University of Cyprus

DEPARTMENT OF CIVIL AND ENVIRONMENTAL ENGINEERING

INTERNAL CURING OF CONCRETE USING HIGHLY ABSORPTIVE NORMAL WEIGHT AGGREGATES

PERICLES ALEXANDROU SAVVA

A Dissertation Submitted to the University of Cyprus in Partial Fulfillment of the Requirements for the Degree of Doctor of Philosophy

JUNE 2018

PERICLES ALEXANDROU SAVVA

εναλλακτικής μεθόδου. Ένας εκ των πιο σημαντικών παραγόντων είναι η ευαισθησία του υλικού σε σχέση με τη δοσολογία, το μέγεθος αλλά και την ποιότητα του εκάστοτε μέσου αυτοσυντήρησης που χρησιμοποιείται. Εξίσου σημαντικός παράγοντας είναι η μείωση των μηχανικών ιδιοτήτων και της ανθεκτικότητας του παραγόμενου σκυροδέματος.

Με σκοπό την διερεύνηση μιας καινούργιας μεθόδου αυτοσυντήρησης, εξετάστηκε η πιθανότητα χρήσης ασβεστολιθικών αδρανών που παράγονται στην Κύπρο. Ένα από τα βασικότερα χαρακτηριστικά των αδρανών στην Κύπρο είναι η υψηλή τους απορροφητικότητα. Η παρούσα διατριβή εστιάζει στην εκμετάλλευση του συγκεκριμένου χαρακτηριστικού με σκοπό την μεταφορά νερού στην μάζα του υλικού, το οποίο σε πρώτο χρόνο δεν θα συμμετάσχει στην ενυδάτωση αλλά θα χρησιμοποιηθεί σε δεύτερο χρόνο για τη διατήρηση της εσωτερικής πίεσης σε υψηλά επίπεδα με σκοπό τη μείωση της συρρίκνωσης και επιπρόσθετα την ενίσχυση του βαθμού ενυδάτωσης του τσιμέντου.

Τα αποτελέσματα απέδειξαν την ικανότητα των αδρανών υψηλής απορροφητικότητας να προσφέρουν αυτοσυντήρηση στο σκυρόδεμα μειώνοντας την αυτογενή συρρίκνωση με σημαντικό θετικό αντίκτυπο στις μηχανικές ιδιότητες και την ανθεκτικότητα του υλικού. Η συγκεκριμένη εφαρμογή αποδείχτηκε εξίσου αποτελεσματική στις περιπτώσεις όπου συμβατικά μίγματα σκυροδέματος είχαν εκτεθεί στο περιβάλον για χρονική διάρκεια ενός έτους. Κατά την συγκεκριμένη περίοδο, εκτός από τις ψηλές θερμοκρασίες, τα μίγματα είχαν υποστεί ψηλές διακυμάνσεις θερμοκρασιών μεταξύ ημέρας και νύκτας. Παρόλα αυτά, τα μίγματα τα οποία είχαν παραχθεί με αδρανή υψηλής απορροφητικότητας είχαν επιδείξει βελτιωμένες μηχανικές ιδιότητες και ανθεκτικότητα σε σχέση με μίγματα που συντηρήθηκαν στο νερό και κάτω από ελεγχόμενες συνθήκες μέσα στο εργαστήριο.

Τέλος με σκοπό την ολοκληρωμένη εξακρίβωση του μηχανισμού αυτοσυντήρησης, συγκεκριμένα μίγματα δοκιμάστηκαν σε μετρήσεις υγρασίας και ποροσιμετρίας υδραργύρου. Για τις μετρήσεις υγρασίας είχε χρησιμοποιηθεί υγρασιόμετρο από το εμπόριο και ταυτόχρονα εξετάστηκε η ανάπτυξη δύο καινοτόμων μετρητών υγρασίας με την χρήση ηλεκτρικής αντίστασης και οπτικών ινών. Τα αποτελέσματα των μετρήσεων υγρασίας έδειξαν ξεκάθαρη διαφοροποίηση των αυτοσυντηρούμενων μιγμάτων η οποία επιβεβαιώνει περαιτέρω την ανάπτυξη του μηχανισμού, ενώ οι εφαρμογές μέτρησης της υγρασίας έδωσαν υποσχόμενα αποτελέσματα ως προς την επιτυχή λειτουργία των αισθητήρων. Τα αποτελέσματα της ποροσιμετρίας υδραργύρου επιβεβαίωσαν την δράση του μηχανισμού αυτοσυντήρησης.

PERICLES ALEXANDROU SAWA

ABSTRACT

Cement hydration and particle flocculation are responsible for concrete solidification. Several physiochemical mechanisms are activated from the moment cement comes in contact with water until the material becomes solid. An ideal maturing period for concrete would be a stress-free situation. However, it is almost impossible for concrete to maintain the same volume from during its early-age. Several mechanisms will develop differential volume variations within the structure of the material which will yield in stress development. Since the material in the early-age will not be able to develop adequate strength, it will crack due to these stresses. The most prominent effect that may cause material damage during the early age is shrinkage. Shrinkage may be classified in various forms, based on the source that causes it. For instance, autogenous shrinkage is mainly caused due to the insufficient quantity of water (low w/c) for cement hydration (self-desiccation) and the fact that the hydration products occupy less space than the raw materials (chemical shrinkage). In addition, a saturated concrete element along with insufficient curing will be the main reasons for the development of differential stress within the materials mass due to drying shrinkage.

The objective of this thesis is to develop an internal curing approach which will focus on reducing these volume variations in order to prevent early-age cracking. Attention was given on delivering additional water within the materials' structure using existing constituents of the mixture. Highly absorptive normal weight aggregates were employed to deliver water for internal curing within the materials' structure.

The results showed that the employment of highly absorptive normal weight aggregates as internal curing agents in concrete mixtures with low w/c ratio was highly efficient in reducing self-desiccation and consequently autogenous shrinkage. The internal curing was efficient in reducing the detrimental effect, on both mechanical properties and durability, of concrete mixtures exposed to adverse environmental conditions, including high temperature and high temperature variations. The method of internal curing was also successfully utilized in concrete mixtures with recycled aggregates.

Finally, in order to verify the action and the effect of the mechanism of internal curing, relative humidity and mercury intrusion porosimeter experiments were conducted on specific mixtures. For the relative humidity measurements, two innovative sensors were developed (electrical and optical fiber) and compared to commercial moisture sensors. The results of the developed sensors were

PERICLES ALEXANDROU SAVVA

very promising whereas the internally cured mixtures showed a humidity retainment within its matrix, which is a direct proof of internal curing action. The mercury intrusion porosimeter experiments verified the effectiveness of the internal curing mechanism and also helped towards clarifying the pore range where the internal curing mechanism acted most prominently.

PERICLES ALEXANDROU SAVVA

ACKNOWLEDGEMENTS

First of all, I would like to express my deepest thanks to my supervisor, Professor Michael Petrou without whose help, this thesis would not have been possible. I am deeply indebted to him for his support and guidance from the very beginning and all the way through.

I would be ungrateful if I did not extend my warmest thanks to Dr. Demetris Nicolaides who has been supportive during all these years.

I would also like to express my deepest thanks to my colleagues and friends Konstantinos Aivaliotis, Michalis Michael, Maria Spanou, Petros Matalas, Giannis Shialos, Stelios Kyprianou, Petros Sotiriou, Antreas Theodosiou, Marios Sophokleous, George Demetriou, Nikos Chousides, Magda Theodosiou, Andri Georgiou and Anna Mina for their support and friendship.

I would like to thank Arsalidou laboratory staff Dr. Loukas Petrou and my PhD committee for allocating their time and providing me with information. MIP equipment was funded by the European Regional Development Fund and the Republic of Cyprus, through the Research Promotion Foundation (Project NEA YPODOMH/NEKYP/0308/17). My deepest thanks go also to Ledra Laboratory and more specifically to Dr. Ioannis Ioannou and Dr. Magda Theodoridou for their contribution and support.

Last but not least, my deepest and warmest thanks goes to my family and friends. This thesis is a result of a great effort, which I could never manage by myself. My special gratitude goes to my wife Stephanie who has been a real support and a true partner through these years.

I dedicate this thesis to my parents, my wife, my son and my closest friends

PERICLES ALEXANDROUSAVVA

Dedicated to my family

PERICLES ALEXANDROU SAVVA

CONTENTS

1. Introduction 30

2. Concrete 32

2.1. History and Background 32

2.2. Cement composition 32

2.3. Cement hydration 33

2.4. Concrete early-age 34

3. Causes and Prevention of Shrinkage in Concrete 36

3.1. Shrinkage 36

3.2. Autogenous, Chemical Shrinkage and Self-desiccation 36

3.3. Drying, Plastic and Carbonation shrinkage 40

3.4. Internal curing 41

3.4.1. Introduction 41

3.4.2. Internal curing mechanism 42

3.4.3. Internal curing methods 44

3.4.3.1. Lightweight aggregates 44

3.4.3.2. Unbound water 45

3.4.3.3. Superabsorbent polymers 45

3.5. Internal curing literature research 47

3.5.1. Lightweight aggregates 47

3.5.1.1. Internal curing using LWA 47

3.5.1.2. Fresh properties 49

3.5.1.3. LWA effectiveness 49

3.5.1.4. Effect on mechanical and durability properties 50

PERICLES ALEXANDROU SAVVA

3.5.1.5. LWA mixtures containing supplementary materials 61
3.5.1.6. Drawbacks of internal curing using LWA 61
3.5.2. Superabsorbent polymers 62
3.5.2.1. Principles and basic experiments 62
3.5.2.2. SAP structure and kinetics effect 73
3.5.2.3. Effect on thermal expansion coefficient 77
3.5.2.4. SAP in other applications 77
3.6. Some Comments Regarding the Literature 79
3.7. Research significance 80
3.8. Synopsis of literature research findings regarding internal curing 80
4. Investigation of internal curing using highly absorptive normal weight aggregates 90
4.1. Objective 91
4.2. Experimental program 92
4.2.1. Materials 92
4.2.2. HANWA aggregates 96
4.2.2.1. Mineralogical composition 97
4.2.2.2. Desorption properties 97
4.2.3. Superabsorbent polymers (SAPs) 98
4.2.4. Internal curing 100
4.1. Experiments 100
4.2. Results and Discussion 102
4.2.1. Chemical shrinkage calculation 102
4.2.2. Autogenous shrinkage 102
4.2.3. Mass Loss 104
4.2.4. Maturing temperature 105
4.2.5. Effect on workability 106

PERICLES ALEXANDROU SAVVA

4.2.6. Compressive strength 108
4.2.7. Open porosity 110
4.2.8. Rapid chloride permeability 111
4.2.9. Sorptivity 112
4.2.10. Relative Humidity 114
4.3. Restrained shrinkage 115
4.3.1. Ring test method 115
4.3.1.1. Experimental setup 116
4.3.1.2. Results and Discussion 118
4.4. Correlations 119
4.5. Internal curing using recycled aggregates 125
4.5.1. Mixtures 125
4.5.2. Experiments and Results 126
4.6. Discussion-Conclusions 127
5. Investigation of internal curing for mitigating high temperature concreting effects 129
5.1. Introduction 129
5.2. Experimental program 130
5.2.1. Mixtures 130
5.2.2. Aggregates 133
5.2.2.1. Mineralogical composition 133
5.2.2.2. Physical and mechanical properties 133
5.2.3. Mixture and internal curing design 134
5.2.4. Experiments and analysis 136
5.2.4.1. Compressive strength 136
5.2.4.2. Vacuum porosity 136
5.2.4.3. Rapid chloride permeability 137

PERICLES ALEXANDROU SAVVA

5.3. Results and Discussion 137
5.3.1. Specimens exposure 137
5.3.2. Compressive strength 138
5.3.3. Durability Indicators 141
5.3.1. Statistical analysis 149
5.3.2. Statistical analysis using SPSS 155
5.3.2.1. Regression analysis 155
5.3.2.2. General remarks 156
5.3.2.3. Descriptive analysis 158
5.4. Conclusions 159
6. Internal curing theoretical verification 162
6.1. Water binding in cementitious system 162
6.1.1. Brunauer, Emmett and Teller (B.E.T.) theory 162
6.1.2. Capillary condensation 163
6.2. Kelvin's Law 163
6.3. Kelvin theorem and mercury intrusion porosimeter – Application on HANWA 164
6.4. Mercury Intrusion Porosimeter on mixtures 169
6.5. Evaluation of HANWA-SSD efficiency using the results of mercury intrusion porosimeter 171
6.6. Volumetric phase distribution 173
6.7. Conclusions 176
7. Innovative techniques for measuring relative humidity in concrete 177
7.1. Introduction 177
7.2. Electrical sensors embedment for the measurement of RH 178
7.2.1. Introduction 178
7.2.2. Sensor Fabrication 178
7.2.3. Experimental Setup 180

PERICLES ALEXANDROU SAVVA

7.2.4. Results & Discussion 180
7.2.5. Conclusions 182
7.3. Fibre optics for measuring relative humidity 183
7.3.1. Polymer optical fibres 183
7.3.2. Concrete relative humidity 185
7.3.2.1. Principles of Fibre Bragg Gratings in Polymer Optical Fibres (FBG-POF) 187
7.3.3. Experimental Program 189
7.3.3.1. Fibre Bragg inscription 189
7.3.3.2. Experimental investigation I 193
7.3.3.3. Experimental Investigation II 194
8. Conclusions and future research 202
8.1. Summary of Conclusions 205
8.2. Recommendations for future research 205
Publications 207
International Journal Publications 207
PhD Related Journal Publications 207
Other Journal Publications 207
Conference Proceedings 209
PhD Related Conference Proceedings 209
Other Conference Proceedings 209
Bibliography 210
ANNEX I: Cement clinker concentration analysis (XRD) 233
CEM I 52.5N 233
CEM II 42.5R 234
ANNEX II: Statistical analysis with SPSS 235

PERICLES ALEXANDROU SAVVA

Regression analysis tables 235
Descriptive analysis 247
Descriptive analysis using all the results included in Chapter 6..... 247
Descriptive analysis using the results included in Chapter 6 excluding NWA 255

PERICLES ALEXANDROU SAVVA

FIGURES

Figure 1-1: Physical mechanisms yielding from cement hydration 31

Figure 3-1: Pore state before and after IC action (a): Unsaturated pore with increased surface tension, (b) IC mediums action, (c) Pore after water replenishment and surface tension reduction 39

Figure 3-2: Disjoining pressure developed from water molecules if water is sufficient 39

Figure 3-3: Chemical and Autogenous shrinkage diagram (Henkensiefken *et al.*, 2008)..... 51

Figure 3-4: Micrograph of crack propagation through a Liapor LWA grain (Lura and Bisschop, 2004) 54

Figure 3-5: NWA ITZ (left) – LWA/NWA ITZ (right) (Bentz, 2009)..... 58

Figure 3-6: Pore created by exhausted SAP particle (Mechtcherine *et al.*, 2006)..... 64

Figure 4-1: Coarse aggregates (NWA and HANWA) sieve analysis according to EN933-1 and EN12620 94

Figure 4-2: Fine aggregates (SAND) sieve analysis according to EN933-1 and EN12620 94

Figure 4-3: Aggregates Young's Modulus 96

Figure 4-4: HANWA desorption properties 98

Figure 4-5: SAP absorptivity in pore fluid 99

Figure 4-6: SAP cumulative particles size distribution 99

Figure 4-7: SAP incremental particles size distribution 100

Figure 4-8: Chemical shrinkage measurement (average of four samples) ASTM C1608..... 102

Figure 4-9: Climatic chamber and strain measurement configuration 103

Figure 4-10: Autogenous shrinkage..... 104

Figure 4-11: Mass loss of mixtures..... 105

Figure 4-12: Maturing temperature..... 106

Figure 4-13: Mixtures' workability 107

PERICLES ALEXANDROU SAVVA

Figure 4-14: Captured image –Threshold image 108
Figure 4-15: Sorptivity values of all mixtures 113
Figure 4-16: Sorptivity testing surface of HANWA and SAP 113
Figure 4-17: Moisture content of control and HANWA-SSD 115
Figure 4-18: Ring test configuration (ASTM C 1581, 2009) 117
Figure 4-19: Ring test configuration 117
Figure 4-20: Environmental chamber and pc units for ring test experiments 117
Figure 4-21: Restrained shrinkage of mixtures control, HANWA SSD and SAP-T1 118
Figure 4-22: Specimens' surface after failure (a) HANWA-SSD (b) control (c) SAP-T1 119
Figure 4-23: Compressive strength of IC-RCA mixtures 127
Figure 4-24: Rapid chloride permeability of IC-RCA mixtures 127
Figure 5-1: Temperature fluctuation for a time interval of two weeks 132
Figure 5-2: Actual maximum and minimum temperature after each mixture exposure to the environment 132
Figure 5-3: All in sieve analysis 135
Figure 5-4: Compressive strength of HANWA mixtures 140
Figure 5-5: Compressive strength of NWA mixtures 140
Figure 5-6: Compressive strength of exposed mixtures 140
Figure 5-7: Compressive strength of water cured mixtures 140
Figure 5-8: Vacuum Porosity (%) 141
Figure 5-9: Sorptivity (i (mm)/t (√ mins)) 141
Figure 5-10: Sorptivity average differences 143
Figure 5-11: Carbonation experiment for NWA (a) and HANWA (b) mixtures 144
Figure 5-12: Porosity vs Apparent Density for exposed specimens 147
Figure 5-13: Porosity vs Apparent Density for water cured specimens 147

PERICLES ALEXANDROU SAVVA

Figure 6-1: Water in C-S-H structure (Feldman and Sereda, 1970) 162

Figure 6-2: Relation between RH and partially empty pores in cement paste (Castro, Bentz and Weiss, 2011) 164

Figure 6-3: Illustration of menisci formation in sealed specimens (Concept based on Henkensiefken, Bentz, et al. 2009) 166

Figure 6-4: HANWA and cement paste cumulative intrusion in MIP 166

Figure 6-5: Aggregates cumulative intrusion (mL/g) 167

Figure 6-6: Aggregates incremental intrusion (mL/g) 167

Figure 6-7: Theoretical empty pores (mL/g) of HANWA-SSD and cement paste according to Kelvin equation 168

Figure 6-8: HANWA theoretical and experimental desorption 169

Figure 6-9: Mercury incremental intrusion for control mixture (mL/g) 170

Figure 6-10: HANWA-SSD mixture mercury incremental intrusion (mL/g) 170

Figure 6-11: Liquid meniscus in a cylindrical pore (Powers and Brownyard, 1947) 171

Figure 6-12: Incremental intrusion of HANWA compared to HANWA mixtures (mL/g) 172

Figure 6-13: Phase distribution of HANWA w/c 0.25 mixture 174

Figure 6-14: Phase distribution of HANWA w/c 0.25 mixture including 0.05 IC water 175

Figure 6-15: Phase distribution of HANWA 0.40 mix design 176

Figure 7-1: Moisture measurement of HANWA-SSD and control mixtures 177

Figure 7-2: Construction of the screen-printed resistivity sensor (left), Concrete cube in an extruded polystyrene box (right) 179

Figure 7-3: Sensor output for the two concrete types 181

Figure 7-4: Normalised resistivity values of the two concrete types 182

Figure 7-5: femtosecond laser (HighQ – femtoRegen) 190

Figure 7-6: Fibre on translation stage for FBG inscription 191

PERICLES ALEXANDROU SAVVA

Table 9 – ANNEX II: Linear regression analysis up to the age of 90 days for porosity..... 239

Table 10 – ANNEX II: Linear regression analysis up to the age of 90 days for porosity (excluding mixtures cast at 40°C)..... 239

Table 11 – ANNEX II: Linear regression analysis up to the age of 365 days for porosity.... 240

Table 12 – ANNEX II: Linear regression analysis up to the age of 28 days for porosity (excluding mixtures cast at 40°C)..... 240

Table 13 – ANNEX II: Linear regression analysis up to the age of 28 days for RCP 241

Table 14 – ANNEX II: Linear regression analysis up to the age of 28 days for RCP (excluding mixtures cast at 40°C)..... 241

Table 15 – ANNEX II: Linear regression analysis up to the age of 90 days for RCP 242

Table 16 – ANNEX II: Linear regression analysis up to the age of 90 days for RCP (excluding mixtures cast at 40°C)..... 242

Table 17 – ANNEX II: Linear regression analysis up to the age of 365 days for RCP 243

Table 18 – ANNEX II: Linear regression analysis up to the age of 365 days for RCP (excluding mixtures cast at 40°C)..... 243

Table 19 – ANNEX II: Linear regression analysis up to the age of 28 days for RCP 244

Table 20 – ANNEX II: Linear regression analysis up to the age of 28 days for RCP (excluding mixtures cast at 40°C)..... 244

Table 21 – ANNEX II: Linear regression analysis up to the age of 90 days for RCP 245

Table 22 – ANNEX II: Linear regression analysis up to the age of 90 days for RCP (excluding mixtures cast at 40°C)..... 245

Table 23 – ANNEX II: Linear regression analysis up to the age of 365 days for RCP 246

Table 24 – ANNEX II: Linear regression analysis up to the age of 28 days for RCP (including mixtures cast at 40°C)..... 246

PERICLES ALEXANDROU SAVVA

EQUATIONS

Laplace's Equation (3-1) 38

Bentz equation (3-2) 51

Young-Laplace equation (6-1) 165

Kelvin equation (6-2) 165

Kelvin/ Young Laplace equation (6-3) 165

Initial porosity (6-4) 174

Chemical shrinkage (6-5) 174

Capillary water (6-6) 174

Gel water (6-7) 174

Gel solid (6-8) 174

Unhydrated cement (6-9) 174

Resistivity equation (7-1) 180

Normalized Resistivity (7-2) 182

Bragg condition (7-3) 188

Shift of the resonance Bragg wavelength (7-4) 188

PERICLES ALEXANDROU SAVVA

SYMBOLS

σ_{cap}	*Capillary pressure*	Pa
γ_p	*Pore fluid surface tension*	N/m
θ	*Liquid-solid contact angle*	*Radians*
γ	*Water surface tension*	N/m
r_{cur}	*Radius of curvature of meniscus*	m
r	*Pore size*	m
R	*Universal gas constant*	$J/mol\,K$
T	*Thermodynamic temperature (Kelvin)*	K
RH	*Relative humidity*	$\%$
V_m	*Molar volume of pore solution*	m^3/mol
M_{LWA}	*Mass of LWA in dry state*	kg
C_f	*Cement content*	kg
CS	*Chemical shrinkage*	ml/g_{cement}
a_{max}	*Maximum expected degree of hydration*	*[-]*
S	*Maximum expected degree of aggregates saturation*	*[-]*
Φ_{LWA}	*Absorption capacity of LWA*	$kg_{water}/kg_{dry\ LWA}$

PERICLES ALEXANDROU SAWA

ABBREVIATIONS

a	*Degree of hydration*
AEA	*Air entrapping agents*
a_{max}	*Maximum expected degree of hydration*
BFS	*Blast furnace slag*
$Ca2^{+}$	*Calcium ions*
CBA	*Coal bottom ash*
CTE	*Coefficient of thermal expansion*
CTRL	*Control mixture*
HANWA	*Highly absorptive normal weight aggregates*
HPC	*High performance concrete*
HSC	*High strength concrete*
IC	*Internal curing*
LWA	*Light weight aggregates*
MIP	*Mercury Intrusion Porosimeter*
NVC	*Normal vibrated concrete*
NWA	*Normal weight aggregates*
OPC	*Ordinary portland cement*
PAM	*Polyacrylamide*

PERICLES ALEXANDROU SAWA

PFA	*Pore fluid absorption*
PVS	*Pre-wetted vacuum saturated*
RCM	*Rapid chloride migration*
RRT	*Round-robin test*
S	*Degree of saturation*
SAP	*Super absorbent polymers*
SCC	*Self-compacting concrete*
SCUC	*Self curing concrete*
SEM	*Scanning electron microscope*
SF	*Silica fume*
SRA	*Shrinkage reducing agents*
SSD	*Saturated surface dry*
w/b	*Water to binder ratio*
w/b_{IC}	*Water to cement ratio for internal curing (additional)*
w/c	*Water to cement ratio*
w/c_{IC}	*Water to cement ratio for internal curing (additional)*

PERICLES ALEXANDROU SAVVA

1. Introduction

Concrete is a material that is generally treated as homogenous. However, in concrete technology the major issues rise from the material's inhomogeneity. Concrete is comprised of three different major phases. The ultimate performance of concrete is affected from the aggregate, cement paste and interfacial transition zone. In order to improve concrete performance, the mechanisms that affect each parameter must be established. The specific procedure was followed in the current research. Based on the classification described above, concrete constituent mechanisms were studied and analyzed in great detail (Figure 1-1), in order to identify ways to increase the material's durability.

The primary objective was to exploit the high absorptivity (up to 5%) of the local aggregates (highly absorptive normal weight aggregates – HANWA) and reverse their detrimental action into beneficial. The idea was to provide water from the inner structure of the material (internal curing – IC) in order to enhance cement hydration, reduce stresses that develop due to lack of water and hence microcracks, in an effort to extend the material's durability. The mechanisms presented in the green shaded shapes in Figure 1-1 represent the main physical mechanisms that cause the material's early-age cracking. The efforts of this research focused on evaluating whether HANWAs were able to reduce self-desiccation and limit the cracking caused by drying shrinkage.

Chapter 2 and Chapter 3 include a description of cement hydration along with the accompanied mechanisms that cause shrinkage and swelling. Chapter 3 examines thoroughly all the established methods and attempts towards internally curing concrete. Chapter 4 focuses on establishing a new IC technique on low water to cement (w/c) ratio concrete mixtures using HANWA-SSD and evaluates the utilization of recycled aggregates as internal curing agents. Chapter 5 examines the possibility of mitigating the effect of high temperature concreting on concrete mixtures with higher w/c using HANWA. Chapter 6 describes the HANWA concrete mixtures' microstructure using theoretical models from the literature and mercury intrusion porosimeter experiments. Chapter 7 describes the development of innovative electrical and fibre optic techniques for the measurement of the material's inner relative humidity (RH). Chapter 8 includes the most prominent conclusions and recommendations for future research. The specific are followed by the authors publications, the bibliography and the annexes.

PERICLES ALEXANDROU SAVVA

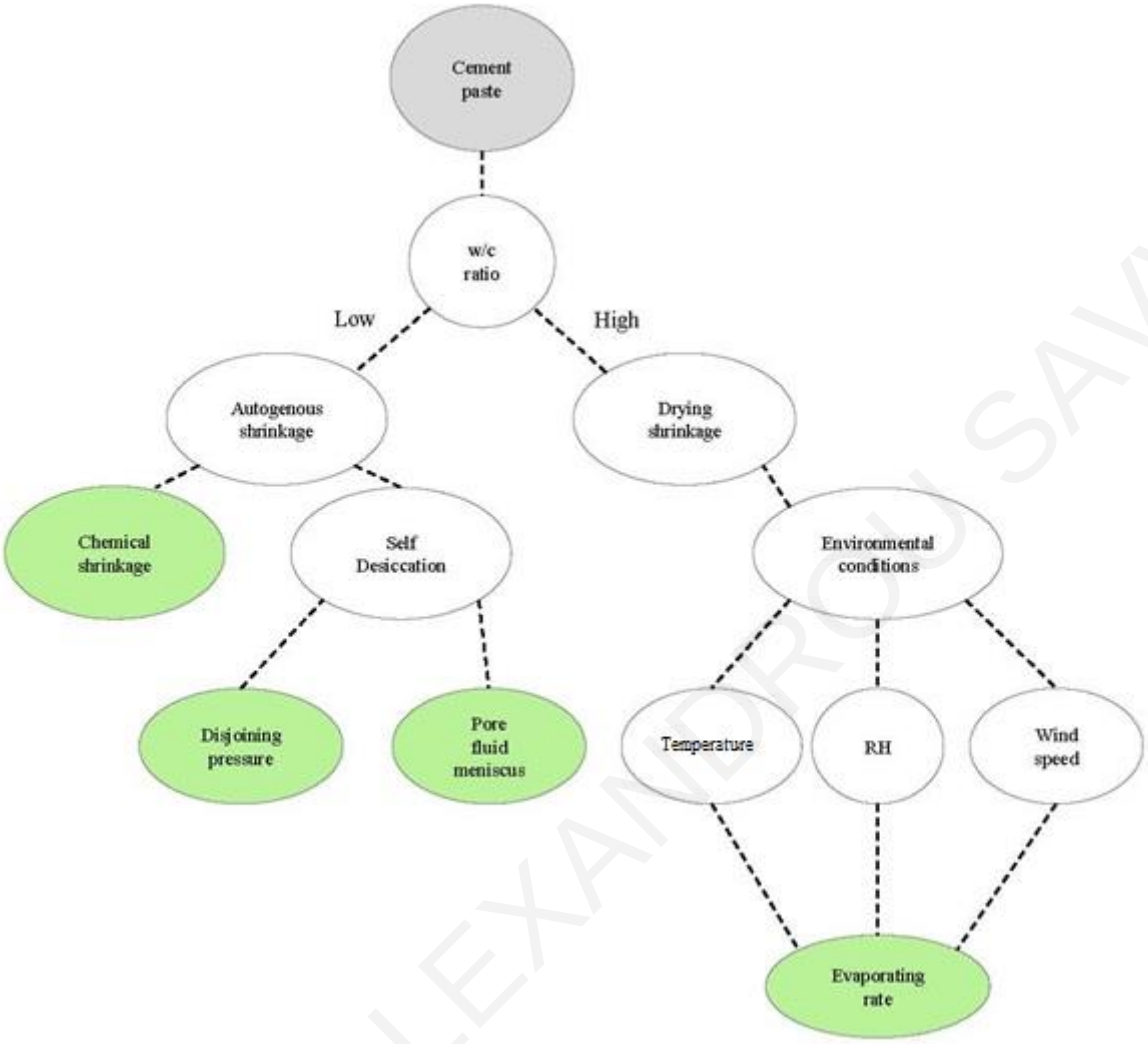

Figure 1-1: Physical mechanisms yielding from cement hydration

PERICLES ALEXANDROU SAVVA

2. Concrete

2.1. History and Background

Due to human readiness to copy nature's processes, concrete is the result of human mimicking nature and producing an artificial rock. The artificial rock known today as Concrete derived due to the agglomeration of particles held together by a binder, widely known as portland cement (Twelvetress, 1905). The word concrete comes from the Latin *concretus* that means grown together, compounded and hardened. Concrete is a material used in the construction industry, consisting of hard inert particles (aggregates), which are bond together using cement and water. Prior to concrete, people were using alternative techniques to obtain a material similar to concrete. The fact that sand and clay mixed with water could yield plastic deformation and shape until the water vapors, provided people the ability to use materials such as these for building heavy and stable structures. The Assyrians and Babylonians used clay as the bonding substance while the Egyptians used lime and gypsum.

During the middle ages, Smeaton was one of the engineers who brought concrete to the front. Portland cement which is the dominant binder used in the construction industry until now was the step further that established concrete as a "recent improvement" as General Pasley refers (Twelvetress, 1905). The first Portland cement was created by Joseph Aspdin, a builder from Leeds, in 1824 who took a p reW*10 0 62pdi

several processes namely autogenous, chemical, and drying shrinkage. These processes are described in detail in chapter 3.

the formation of internal voids is not possible due to the poor strength of the material that causes it to collapse over the voids. During this period of time, autogenous and chemical shrinkage are equal. However, when the material develops adequate strength, voids due to chemical shrinkage form causing a divergence between autogenous and chemical shrinkage. Autogenous shrinkage was first recognized and introduced in concrete technology by Lynam, 1934. In the early years of autogenous shrinkage recognition, its influence was smaller than drying shrinkage, so the attention given to it was not much. In normal strength concrete, autogenous shrinkage is relatively small and its effect on the material's performance is negligible. However, the introduction of high strength concrete in the late 1980's triggered the community towards studying autogenous shrinkage in a greater extent. Advances in concrete technology helped to develop high performance concrete mixtures, characterized by high compressive strength and low permeability. Their performance is attributed to the improved packing of the constituent materials due to the elimination of the coarse aggregates, water content reduction and superplasticizers that result in a dense matrix.

Based on Powers' model, 1 g of cement bounds chemically approximately 0.23 g of water during hydration and 0.19 g of water physically due to adsorption (Powers and Brownyard, 1947). In order to achieve full hydration of cement the minimum water to cement ratio is 0.42. Lower water to cement ratio will result into inadequate amount of water for hydration causing higher capillary tensile forces in the pore structure. Low w/b ratio causes a shortage in water which increases autogenous shrinkage, due to several physical mechanisms known as self-desiccation (Schröfl, Mechtcherine and Gorges, 2012). Self-desiccation is mainly governed by two physical mechanisms. Specifically, the meniscus formation (Figure 3-1-a) and the reduction of disjoining pressure (Figure 3-2). The water-air meniscus which appears in unsaturated pores due to pressure decrease (Kelvin's Law) (Lura, Jensen and Van Breugel, 2003). The RH drop causes a pressure drop within the pore that leads to the formation of water-air menisci (Kelvin's Law) (Lura, Jensen and Van Breugel, 2003). The water menisci lead to a convex surface of the pore water which occurs because of the pressure difference within the pore. The pressure difference also known as capillary pressure increase leads to a surface tension increase (Laplace's Equation (3-1)). The surface tension is counterbalanced from the solid structure, namely the surrounding walls. Consequently, the pore walls develop compressive stress which may lead to contraction or rupture (Figure 3-1 – a) (Lura, Jensen and Van Breugel, 2003; Barcelo, Moranville and Clavaud, 2005; Schröfl, Mechtcherine and Gorges, 2012). When the liquid within a pore evaporates, the tension in the meniscus is transferred to the walls and the pore tends to shrink (Taylor, 1990) as

PERICLES ALEXANDROU SAVVA

shown in Figure 3-1. According to Taylor, the effect may be irreversible due to pore collapse and the specific effect is important at RH levels between 90% and 45% (Taylor, 1990).

The disjoining pressure occurs when the attractive forces between the calcium silicate hydrate (C-S-H) gels are counteracted from the multi-layer water molecules adsorbed on their surface (Taylor, 1990). It develops as a result of adequate amount of water. A drop in RH - which is known to occur earlier in low w/b ratio mixtures - causes the reduction of disjoining pressure, resulting in additional shrinkage (Lura, Jensen and Van Breugel, 2003).

$$p_a - p_w = \sigma\left(\frac{1}{r_1} + \frac{1}{r_2}\right) = \frac{2\sigma}{r_c} \tag{3-1}$$

where $p_a$is the air pressure, p_w is the water or the pore fluid pressure, σ is the surface tension and r_c is the pore radius where r_1=r_2 if the pore section is circular.

It is, therefore, understandable that in order to prevent self-desiccation, additional water should be provided. Since the w/b ratio increase is not possible in high performance concrete, other methods must be employed. Several proposed methods, include the addition of internal reservoirs in order to replenish the consumed water and maintain the RH at high levels, namely, internal curing (IC), (Figure 3-1-b,c), shrinkage reducing agents to reduce pore fluid's surface tension, and expansive minerals to counteract shrinkage (Sant, Bentz and Weiss, 2011). The dispersion of water reservoirs is a well-established method that reduces early-age shrinkage and self-desiccation. The IC water reservoirs are employed to replenish the consumed water and restore the pressure within the pore (Figure 3-1-b). Figure 3-1 demonstrates the surface tension increase due to lack of water, the compressive strength developed on the surrounding walls and the consequent reduction after the IC action.

PERICLES ALEXANDROU SAWA

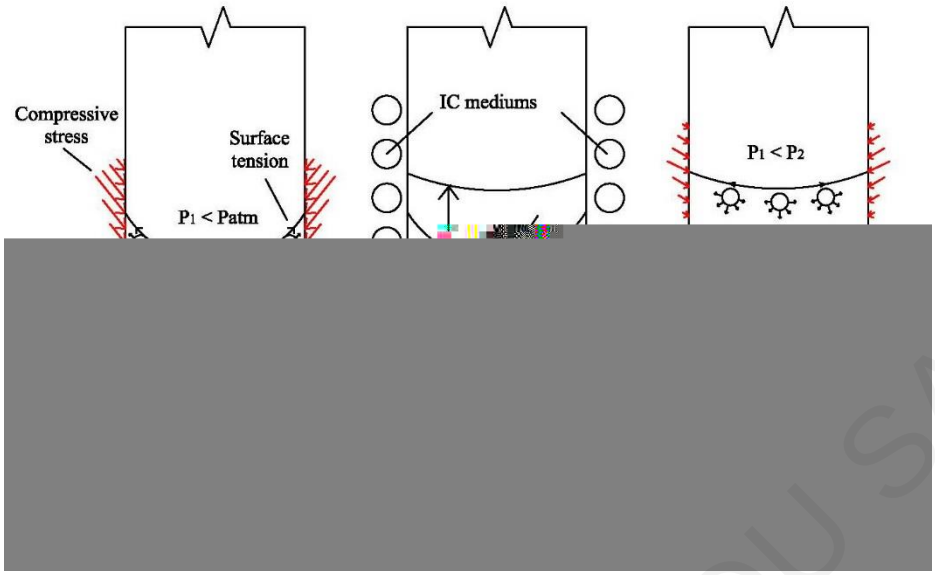

Figure 3-1: Pore state before and after IC action (a): Unsaturated pore with increased surface tension, (b) IC mediums action, (c) Pore after water replenishment and surface tension reduction

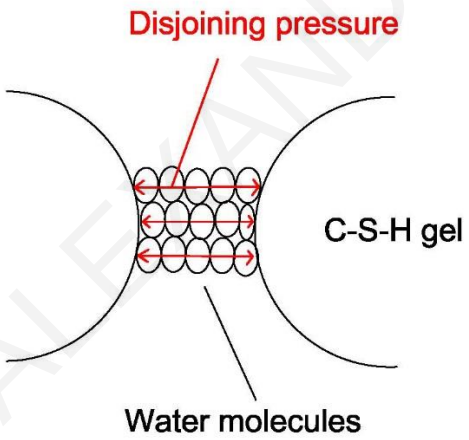

Figure 3-2: Disjoining pressure developed from water molecules if water is sufficient

When autogenous shrinkage in concrete is restrained due to the aggregates, reinforcement, or its own hydrated rigid skeleton, tensile stresses develop. Especially in high performance concrete where the pore structure is extremely dense due to fine pozzolanic materials in the micro and/or nano scale, autogenous shrinkage is even more intense and could cause irreversible damage to the material (Zhutovsky and Kovler, 2010). These phenomena are very intense in early ages when the material does not develop adequate strength, hence cracks formed (Zhutovsky and Kovler, 2010; Craeye, Geirnaert and Schutter, 2011). Due to early-age cracking, the material will perform poorly in terms of diffusivity and permeability, being more vulnerable in aggressive ions attack from the environment

PERICLES ALEXANDROU SAVVA

such as chlorides, sulfates, nitrates and carbon dioxides. Therefore, it is of great importance to prevent the formation of cracks in the early-age of a structure, in order to avoid irreversible damages.

The internal water reservoir method widely known as IC has received great attention during the last decade where several methods were developed in order to compensate self-desiccation and reduce early-age shrinkage. IC attracted great attention after Ole Jensen's comprehensive work (Jensen and Hansen, 2000, 2002) in the early 2000s who included superabsorbent polymers (SAPs) for IC and Dale Bentz who employed lightweight aggregates (LWA) (Bentz, Lura and Roberts, 2005). Both methods are well established with extended research for over than fifteen years. However, both methods evidently exhibit specific drawbacks deteriorating other properties of the material (Table 3-1 and 3-2).

3.3. Drying, Plastic and Carbonation shrinkage

The aforementioned types of shrinkage are caused from cement intrinsic properties. However, when the material is exposed to environmental conditions, it may suffer shrinkage due to high temperature, RH reduction, wind speed and carbonation. More specifically, when the evaporation rate is greater than the bleeding rate, evaporation will occur from the material's matrix, inducing intense vapor diffusion from the material's structure leading to stress development. The specific mechanism is well known as plastic shrinkage, appears in random patterns and forms shallow cracks. Plastic shrinkage refers to the shrinkage observed due to water evaporation which develops tensile stresses on its way out from the matrix. It generally appears during the early age when the material is still in plastic state. The finer the pores of a system the greater the capillary tensile stresses developed at the meniscus hence the higher the contraction (Bentz *et al.*, 1997; Henkensiefken, Castro, *et al.*, 2009; Jin, Gu and Al-Tabbaa, 2014). The volume of the evaporated water will not be equal to the contraction volume of concrete. The reason is that the stress developing due to moisture withdrawal will not always exceed the pore structure in order to fully seal the pore, thus the free water escaped first, will create little or no shrinkage (Neville, 2002). The differential volume changes will generate tensile stresses in concrete and self-restrain due to differential deformation along with concrete low early strength will lead to cracking (Leemann, Nygaard and Lura, 2014).

When a concrete element is exposed to a CO_2 environment, CO_2 gas will ingress the material. If the conditions are favorable (50-80%RH and high diffusivity/permeability coefficient), CO_2 gas in the presence of moisture (H_2O) will convert to carbonic acid (H_2CO_3). H_2CO_3 will react with calcium hydroxide ($Ca(OH)_2$ which is the second in terms of volume product of cement hydration (20-30%)

PERICLES ALEXANDROU SAWA

to form calcium carbonate ($CaCO_3$). Calcium hydroxide $Ca(OH)_2$ dissolution under compressed structure will cause carbonation shrinkage and deposition of calcium carbonate $CaCO_3$. The volume occupied by $Ca(OH)_2$ will be replaced by $CaCO_3$ causing shrinkage.

3.4. Internal curing

3.4.1. Introduction

As explained previously in section 3.2, lower water to cement ratio will result in inadequate amount of water for hydration and finer pores resulting in higher capillary tensile forces in the pore structure. These phenomena are very intense in early ages where the material does not developed adequate strength, hence cracks will be created (Zhutovsky and Kovler, 2010; Craeye, Geirnaert and Schutter, 2011). Due to early-age cracking, the material will perform poorly in terms of diffusivity and permeability being more vulnerable to attack from the environment such from chlorides, sulfates, nitrates and CO_2.

Chemical shrinkage is an intrinsic property of cement, which cannot be manipulated macroscopically. However, self-desiccation can be controlled physically by maintaining the RH of concrete matrix to high levels. Preventing RH drop in concrete benefits the material in multiple, early and long term, ways. A simple way to maintain RH at high level is the use of water curing or impermeable membranes in order to reduce evaporation. The application of external curing is very efficient especially in hot and dry environmental conditions. However, self-desiccation shrinkage cannot be compensated with the use of external curing, in dense structures where the permeability and diffusivity coefficients are very low and water from the exterior cannot travel through the material's structure (Bentz and Snyder, 1999; Akcay and Tasdemir, 2010). The density of high performance concrete which yields to depercolated capillary pores hinders the diffusion of the external moisture throughout the material's structure (Sant, Bentz and Weiss, 2011). Therefore, in order to reach the inner core of the material's body dispersed water reservoirs must be incorporated in the structure. The ideal conditions for concrete maturing would be a constant supply of water throughout its volume for hydration which would not participate in the w/b ratio, along with constant volume from casting to solidification. The aforementioned mechanism would compensate RH drop which occur due to dissolved salts, hydration, drying, self-desiccation and chemical shrinkage. As mentioned, chemical shrinkage cannot be compensated macroscopically and salts dissolution has a minor effect on RH drop (~3-4%) (Lura, Jensen and Van Breugel, 2003), as opposed to self-desiccation which can be diminished by employing internal curing (IC) (Jensen and Hansen, 2000). Drying shrinkage was not evidently compensated by

PERICLES ALEXANDROU SAVVA

the mean of IC. IC is intended to enhance the initial life-period of the material by providing water from the inner structure of the material in order to compensate RH drop. Among others, IC transcendent other shrinkage reducing chemicals that reduce concrete autogenous shrinkage such as shrinkage reducing admixtures which are known to affect mechanical properties (Radlinska *et al*., 2008).

The increased use of high performance concrete led to an increased attention on IC. Although many techniques were proposed for IC, such as the use of various minerals (i.e. magnesium oxide) or artificial reservoirs such as microcapsules, special emphasis was given on techniques with proven applicability such as lightweight aggregates and superabsorbent polymers (Jensen and Lura, 2006). Increasingly in the last two decades, IC gathered special attention and one can observe an increasing trend of new IC techniques as well as an increasing effort towards the optimization of established techniques. An improved maturing period for the material will improve the material's performance and increase the materials durability.

3.4.2. Internal curing mechanism

Concrete is a material with low permeability, therefore with external curing it is impossible for the water to travel throughout the pore structure in order to mitigate self-desiccation and reduce autogenous shrinkage (Bentz and Snyder, 1999; Akcay and Tasdemir, 2010). This phenomenon is more intense in large mass elements where the distance required for the water to travel is longer and in high performance concrete where the permeability is lower than conventional concrete. Concrete will not develop its maximum durability and mechanical properties unless adequate curing is available. Without proper curing, strength could be decreased by 10-20% and permeability could be increased by 20 - 60% (Espinoza-Hijazin and Lopez, 2011). A possible cracking in the interfacial transition zone due to self-desiccation is likely to compromise modulus of elasticity, strength and durability. The objective of incorporating IC in concrete is to compensate early age shrinkage by providing internal curing water, reduce early-age cracks, permeability, ion diffusion, increase resistance to freeze and thaw, deicing chemicals, chemicals attacks, creep, increase durability, increase hydration and strength (Zhutovsky and Kovler, 2010; Castro *et al.*, 2011; ACI Committee 308 and 213, 2013).

In order to withdraw water from smaller pores of IC mediums the negative pressure within the system has to be increased. Besides self-desiccation, which is the principle reason for pressure reduction, the pore size is reduced as the hydration continues and therefore the water withdrawal will continue as

PERICLES ALEXANDROU SAVVA

the specimen ages, due to solidification of the hydration products (Henkensiefken, Castro, *et al.*, 2009). The pressure of the pore fluid drops when chemical and autogenous shrinkage diverge due to solidification forming voids in the internal of the matrix. The RH of the matrix at that time can be a tool to estimate the pressure that develops in the fluid (Henkensiefken, Castro, *et al.*, 2009). Even with a slight drop of RH in the inner core of the material, pressure is developed in the pore fluid and the IC water within the IC medium is withdrawn. It has to be mentioned though that RH at the inner core may observe a drop due to self-desiccation, salts dissolution and drying.

Internal curing is achieved by embedding spatially distributed water reservoirs that will supply additional water to the cement system in order to restore RH equilibrium. The governing force of internal curing is RH drop. When the RH in the cement paste is reduced, suction forces will withdraw water from the medium (ACI Committee 308 and 213, 2013). Henkensiefken et al. clarified that within a system with low pressure the largest pores will empty first (Henkensiefken, Bentz, *et al.*, 2009). Craeye *et al.*, 2011 concluded that any effective water delivering source within the material's structure will produce additional hydration. As the pore size of the paste decreases due to extended hydration, the capillary pressure increases leading to an intense IC water withdrawal. Internal curing is employed in order to maintain high internal RH or replenish the moisture level in concrete and therefore reduce shrinkage (Figure 3-1).

Providing a well dispersed internal curing agent in the material's matrix without compromising its properties is of particular importance in order to maintain or improve the material's durability and mechanical properties. IC good design and implementation are of particular importance since excess free water from the inner core of the material will lead to an increase of the effective w/b and deteriorate the aforementioned properties. Using various IC techniques, autogenous shrinkage was reduced and in certain occasions fully compensated; however, in the majority of the times other properties were negatively affected (Table 3-2). Therefore, the primary concern should be the mechanical and durability improvement alongside autogenous shrinkage reduction. Several materials were proposed for mitigating autogenous shrinkage by the use of internal curing. The main mechanisms are briefly presented below, where the two main established methods are described.

PERICLES ALEXANDROU SAVVA

3.4.3. Internal curing methods

3.4.3.1. *Lightweight aggregates*

3.4.3.1.1. Adsorption

Bentonite clay was suggested due to its high specific surface (>100m^2/g) that allows the adsorption of water molecules within its structure and its swelling ability. However, the high ionic pore fluid of cementitious systems leads to clay agglomeration (Torikai, Sato and Ohashi, 1996).

3.4.3.1.2. Absorption

Porous volcanic rocks such as sponge-like pumice were investigated (Zhutovsky, Kovler and Bentur, 2002). This specific material is formed from magma and dissolved gases and its absorption value may reach up to 27%. The heat treatment (900ºC) of naturally occurring perlite leads to expansion which turns to high absorptivity values up to 200-600%. This characteristic is attributed to the fact that perlite actually contains 2-6% combined water which after the heat treatment evaporates and causes the expansion. It is mostly used for filtration and insulation (Zhutovsky, Kovler and Bentur, 2002).

Liapor and Leca are brand name for clay that also undergoes heat treatment (1200ºC) to expand and reach absorptivity values up to 90%. However, most of the formed pores which occur due to gases from organic materials expansion are closed, yielding in an absorptive value of 17%. Other materials investigated were stalite that yields from heat treatment (1150ºC) of slate whereby entrapped gases lead to interconnected pores. However, the drawback of the specific medium is that the interconnectivity is not as efficient as in other lightweight aggregates and the pores are finer. Additionally, diatomaceous earth was evaluated. The specific material forms from prehistoric single cell algae, diatoms. When the diatoms died, their fossils precipitation formed amorphous silica (opaline) that has a diatomite content of 25-100%. Their size range varies from 5-20 μm with a radial or line symmetry and their absorption range from 50-70% leading to a total water absorption of 100% (Gjorv, 1991).

Moreover, Van et al. employed rice husk ash (RHA) which is a waste from the rice processing industry to enhance the early-age properties of concrete in terms of shrinkage while maintaining other properties intact (Van *et al.*, 2014). RHA is a kind of mesoporous amorphous siliceous material with pore size varying from 2-50 nm, specific pore volume 120 mm^3/g and specific absorption capacity of 0.180 ml/g. The researchers concluded that the utilization of RHA can effectively reduce autogenous shrinkage of concrete and enhance the degree of hydration without noticeable effect on compressive strength. The specific technique extended the internal RH of the mixture.

PERICLES ALEXANDROUSAVVA

3.4.3.2. Unbound water

Microencapsulation is a rising technique in concrete technology. It can be employed in various applications and in various forms and sizes in order to participate as an IC medium or self-healing medium in concrete (Litina, Kanellopoulos and Al-Tabbaa, 2014; Kanellopoulos, Qureshi and Al-Tabbaa, 2015; Giannaros, Kanellopoulos and Al-Tabbaa, 2016). It has many advantages since the size and the material of the capsules can vary according to the application, whereas the fluid carried within the capsules structure can also be modified to serve various applications. The fluid can be either physical such as a simple expansive oxide (MgO) to occupy space and precipitate in pores, up to living organisms such as microorganisms whose urine will react with pore fluid to seal cracks. Microcapsules employed for IC exhibit a specific drawback. The demand for IC water rises due to purely physical mechanisms. Therefore, the capsules' shell failure cannot be controlled chemically. The rupture has to occur at a specific time under certain circumstances governed mainly from anaerobic drop of RH. Therefore, the only mechanism that varies at the specific time is the pore pressure, thus, the shell rupture has to be mechanical. Another proposed technique which was not investigated thoroughly is the emulsification of water in pore fluid. The specific technique lies on the principles of emulsification in other products such as milk, where the emulsifying agent is casein protein and stabilizes the emulsion by forming a protective phase around the dispersed phase (fats).

Liu et al. proposed the incorporation of cenospheres for internal curing (F. Liu *et al.*, 2017). Cenospheres are hollow fly ash particles yielding from power plants. A glass-crystalline external shell is chemically etched to expose the pores that may absorb up to 180%. The absorbed water is readily available for IC. The authors reported a nearly full elimination of autogenous shrinkage and an improvement of the compressive strength.

3.4.3.3. Superabsorbent polymers

SAP were investigated in order to be employed in concrete. SAPs are polymers able to absorb liquid from the surroundings and retain large amount of liquids compared to their weight (Jensen and Hansen, 2000; Siramanont, Vichit-Vadakan and Siriwatwechakul, 2010). SAPs are primarily used in sanitary products such as urine disposal diapers. Their efficiency as water reservoirs used for concrete IC was first recognized by Ole M. Jensen in the early 2000s (Jensen and Hansen, 2000). They are classified into thermoset and thermoplastic polymers where the difference is that the thermoplastic polymers are not chemically cross-linked therefore they can dissolve in a liquid whereas the thermoset polymers are cross-linked (Siramanont, Vichit-Vadakan and Siriwatwechakul, 2010). The SAPs used

PERICLES ALEXANDROU SAVVA

in concrete technology are eminently covalently cross-linked polyacrylates and copolymerized polyacrylamides/ polyacrylates (Jensen and Hansen, 2000). SAP polymerization is carried out by two different techniques. One is the bulk polymerization which is the result of mixing two aqueous solutions including acrylamide, cross-linking agent, accelerator and sodium persulfate (NaPS). The procedure consists of oven drying, rinsing and manual grounding the polymer to irregular shape particles (Siramanont, Vichit-Vadakan and Siriwatwechakul, 2010). Another method is the inverse suspension or water-in-oil technique, which is conducted by adding water droplets that contain the mixture in oil. The polymerization takes place within the water droplets and therefore the particle size is controlled and their shape is spherical. The cross-linking is applied by adding multivalent monomers or by post-polymerization (Schröfl, Mechtcherine and Gorges, 2012).

When a SAP comes in contact with a liquid, the molecules of the liquid are diffused into the SAP to wet the polymer chains, causing a swelling. The weight of the swelled particle to the weight of the dry particle is referred as the swelling ratio. The swelling ratio is determined by various factors such as the cross-linked density, the SAP structure, the surrounding temperature, the liquids pH and ion concentration (Siramanont, Vichit-Vadakan and Siriwatwechakul, 2010). The swelling ratio of a SAP prepared from polyacrylamide (PAM) can be controlled by varying the acid composition because acrylamide contains hydrogen and thus can be deprotonated at high pH and also maintain the ability to polymerize with different amounts of acrylic acid (Siramanont, Vichit-Vadakan and Siriwatwechakul, 2010). This ability of the cross-linked density of the SAP is what determines the particles' carrying capacity. The absorption and desorption rate of SAP is determined by their anionic group density and the particle size (Schröfl, Mechtcherine and Gorges, 2012). The lightly cross-linked polymers are able to absorb greater amount of liquid (Jensen and Hansen, 2000). The cross-link density of a SAP though is not the only factor that determines its carrying capacity. Ion charge and concentration of a liquid will also determine the absorbing amount. SAP macromolecular chain is a polyelectrolyte; when the polymer is dissociated in a liquid it releases positive ions in the solution and bounds negatively charged ions to the chain due to deprotonation. SAP is highly swollen in basic conditions because the negative charges provide the repulsive force on the polymer network (Jensen and Hansen, 2000; Siramanont, Vichit-Vadakan and Siriwatwechakul, 2010). In concrete though, due to the presence of cations within the pore fluid these negative forces are compensated reducing the swelling (Jensen and Hansen, 2000). Schrofl concluded that SAP with high density of anionic groups regardless the cross-linking density are greatly affected by calcium ions ($Ca2^{+}$) presence (Schröfl, Mechtcherine and Gorges, 2012). The carboxylic groups of the polymers complex the $Ca2^{+}$ ions and

PERICLES ALEXANDROU SAWA

the effect of the anion groups inside the SAP diminish. In consequence, SAP anionicity is screened and the swelling ratio decreases because of the reduction in osmotic pressure. Therefore, SAP absorptivity would be affected by the ion concentration of the liquid as well as the ion type. SAP with high density of anionic groups observe high rate absorption and desorption in cement pore solution (Schröfl, Mechtcherine and Gorges, 2012).

3.5. Internal curing literature research

3.5.1. Lightweight aggregates

As opposed to adsorbed and chemically combined water, in the case of physically held mediums such as LWA, the initiation time and the amount of IC water withdrawn depends on the mediums' pore size and the pressure developed. It is a process where due to the underpressure, water is withdrawn from the LWA pores and the replenishment of water within the pores will reduce that pressure as shown in Figure 3-1-(b) and (c). Due to underpressure, the radius of the pore fluid meniscus is reduced causing an increase in surface tension which yields in compression stress from the surrounding material (Figure 3-1-(a)). This mechanism causes the material's shrinkage. Thus providing extra water during this process the consumed water will be replenished and the under pressure will be effectively reduced preventing concrete's shrinkage/early-age cracking. The principle governing the specific mechanism is the high pore size and absorptivity. However, as explained above, the high absorptivity in the majority of the cases occurs due to gas or water expansion within the material's structure. Along with the formation of pores, the material's density is reduced due to the lower weight of air. Therefore, the lightweight aggregates' final structure is characterized by low strength ability and a high air/pores fraction, providing high insulating abilities. It also can be utilized as an IC medium due to its carrying capacity properties. However, the LWA exhibit specific drawbacks discussed hereafter.

3.5.1.1. Internal curing using LWA

One of the very first researchers that recognized the driving force which withdraws water from LWA as well as the ability of LWA to utilize water from their inner structure towards the cement paste was Holm in 1980 (Holm, 1980). Holm studied the performance of lightweight aggregates in marine environments and attributed the increased strength of LWA concrete to an internal supply of water. Holm was the first to use the term internal curing to explain the mechanism. However, the mechanism is being studied in deep since the late 1990s when Weber and Reinhardt (Weber and Reinhardt, 1997), Kohno et al. (Kohno *et al.*, 1999) and Bentur et al. (Bentur, Igarashi and Kovler, 2001) emphasized on the effect of IC using LWA.

PERICLES ALEXANDROU SAVVA

Weber and Reinhardt observed that external curing is not effective in dense paste due to low permeability and diffusivity coefficients (Weber and Reinhardt, 1997). They concluded that the effectiveness of LWA (4-8mm, 24-hour water absorption (WA_{24}) = 20.2%) in concrete with 0.30 w/b ratio by 25% replacement of normal weight aggregates resulted in increased strength with external curing independency. They attributed their findings on extended hydration which was confirmed using X-ray diffraction and led to lower porosity and smaller pores. Weber and Reinhardt, 1997 also concluded that during hydration in an unsealed system, the main mechanism of IC is the capillary suction whereas water evaporation intensifies the phenomenon due to a second humidity gradient. This specific mechanism is responsible for the conclusion drawn regarding the increased compressive strength observed in a dryer environment.

Kohno et al. employed artificial LWA to reduce autogenous shrinkage, which was measured by embedding a strain transducer within the mixture (Kohno *et al.*, 1999). They concluded that the autogenous shrinkage is LWA mixtures was fully compensated as opposed to NWA mixtures. A relation between the autogenous shrinkage, the permeability and the aggregates absorption capacity was extracted. Their final remark was that an increase of LWA would decrease autogenous shrinkage, without clarifying whether the relationship was linear. They had employed LWA after immersion or boiling. The term IC was not used in this specific research.

Bentur *et al.*, 2001, conducted fully and partial replacement (25%) of NWA using Leca LWA and observed no significant strength reduction along with autogenous shrinkage elimination, in high strength concrete mixtures with w/b ratio 0.33 (10% silica fume with respect to cement mass). It was observed that the addition of LWA in air-dry state was as effective as in SSD state regarding autogenous shrinkage.

Regarding the cement paste surrounding the IC medium and the IC medium efficiency, several researchers adopted the method of protected paste. The concept of protected paste was developed in an effort to assess the effectiveness of frost resistance agents. The term “protected” was introduced to explain how much cement paste is protected from frost damage due to air entrainment (Vaysburd, 1996). Powers called the paste surrounding the air void and cured due to expansion space availability, “sphere of influence” (Zhutovsky, Kovler and Bentur, 2011). According to several researchers the durability of the mixture is ensured if the cement paste lies within a minimum distance of 200 μm from the nearest air void. The specific distance is the so called spacing factor. The specific distance is amended in the case of IC according to the IC agent’s water availability, spatial distribution and fraction.

PERICLES ALEXANDROU SAVVA

3.5.1.2. Fresh properties

It is of fundamental importance to evaluate whether the addition of IC medium in concrete will affect its workability. The effect quantification will assist the interpretation of the material's initial and final performance. Lo et al. mentioned that extended LWA pre-wetting time will increase the workability of the mixture due to localized high water content on the LWA surface (Lo, Gao and Jeary, 1999). It was also stated that the water release due to pumping and placing is an unknown parameter, even though it was clarified that intense mechanical vibration may lead to pre-mature water release and segregation (Zhutovsky, Kovler and Bentur, 2002). Poon et al. reported that the addition of SSD LWA may lead to prolonged slump loss (Poon *et al.*, 2004). Collins and Sanjayan employed pre-soaked (4 weeks) coarse LWA (14 mm blast-furnace slag) for IC of alkali-activated slag concrete, as a replacement to NWA (14 mm basalt) (Collins and Sanjayan, 1999). The results showed a reduction in workability as opposed to identical NWA mixtures. The addition of SAP doesn't seem to affect the mixture's workability (Justs *et al.*, 2015). It was reported that SAP mixtures exhibited greater resistance to bleeding as opposed to identical mixtures without SAP addition. The workability in the case where SAP are added to the mixture depends on the amount of IC water, and whether that is deducted from the initial w/b or w/c ratio.

3.5.1.3. LWA effectiveness

In order to evaluate the effectiveness of IC using LWA, several other parameters were examined by various researchers. Maruyama et al. examined the distance that IC water can travel from LWA (32% absorptivity) in high strength concrete (w/b 0.23) using neutron radiography (Maruyama *et al.*, 2009). They concluded that the governing factor that withdraws water from the aggregates core is a concentration gradient. Therefore, the water extraction initiates a few hours after casting and the travel distance varies between 3 mm and 8 mm. They stated that the effectiveness of LWA decreases progressively, due to water exhaustion. The findings of the specific research were in contradiction with other researchers who stated that the governing withdrawal mechanism is a pressure gradient (Bentz *et al.*, 1997; Henkensiefken *et al.*, 2008; Henkensiefken, Bentz, *et al.*, 2009). Zhutovsky et al. stated that the addition of pozzolanic micro fillers such as silica fume reduces the effectiveness of an IC system including coarse LWA, due to the compact network that reduces the travel distance of the IC water (Zhutovsky, Kovler and Bentur, 2004). In another work, Zhutovsky et al. conducted a review work based on the IC experimental progress, aiming to evaluate the concept of protected paste and its applicability on IC concrete mixtures (Zhutovsky, Kovler and Bentur, 2011). The authors concluded that the recommendation to limit the spacing factor to approximately 200 μm cannot be extended to

PERICLES ALEXANDROU SAWA

the IC of high strength concrete, because LWA and SAPs are the IC water sources and thus strongly influence the spacing factor. The authors concluded that the amount, type and particle size have a direct effect on IC effectiveness. According to the authors, the most important parameter seemed to be the availability of IC water and the readiness of the IC agent. They mentioned that the aforementioned properties for LWA are governed based on the aggregates pore structure whereas for SAP based on the particles size.

Akcay and Tasdemir examined the effects of LWA spatial distribution on IC (Akcay and Tasdemir, 2010). More specifically, different sizes and amount of LWA (natural pumice) were employed as a replacement to NWA. An image analysis technique was employed in combination with a protected-paste volume approach in order to estimate the water flow distance from the reservoirs to the paste. The mixtures were manufactured using natural pumice LWA (2-4 mm and 4-8 mm, WA 35% and 30% respectively), constant cement content (497 kg/m^3) and w/b ratio (silica fume 50 kg/m^3) 0.28. The LWA to NWA volume replacement percentages were 10%, 20%, and 30%. The results indicated best-fitted values for travel distance of 1 mm for 3 days of age specimens. The specific conclusion was drawn after different flow distances (0.5 mm, 1.0 mm and 2.0 mm) were compared with the autogenous strain mitigation ratios and the best correlation was observed for 1 mm travel distance (R^2=0.90). As previously clarified, the addition of silica fume in an IC system reduces the systems' effectiveness (Zhutovsky, Kovler and Bentur, 2004). It confirms that the protected paste volume in internal curing can be determined by image analysis. Akcay and Tasdemir confirmed the effectiveness of pre-soaked LWA towards mitigating autogenous shrinkage of concrete.

3.5.1.4. Effect on mechanical and durability properties

Henkensiefken et al. clarified that the performance of an IC system depends on the water availability in terms of quantity and readiness to be utilized by the cement paste, as well as the IC mediums distribution (Henkensiefken, Bentz, *et al.*, 2009). They examined the effect of SSD LWA (expanded shale) IC on sealed and unsealed mortars, employing various replacement percentage of NWA. The IC water required to diminish autogenous shrinkage was calculated based on Bentz and Snyder principle (P. D. Bentz and Snyder, 1999). Bentz equation (3-2) was developed taking into account the final setting time and calculating the voids created due to chemical shrinkage. The equation was based on the approach that the amount of water required for IC is equal to the volume of voids produced due to chemical shrinkage. The specific mechanism was presented graphically in 2008 by Henkensiefken *et al.*, 2008 (Figure 3-3).

PERICLES ALEXANDROU SAVVA

$$M_{LWA} = \frac{C_f \times CS \times \alpha_{max}}{S \times \Phi_{LWA}} \quad (3\text{-}2)$$

where M_{LWA} is the mass of lightweight aggregates, C_f is the cement factor or cement content in kg/m^3, CS is the chemical shrinkage, α_{max} is the maximum expected degree of hydration (0-1), S is the degree of saturation (0-1) and Φ_{LWA} is the aggregates absorption.

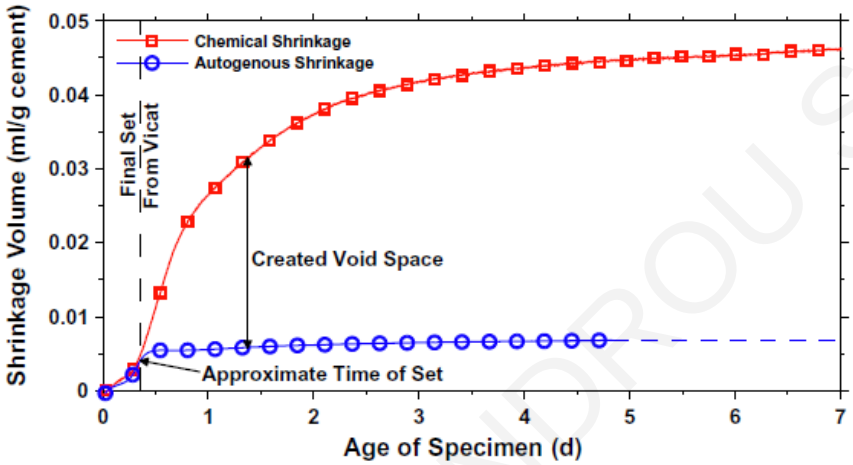

Figure 3-3: Chemical and Autogenous shrinkage diagram (Henkensiefken *et al.*, 2008)

In an effort to estimate the effect of size and quantity inclusion, Akcay *et al.*, 2009, performed optimization of crushed natural pumice LWA to three normal weight aggregate replacements (10%, 20% and 30%), including two different fractions (2-4 mm and 4-8 mm). The LWA had a WA_{24} approximately 34% and were added to the mixture in SSD state. The specific research focused mainly on the mechanical and fracture performance of the specimens. More specifically, compressive strength, static elastic modulus, splitting tension and fracture energy were calculated at 28 days. Moreover, the reduction of autogenous shrinkage was one of the optimization parameters and the specific test was conducted on concrete prisms. The authors concluded that the lower fraction was more effective in reducing concrete autogenous shrinkage. It was also reported that the compressive strength was inversely proportional to the replacement percentage. The fracture properties of the specimens were increased when the mean particle size (LWA) was decreased.

Zhutovsky *et al.*, 2004 reported that the parameters governing the efficiency of IC system including LWA were the aggregates fraction and porosity. Although it was mentioned that the LWA (pumice) replacement necessary to fully diminish autogenous shrinkage was so high that the compressive strength reduction was inevitable. Zhutovsky *et al.*, 2004 concluded that the optimum fraction and

PERICLES ALEXANDROU SAVVA

replacement percentage of LWA to NWA was of great significance in order to reduce autogenous shrinkage without compromising compressive strength.

Byard et al. conducted an examination of fine LWA (expanded shale, shale and slate) IC on 10 different concrete mixtures with three w/c ratios (0.42, 0.36 and 0.30) (Byard, Schindler and Barnes, 2012). The aggregates were added to the mixture in SSD state. A crucial prerequisite towards calculating the required IC water is the knowledge of chemical shrinkage of the cement paste. The calculation of chemical shrinkage was conducted using ASTM C1608 (Zhang *et al.*, 2013). The calculation of autogenous shrinkage was conducted in isothermal conditions. Concrete was cast in rigid cracking framing in order to restrict shrinkage and to calculate the developed stress. Additionally, degree of hydration, compressive strength, splitting tensile strength and static modulus of elasticity were calculated at the age of 0.5, 1, 2, 3, 7 and 28 days. The results showed an increased degree of hydration due to IC. An increase of compressive strength in IC specimens was also exhibited and attributed to the increased degree of hydration and stronger bond between the LWA and cement paste. Autogenous shrinkage and the consequent restrain stress were fully diminished using IC. The high LWA replacement percentage led to a reduced static modulus of elasticity. The authors attributed the delay of early-age cracking formation to the increased tensile strength, the reduction of the autogenous shrinkage and modulus of elasticity.

Zhutovsky et al. examined the effect of LWA (pumice) IC on concrete durability properties. The specific investigation included resistance to chloride penetration, air permeability, water absorption, autogenous shrinkage, drying shrinkage and mass loss on high performance concrete with w/c ratios varying from 0.21 to 0.33 (Zhutovsky and Kovler, 2012). They concluded that the effect of LWA IC on high performance concrete was not detrimental. It was reported that the air permeability was reduced at late ages whereas the sorptivity and mass loss increased. They attributed the sorptivity and mass loss increase to the porosity increase. An improvement of resistance to chloride penetration in high w/c ratio mixtures was also observed.

Henkensiefken et al. examined the effect of IC, using LWA, on concrete fluid transport properties such as water absorption and diffusivity (Henkensiefken, Castro, *et al.*, 2009). In agreement with other researchers (Bentur, Igarashi and Kovler, 2001; Byard, Schindler and Barnes, 2012), they concluded that IC increased the degree of hydration. They stated that the increased degree of hydration which led to a denser microstructure reduced the material's sorptivity (46%) and electrical conductivity (53%) and increased the ITZ density. The specific experiments were conducted on various w/c ratios (0.25, 0.30, 0.35, 0.40) using different LWA replacements (11.0% and 23.7%) whereas the LWA were

PERICLES ALEXANDROU SAVVA

added to the mixture in a dry state. It has to be mentioned that based on ACI IC report published in 2013, the SSD state of the LWA is of crucial importance since the time that each type of aggregates needs to reach SSD varies based on its absorption capacity and surface condition (ACI Committee 308 and 213, 2013). The addition of LWA in an under SSD state may increase – or not sufficiently decrease - the autogenous shrinkage and creep (ACI Committee 308 and 213, 2013).

Cusson *et al.*, 2010 conducted a large scale experiment to assess the performance of LWA IC on high performance concrete bridge decks. It was reported that IC may extend the service-life of high performance concrete for more than 20 years as opposed to conventional concrete and over 40 years for IC including supplementary materials. The specific finding was attributed to the reduction of early-age shrinkage cracking which yields in reduced chloride ions penetration and diffusion. Bridge decks exposed to severe environments (especially snow) suffer a decrease in their service-life due to de-icing agents (salt). The authors conducted a life-cycle cost analysis regarding the aforementioned experiments, where the results revealed a 40% reduced cost for employing high performance concrete instead of conventional concrete in bridge decks and a 63% reduced cost for utilizing IC high performance concrete instead of conventional concrete. The reduction in cost occurred due to the longer service-life and less maintenance required. Additionally, no early-age cracking, increased compressive strength and decreased chloride permeability, freeze-thaw resistance and salt scaling resistance were observed for the IC high performance concrete mixtures.

Collins and Sanjayan added pre-saturated LWA (blast-furnace slag WA_{24} 4.4%) in alkali-activated slag concrete in order to examine the effect of IC (Collins and Sanjayan, 1999). They concluded that the compressive strength measured using cylindrical specimens (100 mm diameter and 200 mm length) was increased for specimens exposed to drying conditions (22ºC and 50% RH) as opposed to water cured and non-IC specimens. The increase in compressive strength was attributed to the IC effect that led to increased degree of hydration, reduced microcracks and moisture content. Additionally, they observed a significant reduction in drying shrinkage (40%) in contradiction with NWA (alkali activated Slag-Basalt) mixtures.

Wasserman and Bentur stated that two similar concrete mixtures (same w/b ratio) including different LWA with the same compressive strength, will not necessarily observe similar compressive strength (Wasserman and Bentur, 1996). The specific observation was associated with the physical and chemical characteristics of the aggregates that affects the mixtures' ITZ, that partly affects the compressive strength. They specifically mentioned that the higher absorption of LWA led to higher cement paste absorption that reduced the water concentration on the specific region yielding in a

PERICLES ALEXANDROU SAWA

denser ITZ. The chemical effect occurred in a later age where a pozzolanic reaction between the aggregate and the alkaline pore solution and $Ca(OH)_2$ impregnated the aggregates pores, resulting in an increased compressive strength.

Lura and Bisschop studied the effect of eigenstrain in LWA concrete and the resulting eigenstress field caused by autogenous and drying shrinkage (Lura and Bisschop, 2004). Three concrete mixtures with SSD LWA were developed. Their difference lied on the LWA fraction size. Liapor 8-16 mm, 4-8 mm and 0-4 mm were employed and the WA_{24} was 18%, which corresponded to 80% of their long-term absorption. The tests focused on the material moisture loss, autogenous and drying shrinkage accompanied by the resulting microcracking. The cement paste modulus of elasticity development was measured. The authors expected to observe a de-bonding of cement paste and LWA due to the early-age paste expansion and LWA shrinkage due to moisture loss. However, no de-bonding was observed due to the low stress exhibited by the cement paste accompanied by the low restrain and high absorption of the LWA that yielded in high quality bond between the LWA and cement paste. Additionally, the drying shrinkage cracking of composites containing LWA was less pronounced than in the NWA mixtures. The reason was the lower modulus of elasticity of LWAs that led to a poorer internal restrain. It is understandable that the aforementioned mechanism allocates additional bulk shrinkage. The lower elastic modulus, strength and the high quality bond may cause the LWA fracture. The specific observation was verified using a micrograph section presenting the crack propagation through a Liapor LWA grain (Figure 3-4).

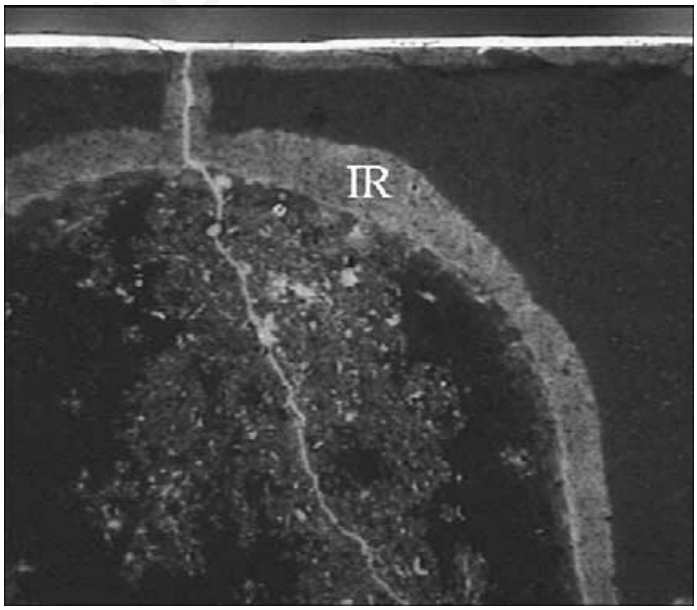

Figure 3-4: Micrograph of crack propagation through a Liapor LWA grain (Lura and Bisschop, 2004)

PERICLES ALEXANDROUSAKIS

Lura et al. conducted an overview of existing experimental works (2005) to evaluate the most prominent and the most insignificant effect of IC in concrete (Lura, Jensen and Igarashi, 2007). They stated that IC has a direct impact on the material's internal RH, degree of saturation and sorption isotherm curves, which in turn affect the material's degree of hydration and autogenous shrinkage. In following, increased degree of hydration and reduced autogenous shrinkage led to improved mechanical properties, porosity, pore size distribution, improved ITZ, reduced self-induced stress and cracking and improved durability indicators. All of the above were considered as a secondary effect exhibited due to the increased degree of hydration and reduced autogenous shrinkage. It was stated that excessive IC mediums utilization may result in a controversial effect on the material. It was suggested that although shrinkage reduction may occur due to large amount of IC agents within the mixture, it will probably lead to reduced modulus of elasticity resulting in increased shrinkage.

Craeye and Schutter developed a vertical configuration for the measurement of autogenous shrinkage (Craeye and Schutter, 2006). They employed two methods of IC, namely LWA (type 1: crushed expanded clay > 2mm, type 2: rounded expanded clay > 4mm) and SAP. The mixture was manufactured with a w/b ratio 0.32 with 475 kg/m^3 cement and 25 kg/m^3 silica fume. A reduction in autogenous shrinkage was observed in the IC mixtures accompanied with a substantial reduction of compressive strength in the order of 20%.

Zhutovsky and Kovler published an experimental research where the effect of LWA IC mediums on the material's strength and durability properties was evaluated (Zhutovsky and Kovler, 2010). The authors focused on the evaluation of durability indicators. Experiments such as resistance to chloride penetration, air permeability, water absorption, drying shrinkage and mass loss were conducted on high performance concrete mixtures with w/c ratios varying from 0.21-0.33 (0.21, 0.25, 0.33). The objective was to quantify the IC impact on high performance concrete as a function of the w/c ratio. The LWA was vacuum saturated pumice with fraction 2.36 mm and 4.75 mm and vacuum WA 73.1%. The researchers concluded that the material's durability performance was not seriously degraded due to the LWA employment. The air permeability of IC mixtures was reduced at later ages, whereas the sorptivity and mass loss were increased due to an increase observed in the total porosity (3-4%). The effect of w/c ratio was manifested in the resistance to chloride penetration tests. The lower w/c ratio IC and reference mixtures observed similar behavior and the higher w/c ratio mixtures observed an improvement. They concluded that IC was beneficial for mixtures with lower w/c ratio. However, it did not result in a perceptible improvement of durability.

PERICLES ALEXANDROUSAKIS

Radlinska et al. compared the effect of shrinkage reducing admixtures as opposed to LWA for mitigating shrinkage in concrete (Radlinska *et al.*, 2008). The evaluation yielded through experimental and theoretical considerations regarding the materials behavior in sealed and unsealed conditions. An unsealed concrete specimen undergoes drying shrinkage and self-desiccation simultaneously as opposed to sealed specimens that experience only self-desiccation. For the comparison purposes, three mixtures were conducted with constant w/c (0.30). The shrinkage reducing admixtures were added as water replacement (5%) and the LWA (rotary kiln expanded shale, WA_{24} 10.5%) were added as a 40% volume replacement of sand. The experiments included restrained and unrestrained volume change measurements and internal RH measurements. It was concluded that shrinkage reducing admixtures reduced shrinkage through capillary pressure-surface tension reduction, while LWA reduced shrinkage by restoring capillary pressure through supplementary water provided. Both systems observed an increased RH value during the early-age (1% for shrinkage reducing admixtures and 10% for LWA). Regarding mass loss measurements for the unsealed systems, it was concluded that both shrinkage reducing admixtures and LWA systems observed a greater loss at equilibrium. Finally, both systems observed a reduction in cracking potential.

In another research work, Mousa et al. conducted two different experimental works to evaluate the effect of two different IC agents on the physical and mechanical performance of concrete (Mousa *et al.*, 2014a, 2014b). More specifically, pre-soaked LWA (leca) at different sand replacement percentages (10%, 15% and 20%) and polyethylene-glycol with various cement replacements (1%, 2%, 3%) were utilized for the specific experiments. Additionally, the cement content, the w/b ratio and the silica fume content varied (300, 400 and 500 kg/m^3, 0.50, 0.40, 0.30 and 15% silica fume addition as replacement to cement weight, respectively). In order to evaluate the physical or durability properties, the authors conducted experiments of mass loss, permeability, volumetric water absorption and sorptivity. For the mechanical properties, compressive strength, indirect tensile strength, flexural strength and modulus of elasticity tests were conducted. The conclusions indicated that the IC mixtures observed an improvement as opposed to the control mixtures, in both mechanical and durability performance. The improved behavior was attributed to the enhanced degree of hydration which ultimately yielded into a more compact/less porous microstructure. A reduction in permeability was observed. However, it was mentioned that excessive usage of IC may result in deteriorated mechanical and durability properties. The specific argument was reflected on the sorptivity and the mass loss experiments for LWA 20% mixtures where an increase was observed in the aforementioned properties. An improvement on the physical properties was observed when poly-ethylene glycol was

PERICLES ALEXANDROU SAVVA

utilized for IC. The addition of silica fume had a beneficial effect, due to reduced mass loss. The authors concluded that the optimum amount of LWA for the specific research was 10%, whereas the optimum chemical agent (poly-ethylene glycol) content was 1%. Comparing the two, poly-ethylene glycol seemed to exhibit superior performance compared to LWA. The same conclusions were also drawn for the mechanical properties, nonetheless the optimum percentage of IC agents was 2% for poly-ethylene glycol and 15% for LWA. Regarding the silica fume addition, the authors mentioned an improvement in the properties. The main conclusion regarding the indirect tensile strength, the flexural strength and the modulus of elasticity was the good correlation of the results with the corresponding values of compressive strength.

Henkensiefken et al. used Pickett's model to determine the shrinkage of the cement paste of a mortar (w/c 0.30, Cement 1228 kg/m^3) containing different volume replacements (7.3%, 14.3%, 25.3%) of LWA (rotary kiln expanded shale aka Kenlite, WA_{24} 10.5%) to NWA (Henkensiefken *et al.*, 2008). Autogenous shrinkage using the corrugated tube method (Mejlhede Jensen and Freiesleben Hansen, 1995) was conducted along with internal RH and growth temperature measurements. They concluded that the inclusion of sufficient LWA reduces the material's autogenous shrinkage and mortar stiffness. However, stiffness reduction is less significant than shrinkage reduction due to the IC reservoirs.

Browning et al. examined the effectiveness of pre-wetted vacuum saturated LWA (expanded shale) in reducing drying shrinkage (Browning *et al.*, 2011). LWA were employed as partial replacement to NWA at percentages of 8.9% to 13.8%. Slag cement was also incorporated as a partial replacement to portland cement at a percentage of 24.1% of concrete volume. Additionally, two types of NWA were employed, namely high-absorptive limestone NWA and low-absorptive granite. The authors observed a minor reduction in the material's density when LWA was utilized, no significant effect on compressive strength and a substantial reduction in shrinkage. Additionally, 30% to 60% of shrinkage reduction was observed when slag cement was utilized regardless of the aggregates. Finally, up to the age of 365 days, drying shrinkage reduction was observed to LWA mixtures as opposed to high and low-absorptive NWA.

Golias et al. examined the influence of the initial moisture content of LWA prior to mixing (Golias, Castro and Weiss, 2012). The aggregates utilized (fine-LWA expanded shale, WA_{24} 17.5% by dry mass, 22.5% vacuum saturated) were pre-conditioned and added to the mixtures in oven-dried state, 24hours pre-soak and vacuum saturation. Eight mixtures with 0.30 w/c ratio, 728 kg/m^3 cement and varying LWA and IC water were manufactured. The experiments focused on the degree of hydration, compressive strength, internal RH, autogenous shrinkage, water sorptivity and LWA desorption

PERICLES ALEXANDROU SAWA

properties. It was reported that when LWA were added in the oven-dried state they absorbed a substantial amount of water prior to setting and returned it to the system through the IC mechanism. This specific amount of water had to be pre-estimated in order to avoid intense self-desiccation phenomena in the early-hours. It was reported that the vacuum saturated LWA were not effective for IC because the majority of the IC water was held in smaller pores and great underpressure was necessary to withdraw the specific amount of water.

Bentz focused on comparing the ITZ for IC LWA mixtures to NWA concrete ITZ, in terms of chloride ion diffusivity (Bentz, 2009). One LWA (expanded shale, WA_{24} 22%) IC mortar mixture was prepared with 0.40 w/c ratio where the LWA were added in a SSD state. The mixtures were tested at 28, 56, 180 and 365 days and the chloride penetration depth was calculated on crushed specimens sprayed with silver nitrate ($AgNO_3$) with the use of image analysis software. It was concluded that the employment of IC had a beneficial effect on ions diffusion within the mixture. The improvement was attributed to the ITZ depercolation and the increased degree of hydration that yielded in a denser microstructure. The fact that LWA concrete observed better ITZ quality due to LWA absorption was verified. Bentz, 2009 supported that the ITZ in the case of LWA exhibited less volume as shown in Figure 3-5. It was stated that percolated ITZ has a large influence on the material's transport properties.

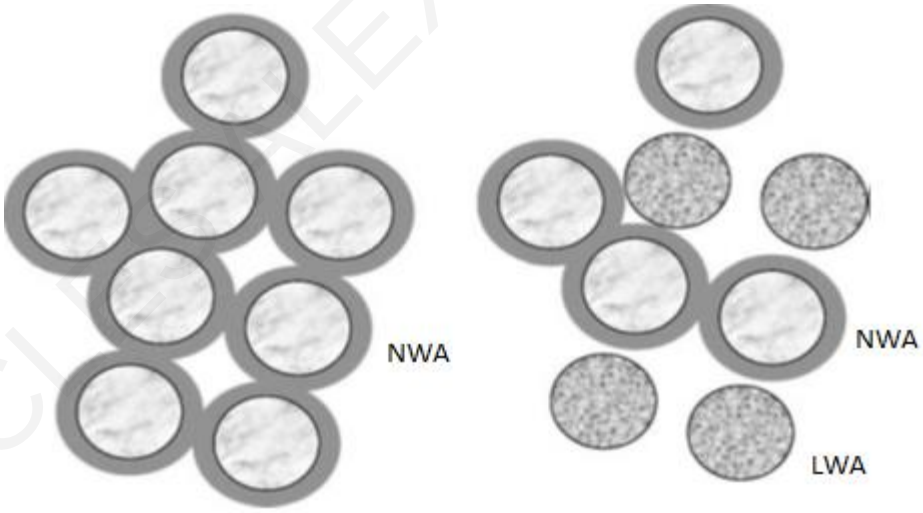

Figure 3-5: NWA ITZ (left) – LWA/NWA ITZ (right) (Bentz, 2009)

Sun et al. examined the IC effects on the microstructure and permeability of ITZ (Sun *et al.*, 2015). Scanning electron microscope (SEM) imaging, transport simulation and hydration modelling techniques were employed to evaluate mortar samples including saturated LWA (expanded shale, WA 14.26%) for IC and plain mixtures (only NWA). The mixtures were characterized by a low w/c ratio

(0.35) in order to intensify the autogenous shrinkage and increase the demand for IC. It was concluded that the IC had a great impact on the material's ITZ microstructure. A permeability solver code (developed in the National Institute of Standards and Technology in the US) was adopted to evaluate the total porosity, the percolated porosity and the permeability of 3D digital samples. The specific solutions verified that the permeability of the IC mixtures was reduced in the specific sections due to pores depercolation and smaller characteristic pore size. Additionally, the authors developed a chemo-thermo-hydraulic model to evaluate the ITZ development process including water transport, heat generation and CSH growth. It was clarified that the utilization of advanced imaging and holistic simulations could picture the development of ITZ and the IC effect in the specific zone.

Husem examined the bond strength between LWA and cement paste and LWA and mortar (Husem, 2003). More specifically, compressive and flexural strength experiments were conducted in an effort to evaluate the quality of the bond on LWA (Biotite-dasitic tuff, WA 14% and 17% for fractions >4mm and <4mm respectively) and NWA (dasitic tuff) mixtures (w/c 0.50). The aggregates mechanical properties were evaluated prior to mixing, in an effort to predict the mixtures corresponding properties. The LWA exhibited a compressive strength of 39.4 MPa and a modulus of elasticity of 4.76 GPa as opposed to the NWA values of 73.4 MPa and 60.0 GPa respectively. Husem concluded that the bond strength of LWA-mortar was less than of NWA-mortar as opposed to LWA-cement paste to NWA-cement paste. The specific observation was attributed to the LWA porosity that enabled cement paste penetration within its structure resulting in a better bond. The mortar viscosity in addition to the pores blocking due to the sand particles are the reasons why mortar is not that efficient in LWA-mortar penetration resulting in a lower quality bond. In terms of compressive strength, the LWA mixture exhibited lower value than the NWA mixture and the cement paste. The flexural behavior of the specific mixtures was slightly improved as opposed to the cement paste yet lower than the NWA mixture.

The effect of internal RH in IC concrete mixtures was studied by Han et al. (Han *et al.*, 2014). The experiments were performed on concrete slabs cured in room environment, where the RH was monitored up to the age of 28 days. The RH behavior was divided in two discrete phases, where the first stage was characterized by a stable RH level (~100%) and the second stage considered the RH reduction. The specific research employed a digital resistance based RH monitor with 3% accuracy, thus the RH drop due to salts dissolution (~3%) did not appear. The specific experiment was conducted using pre-soaked LWA (fly ash based, WA_{7d} 21%, 2.5 mm-6.5 mm) and w/b ratio 0.33. The authors reported that the LWA average pore size was ~100 μm which is preferable for IC. The conclusions

PERICLES ALEXANDROU SAVVA

drawn included a relation between the shrinkage strain of concrete to the pore humidity where an inverse proportionality was observed. Additionally, RH stage one seemed to be prolonged with the addition of LWA which was followed by a reduction of moisture loss (increased RH) in stage two. More specifically, the RH reduction in high performance concrete was 46.5% as opposed to 26.2% for medium LWA replacement and 7.9% for high IC replacement (28 days' age). The last observation was a steeper moisture gradient along the thickness of the slabs for non IC slabs.

Kim *et al.*, 2014 proposed an IC technique using coal bottom ash aggregates. Two different fractions were utilized, namely 0-2 mm and 2-5 mm, whereas 0-2 mm expanded shale was also employed. The w/c ratio of the mixtures was 0.30 where 25% and 50% partial replacement to NWA was conducted. The specific research focused on the chloride diffusion coefficient which was evaluated by measuring the diffusion distance through steady-state and rapid-state penetration tests. Kim et al. conducted X-ray diffraction analysis to detect the crystalline phase of hydration products that could bind chloride. Additionally, electron probe micro analyzer was used to analyze the path of chloride penetration. Porosity and capillary water absorption tests were also conducted on specimens at the age of 28 and 91 days. They concluded that the effect of coal bottom ash in high strength concrete was minor in the diffusion length. However, a significant decrease in the amount of chloride diffusion was observed. They reported that the relationship between concrete porosity and pore connectivity seems to be (merely) affected by the inclusion of this type of aggregates. The specific result led to the conclusion that the pozzolanic reaction of the coal bottom ash did not exhibit a great effect on the pore system.

Iffat, Manzur and Noor, 2016 investigated the possibility of including LWA in concrete to replace external curing, in an effort to reduce the risk of insufficient curing due to the human factor. The authors examined different w/c ratios, LWA replacements and curing conditions. It was concluded that the mixture with 20% replacement of normal aggregates with LWA when covered with polythene sheet exhibited similar water and chloride permeability with a sufficiently cured normal aggregate mixture. The authors suggested that the polythene sheet contributed to the effectiveness of IC.

Zhutovsky and Kovler, 2017 attempted to evaluate the effect of different w/c ratios (0.33, 0.25 and 0.21) on concrete mixture's total shrinkage. The authors conducted various tests on the restrained drying shrinkage, strength, free drying shrinkage and mass loss of concrete mixtures. It was concluded that the w/c ratio had a strong impact on the material's cracking potential. Internally cured mixtures manufactured with w/c ratio lower than 0.30 exhibited lower crack sensitivity and lower drying shrinkage. The reduction of w/c ratio resulted in increased free shrinkage, which was compensated

PERICLES ALEXANDROU SAVVA

with IC. Internal curing had an adverse effect on the compressive strength at early ages that diminished with age. Similar observations were made for tensile splitting strength.

Li et al. examined the possibility of combining internal curing with expansive agents in order to mitigate concrete shrinkage under variable temperature (Li *et al.*, 2017). The authors observed that IC contributed to a reduction in shrinkage. The addition of expansive agents increased the specific action. However, the employment of expansive agents resulted in decreased mechanical properties, which was compensated when expansive agents and LWA were combined. The authors reported an increase in compressive strength and a slight reduction in modulus of elasticity at early-ages.

3.5.1.5. LWA mixtures containing supplementary materials

Regarding fly ash in concrete, Deo and Pofale stated that the water absorbed from the fly ash (WA 16%) was possible to be utilized back to the mixture through an IC mechanism (Deo and Pofale, 2015). In other words, the fly ash itself would be the water reservoir for IC. The fly ash replacement was 25% and the CaO content derived from the chemical analysis was 1.02%, thus class F, without inherent cementitious properties. The authors prepared five different mixtures with constant w/c ratio (0.32) and cement content (450 kg/m^3), varying in fly ash and superplasticizer (SP) content. The experiments included compressive strength, flexural strength, and ultrasonic pulse velocity (UPV) measurements. It was concluded that the addition of fly ash led to better packing and less voids in the mixture. The compressive and flexural strength observed a 15% and 28% increase for mixtures without and with SP respectively. It was also suggested that IC using fly ash could reduce the amount of the microcracks in concrete.

3.5.1.6. Drawbacks of internal curing using LWA

Drawbacks of LWA employed for IC include a preliminary deliberation of IC water which may lead to increased slump, increased w/b ratio (Zhutovsky, Kovler and Bentur, 2002), decreased mechanical and durability properties and poor IC effect. The highly porous LWA after being emptied may act as porous paths for deleterious substances to ingress the mixture (De La Varga *et al.*, 2014). The premature IC water release occurs because the water in LWAs is physically held (Jensen and Lura, 2006) and excess mechanical vibration may overcome the bonds holding the water within LWAs structure. Other issues that may arise include a density and modulus of elasticity decrease, increased porosity, permeability, sorptivity, diffusivity and coefficient of thermal expansion (Bentur, Igarashi and Kovler, 2001; Zhutovsky and Kovler, 2010; Byard, Schindler and Barnes, 2012; ACI Committee 308 and 213, 2013). Jensen mentioned that the major problems of mitigating self-desiccation using

PERICLES ALEXANDROU SAWA

LWA is the inconsistency and the significant reduction in strength and elastic modulus (Jensen and Hansen, 2001). One of the dominant challenges regarding the employment of LWA in concrete is to achieve the required balance between the various properties performance. In general, LWA IC technique is strongly dependent on the physical properties of the LWA medium employed. The specific method is quite delicate. Therefore, a proper design of the content, fraction and handling of the mixture is of vital importance.

3.5.2. Superabsorbent polymers

3.5.2.1. Principles and basic experiments

Ole Jensen and Per Freiesleben Hansen were the first researchers to introduce the idea of IC using superabsorbent polymers (Jensen and Hansen, 2000). The specific research was aiming to discuss a new concept for the prevention of self-desiccation in hardened cement pastes. The authors recognized that the addition of SAP in the mixture would lead to additional macropore induction. Jensen and Hansen employed the phase distribution of a hydrated cement paste developed by Powers in 1948 (Powers and Brownyard, 1947) and modified it to take into account the voids and hydration products yielded from IC. The authors concluded that the mitigation of self-desiccation without impairing strength and durability was possible. They also highlighted the importance of self-desiccation within a cementitious system due to the strain ability of the material at early-ages.

Jensen and Hansen extended their theoretical observations to experimental developments in order to verify the conclusions regarding the SAP applicability and effectiveness (Jensen and Hansen, 2002). A mortar mixture with effective w/b ratio 0.30 (20% silica fume replacement with respect to cement mass) was developed and two different types of SAP at a percentage of 0-0.60% with respect to cement mass were employed. The IC water was calculated to be added as w/c_{IC} 0.05, according to the SAP absorptivity. The first type of SAP were suspension polymerized spherical with 200μm average size and the second was a crushed solution-polymerized ranging from 125μm to 250μm. Restrained ring test was employed to determine the cracking susceptibility of the mortars and the autogenous shrinkage was determined using the dilatometer method developed in 1995 by Jensen and Hansen (Mejlhede Jensen and Freiesleben Hansen, 1995). It was concluded that the SAP were able to fully diminish autogenous shrinkage of a cementitious composite. However, since the SAP addition implied additional porosity a reduction of mechanical properties was expected. The authors mentioned that a fully compensation of autogenous shrinkage may not be necessary. It was proposed that a cross matching of the autogenous shrinkage curves with the restrained test results would provide

PERICLES ALEXANDROU SAVVA

information about the optimum SAP percentage in order to avoid early-age cracking. Additionally, the authors proposed an optimum SAP particle size range at approximately 100μm, in order to ensure full utilization of the IC water and adequate active surface zone. Finally, the authors observed that the addition of 0.30% and 0.60% SAP in the mortars reduce the autogenous shrinkage and their crack susceptibility.

Mechtcherine et al. recognized the damage that autogenous shrinkage can cause, especially on low w/b ratio composites where the phenomenon intensifies (Mechtcherine *et al.*, 2006). A particular mixture was designed for a pavilion built situated in Kaiserslautern for the FIFA World cup 2006 hosted by Germany. The specific mixture was developed from the University of Kaiserslautern for the casting of thin-walled slender columns without conventional reinforcement. The specific design had special requirements such as structural performance and fair-face surface. In order to achieve the aforementioned, the mixture developers employed a self-compacting fibre reinforced cementitious composite with low w/b ratio. The research aimed to assess the impact of IC using SAP on the autogenous shrinkage of the specific mixture. The trial w/b ratio varied from 0.24 to 0.31 (cement and silica fume were added to the mixture). The SAP utilized for the specific project were covalently cross linked acrylamide/acrylic acid copolymers, spherical particles yielded from a suspension polymerization with an average particle size of 200μm (swelled diameter about 3 times larger - Figure 3-6). The rheological behavior of the mixture was not compromised with the addition of SAP in addition to improved resistance to bleeding. The authors observed a reduction in autogenous shrinkage and a clear increase in drying shrinkage in the SAP mixtures. The SAP were exhausted after the first week where an increase in shrinkage was observed. Mechanical properties such as compressive, tensile and flexural strength exhibited a decrease as opposed to non-IC mixtures.

In agreement with other researchers (Mechtcherine *et al.*, 2006), Justs et al. mentioned that the addition of water for SAP IC led to increased drying shrinkage (Justs *et al.*, 2015). It was clarified that SAP had a positive effect on total shrinkage in low w/b ratios where autogenous shrinkage was the dominant mechanism. The effect of SAP was greater in the first days of the materials life cycle, since the water held in the reservoirs is mostly exhausted in later ages.

PERICLES ALEXANDROU SAVVA

Figure 3-6: Pore created by exhausted SAP particle (Mechtcherine *et al.*, 2006)

Mönnig and Reinhardt investigated the effect of drying shrinkage on two types of concrete with IC addition (Mönnig and Reinhardt, 2006). More specifically, the mixtures under investigation included dry SAP and pre-soaked LWAs (expanded clay – Liapor F9.5 <4mm, 4-6.3mm, >6.3mm WA_{24} 19.0%, 16.1%, 15.7% respectively). The SAP utilized (PFA 10g/g) were suspension polymerised and had a medium size of approximately 125μm. The reference mixture was designed with a w/c ratio 0.36, where another mixture without IC was designed with 0.42 w/c ratio. The latter mixture corresponded to the reference mixture (0.36) plus the IC water (0.06), without the IC mediums. The experiments included drying shrinkage, compressive strength and porosity. A reduction in drying shrinkage was observed during the first week in the SAP mixtures. The specific finding was attributed to the water binding and the paste densification. An increase in the compressive strength after the age of 28 days was observed.

Piérard et al. conducted an experimental research to evaluate the effect of water inclusion employing various percentages (0.30% and 0.60%) of SAP (0.9NaCl in demineralised water absorption 65g/g) on concrete properties (w/b ratio 0.33, 427.5kg/m^3 cement and 22.5kg/m^3 silica fume) (Piérard, Pollet and Cauberg, 2006). Autogenous, drying shrinkage and compressive strength tests were conducted. A comparison of the specific technique with existing methods such as shrinkage reducing admixtures and expansive agents was conducted. The researchers continuously monitored the internal RH and the temperature change during the mixtures maturing period. The results indicated an autogenous shrinkage reduction of IC mixtures up to the age of 2 months. The replacement of cement with 0.60% of SAP by mass resulted in a 66% reduction after the age of 6 days. On the other hand, a negative impact on the materials workability, setting time and early-age compressive strength was observed in SAP-IC mixtures. The authors, in agreement with other researchers (Jensen and Hansen, 2002),

PERICLES ALEXANDROU SAVVA

suggested a compromise between autogenous shrinkage reduction and mechanical/durability properties deterioration, by employing an optimum amount of SAP. It was suggested that the autogenous shrinkage could be minimized to prevent early-age cracking but not fully compensated if there is no necessity. It is therefore obvious that an increase in the SAP amount added to the mixture proportionally damage mechanical/durability properties. Furthermore, it was verified that the addition of SAP did not diminish the demand for external curing, since drying shrinkage in the specific mixtures observed an increase. The specific finding was in agreement with other researches described above (Mechtcherine *et al.*, 2006; Justs *et al.*, 2015). The efficiency in autogenous shrinkage reduction for shrinkage reducing admixtures was similar to the 0.30% SAP mixtures (30-40% compared to the reference mixture) whereas their compressive strength reduction was identical. It concludes that the CaO-based expansive agent was the most efficient regarding the autogenous shrinkage reduction.

Craeye et al. conducted a finite element simulation along with concrete mixtures testing in order to establish an optimum SAP content where maximum autogenous shrinkage reduction along with minimum compressive strength decrease will occur (Craeye, Geirnaert and Schutter, 2011). The simulations included the thermal stresses development due to heat of hydration. The experimental work included fresh properties examination (slump, flow and density), mechanical properties (autogenous shrinkage, basic creep, modulus of elasticity, compressive strength and tensile strength) and thermal properties (hydration heat production). The authors reported that autogenous shrinkage reduction was achieved using SAP, due to a swelling gradient developed in the early-age which was higher based on the SAP percentage. However, autogenous shrinkage was not fully diminished. The addition of SAP led to compressive strength and modulus of elasticity reduction whereas a higher addition of SAP led to a higher creep deformation. The heat development in the case of SAP was also increased in terms of rate and magnitude.

Igarashi and Watanabe conducted an experimental work to examine the reduction of autogenous deformation by SAP-IC (Igarashi and Watanabe, 2006). The authors conducted free and restrained shrinkage tests, SEM – backscattered electrons image analysis, SAP spacing factors, compressive and splitting tensile strength measurements. It was reported that the addition of SAP reduced but not fully compensated the autogenous shrinkage in cement paste, even when additional amount of polymers was employed, implying that the relation between SAP amount and shrinkage reduction is not linear. Additionally, a reduction in the macropores diameter was observed. The degree of hydration was not significantly affected by the presence of SAP, especially in the early-ages. The authors estimated that the protected paste due to SAP could not exceed one millimeter, where a dense microstructure would

PERICLES ALEXANDROU SAVVA

reduce even more the specific value. Additionally, a decrease of the materials strength was observed due to SAP addition. The authors highlight the importance of optimizing the fraction of SAP driven by the optimum spacing factor between them.

Reinhardt and Mönnig attempted to evaluate the effect of LWA and SAP on critical material parameters (Reinhardt and Mönnig, 2006). The utilized LWA were expanded clay (Liapor F9.5 <4mm, 4-6.3mm, >6.3mm WA_{24} 19.0%, 16.1%, 15.7% respectively) whereas two types of SAP were employed. The researchers attempted to predict the influence of LWAs and SAP using the DuCOM software (Maekawa, Chaube and Kishi, 1999). It was concluded that the most important aspect regarding SAP were their particle size distribution and water absorption capacity. The compressive strength conducted on IC mortars suffered a slight reduction.

Lura et al. conducted an overview of experimental methods able to describe and evaluate IC and its consequences (Lura, Jensen and Igarashi, 2007). It was mentioned that a direct evidence of IC mechanism activation is the internal RH of the mixture, the degree of saturation and the sorption isotherms. The first consequences were the degree of hydration, the water movement and the autogenous shrinkage, whereas the mechanical properties, the porosity and pores size distribution, the ITZ, the self-induced stress/ cracking and the durability were considered as secondary effects of IC.

Reinhardt et al. conducted an experimental work to compare the effectiveness of SAP on durability indicators, as opposed to conventional air-entrapping agents (Reinhardt, Assmann and Mönnig, 2008). The specific agents are utilized in concrete mixtures to provide space for water expansion, when the concrete casting takes place in cold environmental conditions (below 0ºC). The effect of two different types of SAP (suspension polymerized covalently cross-linked acrylamide/acrylic acid copolymers varying in particles fraction and water absorptivity) and LWA on mortar was evaluated. The mortars were developed with 450kg/m^3 cement in two reference mixtures. The IC mixtures had a w/c ratio of 0.42 (w/c0.36 + w/c_{IC}0.06) and the reference mixtures were conducted with both w/c ratios (0.36 and 0.42). The experimental measurements included compressive strength, tensile strength, modulus of elasticity, drying shrinkage, mercury intrusion porosimeter, freeze thaw resistance, chloride migration and water absorption. The authors concluded that the mixtures with SAP addition performed better than the air-entrapping agent mixtures in freeze and thaw resistance, water absorption and chloride migration experiments. The specific observations were attributed to the microstructure densification occurring due to internal water supply from SAP. It was concluded that the addition of SAP caused slight decrease on mixtures compressive strength, a more pronounced decrease on tensile strength and retardation on drying shrinkage.

PERICLES ALEXANDROU SAWA

Craeye and Schutter employed LWA and SAP (100μm to 800μm) in order to assess the effectiveness of a proposed dilatometer towards measuring autogenous shrinkage (Craeye and Schutter, 2006). Regarding the IC agents, the authors concluded that both LWAs and SAP effectively reduce autogenous shrinkage. However, a clear reduction in strength was observed.

Dudziak and Mechtcherine reported the effectiveness of SAP (suspension-polymerised spherical particles of average size 150 μm) towards reducing autogenous and plastic shrinkage (Mechtcherine *et al.*, 2006). The specific research included two different cement pastes where the first was developed with 0.352 w/c ratio and the second that included IC agent (0.60% SAP by mass of cement) with w/c ratio 0.265. Eight mixtures with various amounts of SAP and one reference mixture were conducted with varying cement content. Plastic deformation, autogenous shrinkage, restrained ring test, Vicat needle (setting time), compression tests and density were the experiments employed to estimate the mixtures' properties. Their experiments on restrained and free shrinkage indicated that SAP IC reduced the mixtures' early-age cracking caused by shrinkage. They concluded that the amount and state of added SAP were the governing factors that determined their impact on the mixtures' performance and properties development. They also reported that the SAP cause retarded setting time and additional porosity that may lead to early-age decreased compressive strength.

Hasholt et al. conducted an extended experimental research comprised of 15 concrete mixtures with 3 different w/c ratios (0.35, 0.40 and 0.50) and SAP (suspension-polymerized covalently cross-linked acrylamide/acrylic acid copolymer) addition to examine the compressive strength of the mixtures (Hasholt, Jespersen and Jensen, 2010a). The experiments included compressive strength, air content and degree of hydration measurements. The authors mentioned a relation between concrete and paste compressive strength, paste strength dependence on gel/space ratio suggested by Powers. They observed that the influence of air voids introduced from SAP on compressive strength could be evaluated in the same way that air content is taken in account using Bolomey formula. It was concluded that the medium SAP addition in low w/c ratio mixture (<0.40) enhanced the degree of hydration yielding in increased compressive strength at late ages, whereas high SAP addition in high w/c ratio mixtures (>0.45) did not increased degree of hydration enough to compensate the additional porosity and consequently reduced the compressive strength. The specific effect stands also for low w/c ratio mixtures at early ages and at high SAP addition. It was also mentioned that according to the modelling results (Powers and Bolomey) the net effect of SAP depended on the mix design and age of the mixture.

PERICLES ALEXANDROU SAVVA

In another work, Hasholt et al. attempted to evaluate the effect of SAP on concrete modulus of elasticity (Hasholt, Jespersen and Jensen, 2010b). The authors separated the mixture in three distinctive phases, namely aggregates, cement paste and air voids. It was mentioned that the addition of SAP changed the elastic properties of the mixtures' because they affected both cement paste and air voids. The authors stated also that the empirical relationships linking various mechanical properties of concrete such as modulus of elasticity and compressive strength given in various codes, cannot apply to mixtures including SAP. At any given moment similar or identical mixtures with and without SAP may observe different properties and the main issue of established empirical models is the air void content. SAP led to increased compressive strength and reduced modulus of elasticity at the same instance. Therefore, the results from an existing empirical model would be misleading. The authors concluded that the mixtures' separation to three different phases promoted the prediction of elastic behavior for mixtures including SAP.

Justs et al. examined the effect of SAP on ultra-high performance concrete (w/c ratio<0.25) (Justs *et al.*, 2015). Solution-polymerized SAP were employed and SEM analysis indicated that SAP cavities were partially filled (over 50%) with portlandite during the process of hydration. For the experiments, solution-polymerized SAP of <63μm particles size were utilized. It was also reported that the hydration peak was shifted and the degree of hydration was increased. However, a decrease on the mechanical properties was observed. The authors reported an autogenous shrinkage reduction of approximately 400 μm/m and compressive strength 149 MPa at the age of 28 days (lower than the corresponding without SAP).

Shen et al. investigated extensively the effect of SAP on the internal RH of concrete (Shen *et al.*, 2015b). Four mixtures were manufactured including a reference mixture and three mixtures including SAP as a replacement to cement (0.05%, 0.15% and 0.25%). The authors concluded that the internal RH was increased proportionally to the IC water increase for sealed and unsealed specimens. Additionally, comparing the sealed and unsealed specimens, the RH was maintained at higher levels for sealed specimens. The decrease rate of RH was lower for SAP mixtures.

The effect of SAP on tensile creep and shrinkage was tested by Assmann and Reinhardt (Assmann and Reinhardt, 2014). They exposed the investigated specimens to various conditions of drying. Crushed acrylamide/acrylic acid SAP with particles size from 50 – 125μm were utilized for the specific research. The authors observed a reduction of 50% in tensile creep in SAP enriched mixtures. It was also reported that the strength for identical w/c ratios was the same regardless the method of

PERICLES ALEXANDROU SAVVA

introducing the specific amount of water in the mixture. They also reported that autogenous and drying shrinkage were reduced when SAP were used.

Hasholt and Jensen conducted a study to investigate the effect of SAP on concrete chloride migration properties based on the chloride migration coefficient and the degree of hydration (Hasholt and Jensen, 2015). The experiments included twenty concrete mixtures which were tested at the age of 7, 14 and 28 days. Three control mixtures were developed whose difference lied on the w/c ratio (0.35, 0.40 and 0.50) and SAP percentages (0.20% and 0.60%) for each one. The SAP were added to the mixture with and without additional water. The authors stated that the gel-space ratio seemed to be the key element that linked the materials age and mixture proportions to the chloride migration coefficient. More specifically, it was mentioned that the greater the gel solid volume relative to the space available for it, the lower the chloride coefficient migration due to the pore structure tortuosity. It was concluded that given an increase of degree of hydration due to SAP and enough space available, the chloride migration coefficient would decrease.

Shen et al. attempted to relate the IC with the early-age expansion, autogenous shrinkage development and autogenous shrinkage to estimate the efficiency of SAP IC in high performance concrete (Shen *et al.*, 2015a). The polymers utilized in the specific research where suspension-polymerized, covalently cross-linked acrylamide/acrylic acid copolymers with particles size distribution varying from 125 to 150μm and WA capacity of 20g/g. It was concluded that the maximum early-age expansion and the time that it occurred increased with the IC water increase whereas the maximum autogenous shrinkage and the autogenous shrinkage rate for IC mixtures decreased. For amounts of SAP varying as 5.35kg/m^3, 16.06kg/m^3 and 26.78kg/m^3, the reduction of autogenous shrinkage at the age of 28 days was 15.1%, 41.5% and 56.0% respectively. Correspondingly, the autogenous shrinkage rate at 5 days was reduced by 27.6%, 41.4% and 48.3%. Moreover, the authors stated that the IC efficiency of SAP decreased with the increase of IC water in concrete. Additionally, the authors proposed a model which correlated early-age expansion and IC water to predict SAP IC mixtures autogenous shrinkage. A good correlation between simulations and experimental results was observed.

Snoeck et al. examined the influence of autogenous shrinkage on mixtures containing supplementary materials such as fly ash and blast-furnace slag (Snoeck, Jensen and De Belie, 2015). The mixtures were manufactured using the same w/b ratio (0.30). Two types of SAP were used for the specific research designated as SAP-A, a copolymer of acrylamide and sodium acrylate (particle size 100.0±21.5μm), and SAP-B, a cross-linked potassium salt polyacrylate (particle size 476.6 ± 52.9μm). Both SAP were bulk-polymerized and consisted of irregular crushed particles. The extra water for IC

PERICLES ALEXANDROU SAVVA

mixtures was estimated at w/b_{IC}=0.054. The replacement of the supplementary materials was conducted with cement replacement. Class F fly ash was added to the mixture in a replacement percentage of 15%, 30% and 50%. Blast-furnace slag was added in the same percentages with an additional replacement of 85% for the latest. Autogenous shrinkage in mixtures containing supplementary materials observed a delay due to the retarded pozzolanic activation. Despite the delayed peak of autogenous shrinkage, the SAP were still efficient in reducing the effect.

Snoeck et al. evaluated the effect of SAP on the microstructure of cementitious materials with the use of sorption isotherms (Snoeck *et al.*, 2015). Static and dynamic vapor sorption experiments were conducted along with nitrogen absorption experiments. The cement pastes were manufactured with four different w/c ratios 0.50, 0.46, 0.41 and 0.35, whereas the SAP percentages where 0.50% and 1.00% with respect to cement mass. Two types of bulk-polymerized and irregular crushed particles of SAP were tested. SAP type A was copolymer of acrylamide and sodium acrylate with particle size 100.0 ± 21.5μm and SAP type B was a cross-linked potassium salt polyacrylate with particles size 477±53μm. The results showed that the addition of SAP in cement pastes without adding extra water lead to a decreased micro (<2nm) and meso (2nm-50nm) pore range whereas the addition of extra water based on the polymers absorption exhibited no significant change in the micro level and slight increase in the meso pore level. The authors stated that the effective w/c ratio was important instead of the total w/c ratio (including the polymers).

A comprehensive experimental work (round-robin test) performed by 13 international research groups representing fifteen institutions in the framework of the activities of the RILEM technical committee 225-SAP was conducted, in order to evaluate the effect of internal curing by using superabsorbent polymers (SAP) on autogenous shrinkage and other properties of a high-performance fine-grained concrete (Mechtcherine *et al.*, 2013). Two different SAP (acrylic acid) with the same amount of anionic groups where utilized for the specific work. Their difference lied on the cross-linking density which was denser for SAP1, the polymerization technique where SAP1 was bulk polymerized/crushed and SAP2 was spherical particles and on the particles size distribution where SAP1 was coarser (~average=750μm) than SAP2 (~average=300μm). Both types of SAP were added to the mixture in a percentage of 0.30% by cement mass in a dry state while the IC water was added above the initial w/c (SAP1: 21kg water/m^3 concrete and SAP2: 28kg water/m^3 concrete). The mix design was kept constant despite the fact that every laboratory was using local materials. More specifically, the cement content was 700kg/m^3 with an additional 70kg/m^3 silica fume and a w/b ratio of 0.30. The experimental methods for the fresh state included slump flow test, fresh state density and air content,

PERICLES ALEXANDROU SAVVA

setting time (UPV, autogenous shrinkage, Vicat needle), autogenous shrinkage (most participants used the dilatometer method to estimate the longitudinal deformation of corrugated tubes (Mejlhede Jensen and Freiesleben Hansen, 1995)). Regarding the hard state, bending and compressive strength experiments were conducted. The experiments indicated that both types of SAP effectively mitigated autogenous shrinkage highlighting the SAP IC robustness towards compensating autogenous shrinkage. More specifically, the addition of SAP1 led to a decrease in early age autogenous shrinkage of 80% which ended up to 44% at the age of 28 days and 50% to 32% correspondingly for SAP2. The researchers also reported a loss in compressive and flexural strength when SAP were employed even though a few participants observed the contrary. It was also stated that the shape and particles size of the polymers had a major influence on the materials strength. The spherical and finer particles exhibited greater shrinkage than the crushed particles. However, it was not clarified which of the two parameters affect the materials performance the most. The polymers kinetics had a great influence on the mechanical performance of the mixtures since an early water release increased the effective w/c ratio in a premature stage where IC demand was disproportional to the supply. A further investigation supported that the consistent reduction in high performance concrete compressive strength could be surpassed by a proper design, regarding the dosage and the curing of each mixture (RILEM TC 225-SAP, 2012). It continues suggesting that the interest must focus on achieving IC without affecting other properties of the material.

In addition to compressive strength, other properties of the material are affected by the introduction of IC. Modulus of elasticity and flexural strength deteriorate due to insufficient stiffness and increased porosity (Zhutovsky and Kovler, 2010; Byard, Schindler and Barnes, 2012; Mechtcherine *et al.*, 2013). Additionally, in NWA mixtures the permeability is governed by the cement paste permeability. In mixtures including LWA the permeability may be influenced by the properties of LWAs. A reduction in permeability and diffusivity can be expected in IC mixtures due to extended hydration that leads in capillary pores depercolation. In both SAP and LWA IC methods, additional porosity is expected to be introduced in the mixture (RILEM TC 196-ICC Rep 41-6, 2007).

Shen et al. attempted to predict the internal relative humidity of concrete, considering the w/c and the age of concrete enriched with SAP (Shen *et al.*, 2017). The authors presented a model that predicts the early age RH of concrete enriched with SAP. Ding et al. studied the relationship between the SAP dosage and the concrete compressive strength (Ding, Zhang and Zhang, 2017). The material compressive strength was affected from the w/c ratio, the SAP dosage and the SAP particles size. An increased SAP particle size resulted in an increased early-age strength. However, a detrimental effect

PERICLES ALEXANDROUSAKIS

on the later-age strength (28 days) due to residual cavities was observed. The authors concluded that the SAP dosage must not exceed 0.20%.

Wehbe and Ghahremaninezhad examined the effect of shrinkage reducing admixtures with SAP, on concrete autogenous shrinkage, hydration and microstructure (Wehbe and Ghahremaninezhad, 2017). It was shown that the specific combination resulted in increased shrinkage as opposed to the SAP enriched mixture especially in early-ages. The addition of shrinkage reducing admixtures caused a shift of the temperature-peak as opposed to the SAP and shrinkage reducing admixtures combined. The SAP- shrinkage reducing admixtures mixture showed higher degree of hydration than the shrinkage reducing admixtures mixture due to internal curing. However, the SAP- shrinkage reducing admixtures mixture exhibited lower compressive strength and electrical resistivity than the mixture with SAP and the mixture with shrinkage reducing admixtures. An examination of the SAP-shrinkage reducing admixtures mixture with SEM showed a distribution of 10-20μm pores, where the authors attributed the reduced compressive strength.

Olawuyia and Boshoff conducted a volume analysis on the three dimensional influence of SAP and curing age on the air void distribution on high performance concrete. (Olawuyi and Boshoff, 2017). The specific analysis was conducted on mixtures with various w/b ratios, various SAP percentages and particles size. The pore distribution was analyzed using X-ray computed tomography. The high performance mixtures enriched with SAP exhibited higher porosity and larger size of pores, according to the polymers distribution in dry state. It was reported that an optimum SAP dosage (~0.3%) accompanied with a regulated IC water (less than the SAP absorbing capacity) may result in a fully diminished porosity caused from SAP.

Ma et al. examined the effect of SAP on the pore structure and properties of high performance cement-based materials with w/b ratio 0.18-0.24, in 60% of RH (Ma *et al.*, 2017). It was concluded that at the same effective w/b ratio, SAP inclusion resulted in reduced strength, increased drying shrinkage, increased chloride ion coefficient and increased absorption. However, at a same total w/b ratio, the SAP inclusion resulted in increased strength, decreased permeability and decreased drying shrinkage. It was mentioned that SAP reduced the amount of pores with a diameter higher than 100μm. The authors stated that larger SAP particles contributed to a better 28^{-day} behavior.

Liu et al. conducted an overview of the internal curing method, including both LWA and SAP in their discussion (J. Liu *et al.*, 2017). They divided internal curing agents into two categories, according to their absorbing mechanism. It was noted the due to their pore structure, LWA and SAP may possibly

PERICLES ALEXANDROU SAVVA

cause strength decrease in high performance concrete. Internal curing would increase the degree of hydration resulting in increased chemical shrinkage, reduction or elimination of autogenous shrinkage and increased drying shrinkage.

3.5.2.2. SAP structure and kinetics effect

Pedro Esteves attempted to give a better understanding on the absorption kinetics of SAP in synthetic pore fluid (Esteves, 2010, 2011). The utilized spherical polyelectrolyte polyacrylamide polymers employed had a fraction size varying between 50 to 500 μm. The synthetic pore fluid was reproduced based on the cement compounds dissolved in water determined by ion chromatographic analysis ([mmol L^{-1}]: [Na^+] = 200, [K^+] = 500, [Ca^{2+}] = 1, [SO^{2-}_4] = 15, [OH^-] =672) (Page and Vennesland, 1983; Lura, 2003). It was concluded that the size of the polymers had a significant effect on the absorption kinetics of polyacrylate-based polymers. Esteves developed a model based on the Fick's second law to express the physical or volumetric change of the polymers within the pore fluid after an instantaneous liquid uptake that takes place at the instant of submersion. The specific model was extended to capture the absorption kinetics of a given particle size distribution. Esteves concluded that the gravimetric method of estimating SAP absorptivity may lead to uncertainties regarding the adsorbed water. It was added that the finer the particles size the greatest the surface exposed to Van der Waals forces leading to uncertainties regarding the polymers absorption. Additionally, Esteves mentioned that Fick's law of diffusion can be extended and apply to the kinetics of SAP absorption. It was clarified though that the amount of water added to the mixture would affect the particles absorptivity due to ions concentration variations. Finally, Esteves reported that the polymers' particles size influenced the rate of absorption and the maximum absorption capacity, whereas the high particles diameter led to great absorption capacity.

Dudziak and Mechtcherine attempted to approach the kinetics of water migration and consumption in order to provide key information regarding IC using SAP (Dudziak and Mechtcherine, 2010). The specific research was conducted on ultra high performance concrete with and without IC, where the mixtures were adopted from another research work (Mechtcherine *et al.*, 2006). The researchers conducted free autogenous and total shrinkage experiments, ultrasonic and temperature experiments. The results indicated that the water deliberation from SAP took place close to the final setting time of the control mix. It was mentioned that the calculation of IC water based on Power's model underestimates the required amount of water. It highlights the principle of Power's model that explicitly demonstrates the phase change of a volumetric stable, air free cement paste fairly independent of the cement type, w/c ratio and degree of hydration.

PERICLES ALEXANDROU SAVVA

Schröfl et al. studied the relation between the molecular structure of SAP and their efficiency towards reducing autogenous shrinkage (Schröfl, Mechtcherine and Gorges, 2012). It was mentioned that the presence of Ca^{2+} ions in the alkaline solution affected the liquid uptake and release kinetics as opposed to other saline solutions and distilled water. SAP with high density anionic groups had a greater rate of cement pore fluid absorption and release, as opposed to SAP with lower density of anionic groups that did not release the pore fluid in the assessed time interval. The authors mentioned that the cross-linking density of the polymers had no pronounced influence on the high anionic density SAP. It was stated that the high anionic density SAP had an influence of mortars autogenous shrinkage only during the acceleration period of the cement paste whereas the lower density polymers extended their effect on the deceleration period as well. None of the polymers employed in the specific research had a negative effect on the materials compressive strength.

Siramanont et al. compared suspended and bulk SAP in terms of concrete internal curing (Siramanont, Vichit-Vadakan and Siriwatwechakul, 2010). The comparison was conducted on concrete compressive strength, SEM of the microstructure and porosity. It was assumed that the mixtures that contained bulk SAP would perform better in terms of compressive strength than those containing microsphere SAP, whereas the mixtures containing microsphere SAP would perform even poorer than the mixtures without SAP addition. The SAP enriched mixture cured in water exhibited lower compressive strength than concrete without SAP. Other tests such as sorptivity and porosity were consistent with the compressive strength findings. The specific findings though came in contradiction to other research findings (Jensen and Hansen, 2002) which concluded that the inclusion of spherical macropores from SAP microspheres would be more beneficial for strength and durability of concrete rather than irregular shaped pores.

Mechtcherine et al. examined the effect of two different types of SAP (acrylic acid and acrylic acid with acrylamide) on yield stress and viscosity of cement-based mixtures (Mechtcherine, Secrieru and Schröfl, 2015). The specific polymers also varied in cross-link density. The cross-link density is one of the main factors that affect the polymers absorptivity, namely, the higher the density the lower the absorptivity. The authors developed three reference mortars which undergone continuous rheological examination for 90 minutes. The conclusions indicated that the distinct kinetics of the polymers governed by their chemical composition was the key parameter that governed the rheological properties. Additionally, it was found that the addition of various grading of SAP affected the development of yield stress and viscosity with time. More specifically, the finer particles of SAP provided higher yield stress and plastic viscosity due to greater total absorption. The authors also

PERICLES ALEXANDROU SAVVA

attributed the effect of SAP on the rheological behavior on the w/b ratio, the superplasticizer and the silica fume. The addition of silica fume hindered the water absorption from SAP because of silica finest structure.

Schroefl et al. examined the sorption kinetics of two different type of SAP in cement-based mixtures using neutron tomography and correlated the findings with the progress of hydration (Schroefl *et al.*, 2015). One cement paste including silica fume (w/c=0.42) and two without silica fume were examined (0.25 and 0.50). The authors classified the two types of SAP into retentive and self-release categories meaning that the polymers release the held moisture in a different way. The SAP where crushed polymerized where the first type of SAP (SAP 1- acrylic acid) had the maximum relative anionicity which is known to affect the absorptivity. SAP 2 was a cross-linked copolymer composed of the two main monomers acrylic acid and acrylamide. The percentage of SAP were adjusted to 0.30% by weight of cement. It was concluded that desorption from SAP 1 began very early therefore the releasing mechanism was the self-retention of the polymers with respect to the saline of the pore fluid. The specific finding was considered as a drawback since the polymers utilized for IC are intended to release their moisture according to the mixture demand (RH drop). The authors stated that the SAP 2 was more efficient than SAP 1. Regarding SAP 2, the water release was initiated simultaneously with the activation period, namely at the exact time where the water demand begins to occur. The whole amount of water was released, however, the kinetics varied according to the state of mixture. More specifically, the polymers in the paste with high w/c observed a moderate early-age (first hours) water release in contradiction to the other two pastes where the majority of the IC water was released throughout the acceleration period. The authors attributed the autogenous shrinkage reduction to the coordinated water release and water demand.

Wang et al. investigated the cement paste on the surrounding area of the swelled SAP and its properties (Wang *et al.*, 2016). In order to magnify the effects, the authors employed high particle size polyacrylic acid-based polymers (1.5mm-2.0mm in collapsed phase and 4-5mm in swelled phase). The investigation included hydration, capillary pore structure, microstructure and microhardness. It was concluded that the degree of hydration in the specific area was 5% higher than the outer volume of the surrounding paste, indicating a w/c increase of 0.04. Moreover, capillary porosity was increased in early-age and decreased in later ages due to SAP activation (IC). The denser region in the SAP surrounding area reflected in the higher microhardness, increased degree of hydration and pore structure of the specific area.

PERICLES ALEXANDROU SAVVA

Azarijafari et al. examined the effect of pre-soaked SAP on self-consolidating lightweight concrete with and without the incorporation of silica fume (Azarijafari *et al.*, 2016). More specifically the fractions 1-4 mm and 0.3-1 mm of polymers were employed. The researchers concluded that the employment of SAP resulted in improved static stability and passing ability of the mixtures, with additional improvement in the static stability when silica fume was added. Additionally, a reduction in the compressive strength at the age of 7 and 28 days was observed, regardless of the polymers fraction. The specific loss was recovered when silica fume was added at a percentage of 15%. Moreover, durability related experiments such as water absorption and electrical resistivity showed a deterioration when SAP were employed, with a high detrimental impact in the case of coarser SAP. Finally, the researchers observed a shrinkage reduction in the case of SAP enriched mixtures, with a higher reduction observed when finer SAP were employed. The specific was attributed to an enhanced IC due to better dispersion of polymers.

Wang et al. examined the effect of SAP on their vicinity volume (Wang *et al.*, 2016). They used large SAP particles (1.5-2mm) to evaluate their effect on the hydration kinetics, the degree of hydration, the capillary pore structure, the microhardness and microstructure according to the SAP desorption properties. It was concluded that the SAP promotes the cement hydration at the surrounding cement paste. The degree of hydration at the specific areas was increased by 5% or equivalent w/c ratio 0.04, which was in agreement with the theoretical amount of water added for IC. Additionally, an early-age porosity increase was observed which was reduced at late-age. The authors clarify that SAP desorption occurred due to osmotic pressure at early-age and due to humidity gradient in late-age. The degree of hydration and the porosity were calculated using the loss on ignition and Brunauer-Emmett-Teller (BET) theory respectively and verified using backscattered images (BSE). Finally, the microhardness of the affected zone was higher than the unaffected zone. The specific was attributed to the increased degree of hydration which yielded in decreased capillary porosity.

Mechtcherine et al. examined the effect of various types of SAP on the kinetics of fresh mortars and more specifically on their yield stress and plastic viscosity (Mechtcherine, Secrieru and Schröfl, 2015). The authors mentioned that the sorption properties of SAP were affected by their anion concentration, cross link density and the ion concentration of the surrounding substance. It was found that the finer polymers caused the highest yield stress and plastic viscosity due to higher surface area that resulted in greater total absorption and rapid equilibrium. In addition, the authors observed that SAP absorption capacity was less in mortars that contained silica fume.

PERICLES ALEXANDROU SAVVA

Kang et al. examined the absorption kinetics of SAP using a modified tea-bag test, in order to reduce the risk of overestimating SAP absorption capacity (Kang, Hong and Moon, 2017). The SAP were examined in artificial pore solutions, with various w/c ratios. It was shown that an increase in w/c ration resulted in an increased early SAP absorptivity, due to higher dilution. However, the decreased OH^- concentration resulted in higher Ca concentration that yielded into lower secondary absorptivity. The addition of silica fume did not change SAP kinetics dramatically. The addition of acidic superplasticizer resulted in increased cation concentration (Na and Ca) which reduced SAP absorptivity in both short and long term.

3.5.2.3. Effect on thermal expansion coefficient

According to Wyrzykowski and Lura, low w/c ratio lead to an increased (up to 70%) coefficient of thermal expansion (CTE) in cement mixtures at early ages, due to RH changes induced by temperature changes. The authors showed that the utilization of SAP in cement mixtures can reduce the CTE increase effect (Wyrzykowski and Lura, 2013). The authors developed cement paste and mortar mixtures where shrinkage and CTE measurements were conducted. Based on the experiments, cement paste mixtures reached values of 25μm/m/ºC on 0.30 w/c ratio whereas the addition of fine aggregates lowered the CTE value to 18μm/m/ºC on 0.30, all at 7 days. The specific reduction was attributed to the aggregates addition since a coefficient of 9μm/m/ºC was adopted for the specific aggregates based on the literature. Additionally, the researchers mentioned that the steepest CTE rise for non-IC mixtures was observed at the first 3-4 days of maturing. It was concluded that the CTE was down to the 60-70% of their original value and attributed to the RH at high levels.

3.5.2.4. SAP in other applications

3.5.2.4.1. Self-Compacting Concrete (SCC)

Lura and Terrasi examined the effect of SAP and propylene fibres on fire spalling of carbon fibre reinforced plastic-prestressed self-compacting concrete (Lura and Terrasi, 2014). High performance concrete is prone to explosive spalling when exposed to fire because of its depercolated pore network which restricts the violent vapor escape. Polypropylene fibres are added to the mixtures in order to intentionally introduce air channels during the fire and allow the vapor to evacuate. It was stated that excessive addition of fibres in self-compacting concrete may damage its flowing properties, therefore the specific applications have certain restrictions. The employment of SAP provides earlier network percolation due to the macropores introduced by the polymers reducing fire spalling. The authors

PERICLES ALEXANDROU SAVVA

reported a negative effect on the mixtures compressive strength and fresh properties due to SAP addition.

Azarijafari et al. investigated the effect of SAP with various fineness Lightweight SCC (Azarijafari *et al.*, 2016). SAP with particles size varying from 0.3 to 1 mm and 1 to 4 mm were utilized in 1.5% binder replacement. The mixtures were examined on the basic SCC experiments, namely, slump flow, T500, V-funnel, and J-ring and on basic mechanical and durability experiments such as compressive strength, water absorption, electrical resistivity, and total shrinkage. It was concluded that SAP improved the passing ability and the static stability or yield stress of the SCC mixtures. Additionally, a decreased compressive strength at the age of 7 and 28 days was observed which was more prominent for the coarse SAP. However, the addition of supplementary materials such as silica fume compensated the loss in compressive strength. In addition, the SAP exhibited a negative impact on electrical resistivity and water absorption especially in the case where coarse SAP were utilized. Finally, a significant (50%) reduction of shrinkage was observed in the SAP-enriched mixtures where the fine SAP were more efficient than the coarse.

3.5.2.4.2. Self-healing

Huang et al. supported that the isolation of saturated SAP within waterproof capsules could prevent their moisture loss at early-ages and fracture when a crack intersects the confined particles due to low strength (Huang, Ye and Breugel, 2010). The moist stored in the SAP would be desorbed from the polymers, diffused and transported in the crack leading to additional hydration products formation and/or calcium carbonation salts that will eventually seal the crack and restrict deleterious ion transformation within the matrix. The aforementioned mechanisms (desorption, diffusion and transportation) were simulated using finite difference method. The authors mentioned that the driving force behind the moisture transportation was the humidity gradient within. The internal RH was increased from 82.5% to 99.5% in a time interval of 10 minutes. The aforementioned conclusions were drawn based on the modelling results. It was reported that the water penetration depth 48 hours after the capsules fracture was 2mm and attributed to the low degree of concrete saturation (0.25) and low porosity (20%).

Lee et al. conducted experimental research to assess the ability of SAP to provide self-healing properties on cement pastes and mortars (Xiang *et al.*, 2010). For the specific research various amounts of SAP were utilized. The specimens were loaded to create a through crack ranging from 100-400μm and then exposed to 0.2M sodium chloride solution with a pressure gradient 4 and

PERICLES ALEXANDROU SAVVA

controllable flow rates. The polymers employed were polyacrylate or polyacrylate-co-acrylamide. The researchers reported that the cement paste specimens containing 5% SAP had observed a cumulative flow reduction of 80% as opposed to the control mixtures. The mortar mixtures including SAP in lower percentage exhibited a flow reduction of 85%. The authors concluded that the polyacrylate-co-acrylamide polymers and the larger particles size were more effective than the polyacrylate and lower particles size in terms of self-healing. The w/c ratio in the specific research was not constant and the mechanical properties were not reported.

3.6. Some Comments Regarding the Literature

Deo and Pofale conducted experimental research to assess the possibility of utilizing fly ash in concrete mixtures as IC agent (Deo and Pofale, 2015). In the conclusions section a comment regarding the beneficial effect of fly ash as an IC agent was made, highlighting the fact that sand replacement with fly ash can reduce cracks in concrete. It has to be mentioned though that the specific conclusion was derived indirectly, due to an increased compressive and flexural strength. It is believed that the specific argument would be reinforced if durability measurements, restrain shrinkage or free shrinkage experiments were conducted. Zhutovsky and Kovler conducted experimental work where the effect of LWA IC mediums on the materials strength and durability properties was evaluated (Zhutovsky and Kovler, 2010). It was mentioned that the reduction of w/c for IC mixtures had a beneficial effect on drying shrinkage. It is well known though that drying shrinkage is being reduced as the w/c reduces, regardless of IC presence, thus the specific observation cannot be attributed to a beneficiary effect of IC. Mousa et al. conducted two different experimental works to evaluate the physical and mechanical performance of two different IC agents on concrete (LWA and poly-ethylene glycol) (Mousa *et al.*, 2014a, 2014b). In their research regarding the impact of IC on concrete physical properties, the authors claimed that the addition of silica fume had a beneficial effect, due to reduced mass loss. It has to be reminded that the IC systems effectiveness is partially determined from the distance that IC water can travel from the reservoir to the cement paste. Therefore, the reduced mass loss due to silica fume addition is expected due to its fineness and thus it is not an indicator of IC effectiveness. Zhutovsky verified that the addition of silica fume reduces the effectiveness of an IC system due to water retainment that restricts its access or diffusion to a broad cement paste volume (Zhutovsky, Kovler and Bentur, 2004). Regarding the mechanical properties, the authors mentioned an improvement for the mixture with silica fume. However, a mixture with silica fume and no IC was not conducted, therefore the improvement cannot be attributed to the IC. Assmann and Reinhardt (Assmann and Reinhardt, 2014) reported that the strength for identical w/c ratios was the same regardless the method

PERICLES ALEXANDROU SAVVA

of introducing the specific amount of water in the mixture. The specific conclusion points out the effect of SAP on the compressive strength implying that the SAP at the early age of the mixtures life-cycle has the same effect on mechanical properties as the free water. The specific argument is invalid because SAP provide moisture to the mixture when the mixture demands it. Therefore, the water provided from SAP will be fully utilized for hydration.

3.7. Research significance

The technique of internal curing IC aroused at the beginning of the last century and much advancement were achieved since. It is an on-going research topic and attracts great attention since the advantages of establishing an IC technique are both short and long term. Improved performance during the structures service life as well as extended life-cycle are two of the main benefits that contribute to a lower construction and maintenance cost ensuring environmental sustainability.

The main objective of IC is to provide additional water in a dense concrete to reduce the early-age shrinkage. The quantity of IC water required to compensate autogenous shrinkage can be calculated based on Bentz equation (3-2) (P. D. Bentz and Snyder, 1999). The difficulty in IC is to provide the full quantity of IC water without compromising the material's performance. For example, increasing LWA in order to satisfy the IC requirements may endanger the mechanical properties of the mixture. Employing SAP to compensate autogenous shrinkage has proven to be a very effective method but the material's mechanical properties are evidently deteriorated (Table 1 and 2). Furthermore, using shrinkage reducing agents in the mixture, although durability indicators may remain unaffected, the compressive strength is reduced (Lopes *et al.*, 2013). The effort of this research focus on establishing IC various w/c ratio concrete mixtures stored in various conditions without reducing any other properties of the material. The aggregates employed in this research were high-absorptive normal weight aggregates (HANWA) that exhibit high absorption capacity (thorough description in Section 4.2). Preliminary results indicate that HANWA benefits IC and sound mechanical properties that ensure the mixtures serviceability. More details regarding the aggregates formation and properties can be found in section 4.2.

3.8. Synopsis of literature research findings regarding internal curing

So far, the main techniques which were practically applied for internal curing were superabsorbent polymers and lightweight aggregates. The main criteria to select the appropriate IC technique should focus on the cost, effectiveness and applicability. Many techniques are not being used due to their high cost and sensitive nature (microcapsule) where others more cost-effective are not being used due

PERICLES ALEXANDROU SAVVA

to their poor IC effectiveness (Bentonite clay). Additionally, the performance of an internal curing system depends on several parameters such as the pore structure, the size and the distribution of the agent, the readiness by which the medium releases the curing agent as well as its carrying capacity in terms of IC agent which in most cases is water (Henkensiefken, Bentz, *et al.*, 2009). It is therefore concluded that the IC agent should be selected based on the application since the parameters under consideration are complex. A synopsis of the experimental and theoretical work found in the literature is presented in Table 3-1 and Table 3-2.

Table 3-1: Synopsis of literature research findings regarding internal curing

Researchers	IC method	Main findings
(Holm, 1980)	LWA	• Extended hydration • Increased compressive strength
(Weber and Reinhardt, 1997)	LWA	• Increased compressive strength • Porosity decrease • Increased degree of hydration • Increased hydration products
(Collins and Sanjayan, 1999)	LWA in AAS concrete	• Increased compressive strength (curing 22°C-50%RH) • Decreased compressive strength for water cured specimens • Lower drying shrinkage in IC mixtures
(Collins and Sanjayan, 1999)	Saturated BFS in AAS concrete	• Increased compressive strength at 7 days • Decreased drying shrinkage at 7 days
(Kohno *et al.*, 1999)	Artificial LWA	• Autogenous shrinkage decrease • Autogenous shrinkage link with LWA permeability and adsorption capacity
(Lo, Gao and Jeary, 1999)	LWA	• Extended pre-wetting lead to increased workability • Intense mechanical vibration may lead to pre-mature water release
(Bentur, Igarashi and Kovler, 2001)	LWA	• Autogenous shrinkage reduction or full elimination • Extended hydration • Reduction of autogenous shrinkage stress

PERICLES ALEXANDROU SAVVA

(Zhutovsky, Kovler and Bentur, 2002)	LWA	• Autogenous shrinkage elimination • Reduced compressive strength • Increased cost
(Husem, 2003)	LWA	• LWA-mortar bond strength lower than NWA-mortar bond strength • LWA-cement paste strength higher than NWA-cement paste strength • LWA mixture had lower compressive strength than NWA mixture and plain cement paste mixture • LWA mixture had lower flexural strength than NWA mixture yet higher than plain cement paste mixture
(Zhutovsky, Kovler and Bentur, 2004)	LWA	• Autogenous shrinkage elimination • Reduced compressive strength • Silica fume affects IC negatively
(Lura and Bisschop, 2004)	LWA	• Lower eigenstresses • Greater bulk shrinkage • Reduced aggregates restrain
(Le Roy, Parant and Boulay, 2005)	LWA	• Compressive strength inversely proportional to particles inclusion size
(Craeye and Schutter, 2006)	LWA	• Reduced autogenous shrinkage • Decreased compressive strength
(Lura, Jensen and Igarashi, 2007)	Overview LWA techniques	• IC affects directly mixtures RH, S, and sorption isotherms • Increased degree of hydration • Reduced autogenous shrinkage • Improved mechanical properties, porosity, microstructure interconnectivity, ITZ • Reduced self-induced stress and cracking • Improved durability indicators • Delicate method (excessive IC may have controversial effects)
(Henkensiefken *et al.*, 2008)	LWA	• Reduced autogenous shrinkage • Reduced mortars stiffness
(Bentz, 2009)	LWA	• IC beneficial effect on chloride ions diffusion • Denser ITZ

PERICLES ALEXANDROU SAVVA

		• Microstructure depercolation
(Henkensiefken, Castro, *et al.*, 2009)	LWA	• Increased degree of hydration • Reduced sorptivity • Reduced electrical conductivity • Increased ITZ density
(Akcay and Tasdemir, 2009)	LWA	• Lower LWA fraction more efficient autogenous shrinkage reduction • Compressive strength inversely proportional to particles inclusion size • Particles size decrease led to fracture properties increase
(Cusson, Lounis and Daigle, 2010)	LWA	• No early-age cracking • Increased compressive strength • Decreased chloride permeability • Decreased freeze-thaw resistance • Decreased salt scaling resistance • 63% reduced cost (due to longer service-life and reduced maintenance cost)
(Browning *et al.*, 2011)	Pre-wetted vacuum saturated LWA	• Drying shrinkage reduction • Similar compressive strength • Minor density reduction • Substantial shrinkage reduction when slag cement was used
(De La Varga *et al.*, 2012)	fly ash (class C) - LWA	• Reduced modulus of elasticity • Decrease autogenous shrinkage due to retarded hydration in the case of fly ash addition • Increased early-age strength
(Byard, Schindler and Barnes, 2012)	LWA	• Increase degree of hydration due to IC • Increased compressive strength • Autogenous shrinkage elimination • Elastic modulus reduction with high LWA replacement levels • Increased tensile strength
(Golias, Castro and Weiss, 2012)	Pre-wetted vacuum saturated LWA	• Delicate design • Reduced autogenous shrinkage • Slight increase of compressive strength

PERICLES ALEXANDROU SAVVA

		• LWA saturation may retain water in smaller pores
(Zhutovsky and Kovler, 2012)	LWA	• Air permeability reduction at later ages on IC mixtures • Sorptivity and mass loss increased at later ages on IC mixtures • Porosity increase • Improved chloride resistance
(Mousa *et al.*, 2014a)	LWA – Poly ethylene glycol	• Increased degree of hydration • Improved compressive, tensile and flexural strength • Improved modulus of elasticity • Excessive IC led to degradation (sorptivity and mass loss increase) • Poly ethylene glycol exhibited superior performance as opposed to LWA
(Mousa *et al.*, 2014b)		• Improved water absorption, permeability, sorptivity and mass loss
(Han *et al.*, 2014)	fly ash - LWA	• RH level was inversely proportional to the shrinkage strain • Moisture gradient is steeper from the core to the edge of the elements for non-IC mixtures
(Kim *et al.*, 2014)	CBA	• Chloride diffusion reduction • Porosity interconnectivity relation is affected negatively • Pozzolanic reaction of CBA does not have great effect on the pore system
(De La Varga *et al.*, 2014)	fly ash and LWA	• High absorptivity at early ages for LWA mixtures • Lower chloride penetration • fly ash -LWA higher resistivity due to denser microstructure • IC had not additional contribution in fly ash mixtures in terms of ion transport
(Sun *et al.*, 2015)	LWA	• Reduced permeability • Pores depercolation • Smaller pores size
(Deo and Pofale, 2015)	fly ash	• Better packing/less voids • Compressive strength increase

PERICLES ALEXANDROU SAVVA

		• Flexural strength increase
(Zhutovsky and Kovler, 2017)	LWA	• Reduced early age compressive strength • Recovered compressive strength • Reduced w/c ratio caused increased shrinkage, which was counteracted with IC
(Li *et al.*, 2017)	LWA and expansive agents	• Reduced shrinkage • Increased compressive strength • Reduced modulus of elasticity
(Jensen and Hansen, 2000)	SAP	• Self-desiccation reduction
(Jensen and Hansen, 2002)	SAP	• Self-desiccation reduction • RH replenishment • Autogenous shrinkage elimination • Change of setting time • Change of rheology • Additional porosity • Possible mechanical properties deterioration
(Mönnig and Reinhardt, 2006)	SAP	• Drying shrinkage decrease during the first week • Increased compressive strength
(Mechtcherine *et al.*, 2006)	SAP	• Workability was not affected • Better performance regarding bleeding • Reduction in autogenous shrinkage • Drying shrinkage significant increase • Autogenous shrinkage increase after 1 week • Reduction of compressive strength • Reduction of tensile strength • Reduction of flexural strength
(Piérard, Pollet and Cauberg, 2006)	SAP shrinkage reducing admixtures	• Autogenous shrinkage reduction • Negative impact on workability, setting-time • Negative impact on compressive strength • Drying shrinkage increase • Shrinkage reducing admixtures compressive strength reduction
(Reinhardt and Mönnig, 2006)	SAP LWA	• Results are affected from SAP size and absorption capacity

PERICLES ALEXANDROU SAVVA

		• Compressive strength slight reduction
(Mechtcherine *et al.*, 2006)	SAP	• Early-age crack decreased • Free and restrained shrinkage decreased • Amount and state of SAP determine the mixtures performance • Retarded setting • Additional porosity • Early-age compressive strength decrease
(Craeye and Schutter, 2006)	SAP LWA	• Autogenous shrinkage reduction in both methods • Compressive strength reduction in both methods
(Igarashi and Watanabe, 2006)	SAP	• Autogenous shrinkage reduction- not fully compensated • Macropores diameter reduction • No significant increase of degree of hydration especially at early-ages • Compressive strength decrease
(Reinhardt, Assmann and Mönnig, 2008)	SAP AEA	• Better performance from SAP in freeze and thaw, water absorption and chloride migration • Slight decrease of compressive strength • Decrease of tensile strength • Retardation of drying shrinkage
(Hasholt, Jespersen and Jensen, 2010a)	SAP	• Enhanced degree of hydration (w/b<0.40) • Increased compressive strength at later ages (w/b<0.40) • Decreased compressive strength at early ages (w/b<0.40 and high SAP content) • Not significant contribution on the degree of hydration (w/b>0.45) • Compressive strength decrease (w/b>0.45)
(Siramanont, Vichit-Vadakan and Siriwatwechakul, 2010)	SAP	• Reduced compressive strength • Increased sorptivity and porosity
(Craeye, Geirnaert and Schutter, 2011)	SAP	• Autogenous shrinkage reduction- not fully compensated • Compressive strength reduction • Modulus of elasticity reduction • Higher creep deformation

PERICLES ALEXANDROU SAVVA

		• Heat development increase
(Schröfl, Mechtcherine and Gorges, 2012)	SAP	• No harmful impact on compressive strength
(Mechtcherine *et al.*, 2013)	SAP	• 13 laboratories participated • Compressive strength reduction • Autogenous shrinkage reduction • Flexural strength reduction
(Assmann and Reinhardt, 2014)	SAP	• Tensile creep reduction • Autogenous and drying shrinkage reduction • Identical compressive strength
(Lura and Terrasi, 2014)	SAP for moisture evacuation during fire	• Reduced spalling of high performance concrete due to fire event • Reduced compressive strength • Poor performance regarding workability
(Justs *et al.*, 2015)	SAP	• Degree of hydration peak shift • Autogenous shrinkage reduction • Compressive strength reduction
(Hasholt and Jensen, 2015)	SAP	• Increased degree of hydration • Decreased chloride migration coefficient
(Shen *et al.*, 2015a)	SAP	• Maximum early-age expansion was increased when IC water was utilized • Maximum autogenous shrinkage and maximum shrinkage rate were decreased when IC water was utilized
(Snoeck *et al.*, 2015)	SAP	• Autogenous shrinkage rate decreased
(Snoeck, Jensen and De Belie, 2015)	SAP	• Micro and meso pores decrease for non-additional IC water • Meso pore increase when additional water was utilized
(Mechtcherine, Secrieru and Schröfl, 2015)	SAP	• Various grading of SAP affects the yield stress and viscosity • The finer the particles the greater the aforementioned parameters
(Ding, Zhang and Zhang, 2017)	SAP	• Increased size of SAP result in increased early-age strength and decreased later-age (28 days) strength

PERICLES ALEXANDROU SAVVA

		• Increased SAP dosage (>0.2%) result in reduced compressive strength
(Wehbe and Ghahremaninezhad, 2017)	SAP and shrinkage reducing admixtures	• SAP and shrinkage reducing admixtures result in reduced compressive strength due to formation of voids • SAP and shrinkage reducing admixtures result in reduced electrical resistivity
(Olawuyi and Boshoff, 2017)	SAP	• Increased Porosity • Porosity may be decreased when SAP dosage and IC water are adjusted
(Ma *et al.*, 2017)	SAP	• Same effective w/b ratio • Reduced compressive strength • Increased drying shrinkage • Increased absorption • Increased chloride ion coefficient • Same total w/b ratio • Increased compressive strength • Reduced drying shrinkage • Decreased permeability

Table 3-2: IC methods-summary

		LWA	SAP	Other
		Number of Studies		
Fresh properties				
Autogenous shrinkage	Reduction	7	13	2
	Elimination	1	1	-
Drying shrinkage	Beneficial	2	4	2
	Detrimental	-	4	-
Degree of hydration	Beneficial	4	3	1
	Detrimental	-	1	-
Mechanical properties				
Compressive strength	Beneficial	9	3	4

PERICLES ALEXANDROU SAVVA

	Detrimental	7	18	1
Tensile strength	Beneficial	3	-	1
	Detrimental	-	3	-
Flexural strength	Beneficial	2	-	1
	Detrimental	1	3	-
Modulus of elasticity	Beneficial	1	-	1
	Detrimental	2	2	1
Durability indicators				
Porosity	Beneficial	2	3	1
	Detrimental	1	5	1
Chloride migration	Beneficial	4	2	1
	Detrimental	-	-	-
Permeability	Beneficial	6	1	1
	Detrimental	-	1	2
Sorptivity	Beneficial	2	1	2
	Detrimental	2	2	-
ITZ quality	Beneficial	3	-	-
	Detrimental	-	-	-
Electrical resistivity	Beneficial	-	-	-
	Detrimental	-	1	-

PERICLES ALEXANDROU SAVVA

4. Investigation of internal curing using highly absorptive normal weight aggregates

The fact that IC has a beneficial effect on concrete was established through extensive literature review, presented in Chapter 3, and it can be stated that in low w/c or w/b cementitious mixtures the employment of IC reduces or fully eliminates early-age shrinkage. However, the topic of an optimum methodology or technique is still under research since the results from various laboratories are in contradiction (Table 3-2). The most established techniques still have several significant drawbacks that restrict their wide adoption in the construction sector (Table 3-2). Additionally, the cost of some of these techniques is another restricting factor for the implementation of the IC technique in conventional structures. The objective of this research was to develop an IC technique that overcomes most of the drawbacks and establish the methodology towards gaining better properties from low quality aggregates.

In order to prevent self-desiccation in a concrete mixture, it is necessary to maintain RH at high levels. The matrix of high performance concrete, which yields to depercolated capillary pores, hinders the diffusion of the external moisture throughout the material's structure (Sant, Bentz and Weiss, 2011). Therefore, in order to reach the inner core of such material's mass, dispersed water reservoirs must be employed. It is implied that a better dispersion will result in a uniform water utilization throughout the material's matrix increasing IC effectiveness. Two well established methods of IC are the use of SAP and LWA. Both methods have drawbacks. The addition of SAP weakens the material due to additional porosity and the addition of LWAs compromises the mechanical and transport properties of the material due to the introduction of porous and mechanically weak materials (Zhutovsky and Kovler, 2010). Byard reported that internally cured mixtures' (LWA) compressive strength decreases slightly in comparison with the corresponding reference mixtures' compressive strength (Byard, Schindler and Barnes, 2012). A round-robin test (RRT) conducted by 13 different laboratories across the world used the same mix design but local aggregates and examined the effect of including SAP in concrete. The majority of the researchers reported a decrease in compressive strength for concretes including SAP. Nevertheless, in some cases, an improvement in compressive strength was observed (Mechtcherine *et al.*, 2013). However, some researchers support that compressive strength reduction is not a consequence of SAP inclusion in concrete (Lura *et al.*, 2006). The consistent reduction in high performance concrete compressive strength can be surpassed by proper design, regarding the dosage and the curing of each mixture (RILEM TC 225-SAP, 2012). This suggests that the interest must be focused on achieving IC without affecting other properties of the material. Furthermore, other

PERICLES ALEXANDROU SAVVA

properties of the material are affected by the introduction of IC. Young's modulus and flexural strength seem to decrease due to lower stiffness and increased porosity (Zhutovsky and Kovler, 2010; Byard, Schindler and Barnes, 2012; Mechtcherine *et al.*, 2013). Additionally, in NWA mixtures, the permeability is governed by the cement paste permeability. In concrete mixtures including LWA, the permeability is influenced by the properties of LWA. A reduction in permeability and diffusivity can be expected in IC mixtures due to extended hydration that leads in capillary pores depercolation. However, in both SAP and LWA IC methods, additional porosity is expected to be introduced in concrete (RILEM TC 196-ICC Rep 41-6, 2007). Finally, it is reported that an IC design may yield to a compromise where certain material's properties are inevitably reduced in order to reduce shrinkage (Piérard, Pollet and Cauberg, 2006). It is, therefore, understandable that both methods are sensitive and in several occasions trial experiments may be required prior to any application.

4.1. Objective

The objective of this chapter was to evaluate the effectiveness of using HANWA as an IC agent without compromising the mechanical or durability properties of high performance concrete. It has to be mentioned that the aggregates employed for the control mixtures (NWA) were transferred from a source that is not available to the local construction companies. The HANWA aggregates come from one of the main local sources of aggregates. Therefore, the emphasis is on improving the specific poor quality material, by reversing its negative characteristic, very high absorption, into a beneficial action, IC. The principles of the specific work can be modified and be applicable in other applications (i.e. recycled aggregates) and countries.

The IC mechanism was thoroughly explained in the preceding chapters. The physical mechanism of achieving IC requires the RH decrease in the material's structure which is inevitable due to the intrinsic properties of cement, and a media that will be able to supply water in order to maintain or replenish the consumed moisture. The scope of this chapter is to employ, assess and establish the utilization of HANWA to deliver the required amount of IC water and achieve autogenous shrinkage reduction. Additionally, it is anticipated that the density of the specific aggregates will be the key factor towards expecting better performance of the HANWA-IC technique as opposed to LWA and SAP methodologies.

PERICLES ALEXANDROU SAWA

4.2. Experimental program

4.2.1. Materials

The cement utilized for this research was CEM I 52.5R (Table 4-1 and Table 4-3). Due to the type of cement, it was expected that the mixtures would develop their properties earlier. Therefore, out of the four tests scheduled for each mixture (3, 7, 28 and 90 days), two tests were conducted during the first week after casting. The mixtures workability was measured with respect to the required amount of polycarboxylate polymer superplasticizer (SP) added to the mixture. The objective was to maintain the slump within the range of 100±30 mm. The fraction of the coarse aggregates utilized was 4-10 mm. A similar fraction (4-8 mm LWA) was also used by Weber and Reinhardt in 1997, who established their IC effectiveness. The aggregate water absorption at 24 hours (WA_{24}) was measured according to EN-1097-6 (EN 1097, 2013) (Table 4-2) and the aggregates sieve analysis is provided in Figure 4-1 and Figure 4-2 (EN 933-1 and EN 12620). Both HANWA and NWA are crushed limestone aggregates. The compressive strength and modulus of elasticity of both types of aggregates utilized for this experimental program (HANWA and NWA) were tested according to EN 1926 (EN 1926, 2006) and EN 14580 (EN 14580, 2005), respectively.

Table 4-1: Chemical composition for CEM I 52.5R

CaO Free	0.344
C_3S	106.899
C_2S	24.136
C_3A	2.364
C_4AF	7.878

Table 4-2: Aggregates properties EN 1097 (EN 1097, 2013)

	Specific Gravity, ρ_a (g/cm^3)	Specific Gravity, ρ_{ssd} (g/cm^3)	Water Absorption, WA_{24}	Fraction (mm)
NWA	2.74	2.77	1.1%	4/10
HANWA	2.30	2.42	5.2%	4/10
SAND	2.63	2.66	1.2%	0/4

PERICLES ALEXANDROU SAVVA

The average compressive strength of six cylindrical specimens was 33.5 MPa (standard deviation 4.4 MPa) for HANWA and 80.3 MPa (standard deviation 5.7 MPa) for NWA, whereas, their modulus of elasticity was 19.3 GPa and 78.3 GPa, respectively (Figure 4-3).

Table 4-3: Typical cement properties for portland-composite cement EN197-1 CEM I 52.5R

Chemical Analysis	
Loss on Ignition %	4.46
SiO2 %	18.91
Al2O3 %	4.23
Fe2O3 %	2.99
CaO %	61.99
SO3 %	3.51
MgO %	1.79
Na2O %	0.34
K2O %	0.58
Chlorides %	0.02
Mechanical and Physical properties	
Specific surface, Blaine (m2/kg)	400
Normal consistency % H2O	28
Initial setting time (Vicat) min	220
Soundness expansion (Le Chatelieur) min	0-1

PERICLES ALEXANDROU SAVVA

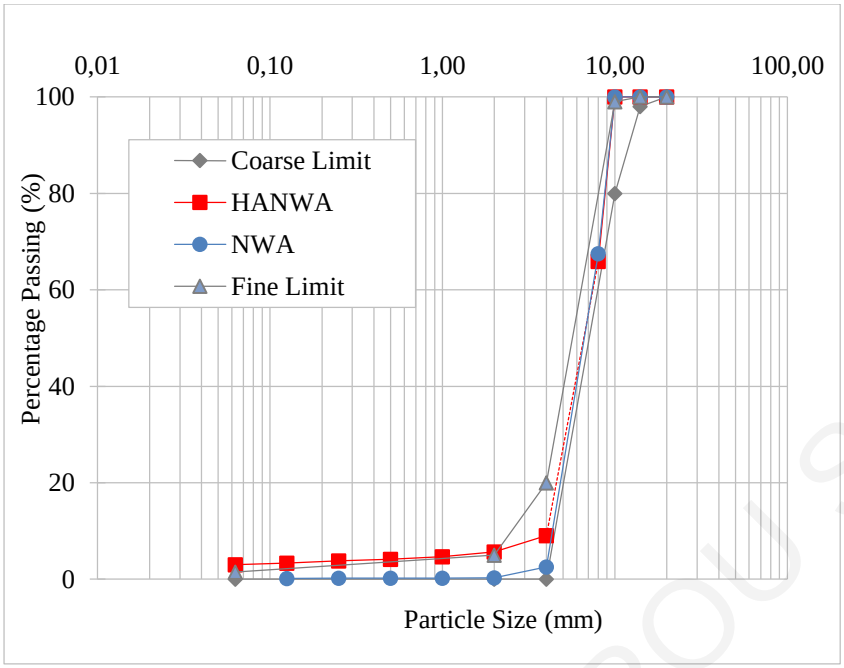

Figure 4-1: Coarse aggregates (NWA and HANWA) sieve analysis according to EN933-1 and EN12620

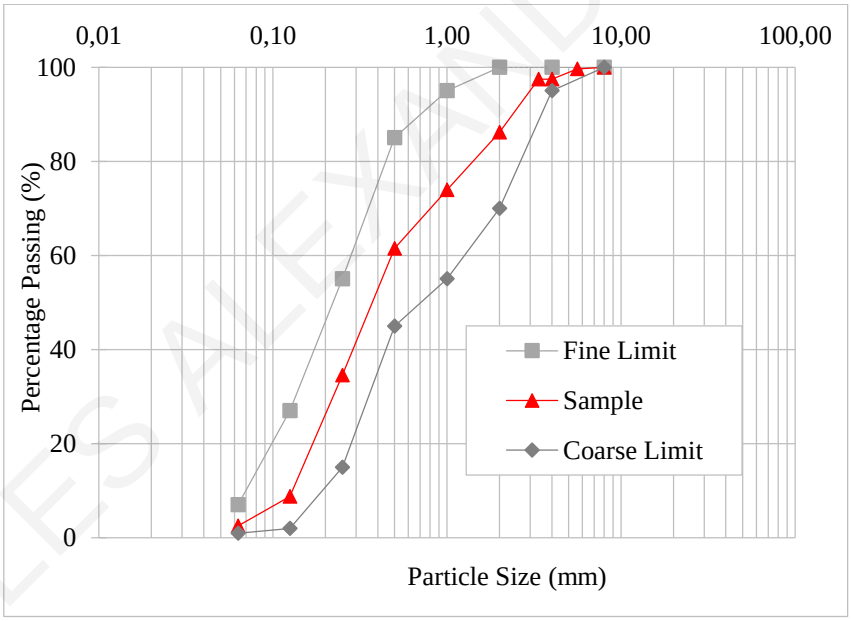

Figure 4-2: Fine aggregates (SAND) sieve analysis according to EN933-1 and EN12620

Five mixtures with low w/c ratio (0.25) were designed (Table 4-4). It was expected that autogenous shrinkage would be more intense in such low w/c ratio mixtures, thus the IC mediums intended to reduce autogenous shrinkage would be better evaluated. In order to reduce autogenous shrinkage, three IC mediums were employed. HANWA in two different states (SSD and DRY) and two types of SAP were compared. HANWA were added in two different conditions in order to clarify whether a saturated-surface dry (SSD) condition would affect the material's performance as opposed to a dry

PERICLES ALEXANDROU SAVVA

state (DRY). A water correction based on the aggregates' absorption was done for the dry aggregates. SAPs were employed in order to compare their effectiveness as opposed to HANWA. The calculation procedure of IC water is discussed in Section 4.2.4.

The mixtures were prepared in a horizontal rotary mixing machine. The slump of each fresh concrete mixture was measured in order to maintain consistent workability. The mixing constituents were maintained in a chamber for 24 hours before mixing to ensure constant temperature. After the specimens were cast, the molds were covered with wet burlaps in order to prevent moisture loss to the environment. 24 hours after casting the specimens were demolded and wrapped with polyvinyl chloride membrane in order to provide sealed conditions for curing. The efficiency of the membrane was verified with consecutive mass measurements. After mixing, the mixtures were tested for autogenous shrinkage and mass loss (Section 4.2.2 and 4.2.3).

Table 4-4: Mix constituents (kg/m^3) ACI 211.1-91 (America Concrete Institute, 2002)

	Control	HANWA-SSD	HANWA-DRY	SAP-T1	SAP-T2
CEM I 52.5R	864	864	864	864	864
Water	216	216	216	216	216
Coarse	854	854	854	854	854
Sand	499	344	344	383	383
SP (%)	0.09	0.05	0.05	0.04	0.23
SAP	-	-	-	1.5	1.7
IC water	-	44	44	44	44
Slump	70	100	85	85	80

PERICLES ALEXANDROU SAWA

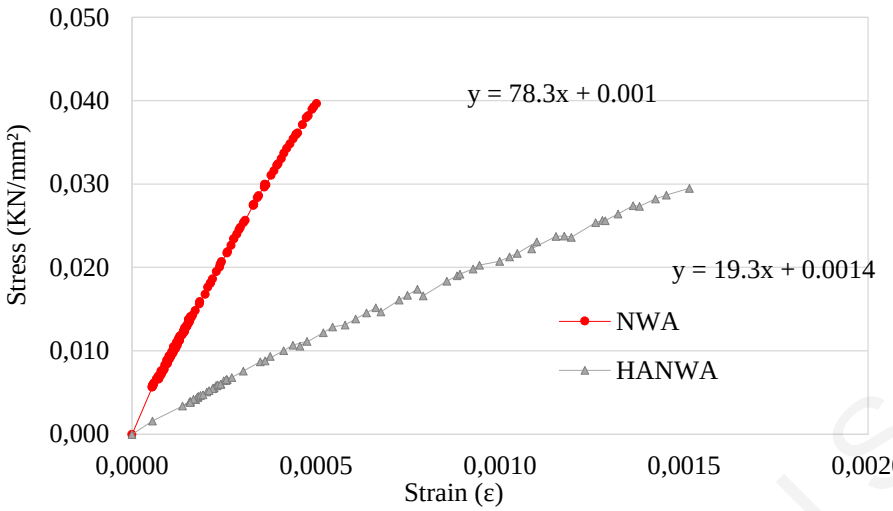

Figure 4-3: Aggregates Young's Modulus

4.2.2. HANWA aggregates

When the production of concrete started in Cyprus, the aggregates where mostly collected from nature, especialy from estuaries. The specific aggregates were rounded due to friction, since their source was the high mountain range of Troodos. The specific source was gradually replaced from Pentadaktylos limestone, which had superior quality and low quarry cost, since it was a byproduct of lime factories. Its utilization was suspended after the Turkish invasion and occupation. Afterwards, aggregates were collected from rivers and coasts up to the point that better sources were located in the South part of Cyprus. Since then the conctruction industry is working with the specific sources of aggregates. The main quarries are located in Farmakas and Parekklisia. The aggregates found in the south part of Cyprus nowadays are mainly diabase, limestone and limestone sand. The highest quality aggregates, as mentioned previously, are limestone located at Pentadaktylos. However, their utilization is not possible due to the lack of conformity marking required for products sold in the European Economic Area and their high cost. Cyprus now is "obliged" to use the best between the "worse" sources of aggregates. It has to be noted that the diabase aggregates exhibit higher quality than the limestone aggregates and that is the reason why the specific source is mostly utilized in the construction sector. The main drawback of the limestone aggregates is their high absorption (up to 5.0%). The specific disadvantage causes serious problems in terms of strength and durability, and any solutions may cause construction cost increase.

PERICLES ALEXANDROU SAVVA

4.2.2.1. Mineralogical composition

HANWA contain mainly micritic calcite which in restricted areas yields to microspar. Ioannou et al. observed the specific aggregates under microscope in order to interpret their high absorptivity (Ioannou *et al.*, 2010). Fossils, whose composition is mainly recrystallized sparry calcite, were observed, whereas micritic endoclasts and non-carbonate grains such as quartz, chert and spinel were sparsely observed. Traces of anhydrite were also observed. Their high absorptivity was attributed to the significant intraparticle porosity obtained within fossils, whereas elongated pores were formed due to recrystallization of spar crystals. The limestone contains mainly calcite at 85-90%, ankerite at 8-12% and in lower quantites quartz, albite and hematite. The main oxides of the limestones were chemically analysed and the following results were observed: CaO=44-46%, MgO=6-9%, SiO2=2-3% and in lower quantities Al2o3 and Fe2O3. The rest percentage corresponds to the loss of ignition (CO_2).

The NWA aggregates source is located in the Keryneia Terrane which is one of the three main allochthonous geological formations, which forms the main carbonate masses of the Pentadaktilos mountain range. The specific formation is composed of massive to thickly bedded dolomitic limestones (Cyprus Geological Survey Department, 2016)**.**

4.2.2.2. Desorption properties

The principle characteristic of an IC medium is its ability to absorb, hold and release moisture. Therefore, in order to design an IC mixture, absorption and desorption properties must be known. The aggregate used were tested for water absorption WA_{24} based on EN 1097 (2013) and presented in Table 4-2. In order to assess the aggregates behavior in the matrix their desorption isotherms have to be calculated. Desorption isotherms represent the materials mass loss as a function of various RH at constant temperature (Castro *et al.*, 2011). As mentioned previously, the main mechanism that will withdraw water from the aggregates pores is the under pressure developed due to chemical shrinkage and RH fall. Therefore, it is necessary to assess whether the IC medium will be able to provide adequate moisture in proper timing to ensure IC. Castro *et al.*, 2011, reported that an efficient IC medium would release water at high RH (i.e.93%) whereas a less efficient medium will release its water at lower RH values. Bentz *et al.*, 2005, declared that the water from the aggregates pores has to be released before the cement matrix RH levels drop below 85%.

An indirect way to check aggregates suitability is by assessing the aggregates ability to release moisture at high RH-levels. The HANWA used in this research were washed in a 63 μm sieve and

PERICLES ALEXANDROU SAWA

then oven dried until constant mass was reached. The aggregates were then placed in a wire basket and immersed in 22^{o}C water for 24h. The aggregates surface was then dried using a towel, according to the aggregates absorption method (EN 1097, 2013) and the sample was placed in an environmental chamber and exposed to constant temperature (22°C) with gradual RH decrease (1%) and their mass loss was recorded (Figure 4-4). HANWA aggregates were also examined in mercury intrusion porosimeter (MIP - Figure 6-4, Figure 6-5, Figure 6-6). The results presented in Figure 4-4 represent the average of two measurements with low variation, less than 2%. Based on Figure 4-4, the HANWA aggregates release 65% of their moisture at 93% RH, whereas another 15% of their moisture is released to a RH level of 85%. It is expected, therefore, that HANWA will be able to provide the majority of IC water at early-ages. It was expected that due to their smaller pores as opposed to LWAs, which is reflected on the desorption curve, the HANWA beneficial effect would occur more gradually and last for a longer period of time.

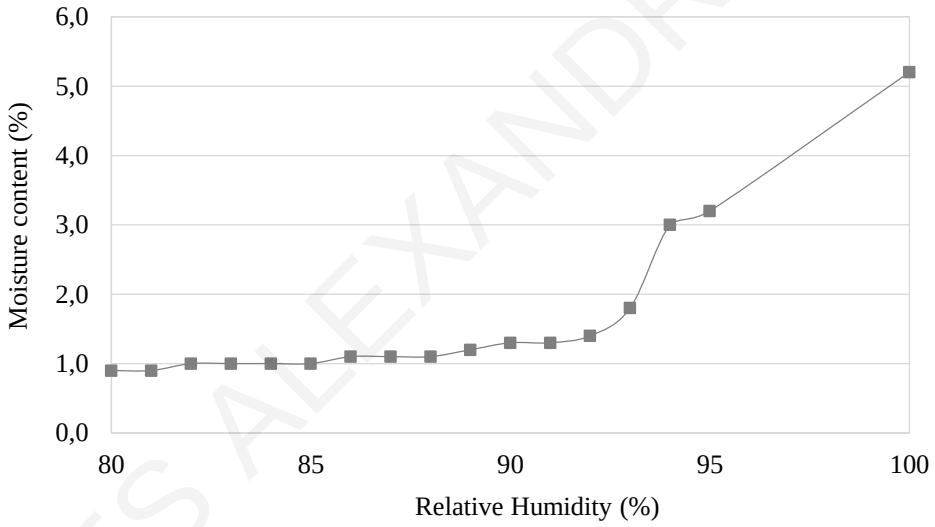

Figure 4-4: HANWA desorption properties

4.2.3. Superabsorbent polymers (SAPs)

The utilized SAPs were poly (acrylic acid) partial sodium salt for type 1 (SAP-T1) and poly (acrylic acid), partial potassium salt, slightly cross-linked for type 2 (SAP-T2). The polymers were tested suspended in pore solution using the teabag method. The pore fluid was obtained after mixing cement with water and acquiring the fluid on the top of the sediment cement paste. The pore fluid was tested based on the American Public Health Association (APHA) Association American Public Health, 2005). The results of the ion concentration were SO_4^{2-} 4 g/L, Ca 0.68 g/L, Na 0.77 g/L and K 24.8 g/L. The polymers absorbing capacity was 29 g/g for SAP-T1 (150 g/g in tap water) and 26 g/g for

PERICLES ALEXANDROU SAVVA

SAP-T2 (85 g/g in tap water) (Figure 4-5). Therefore, the amount of SAP required to carry the necessary quantity of IC water was 0.18% and 0.20% with respect to cement mass for SAP-T1 and SAP-T2 respectively. SAP particles size distribution is presented in Figure 4-6 and Figure 4-7. The polymers average particle size was 441 μm for SAP-T1 and 384 μm for SAP-T2.

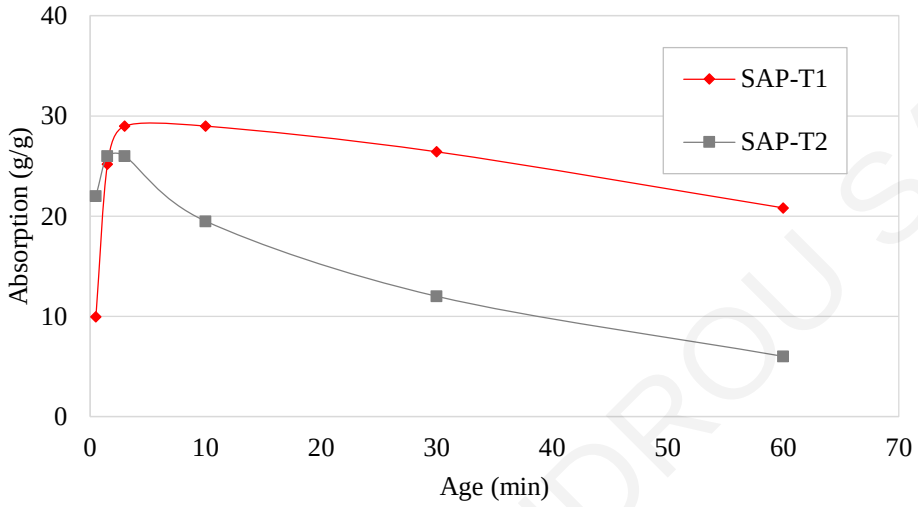

Figure 4-5: SAP absorptivity in pore fluid

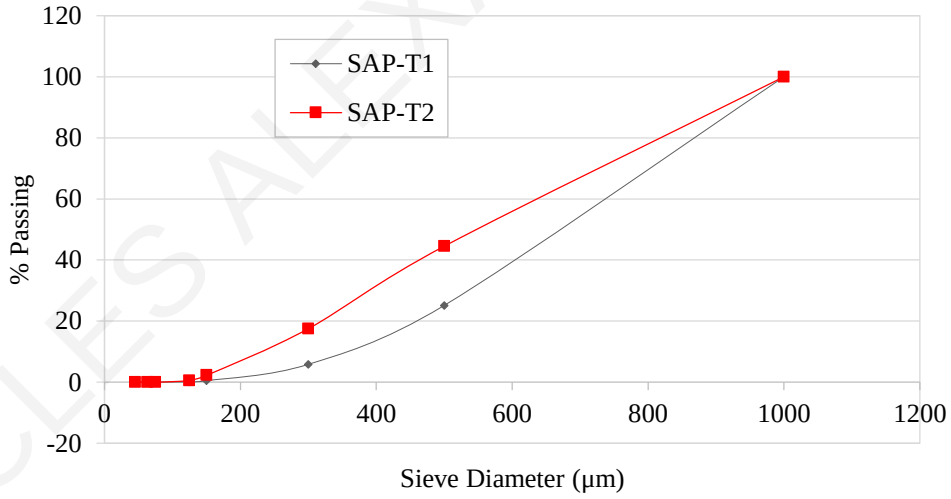

Figure 4-6: SAP cumulative particles size distribution

PERICLES ALEXANDROU SAVVA

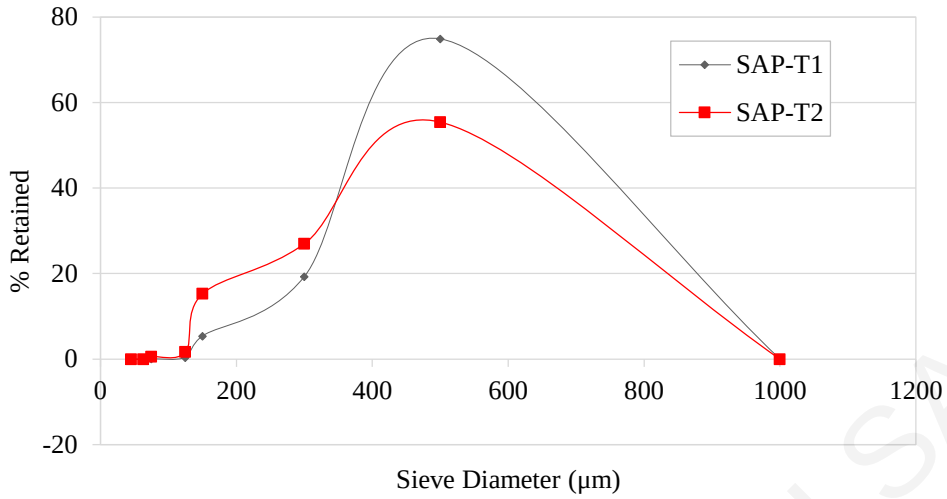

Figure 4-7: SAP incremental particles size distribution

4.2.4. Internal curing

The amount of coarse aggregates and SAP was calculated based on the IC water requirements extracted from Bentz equation (3-2) (D. P. Bentz and Snyder, 1999), according to the aggregates desorption (Figure 4-4) and the SAP absorption properties (Figure 4-5). According to Bentz equation, the aggregate degree of saturation and absorption capacity, the chemical shrinkage of the cement paste, the expected maximum degree of hydration and the cement content should be known. The cement chemical shrinkage was measured according to ASTM C1608 (ASTM C1608, 2008) – Section - 4.2.1 (Figure 4-8). The maximum degree of hydration (a_{max}) was estimated based on $a_{max} = (w/c)/0.36$ (RILEM TC 196-ICC Rep 41-4, 2007). Based on Figure 4-4, a more conservative approach regarding the degree of saturation should be followed. The aggregates desorption below 90% RH reaches 1% which corresponds to approximately 80% of their SSD absorption (5.15%). The amount of SAP required to carry the necessary quantity of IC water was 0.18% and 0.20% with respect to cement mass for SAP-T1 and SAP-T2 respectively.

4.1. Experiments

The experiments conducted to evaluate the IC efficiency using HANWA, are presented in Table 4-5 and described below. One prismatic specimen (40mm x 40mm x 160mm) from each batch was wrapped in membrane and stored in a controlled environment. After the specimens were solidified, two rectangular sections (7mm x 35mm) of membrane at the specimen's longitudinal opposite faces were removed using a surgical blade and the free surface was covered with epoxy resin. After the

PERICLES ALEXANDROU SAVVA

resin was solidified, 30 mm strain gauges were attached at each side and the specimens were wrapped again in order to isolate the specimens and the gauges from external moisture. The employed method ensured that the measured deformations would represent only longitudinal displacements of the specimen, and no moisture exchange would occur. Similar specimens with the ones utilized to measure autogenous shrinkage were cast in order to record their mass loss. The mass loss experiment is an indicator of the water retention of the investigated mixtures (Mousa *et al.*, 2015).

The compressive strength experiments were conducted according to EN 12390-3 (EN 12390 - 3, 2002). For compressive strength, cubic specimens were cast in 100 x 100 x 100 mm molds and tested at 3, 7, 28 and 90 days.

The experiments for the open porosity and sorptivity measurement were conducted in accordance to another research work (Kanellopoulos, Petrou and Ioannou, 2012) at 3, 7, 28, 90 days and 7, 28 and 90 days respectively. The open porosity value describes the ratio of the volume of the open pores to the total volume of the sample. The sorptivity value represents the material's absorptivity with respect to time. For the porosity experiments, the specimens were kept in a sealed chamber and the pressure was gradually lowered using a vacuum pump. The specimens were subjected to vacuum for 24 hours before being immersed in water. After 24 hours, their immersed and saturated mass were recorded before being placed in an oven at a constant temperature of 105^{o}C to remove the free water. After constant mass was reached, the dry mass of the specimens was recorded and the porosity of each specimen was calculated. The sorptivity measurement was conducted on dry specimens. The sorptivity test was previously used as a durability indicator (Kanellopoulos, Petrou and Ioannou, 2012).

The rapid chloride permeability (RCP) (ASTM C 1202, 2009) tests were conducted at 7, 28 and 90 days. The RCP experiment consisted of measuring the amount of chloride ions passing through the 50 mm thick cylindrical concrete specimens. The RCP cylindrical disks (Diameter 100 mm, Height 50 mm) were extracted from the mid-height of three different cylindrical specimens (Diameter 100 mm, Height 200 mm). The specimen sides were immersed in sodium chloride and sodium hydroxide and a potential difference of 60 V was maintained. The total charge passed, in coulombs, relates the resistance of the specimen to chloride ion penetration. Each specimen was conditioned according to ASTM C 1202 2009.

Two methods of curing were employed in order to assess the effect of external curing. One series of specimens was immersed in a water tank with constant temperature (23±1^{o}C) whereas another series

PERICLES ALEXANDROU SAVVA

was wrapped with polyvinyl chloride membrane and stored in a room with controlled temperature (23±1^{o}C). The cement hydration temperature evolution was monitored (Figure 4-12).

Table 4-5: Experiments for evaluation of IC efficiency using HANWA

Fresh state	**Mechanical properties**	**Durability properties**
Slump test	Compressive strength	Porosity
Maturing temperature		Sorptivity
		Rapid chloride permeability

4.2. Results and Discussion

4.2.1. Chemical shrinkage calculation

The chemical shrinkage was calculated according to ASTM C1608 2008 (Figure 4-8). Cement paste was mixed and placed in sealed vessels with water, covering the material's top surface. A cylindrical scale was embedded on the sealing rubber in order to monitor the material's shrinkage. In order to avoid evaporation, oil was added on the surface of the vessel water. The material's shrinkage was monitored through macroscopic inspection until constant indication was reached. The cement paste observed a chemical shrinkage equal to 6ml/100g of cement.

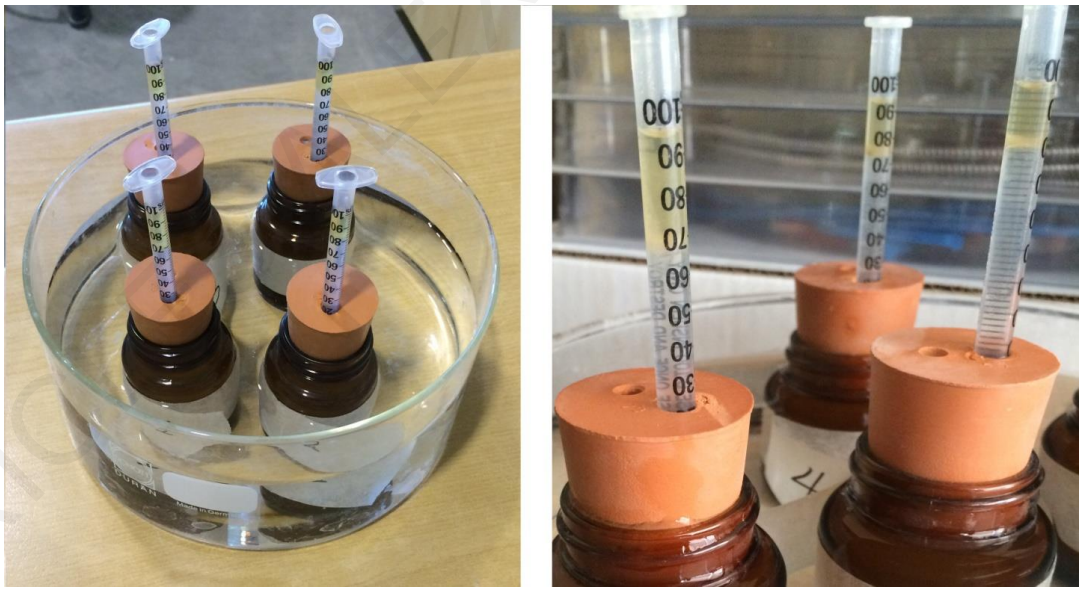

Figure 4-8: Chemical shrinkage measurement (average of four samples) ASTM C1608

4.2.2. Autogenous shrinkage

The effectiveness of an IC medium is reflected on the mixture's shrinkage since the implementation of IC aims to reduce the early-age volume variations that cause excessive internal stress and lead to

cracking. Therefore, autogenous shrinkage experiments were conducted in order to evaluate the effectiveness of the selected IC medium. Sealed concrete prisms with strain gauges attached on their longitudinal opposite faces were tested for 7 days after final setting. The mixtures were cured for 7 hours after casting and directly sealed after demolding with polyvinyl chloride membrane. The membrane at the strain gauges' location was removed using surgical blade and epoxy resin covered the surface. After the resin was solidified the strain gauges were attached and the specimen was wrapped again with membrane to ensure no moisture exchange with the environment. The experiments were conducted in an environmental chamber with constant temperature (22±1^{o}C) and RH (50±1%). Each strain gauge was connected to a strain indicator and the results were logged using pc units with a time interval of 15 minutes (Figure 4-9).

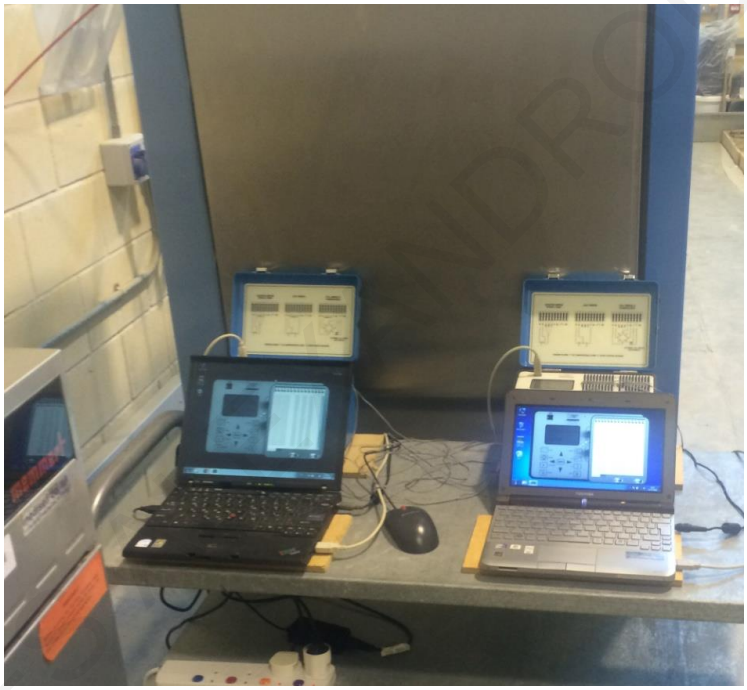

Figure 4-9: Climatic chamber and strain measurement configuration

The results of the autogenous shrinkage experiments are presented in Figure 4-10. As explained above, insufficient water in the material's pores would increase autogenous shrinkage. It was, therefore, expected that the control mixture would exhibit the highest autogenous shrinkage (Figure 4-10). The decrease of autogenous shrinkage in the IC mixtures demonstrated that the IC water was successfully distributed within the mixture's body increasing RH and reducing the materials' shrinkage. Mixtures HANWA-SSD, HANWA-DRY and SAP-T2 managed to reduce significantly autogenous shrinkage whereas SAP-T1 fully diminished it. More specifically, HANWA-SSD, HANWA-DRY and SAP-T2 exhibited around 50% lower autogenous shrinkage than the control mixture. The state of HANWAs

prior to entering the mixture does not affect the autogenous shrinkage. However, the mechanism of the autogenous shrinkage mitigation, is different for HANWA-SSD and HANWA-DRY. It seems that in HANWA-SSD the dominating mechanism is the IC whereas in the HANWA-DRY is the increase of the w/b ratio. The HANWA-SSD reduces autogenous shrinkage according to the mix design and known parameters such as self-desiccation, RH reduction and aggregates absorption, whereas HANWA-DRY autogenous shrinkage reduction occurred due to higher w/c ratio than the one designed. Finally, SAP mixtures exhibited the lowest autogenous shrinkage. It was anticipated that the specific polymers would perform very efficiently during the first days because at the age of 60 minutes the polymers are providing the majority of their water back to the mixture (Figure 4-5). Schröfl reported that SAP which observe an early desorption are likely to be effective for internal curing only at early-ages (Schröfl, Mechtcherine and Gorges, 2012).

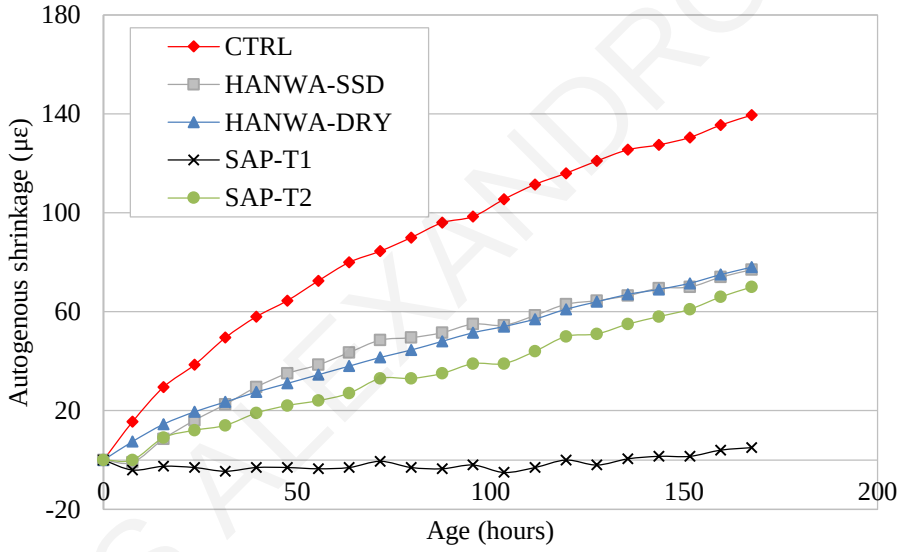

Figure 4-10: Autogenous shrinkage

4.2.3. Mass Loss

The mixtures' mass loss was necessary to determine whether a premature water release occurred, causing an increase to the effective w/b ratio. In the specific research, control, HANWA-SSD and SAP-T1 mixtures were investigated regarding their retention properties. Figure 4-11 presents the mass loss of the three aforementioned mixtures for a time period of 12 days.

PERICLES ALEXANDROU SAVVA

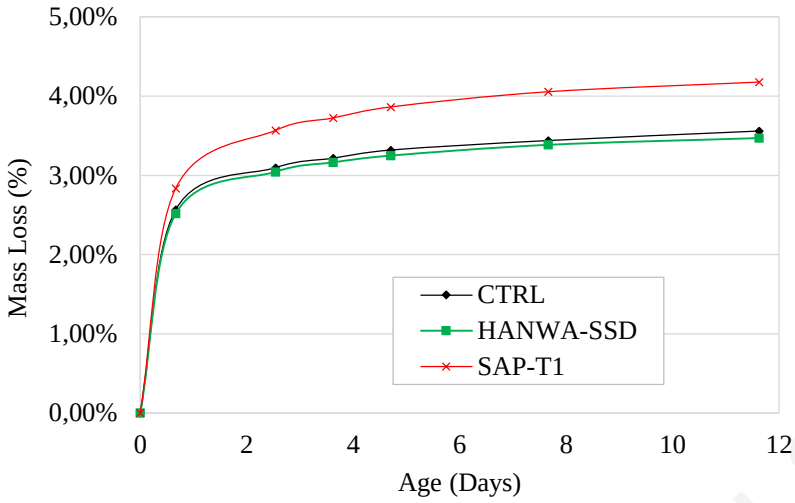

Figure 4-11: Mass loss of mixtures

It was observed that the SAP enriched mixture observed a greater mass loss as opposed to the control and HANWA-SSD mixture. This was in agreement with the SAP-T1 absorption/desorption properties (Figure 4-5). Additionally, the HANWA-SSD mixture exhibited identical mass loss with the control mixture. This finding is an indicator of a good water retention by the HANWA-SSD that does not allow premature water release. Moreover, the specific characteristic along with the findings presented in Figure 4-4 verified the suitability of the specific medium to be employed for IC purposes.

4.2.4. Maturing temperature

Three thermocouples were embedded in a concrete prism at three mid-height points along the specimen right after the mixtures were cast. The specimen was sealed to ensure no moisture exchange and the temperature was kept constant (23±1^{o}C). The mixture's maturing temperature was monitored until constant temperature was reached. Based on Neville (2002), the rate of heat evolution is comprised of three temperature peaks. The first which is the highest occurs at the point the cement comes in contact with water; its duration is very short and corresponds to the surface hydration of the cement particles and especially C_3A. The second peak happens at approximately 10 hours after the initial contact but occasionally can be observed as early as 4 hours. The third stage is observed in most types of cement and occurs due to an extended hydration of C_3A because of gypsum exhaustion. Gypsum is added in cement production in order to prevent the violent hydration that occurs after C_3A comes in contact with water. On Figure 4-12, the second stage of heat evolution is clearly observed as well as a very smooth increase at late hours which is likely to correspond to gypsum depletion.

The HANWA-IC mixtures exhibit a higher temperature at the second stage and this is attributed to the availability of IC water which is supplied to the mixture from the aggregate walls. It can be

PERICLES ALEXANDROU SAVVA

observed though that the slope of HANWA-SSD is steeper. It has to be mentioned that water is withdrawn from HANWA when the RH drops and negative pressure is developed within the material's pores. It is, therefore, concluded that the HANWA-DRY aggregates do not absorb the whole additional quantity of water which finally participates in the w/b ratio delaying the RH drop. It was clearly stated in the literature that the heat evolution during hydration is directly related to the degree of hydration (Double and Hellawell, 1977). The increased temperature peak is attributed to higher w/c ratio. Furthermore, SAP-T1 and control mixtures observed similar heat evolution; however, the SAP peak value is slightly shifted. The results of RILEM RRT (Mechtcherine *et al.*, 2013) showed that mixtures including IC water would observe an increased setting time. SAP-T2 exhibits a very different maturing behavior from the other mixtures. However, this is beyond the objective of the current investigation. It has to be mentioned though that the specific type of polymers observed a high reduction in mass at the first hours during the tea-bag test (Figure 4-5).

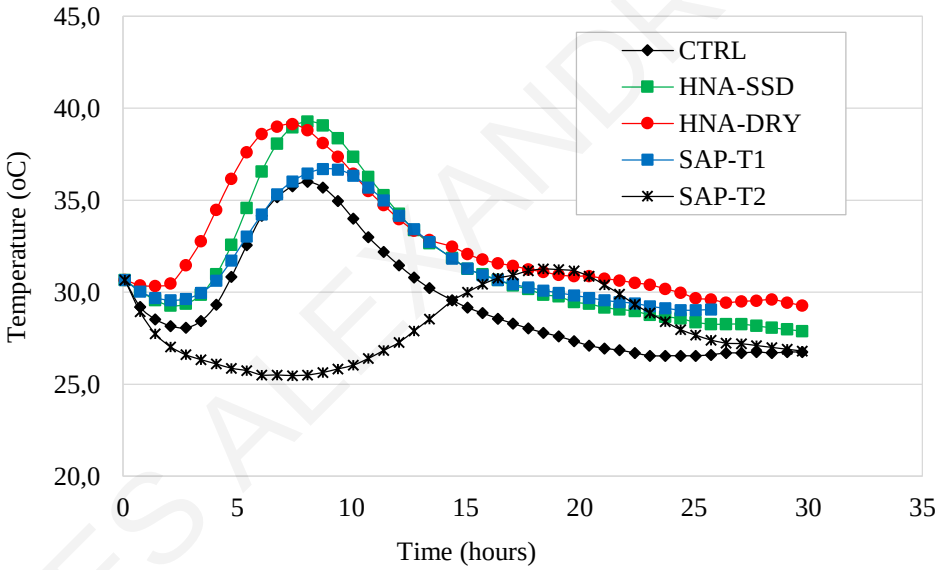

Figure 4-12: Maturing temperature

4.2.5. Effect on workability

The mixture's workability was evaluated with respect to the required amount of SP added to the mixture (Figure 4-13). HANWA-SSD, HANWA-DRY and SAP-T1 mixtures exhibited similar rheological behavior. The specific mixtures required an amount of 0.4 – 0.5%, with respect to cement mass, of SP to obtain the required workability. The HANWA-SSD mixture achieved a slight increased slump, 15 mm higher, as opposed to HANWA-DRY mixture even though the SP amount was the same. The specific variation was attributed to the instant adhesion of cement particles on the aggregates surface that smoothed out their rough surface. The control mixture required higher amount

PERICLES ALEXANDROU SAVVA

of SP in order to fulfill the slump requirements whereas SAP-T2 mixture required a very high amount of SP in order to obtain an acceptable workability (100±30 mm). The aggregates (HANWA and NWA) were examined using an image analysis software (ImageJ (Ferreira and Rasband, 2012)) in order to assess their circularity. Stereoscopy and image analysis techniques were developed and used in the industry for material development and improvement. Image analysis is a non-destructive technique that allows the operator to repeat various experiments and evaluate the results precision (Sumanasooriya and Neithalath, 2009). The aggregates threshold was adjusted based on their grayscale in order to convert the black and white image into a binary image (Figure 4-14). The binary image was used from the analysis software to clarify the matter in consideration and calculate the required circularity. The measurements were expressed as a number between 0.00 and 1.00, where 1.00 corresponds to a completely circular particle. As the measurement approaches 0.00, the corresponding particle approaches an increasingly elongated shape. The measurements were conducted on a minimum of 75 particles from each batch and both aggregates exhibited similar degree of circularity (HANWA: 0.61, NWA: 0.64).

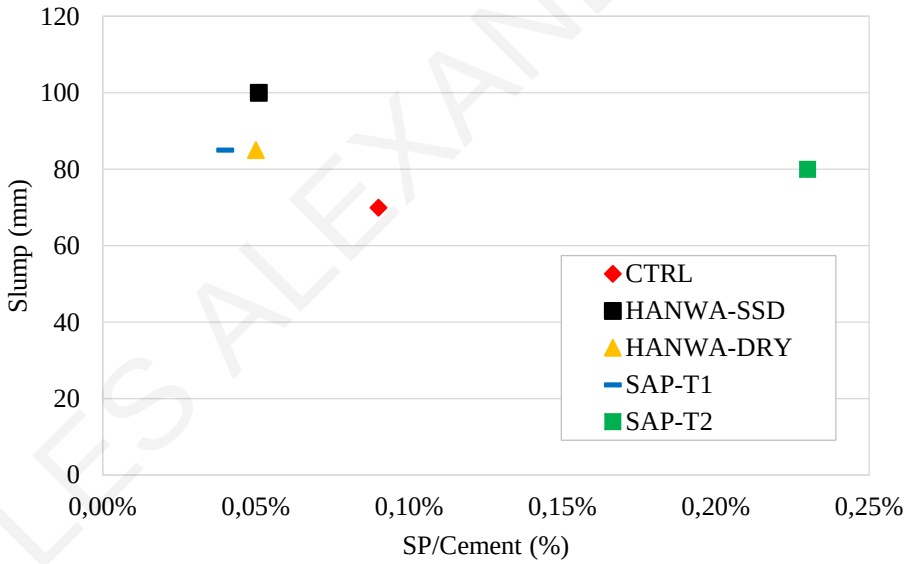

Figure 4-13: Mixtures' workability

PERICLES ALEXANDROU SAVA

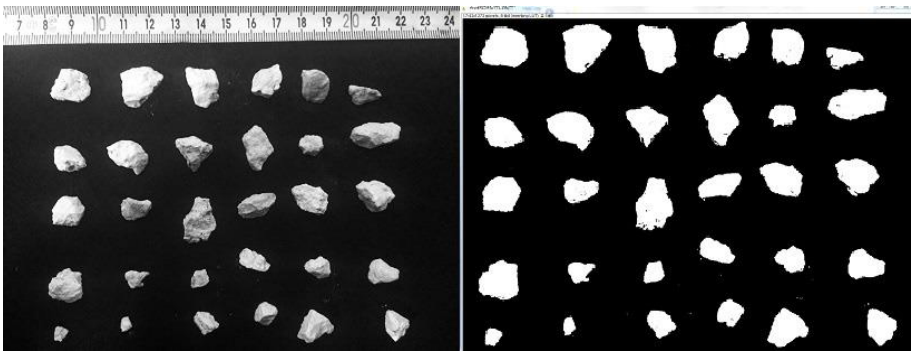

Figure 4-14: Captured image –Threshold image

It can be concluded that the different behavior is exclusively attributed to the IC mediums. HANWA-SSD, HANWA-DRY and SAP-T1 seem to benefit the mixtures workability whereas the control and SAP-T2 mixtures require higher amount of SP due to the lack of water. The workability variations caused by SAP strongly depend on the polymers absorption capacity, absorption rate and the additional water entering the system (RILEM TC 196-ICC Rep 41-5, 2007).

4.2.6. Compressive strength

The results of compressive strength as well as the standard deviation are presented on Table 4-6. The control mixture's compressive strength was expected to obtain the highest value due to the lack of IC materials and weak porous mediums. In fact, up to the age of 28 days, the control mixture developed the highest compressive strength as opposed to the rest of the mixtures, except from SAP-T2 in water curing regime. Interestingly, at the age of 90 days in all curing regimes, the control mixture exhibited a loss (average reduction = 5.3 MPa) in compressive strength. However, due to the high standard deviation (average SD = 7.2 MPa) observed, it could not be concluded that the material suffered a real reduction. It has to be mentioned thought, that the degree of hydration of a conventional concrete mixture with dense microstructure and no IC agents, is expected to be reduced exponentially with time (Cervera *et al.*, 2002). It is reasonable to expect a similar compressive strength at 28 and 90 days.

On the contrary, the HANWA-SSD mixture continued developing higher compressive strength with time. This was attributed to the extended hydration which was anticipated because of the dispersed IC sources of water. The aggregates small pores were expected to provide their water at lower RH levels, i.e. later-age. This was reflected on the results, since its compressive strength at the age of 90 days overcame the control mixture's compressive strength. Furthermore, the compressive strength of HANWA-SSD was on the average 11.5% higher than the HANWA-DRY at the age of 90 days. It is presumed that part of the water added for aggregate's humidity state correction in HANWA-DRY participated in the effective w/c ratio.

PERICLES ALEXANDROU SAVVA

The SAP mixtures observed reduced compressive strength at the early ages, which however, was fully recovered by the age of 28 days. SAP-T1 mixture observed an additional increase at the age of 90 days under water curing conditions. Since the specific behavior has not been observed in the membrane cured specimens and considering the SAP water exhaustion (Figure 4-5), the compressive strength increase cannot be attributed to an IC action. It is presumed that numerous parameters such as zero autogenous shrinkage (Figure 4-10) and easier external moisture diffusion due to increased porosity caused by SAP (Table 4-7), contributed to a better microstructure and an increased degree of hydration. Snoeck et al., using the water vapor sorption technique, confirmed that the amount of mesopores of SAP enriched mixtures was slightly higher (Snoeck *et al.*, 2015). On the other hand, the SAP-T2 mixtures exhibited a small decrease (average reduction = 4.5 MPa) in compressive strength at the age of 90 days. However, due to the high standard deviation (average SD = 6.8 MPa) observed, it could not be concluded that the material suffered a real reduction.

Table 4-6: Compressive strength (MPa)

	3 DAYS		7 DAYS		28 DAYS		90 DAYS	
	f_{cm}	SD	fcm	SD	fcm	SD	fcm	SD
	Membrane cured specimens							
CTRL	84.6	3.9	82.1	4.4	93.2	4.5	88.5	6.8
HANWA-SSD	76.2	3.8	76.7	0.7	80.3	3.2	86.1	3.4
HANWA-DRY	71.8	1.1	67.6	5.3	75.6	3.8	75.9	3.9
SAP-T1	62.6	4.1	72.9	2.3	80.4	5.1	81.7	1.6
SAP-T2	66.0	4.7	67.3	5.4	81.6	8.1	78.7	7.4
	Water cured specimens							
CTRL	71.7	5.8	79.7	5.6	80.9	6.6	75.0	7.6
HANWA-SSD	76.6	*2.4*	74.9	*4.0*	74.9	*4.0*	81.5	*3.9*
HANWA-DRY	62.7	*5.2*	73.0	*2.6*	74.3	*2.6*	74.4	*5.2*
SAP-T1	66.3	*2.3*	71.1	*2.0*	80.2	*3.4*	92.9	*4.1*
SAP-T2	58.8	*8.9*	66.5	*7.2*	84.7	*4.9*	78.6	*6.2*

PERICLES ALEXANDROU SAVVA

4.2.7. Open porosity

Table 4-7: Vacuum porosity

	3 DAYS	7 DAYS	28 DAYS	90 DAYS
	Membrane cured specimens			
Control	12.5%	11.4%	9.4%	8.2%
HANWA-SSD	14.8%	14.0%	13.7%	12.7%
HANWA-DRY	15.5%	14.7%	16.6%	17.1%
SAP-T1	17.5%	15.2%	15.3%	14.5%
SAP-T2	17.3%	16.3%	15.2%	14.7%
	Water cured specimens			
Control	12.8%	12.0%	9.9%	8.2%
HANWA-SSD	15.6%	14.8%	14.1%	13.6%
HANWA-DRY	15.1%	15.0%	15.6%	16.3%
SAP-T1	18.0%	16.2%	15.6%	14.2%
SAP-T2	17.4%	16.7%	15.3%	15.0%

The porosity values of the mixtures are presented in Table 4-7. The control mixture exhibited the lowest porosity in comparison with the IC mixtures. As mentioned previously, IC implementation has specific disadvantages, since extra porosity or porous materials are being added to the mixture. SAP mixtures exhibited high porosity at early-ages, which was anticipated. However, the expected reduction of porosity at 28 days was not reflected in the results of the membrane cured specimens. This was attributed to the fact that the specific polymers utilized in this research were likely to exhaust their IC ability at early ages (Figure 4-5). A premature exhaustion led to an increased w/b ratio that subsequently led to an increased porosity. Moreover, the space occupied by the polymers particles remained empty and the occupied volume was added up to the total porosity. On the other hand, the HANWA-SSD mixture exhibited a very good performance in terms of porosity at later-age, compared to the other IC mixtures. It seems that the specific IC medium was able to provide IC water even at later ages. It is noticeable that the membrane curing method seemed to be slightly more effective than the water curing method. Furthermore, the HANWA-DRY mixture performed poorly in comparison with the HANWA-SSD mixture. It seems that the specific aggregates did not absorb the total quantity of added water.

PERICLES ALEXANDROU SAVVA

4.2.8. Rapid chloride permeability

Table 4-8: RCP results (Coulombs)

	7DAYS	28DAYS	90DAYS	Reduction rate 7 to 90 days (Coul. /Day)	Average (Coul. /Day)
	Membrane cured specimens				
Control	3695	2352	1378	25	25
HANWA-SSD	5850	3022	2137	38	38
HANWA-DRY	5433	4410	2202	38	
SAP-T1	6554	3831	2198	47	39
SAP-T2	4972	4258	2333	32	
	Water cured specimens				
Control	3228	2088	1168	23	23
HANWA-SSD	5736	3978	1974	42	39
HANWA-DRY	4576	3556	1606	35	
SAP-T1	6249	3714	2228	43	37
SAP-T2	5100	3648	2314	31	

The specific experiments were conducted on disk specimens, as explained in section 4.1. Based on Table 4-8, the control mixture exhibited the lowest permeability value. The specific mixture included NWA and no IC agent. It is presumed that its dense microstructure due to the constituent materials and the aggregates' low absorptivity yielded in a refined pore network. Several conclusions can be drawn by observing the evolution of RCP reduction in Table 4-8. Specifically, all the mixtures exhibited a similar reduction (approximately 60%) from day 7 to day 90 except SAP-T2. The specific mixture seemed to suffer an early-age water exhaustion and therefore IC contribution was diminished after the first days of the material's life-cycle. Nevertheless, despite the identical reduction observed in all mixtures, the reduction rate and the average reduction rate, presented in Table 4-8, demonstrate the effectiveness of IC methods in contrast to the control mixture. The specific mixtures exhibited high RCP in the early-ages due to additional porosity yielded by the IC mediums, which however was compensated by an enhanced degree of hydration that occurred at a later stage. It is clearly observed in Table 4-8 that the IC mixtures exhibited a steeper RCP reduction as opposed to the control mixture.

PERICLES ALEXANDROU SAVVA

On average the IC mixtures observed an approximate 35% higher reduction rate as opposed to the control mixture.

SAP-T2 mixture exhibits the lowest reduction rate among the IC mixtures. However, it has to be stated that the specific mixture along with the control exhibited the lowest RCP values at early-ages (7days). Moreover, the control mixtures exhibited the lowest RCP values at 90 days. HANWA mixtures observed an RCP value around 2000 Coulombs which is satisfactory, considering the poor quality of the specific aggregates. Furthermore, the curing method does not seem to highly affect the results. It is worth noticing, however, that the majority of the specimens subjected to water curing had consistently exhibited lower RCP values. In fact, on the average, the water cured specimens exhibited around 6% lower RCP values as opposed to the membrane cured specimens.

4.2.9. Sorptivity

Sorptivity was measured at the age of 7, 28 and 90 days (Figure 4-15, Figure 4-16, Table 4-9). The experiments were conducted according to (Kanellopoulos, Petrou and Ioannou, 2012). It is important to highlight the IC mixtures sorptivity between the 7^{th} and the 28^{th} day, which reveals the IC action. However, the most significant conclusion is the mixtures' increase in sorptivity at the age of 90 days. It has to be reminded that the aggregates used in the current research work were limestone. Matschei et al. mentioned that the addition of coarse limestone aggregates in cement mixtures may result in a delayed reaction between the two (Matschei, Lothenbach and Glasser, 2007). The kinetics of the specific reaction are expected to be slower due to the size of the aggregates that result in lower available surface area for reaction and lower species diffusion towards the region where the reaction occurs. It is expected that the specific reaction will form a porous structure at the region, probably due to the formation of ettringite. It is understandable that the specific region is the interfacial transition zone (ITZ). Therefore, the compressive strength immunity can be explained. The sorptivity increase at the 90^{th} day was more prominent in the SAP mixtures. The polymers addition within the mixtures structure is expected to increase the porosity of the specimen evenly, due to their small particle size (~0.4 mm - 4.2.3) in contrast to the aggregates whose smallest particle size was 4 mm (4.2.2) as illustrated in Figure 4-16. Therefore, the sorptivity measurement on a given surface is possibly higher in SAP mixtures than HANWA mixtures. In all cases, the controlled curing specimens exhibited higher sorptivity than the membrane curing specimens. Finally, comparing the average sorptivity with respect to the control mixtures, the HANWA-SSD, the HANWA-DRY, the SAP-T1 and the SAP-T2 mixtures exhibited 22%, 30%, 26%, and 28% higher sorptivity than the control mixture, respectively.

PERICLES ALEXANDROU SAWA

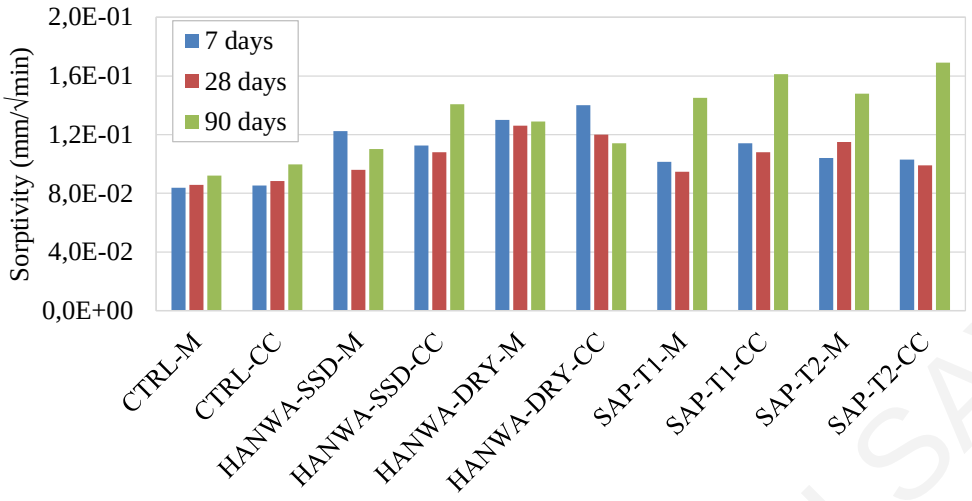

Figure 4-15: Sorptivity values of all mixtures

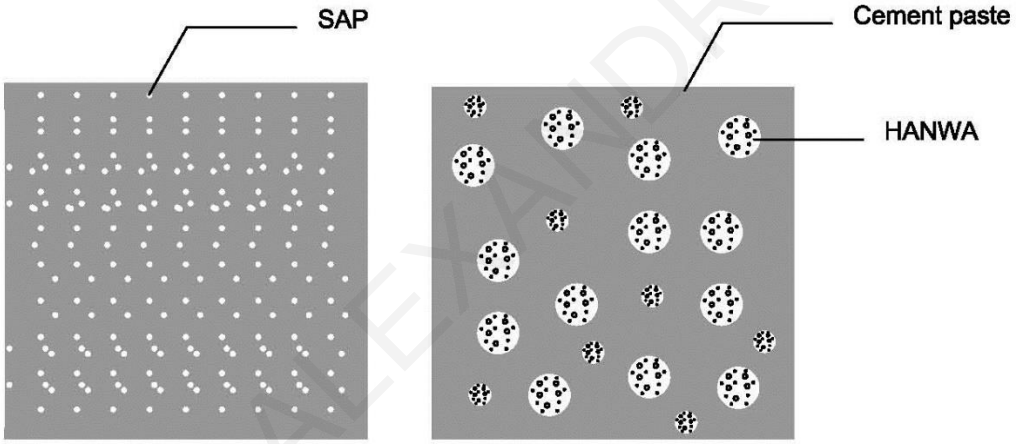

Figure 4-16: Sorptivity testing surface of HANWA and SAP

Table 4-9: Sorptivity values of all mixtures (mm/√min)

	Membrane cured specimens		
Control	0.084	0.086	0.092
HANWA-SSD	0.122	0.096	0.110
HANWA-DRY	0.130	0.126	0.129
SAP-T1	0.101	0.095	0.145
SAP-T2	0.104	0.115	0.148

PERICLES ALEXANDROU SAVVA

	Water cured specimens		
Control	0.085	0.088	0.100
HANWA-SSD	0.113	0.108	0.141
HANWA-DRY	0.140	0.120	0.114
SAP-T1	0.114	0.108	0.161
SAP-T2	0.103	0.099	0.169

4.2.10. Relative Humidity

RH drop develops the demand for IC and initiates the IC mechanism. The RH monitoring during the material's maturing period is of essential importance in order to clarify the material's need for IC and quantify the IC medium's efficiency. Commercial RH sensors were utilized for RH measurement. For the specific experiments, two commercial moisture sensors were utilized in order to evaluate the inner moisture condition of the two basic mixtures (control and HANWA-SSD) with respect to time (Figure 4-17). More specifically the ML3 thetaprobe soil moisture sensors with an accuracy of ± 0.01 m3.m-3 (1%) from Delta-T company were utilized with an analogue data logger. The measurements were continuously recorded at preset time intervals on a computer, via a nine pin RS232 cable. It has to be mentioned that the experiments were conducted at the same time and moisture exchange was restricted using water insulation. In addition, the temperature was kept constant at 22^{o}C (±2^{o}C). The mixtures mix design (Table 4-4) was the same as in the mixtures presented in section 4.2.1. The raw materials including water were kept at constant temperature (22^{o}C (±2^{o}C)) for 24 hours prior to mixing.

The results showed that between the second and the third day, the two mixtures' moisture content observed a divergence, which is interpreted as the HANWA pore water being diffused within the materials structure. More specifically, the specific figure justifies the initiation of IC using HANWA. It has to be mentioned that the specific measurements are going to be conducted using a fibre optic technique developed within the framework of the current research work, in order to verify the results.

PERICLES ALEXANDROU SAVVA

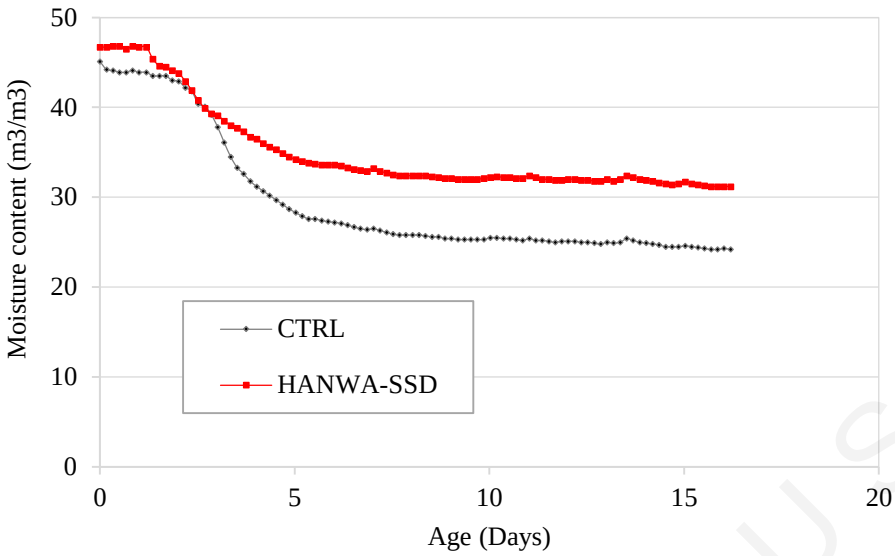

Figure 4-17: Moisture content of control and HANWA-SSD

4.3. Restrained shrinkage

4.3.1. Ring test method

Testing shrinkage is generally classified in two groups: Restrained and unrestrained shrinkage test methodologies. Tritsch *et al.*, 2005 divided the restrained shrinkage tests into three categories: plate tests, linear tests, and ring tests. Several studies performed different techniques to identify the shrinkage cracking tendency of concrete using a wide range of test apparatus. ASTM C 157-04 tests are commonly used to evaluate the free shrinkage of a concrete mixture (Sant, Lura and Weiss, 2006). Free shrinkage by itself is very difficult to predict whether cracking will appear in concrete. It was clarified though that the main factors that affect the material's shrinkage and cracking possibility are related to a combination of many factors considering the magnitude of free shrinkage, elastic modulus, degree of restraint, the rate of shrinkage, creep and stress relaxation and fracture toughness (Table 4-10) (Weiss, Yang and Shah, 2000). The shrinkage and cracking propensity of concrete using the restrained ring test method was studied thoroughly during the last decade (Weiss, Yang and Shah, 2000; Tritsch, Darwin and Browning, 2005; Gao, Zhang and Han, 2013; Choi *et al.*, 2015). Restrained shrinkage test methods have as a target to measure the related shrinkage-cracking rather the shrinkage mechanism itself. The ring test method became the most common and popular technique used to evaluate or identify the shrinkage cracking potential of concrete.

PERICLES ALEXANDROU SAVVA

Table 4-10: Properties that affect the shrinkage of concrete

Property	Critical parameters
Evaporation rate and duration	Environmental conditions, water content
Elastic Modulus	ITZ, w/b ratio, aggregates
Free shrinkage	Cement type, w/b ratio, curing conditions
Degree of restraint	Aggregates, age
Creep	w/b ratio, loading, ITZ, bond
Stress relaxation	ITZ, aggregates, bond

4.3.1.1. Experimental setup

Many different concrete rings were tested under a variation of restrained conditions. Although concrete testing is a standardized method (ASTM C 1581, 2009), various attempts were made for a better understanding of the stress development by changing the shape and dimensions of the configuration (Dong *et al.*, 2016). The dimensions of the concrete ring, as well as the test procedure, vary greatly in the literature (Hossain and Weiss, 2004; Eppers, 2010; Briffaut *et al.*, 2011; Dong *et al.*, 2016). The concrete ring is cast around a steel ring. As the concrete dries out, it undergoes shrinkage but the steel reactively prevents the shrinkage providing restraint to concrete. The restraint leads to stress development in the circular direction. The dimensions of the samples can be designed in such way (thin wall) to approximate uniaxial tension as a cause of restraint.

The specific test restrains the cast material which exerts force on a steel ring in its effort to shrink. Similar forces are exerted from fresh concrete on formworks, adjacent structures (Eppers, 2010), or within its own volume when it is a mass structure. These forces are converted in deformations which are monitored using three embedded strain gauges. The material will exert high deformation if autogenous and drying shrinkages are high. High autogenous shrinkage will be caused by low w/c ratio and high drying shrinkage will be caused due to extreme environmental conditions and high w/c ratio.. The ring test configuration is shown in Figure 4-18 and Figure 4-19 whereas the testing environment was maintained at 23.0±2.0°C temperature and 50±4% RH in an environmental chamber (Figure 4-20), according to (ASTM C 1581, 2009).

PERICLES ALEXANDROU SAVVA

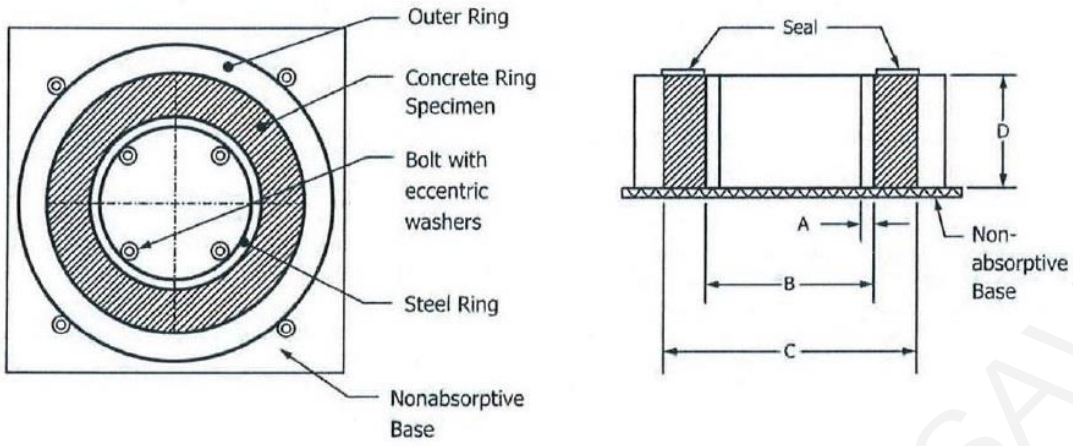

Figure 4-18: Ring test configuration (ASTM C 1581, 2009)

Figure 4-19: Ring test configuration

Figure 4-20: Environmental chamber and pc units for ring test experiments

PERICLES ALEXANDROU SAVVA

4.3.1.2. Results and Discussion

The results from the restrained shrinkage experiments on the three mixtures investigated (control, HANWA-SSD and SAP-T1, mixtures are provided in Table 4-4) are presented in Figure 4-21. It can be seen that HANWA-SSD cracked approximately 6 days after the control mixture, whereas the SAP-T1 mixture failed a few hours after the control mixture. The specific finding is in agreement with various researchers who stated that SAP increase, or do not decrease the material's drying shrinkage (Mechtcherine *et al.*, 2006; Piérard, Pollet and Cauberg, 2006; Justs *et al.*, 2015). The specimens were analyzed by Image J analysis (Ferreira and Rasband, 2012) in order to estimate their crack width (Figure 4-22). It was concluded that the HANWA-SSD specimen had an average crack width of 0.24 mm as opposed to the control and SAP-T1 specimens which had an average crack width of 1.93 mm and 1.79 mm respectively. Moreover, the shrinkage development rate in the case of the SAP mixture was 50% higher as opposed to the HANWA-SSD mixture and 33% higher for the control as opposed to the HANWA-SSD mixture.

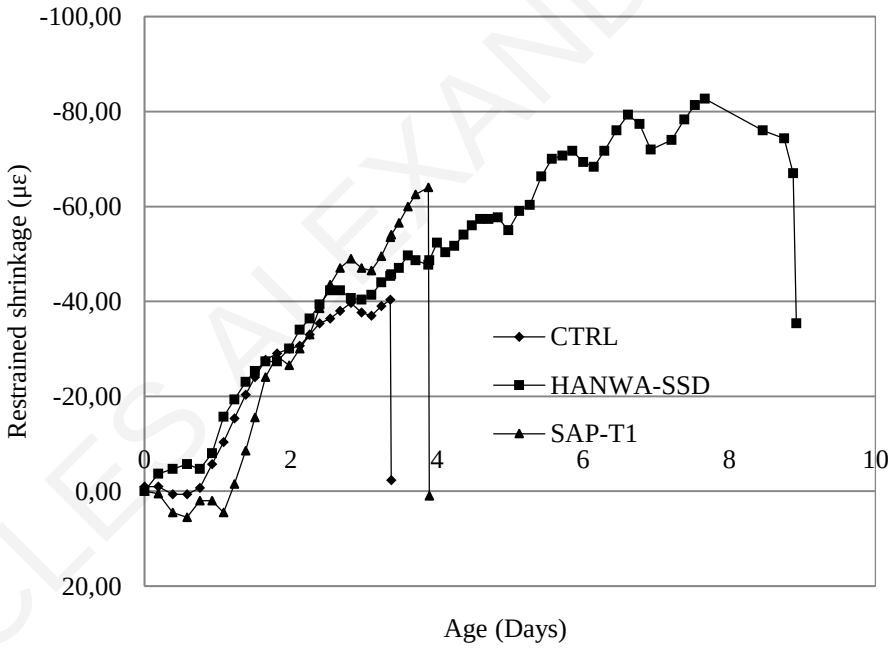

Figure 4-21: Restrained shrinkage of mixtures control, HANWA SSD and SAP-T1

The control specimen exhibited intense microcracking which was visible (Figure 4-22-b) prior to failure. This was an indicator of the intense drying shrinkage that developed within the material's structure, as opposed to both IC mixtures HANWA-SSD (Figure 4-22-a) and SAP-T1 (Figure 4-22-c).

PERICLES ALEXANDROU SAWA

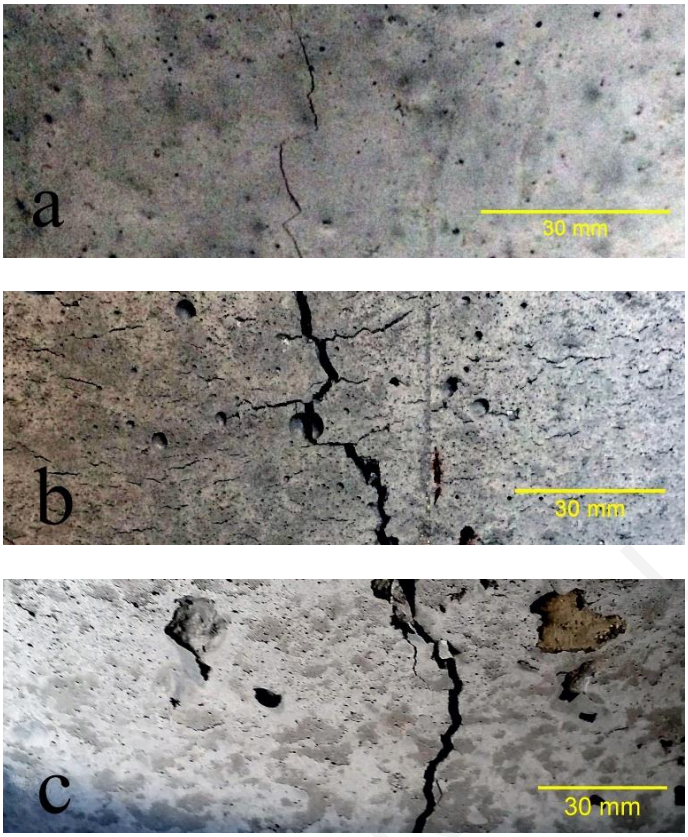

Figure 4-22: Specimens' surface after failure (a) HANWA-SSD (b) control (c) SAP-T1

4.4. Correlations

The results of the compressive strength, porosity, RCP and sorptivity were analyzed using the coefficient of determination denoted as R^2. It has to be said that the correlation coefficient is an indicator of the mixtures consistency and as such, it doesn't reflect a mixtures quality. The properties denoted "Membrane cured" and "Water cured" represent average values of the specimens cured under the specific conditions, regardless of the type of aggregates or IC inclusion. Each coefficient represents the material's property for all time intervals, 3, 7, 28 and 90 days. Therefore, each coefficient of determination was calculated using four points.

Based on Table 4-11, the most important conclusions is the excellent correlation between the Porosity and the RCP values (average R^2: 0.97). The only mixture that observed slightly lower degree of correlation (R^2: 0.86) was SAP-T2. The compressive strength of IC mixtures HANWA-SSD and SAP-T1 observed an excellent correlation with the RCP values. On the average, all the mixtures exhibited excellent property correlations, except SAP-T2, which exhibited a good correlation, and the control which exhibited a poor correlation.

PERICLES ALEXANDROU SAVVA

Table 4-11: Coefficient of Determination (R^2) for linear correlation of various properties of the mixtures (fcm: Compressive strength, P: Porosity, RCP: Rapid chloride permeability)

	RCP	fcm	P	S	Sorptivity	fcm	P	Porosity	fcm
All		0.80	1.00	0.54		0.13	0.56		0.92
M		0.78	0.99	0.51		0.09	0.41		0.87
C		0.84	0.96	0.57		0.19	0.75		0.94
Control		0.53	0.99	0.86		0.87	0.79		0.36
HANWA SSD		0.99	0.95	0.05		0.08	0.18		0.81
HANWA DRY		0.61	0.98	0.67		1.00	0.53		0.82
SAP-T1		0.99	1.00	0.50		0.60	0.45		0.74
SAP-T2		0.34	0.86	0.88		0.07	0.55		0.89
Average		0.73	0.97	0.57		0.38	0.53		0.79

The same procedure was followed for the mixtures' aging. The coefficient of determination, R^2, of each mixture was evaluated with respect to their age. Each value represents the average of all properties (RCP, P, fcm, S) plotted with respect to their age (3, 7, 28, 90days). The specific coefficients were calculated for both linear and logarithmic time scale, in order to evaluate whether the property development rate was decreased with respect to time. Observing Table 4-12, the HANWA-SSD exhibited an excellent linear behavior regarding its properties development. This was attributed to the material's ability to retain its IC effectiveness even after the 28 days, contributing to a continuous hydration. This was confirmed also from the mercury intrusion porosimeter results (Section 6.4). It is well known that water from IC mediums' small pores will be withdrawn at lower pressure level, which is likely to be developed in an isolated pore system with low RH. SAP-T1 mixture also observed a good linear correlation, although its logarithmic correlation was better. The specific mixture observed a compressive strength increase from 28 to 90 days, explained in section 4.2.6. HANWA-DRY and SAP-T2 mixtures observed a completely different behavior. More specifically, these mixtures exhibited an excellent correlation when their age was plotted on a logarithmic scale versus their properties. This was attributed to the water consumption due to hydration and lack of extra water for additional hydration. Finally, the control mixture exhibited a moderate to good correlation with the linear age scale, where its correlation was highly improved when the age was plotted on a logarithmic scale.

PERICLES ALEXANDROU SAVVA

Table 4-12: Coefficient of Determination (R^2) for linear and logarithmic correlation of different properties and age

	Linear				Logarithmic			
	fcm	P	RCP	S	fcm	P	RCP	S
All	0.58	0.70	0.91	0.82	0.91	0.94	1.00	0.52
M	0.60	0.73	0.90	0.80	0.87	0.97	1.00	0.50
C	0.50	0.65	0.92	0.83	0.84	0.88	1.00	0.53
Control	0.79	0.81	0.88	1.00	0.42	0.99	1.00	0.88
HANWA SSD	0.92	0.81	0.84	0.34	0.91	0.97	0.99	0.09
HANWA DRY	0.58	0.64	0.99	0.59	0.91	0.85	0.94	0.87
SAP-T1	0.80	0.81	0.83	0.88	0.99	0.81	0.99	0.60
SAP-T2	0.38	0.70	0.97	0.96	0.76	0.96	0.97	0.76
Average	0.64	0.73	0.91	0.78	0.83	0.92	0.99	0.59

Additionally, the results were grouped according to the IC medium and curing regime at first, and IC medium in following (Table 4-13 and Table 4-14). Comparing the performance of the IC mediums as opposed to the control mixture, it was observed that even though the late-age porosity values of the later was significantly lower, it was not reflected on the compressive strength as well. Moreover, the membrane cured specimens regarding the control mixture exhibited improved compressive strength and slightly poorer durability properties, compared to the water cured specimens. Similar behavior was observed in the HANWA mixtures, while the two curing regimes of the SAP mixtures didn't show any significant differences. The retardation of hydration occurring in the control mixture, which was also verified in Table 4-12 where the control compressive strength exhibited an excellent correlation with the age on a logarithmic scale, might occurred due to space limitations, namely gel/space ratio, and lack of available water for hydration. Finally, observing the early and late-age RCP and porosity of the IC mixtures, it can be seen that the RCP reduction was much more efficient (approximately 60%) than the porosity (16% for HANWA and 3.5% for SAP). As mentioned previously, the IC mediums are either porous mediums or polymers whose exhaustion creates additional porosity. The difference between SAP and a porous medium, is that the latter is likely to exhibit a "sealed surface" at later-ages, because enhanced hydration occurs in the region of the

PERICLES ALEXANDROS SAVVA

aggregates surface. Therefore, even if their inner structure will remain porous, the moisture diffusion within their structure will be much more difficult. That was most likely the reason why the HANWA mixtures observed a greater reduction in porosity and RCP, as opposed to the SAP mixtures. Moreover, it was anticipated that IC mediums would be more efficient in sealing the pore network as opposed to decreasing the total open porosity. The specific conjecture was based on the ability of IC water, to travel only a certain distance away from their source (P. D. Bentz and Snyder, 1999), thus their effectiveness in sealing pores larger than a few hundred of micrometers will be limited.

PERICLES ALEXANDROU SAVVA

Table 4-13: Grouped results according to IC medium

		3 DAYS				7 DAYS				28 DAYS				90 DAYS			
		fc Mpa	Porosity %	RCP Coul.	Sorptivity mm/t^1/2	fc Mpa	Porosity %	RCP Coul.	Sorptivity mm/t^1/2	fc Mpa	Porosity %	RCP Coul.	Sorptivity mm/t^1/2	fc Mpa	Porosity %	RCP Coul.	Sorptivity mm/t^1/2
Control	M	84.64	12.77%			82.09	11.99%	3695	8.37E-05	93.18	9.88%	2352	8.57E-05	88.53	8.77%	1378	9.22E-05
	C	76.68	12.48%			79.68	11.42%	3228	8.53E-05	70.25	9.40%	2088	8.84E-05	75.00	8.22%	1168	9.97E-05
HANWA	M	74.04	16.79%			72.13	15.48%	5642	1.26E-04	77.92	14.83%	3716	1.11E-04	81.01	13.91%	2170	1.20E-04
	C	69.65	16.15%			73.98	14.63%	5156	1.26E-04	77.16	14.48%	3767	1.14E-04	77.91	13.59%	1790	1.27E-04
SAP	M	64.31	16.25%			70.13	15.83%	5763	1.03E-04	81.03	15.45%	4045	1.05E-04	80.24	15.65%	2266	1.47E-04
	C	60.10	16.42%			70.83	15.51%	5675	1.09E-04	82.42	15.90%	3681	1.04E-04	85.74	15.89%	2271	1.65E-04

PERICLES ALEXANDROU SAWA

Table 4-14: Grouped results according to curing regime and IC medium

	3 DAYS				7 DAYS				28 DAYS				90 DAYS			
	fc Mpa	Porosity %	RCP Coul.	Sorptivity mm/t^1/2	fc Mpa	Porosity %	RCP Coul.	Sorptivity mm/t^1/2	fc Mpa	Porosity %	RCP Coul.	Sorptivity mm/t^1/2	fc Mpa	Porosity %	RCP Coul.	Sorptivity mm/t^1/2
Control	80.66	12.63%			80.89	11.70%	3462	8.45E-05	81.72	9.64%	2220	8.70E-05	81.77	8.50%	1273	9.59E-05
HANWA	71.84	16.47%			73.05	15.05%	5399	1.26E-04	77.54	14.66%	3742	1.13E-04	79.46	13.75%	1980	1.23E-04
SAP	62.20	16.33%			70.48	15.67%	5719	1.06E-04	81.73	15.68%	3863	1.04E-04	82.99	15.77%	2268	1.56E-04

PERICLES ALEXANDROU SAWA

4.5. Internal curing using recycled aggregates

A batch of recycled aggregates (RCA) was utilized for evaluating whether the specific "waste" materials could be used for concrete production. RCA in Cyprus are being used only in secondary applications such as road embankment etc., and the effort focused on improving their performance in order to increase their value. A major drawback of RCAs utilization in primary concrete structures is the attached old mortar, which decreases the material's quality. More specifically, the attached mortar causes a double interfacial transition zone (ITZ) which is known to exhibit higher porosity than the rest of the mixture being a "weak zone" that determines various properties of the material's final performance. In addition, the adhered mortar is characterized by high porosity and cracks that weaken the material's performance even more. It has to be mentioned that the adhered mortar is not negligible since it constitutes 30-35% of the old cement paste volume (Poon, Shui and Lam, 2004). In an effort to reduce the excessive mortar, Demetriou added RCAs in an inclined rotating machine, full with water (similar to Los Angeles test – ASTM C131) and rotated for approximately 2 hours (Demetriou, 2014). The same method was followed herein where the treated aggregate was named RCA-T and the non-treated RCA-F. In addition, the specific aggregates were used as IC agents according to their absorption and desorption behavior. The specific chapter aims to employ RCAs in concrete mixtures in order to evaluate their performance and their IC effectiveness.

4.5.1. Mixtures

Both RCA-F and RCA-T have a sufficient absorption (7.2% and 4.5% respectively) to carry IC water and also good water desorption properties, since both types of aggregate released more than 50% of their water at RH levels higher than 90%. In addition, since the aggregates IC applicability was established, small trial mixes were designed in order to verify their effectiveness in concrete. For the specific tests, it was decided that, a low w/c ratio would be more appropriate, in order to reduce the water availability and thus intensify the IC action. Therefore, three concrete mixtures with 0.25 w/c ratio were designed (Table 4-15). The mixtures included a control mixture with normal weight aggregates (NWA) (4-10 mm and 0-4 mm), a mixture with 100% RCA replacement of coarse aggregates and NWA 0-4 mm and an identical mixture with RCA-T. It has to be mentioned that the RCA quantity was calculated based on IC water requirements yielded from Bentz equation (3-2) and the RCA absorptivity. However,

PERICLES ALEXANDROU SAWA

since the RCA-F and the RCA-T water absorption was different, the aggregate quantity had to be varied in order to deliver the same amount of IC water. Therefore, it was decided that the amount of aggregates will be based on the RCA properties to carry a portion of the required water. The main reason was to maintain similar mix design in order to have comparable results.

Table 4-15: RCA mixtures design

	Control	RCA-F	RCA-T
	kg/m^3	kg/m^3	kg/m^3
CEM II 42.5 R	864	864	864
Water	216	216	216
4/10	620	620	620
Sand	597	556	583
w/c	0.25	0.25	0.25

4.5.2. Experiments and Results

The mixtures were tested for compressive strength (EN 12390-3) at the age of 1, 3,7,14, 28 and 56 days (Figure 4-23) and chloride resistance (ASTM C-1202) at the age of 1, 3,7,14 and 28 days (Figure 4-24). The RCA mixtures exhibited low compressive strength during the first day. The initiation of IC contributed to a high rate of compressive strength development. The RCA mixtures exhibited an average increase of 39% in compressive strength from day 1 to day 28 as opposed to a 12% increase for the control mixture. The IC action enhanced the degree of hydration. Regarding RCP, the RCA-F mixture observed a lower initial reduction as compared to the other two mixtures. The RCA-T observed the lower final RCP. The IC mechanism of RCA-F mixture was expected to initiate from early-ages as opposed to the RCA-T. It was mentioned previously (Section 4.5.1) that the utilized IC water would be less for RCA-T, due to different water absorption from RCA-F, in order to maintain comparable mixtures. It is also known that absorption begins from the smallest pores and desorption from the largest. Therefore, the IC water utilized for RCA-T was expected to be stored in the smallest pores and be diffused in the mixture at later stages. Indeed, the results reveal that the mixture did not performed very well in the early-ages but observed an exceptional improvement at later-ages.

PERICLES ALEXANDROU SAVVA

On the other hand, the RCA-F mixture which was fully saturated performed poorly in compressive strength during the first day but highly improved during the early and later-ages.

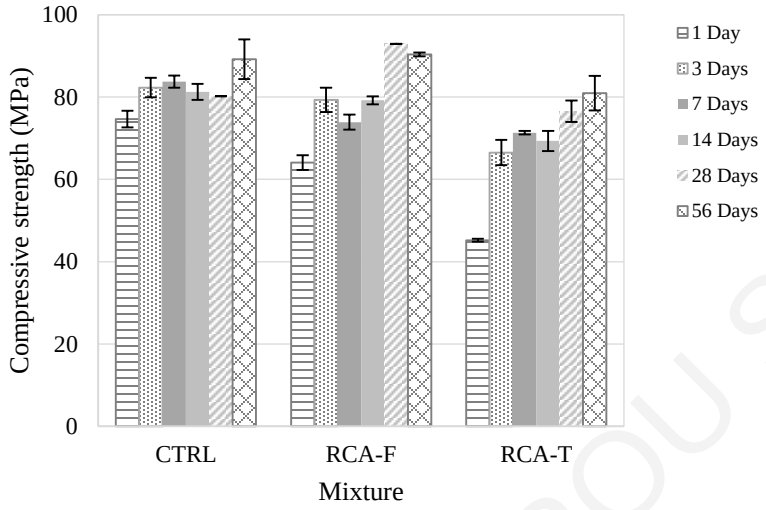

Figure 4-23: Compressive strength of IC-RCA mixtures

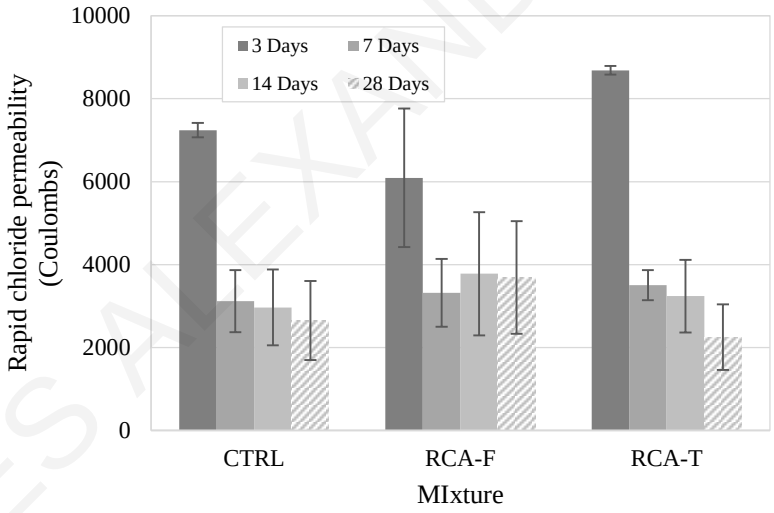

Figure 4-24: Rapid chloride permeability of IC-RCA mixtures

4.6. Discussion-Conclusions

The objective of this research was to develop an IC method, aiming to reduce early-age shrinkage and maintain the materials' properties intact. The specific objective was fulfilled considering that the IC mixtures including HANWA-SSD exhibited similar mechanical and durability properties with the control mixture. HANWA-SSD performed very well in reducing autogenous shrinkage. HANWA-SSD mixtures recovered the inevitable early-age loss in

PERICLES ALEXANDROU SAVVA

compressive strength and continuously gained strength due to the presence of water from the inner core. Their IC effectiveness was also demonstrated by the RCP experimental results. In comparison with the rest of the IC mixtures, HANWA-SSD is the only mixture that consistently exhibited a reduction in porosity with time. It was showed that the specific IC medium utilized IC water even at later ages. The ring test showed that the HANWA-SSD mixture cracked 6 days after both control and SAP mixtures and exhibited 87.5% and 86.5% lower crack width than the control and the SAP mixture.

The performance of concrete including RCA can be improved using the method of IC. The mixture design has to be conducted based on the cement requirements, in order to compensate self-desiccation. It was shown that the RCA mixtures exhibited identical or even better properties than the conventional concrete mixture (i.e. control – Section 4.2) in both compressive strength and RCP experiments.

The specific results constitute the extension of the current research and prepare the field for an extended research regarding IC on waste materials such as recycled aggregates, regardless of their poor properties. It also supports the argument that extending the principles of IC can be extended on materials other than LWAs and HANWAs, succeeding in yielding useless materials into high performance materials with a wide range of applications. The successful application of IC on RCA will contribute to a better utilization of waste materials, ensuring environmental sustainability.

PERICLES ALEXANDROU SAVVA

5. Investigation of internal curing for mitigating high temperature concreting effects

5.1. Introduction

Cement hydration is an exothermic reaction where the amount of energy released is an indicator of the rate of hydration. Concrete strength depends mainly on the cement type and particles size, rate and degree of hydration as well as the aggregates quality. The rate and degree of hydration determine the amount and quality of the cement paste which is the bonding agent for the aggregates. A rapid hydration rate will create an outer shell on the cement grains with low permeability that will eventually restrict water vapor from diffusing within the grains to trigger additional hydration (Taylor, 1990; Kjellsen and Detwiller, 1992). Therefore, the ultimate degree of hydration is strongly dependent on the rate of hydration. Furthermore, the cement products after a rapid hydration will probably observe poor physical structure due to higher porosity (Neville, 2002). The rapid nucleation of the cement grains leads to intense flocculation of hydration products in the vicinity of the cement grain hindering the even distribution of products within the available space. The poor dispersion of hydration products will lead to additional porosity and eventually decrease of the concrete strength due to stress concentration. Additionally, the curing temperature affects the material's deformation (shrinkage/swelling) rate at early ages. The material's contraction in low w/b ratios is inevitable due to intense autogenous shrinkage and self-desiccation, whereas mixtures with higher w/b ratio suffer contraction due to drying shrinkage. An intense rate of hydration increases the rate of autogenous shrinkage, inducing stress within the material's structure (Chu *et al.*, 2012). In the case where curing temperature observes fluctuations it is expected that the material undergoes contraction/ expansion cycles leading to cracking which eventually deteriorates the material's durability and mechanical performance.

It was proven that IC is effective in reducing autogenous shrinkage by replenishing consumed water within the material's structure. In the case where concrete is cast and cured in hot and dry environment, plastic shrinkage will be intensified resulting in decreased quality. Plastic shrinkage enhances menisci formation, which yields in tensile stress development. If the evaporation rate is high, the rate and magnitude of the developed stresses will overcome concrete strength resulting in crack formation. However, if the evaporated surface water is

PERICLES ALEXANDROU SAVVA

replenished from the inner core, the menisci formation will be prevented and the cracks are expected to be reduced.

Espinoza-Hijazin and Lopez attempted to evaluate the effectiveness of IC in concrete mixtures with w/c ratio higher than 0.42 (Espinoza-Hijazin and Lopez, 2011). As mentioned, 0.42 w/c ratio represents the minimum ratio that allows the whole cement quantity to be hydrated. The specific finding yielded from Powers comprehensive models developed in 1948 (Powers and Brownyard, 1947). IC mainly improves concrete through self-desiccation reduction, which yields due to lack of sufficient water in the system. The authors aimed to assess the effectiveness of IC on concrete members exposed to drying conditions (RH 50%). The experiments included degree of hydration, compressive strength and chloride ion permeability at the age of 90 days, for five different w/c ratios (0.400, 0.425, 0.450, 0.475 and 0.500). The IC agent was LWA (expanded clay sand) with size range 0.5-8.0 mm and WA_{24} 21.2%. It was concluded that the IC mixtures performed much better in terms of mass loss than the non-IC mixtures. Additionally, it was also mentioned that the IC mixtures observed a 15% increase in the degree of hydration which had direct impact on the compressive strength (19% increases) and chloride ion penetration (30% decrease).

This chapter presents the results of a research that focuses on employing HANWA in order to evaluate their efficiency towards improving concrete performance under hot weather conditions.

5.2. Experimental program

5.2.1. Mixtures

Sixteen different mixtures were prepared (Table 5-1) in order to evaluate the effect of mixing and curing temperature on concrete mechanical and durability properties. The mixture's variables were the moisture state of aggregates (SSD for HANWA and lab-dry for NWA), the curing regime and the mixing and curing temperatures. More specifically, mixtures were prepared using two different types of aggregates, cured at two different curing regimes and cast at four different temperatures, as presented in Table 5-1. The water cured specimens were immersed in water tanks right after their demolding. The water temperature was identical to the manufacturing temperature. The concrete specimens were cured at the corresponding temperature up to the age of testing or up to the age of 28 days, whichever came first. After the 28 days the water tank temperature was reduced to the standard temperature (20±2°C). The

PERICLES ALEXANDROU SAWA

workability of the mixtures was kept constant (slump test 75 ± 25mm) by adjusting the superplasticizer quantity.

Table 5-1: Mixtures variables

Aggregates	Curing Regime	Cast temperature	No. of mixtures
HANWA Highly absorptive (H) Saturated Surface Dry (SSD)	Exposed (E)	22ºC (22) 30ºC (30) 35ºC (35) 40ºC (40)	4
	Water cured (C)	22ºC (22) 30ºC (30) 35ºC (35) 40ºC (40)	4
NWA Low absorptive (L) Lab Dry	Exposed (E)	22ºC (22) 30ºC (30) 35ºC (35) 40ºC (40)	4
	Water cured (C)	22ºC (22) 30ºC (30) 35ºC (35) 40ºC (40)	4

The specimens were encoded according to their production and curing variables. For instance, 22EL corresponds to the mixture produced at 22ºC using NWA (L) and exposed to the environment (E).

The first mixture of the experimental program was cast at the beginning of July, and before the end of the specific month all the mixtures intended to be exposed to the environment were completed. The specific batch of specimens tested were directly exposed to the environment, exposed to direct sun (~six hours per day and moderate RH (~55%)), as opposed to the control water cured specimens (mixtures designated with C) where the water curing temperature was constant and corresponded to the casting temperature. All specimens were kept in laboratory conditions until demolding (24h). The ambient environmental temperature was continuously

PERICLES ALEXANDROU SAVVA

monitored with the use of thermocouples. The maximum and the minimum ambient temperatures recorded in the storing environment were 44.3^{o}C and 21.2^{o}C (Figure 5-1), whereas the largest and smallest day to night fluctuations were 22^{o}C and 8.5^{o}C respectively. It has to be noted though, that over 80% of the days monitored had a temperature fluctuation exceeding 15^{o}C (Figure 5-1). In Figure 5-2, each vertical line intersects the value of the maximum and the minimum ambient environmental temperature on the day of each mixture's initial exposure.

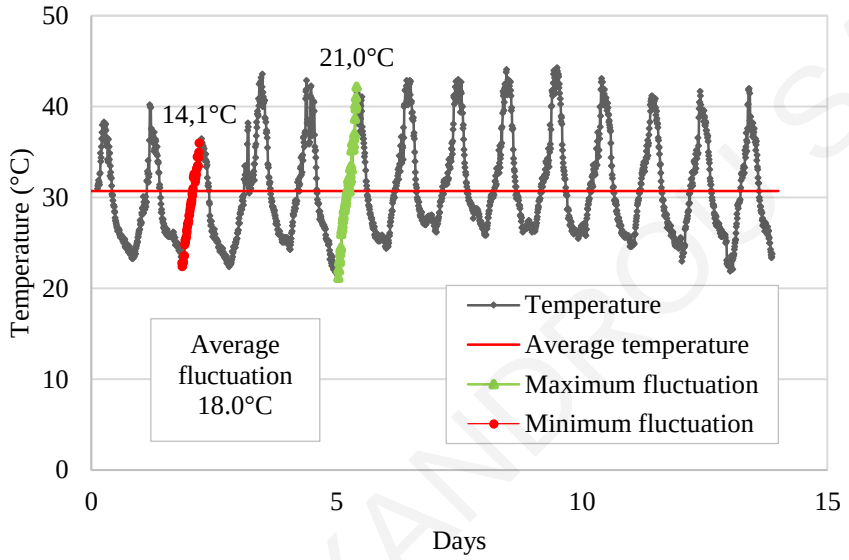

Figure 5-1: Temperature fluctuation for a time interval of two weeks

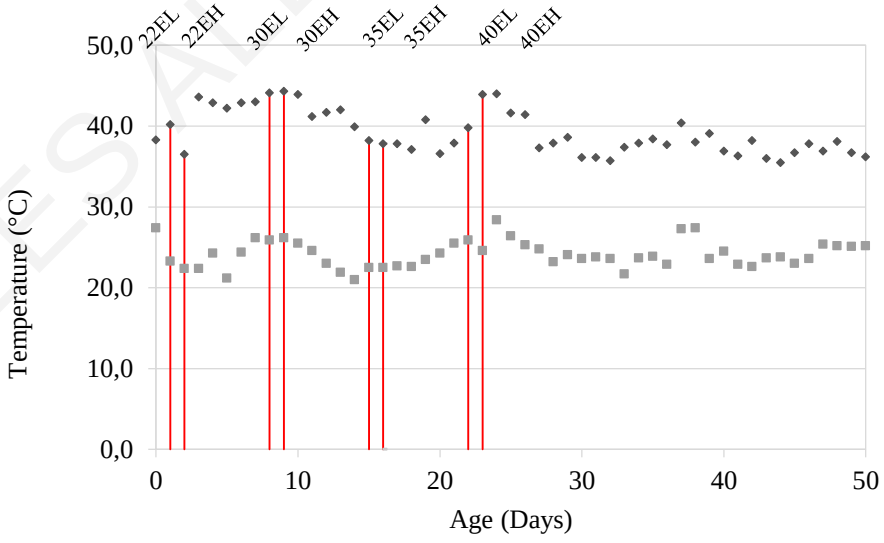

Figure 5-2: Actual maximum and minimum temperature after each mixture exposure to the environment

PERICLES ALEXANDROS SAVVA

5.2.2. Aggregates

5.2.2.1. Mineralogical composition

Both HANWA and NWA were crushed limestone aggregates. HANWAs source is located in the Troodos mountain range. It contains mainly micritic calcite which in restricted areas yields to microspar. The aggregates contain fossils whose composition is mainly recrystallized sparry calcite in addition to minor quantities of micritic endoclasts, non-carbonate grains such as quartz, chert, spinel and also traces of anhydrite (Ioannou *et al.*, 2010). Their observed high absorptivity is due to the significant intraparticle porosity obtained within fossils, whereas elongated pores are formed due to recrystallization of spar crystals. NWA source is located in the Keryneia Terrane and is one of the three main allochthonous geological formations, which forms the main carbonate masses of Pentadaktilos mountain range. The specific formation is composed of massive to thickly bedded dolomitic limestones (Cyprus Geological Survey Department, 2016).

5.2.2.2. Physical and mechanical properties

The aggregate physical properties were measured according to EN 1097-6 (EN 1097, 2013) and are listed on Table 5-2.

Table 5-2: Aggregates properties

Type	Fraction (mm)	Bulk Specific Gravity, ρ_b (kg/m^3)	SSD Specific Gravity, ρ_{ssd} (kg/m^3)	Water Absorption, W_{24} (%)
NWA	8/20	2.71	2.74	1.00
	4/10	2.71	2.76	1.60
HANWA	8/20	2.52	2.58	2.35
	4/10	2.41	2.52	4.65
SAND	0/4	2.60	2.70	1.29

The compressive strength and modulus of elasticity of both types of aggregates utilized for this experimental program (HANWA and NWA) were tested according to EN 1926 (EN 1926, 2006) and EN 14580 (EN 14580, 2005), respectively. The average compressive strength of six

PERICLES ALEXANDROU SAWA

cylindrical specimens was 33. 5 MPa (standard deviation 4.4 MPa) for HANWA and 80. 3 MPa (standard deviation 5.7 MPa) for NWA, whereas, their modulus of elasticity was 19.3 GPa and 78.3 GPa, respectively.

5.2.3. Mixture and internal curing design

The amount of cement and the w/c ratio were aligned with the practice applied by the local construction sector. The cement utilized in this research was CEM II 42.5R with a Blaine specific surface of 430 m^2/kg. The mixture design was performed based on ACI 211.1 (America Concrete Institute, 2002) (Table 5-3). The baseline of the mixture design was the amount of aggregates required to deliver IC water within the mixtures. The internal curing (IC) water was calculated based on Bentz equation (P. D. Bentz and Snyder, 1999; Bentz, Lura and Roberts, 2005). The cement chemical shrinkage was calculated based on ASTM C1608 (Zhang *et al.*, 2013). The use of coarse aggregate fractions (8/20 mm and 4/10 mm) was considered as a drawback due to the low expected degree of dispersion within the matrix. However, the main objective was to evaluate the performance of construction common practice mixtures, in an effort to improve their properties. The NWA mixtures coarse aggregates were kept fairly constant in order to make the mixtures (HANWA and NWA) comparable. The coarse aggregates density differences are reflected in the fine aggregates quantities. Considering the all-in aggregate gradation, however, the difference between HANWA and NWA is negligible (Figure 5-3 and Table 5-4).

Table 5-3: Mixture constituents (kg/m^3)

	NWA	HANWA
Cement II 42.5R	512	512
Water	205	205
Coarse aggregates 8/20 mm	336	332
Coarse aggregates 4/10 mm	671	665
Limestone sand 0/4 mm	627	577

PERICLES ALEXANDROU SAWA

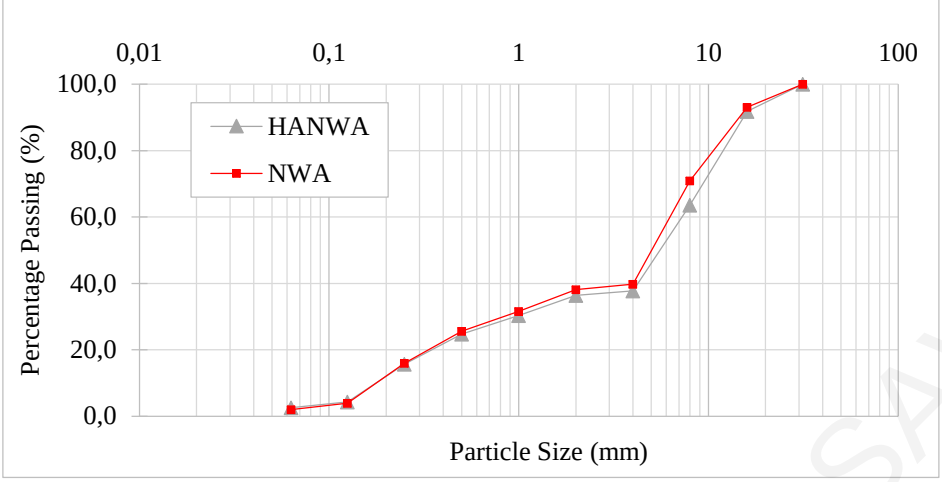

Figure 5-3: All in sieve analysis

Table 5-4: Aggregates and all-in mixtures sieve analysis

	Cumulative passing percentage							
	HANWA				NWA			
	0/4 mm	4/10 mm	8/20 mm	ALL IN	0/4 mm	4/10 mm	8/20 mm	ALL IN
Sieve size (mm)	36.4%	42.4%	21.2%	100%	38.4%	41.1%	20.5%	100%
31.5	100.0	100.0	100.00	100.0	100.0	100.0	100.00	100.0
16	100.0	100.0	61.63	91.9	100.0	100.0	65.87	93.0
8	100.0	63.4	1.30	63.5	100.0	78.1	1.26	70.7
4	98.9	3.7	1.05	37.7	98.9	2.8	0.62	39.2
2	96.1	2.9	1.03	36.4	96.1	1.6	0.61	37.6
1	79.6	2.7	1.00	30.3	79.6	1.3	0.58	31.2
0.5	64.4	2.7	0.97	24.7	64.4	1.2	0.55	25.3
0.25	39.5	2.6	0.91	15.7	39.5	1.2	0.53	15.8
0.125	8.6	2.5	0.82	4.3	8.6	1.1	0.44	3.8
0.063	4.0	2.2	0.71	2.5	4.0	1.0	0.37	2.0

PERICLES ALEXANDROU SAVVA

5.2.4. Experiments and analysis

The measured properties included compressive strength (Table 5-5) (EN 12390 - 3, 2002) vacuum porosity (Table 5-6) (Kanellopoulos, Petrou and Ioannou, 2012), sorptivity () (Kanellopoulos, Petrou and Ioannou, 2012) and rapid chloride permeability(Table 5-8) (ASTM C 1202, 2009). The experiments were conducted at 3, 7, 28, 90, 365 days. The average coefficient of variation of the porosity measurements was <4% and the corresponding coefficient of variation for sorptivity measurements was <7%. Due to the large volume of data, the coefficient of determination was determined for the combination of the tested properties based on their average values. At first, the average values were calculated and plotted according to the testing age (up to the age of 90 days (Table 5-9 – 4 points) and up to the age of 365 days (Table 5-10 - 5 points)). For each comparison, only the effect of the parameter under investigation was considered. For instance, the value designated with the letter "E" (Table 5-9) represents the average of all the exposed specimens including all the type of aggregates and cast temperatures. The specific properties were plotted according to the corresponding average values tested at the ages of 3, 7, 28, 90 and 365 days. The specific analysis was conducted considering each parameter (curing regime (Exposed – "E", control cured – "C"), type of aggregates (HANWA – "H", NWA- "L"), cast temperature and testing age). The yielding averages were plotted combining two parameters at a time (e.g. compressive strength vs porosity) for each time interval. The same procedure was applied and the resulting averages were plotted for each property versus the time intervals instead of another property in order to extract each property trend of development, up to the age of 90 and 365 days (Table 5-11 and Table 5-12 respectively). The specific analysis was done on both linear and logarithmic scales.

5.2.4.1. Compressive strength

The compressive strength was conducted according to EN12390 (EN 12390 - 3, 2002) using three cubic specimens (100x100x100 mm) for each test. The results presented in Figure 5-4, Figure 5-5, Figure 5-6, Figure 5-7 and Table 5-5, represent the average of these specimens and the coefficient of variation was < 10%.

5.2.4.2. Vacuum porosity

The experiments were conducted based on the procedure described by Kanellopoulos et al. 2012. The specimens were kept in a sealed chamber and vacuum was applied. The specimens

PERICLES ALEXANDROU SAVVA

were subjected to vacuum for 24 hours before being immersed in water. Subsequently, the specimens were stored for another 24 hours in water in order become saturated and the immersed and saturated masses were recorded. Then, the specimens were placed at 105^{o}C and as soon as a constant mass was reached, the dry mass of the specimens was recorded. It has to be noted that the results correspond to three cubic specimens conducted on different specimens at each time interval. The coefficient of variation was < 2% in each experiment.

5.2.4.3. Rapid chloride permeability

The rapid chloride permeability (RCP) test was conducted based on ASTM C1202 (ASTM C 1202 - 2008). The experiment assesses concrete ability to resist chloride intrusion. The specific test is widely used because it requires low amount of time and it is easy to be conducted (Riding *et al.*, 2008). The experiment measures the electrical conductivity or resistance of a 50 mm thick disk concrete specimen for a period of 6 hours. It is assumed that the resistivity is directly related to the pore network or concrete permeability. Rapid chloride permeability test can be used for quality control and concrete durability research (Bentz, 2007).

The specimens were positioned in a measuring cell which contained a fluid reservoir at each face. One reservoir was filled with sodium chloride (NaCl) solution and the other with a sodium hydroxide solution (NaOH). The reservoir containing NaCl was connected to the negative terminal and the NaOH reservoir to the positive terminal of the microprocessor power supply unit. Specimens that exhibited high charge indicated a highly permeable mixture.

5.3. Results and Discussion

5.3.1. Specimens exposure

It was expected that the high temperature fluctuations would cause high stress cycles to the exposed specimens. Considering the material's structure especially during the first days of its development, the difference of the constituent aggregates and cement paste stiffness and the size and shape of the concrete element were expected to cause a restrain. The magnitude of restrain depends on various parameters including the shape and size of the concrete element, the aggregates fraction and modulus of elasticity. The restrain is intense in the early-ages when the cement chemical reactions reach their peak. Cement is a thixotropic material that undergoes swelling and shrinkage until its solidification, while aggregates are chemically inert materials

PERICLES ALEXANDROU SAVVA

with constant predetermined characteristics. Considering these characteristics, the development of differential shrinkage is anticipated in concrete elements.

Comparing the two types of aggregate used in the current chapter, the aggregates used for the control mixtures (NWA) exhibited more than four times higher modulus of elasticity than the HANWA (Section 5.2.2.2). The higher modulus of elasticity was expected to allow lower deformation to the cement paste of the mixtures cast with NWA which would cause higher stresses at critical areas such as ITZ.

5.3.2. Compressive strength

The compressive strength values of the mixtures are presented in Figure 5-4 to 5-7 and Table 5-5. Considering the mixtures produced with HANWA (Figure 5-4), the exposed mixtures, exhibited higher compressive strength than the water cured mixtures. On average, the exposed HANWA mixtures exhibited a compressive strength of 57.1 MPa as opposed to 50.5 MPa of the water cured specimens, whereas their ultimate compressive strength (365 days) was 64.6 MPa to 58.7 MPa respectively. The specific was attributed to the IC water that replenished the consumed water and enhanced the degree of hydration.

The exposed NWA mixtures observed a slightly higher compressive strength than the water cured specimens at the early-age (3 and 7 days) which was reversed at the age of 28 days (Figure 5-5). Additionally, the compressive strength development of the NWA water cured mixtures was much more consistent than any series of mixtures. Specifically, no specimen of the specific series observed a reduction when compared with a previous age of testing. The NWA water cured mixtures observed an average compressive strength of 66.2 MPa as opposed to 61.9 MPa of the exposed specimens. The specific difference was increased to 11.9 MPa at the age of 365 days (Exposed: 67.7 MPa, Water cured: 79.7 MPa). This highlights the effect of the curing conditions on the material's compressive strength. Regarding the exposed mixtures, it is believed that the most prominent damage that caused the reduction of compressive strength was located at the area of the interfacial transition zone, because of the high temperature fluctuation (Figure 5-1).

PERICLES ALEXANDROU SAVVA

Table 5-5: Compressive strength (MPa)

	Average compressive strength (μ) - standard deviation (σ) - MPa									
	3		7		28		90		365	
Days	μ	σ	μ	σ	μ	σ	μ	σ	μ	σ
22EH	42.2	*1.7*	53.6	*4.3*	60.6	*2.7*	52.0	*3.8*	60.2	*4.2*
22EL	53.3	*1.3*	56.8	*3.8*	62.9	*1.8*	52.7	*1.8*	72.4	*3.4*
30EH	53.3	*2.3*	60.9	*2.8*	65.5	*1.8*	54.7	*5.3*	68.5	*3.5*
30EL	55.8	*0.9*	58.1	*5.4*	63.3	*1.8*	56.4	*5.1*	68.7	*2.4*
35EH	62.9	*7.0*	51.1	*0.6*	70.9	*0.1*	66.9	*2.6*	68.6	*3.8*
35EL	60.8	*3.3*	66.2	*3.0*	60.5	*0.9*	69.8	*1.8*	72.9	*4.3*
40EH	43.4	*0.4*	45.9	*3.4*	49.6	*0.7*	48.9	*0.7*	61.1	*4.7*
40EL	59.9	*3.3*	65.0	*1.4*	57.6	*0.3*	67.8	*2.6*	56.9	*5.1*
22CH	40.9	*3.4*	45.8	*1.0*	50.6	*3.5*	57.4	*1.5*	64.5	*4.2*
22CL	51.5	*0.5*	55.4	*0.9*	67.1	*2.9*	74.0	*5.5*	73.1	*3.0*
30CH	40.0	*2.5*	47.0	*1.2*	53.9	*1.6*	52.1	*0.8*	51.9	*5.5*
30CL	52.4	*4.2*	56.8	*4.0*	65.4	*4.7*	66.8	*0.5*	73.4	*2.9*
35CH	47.7	*1.3*	50.0	*2.1*	51.3	*5.6*	57.1	*1.4*	59.2	*5.3*
35CL	55.6	*3.1*	62.5	*0.9*	69.3	*4.0*	75.6	*2.2*	82.9	*3.3*
40CH	30.2	*2.0*	47.7	*0.9*	50.2	*4.2*	53.4	*1.2*	59.1	*5.4*
40CL	56.8	*3.4*	62.5	*2.6*	64.8	*1.9*	69.6	*1.8*	89.2	*3.0*

Observing Figure 5-6 it can be seen that the NWA mixtures performed in a more consistent way than the HANWA mixtures. However, the compressive strength of HANWA exposed mixtures at the later-ages was highly improved. More specifically, the HANWA exposed mixtures cast at 30ºC and 35ºC observed an average compressive strength of 62.3 MPa whereas the corresponding NWA mixtures observed an average compressive strength of 63.2 MPa Table

PERICLES ALEXANDROUSAVVA

5-5). In addition, the same mixtures at 365 days observed an average compressive strength of 68.5 MPa to 70.8 MPa respectively.

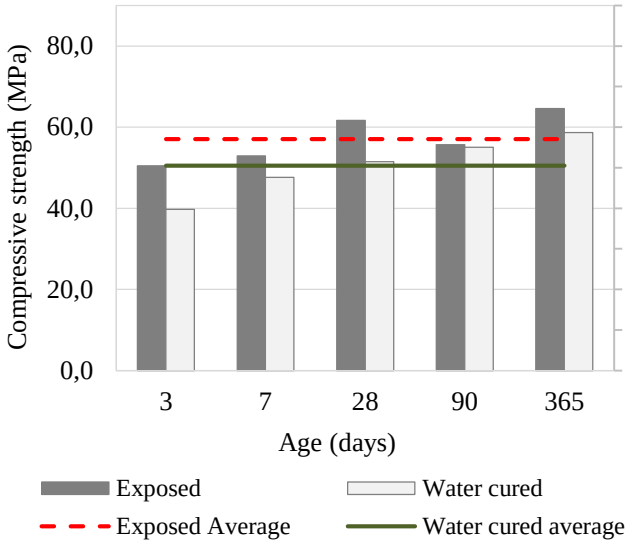

Figure 5-4: Compressive strength of HANWA mixtures

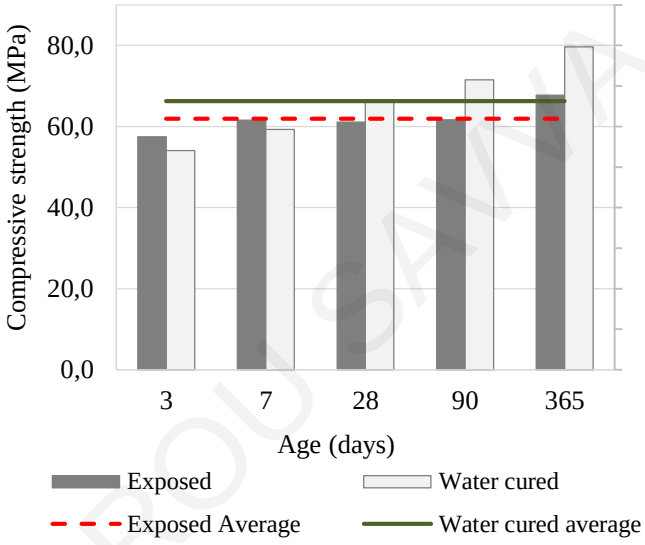

Figure 5-5: Compressive strength of NWA mixtures

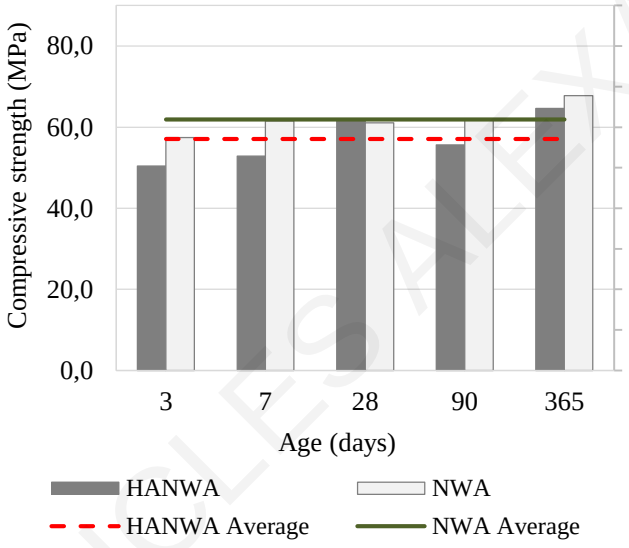

Figure 5-6: Compressive strength of exposed mixtures

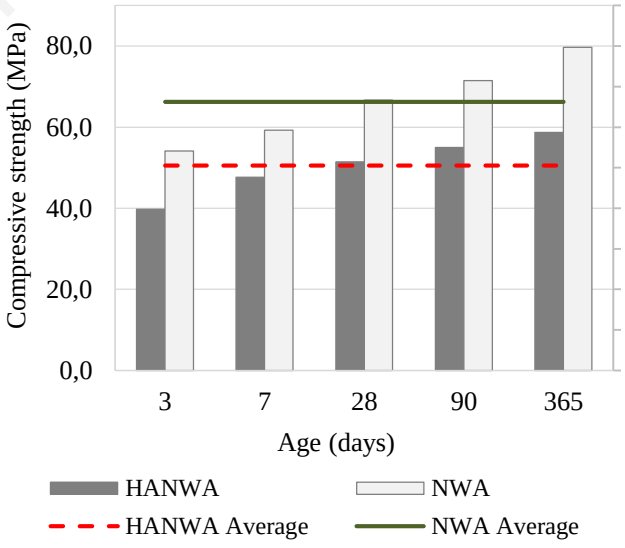

Figure 5-7: Compressive strength of water cured mixtures

As stated previously, this was attributed to the IC that replenished the loss of water and increased degree of hydration and the improved ITZ due to the better adhesion of cement paste. A pronounced characteristic of the specific results is the uncertainty regarding the mixtures cast at 40^{o}C. The specimens of the specific mixtures showed a decreased compressive strength in the

PERICLES ALEXANDROU SAVVA

three out of four occasions tested (EH, CH and EL). The main drawback of the specific mixtures was the variability and unpredictability of their future behavior, since sharp unexpected strength drops or rises were observed. The most important conclusion regarding the compressive strength of the specific series was the reverse behavior regarding the HANWA exposed and HANWA control cured to the corresponding NWA mixtures.

5.3.3. Durability Indicators

The vacuum porosity experiments and the sorptivity were conducted according to (Kanellopoulos, Petrou and Ioannou, 2012) at the age of 3, 7, 28, 90, and 365 days. The average values of each mixture at each curing regime are presented in Figure 5-8 and Figure 5-9. The most prominent conclusion is the consistent behavior observed in both porosity and sorptivity experiments. More specifically, the HANWA mixtures exposed to the environment (except the mixture cast at 40^{o}C) observed improved behavior as opposed to the water cured mixtures, similarly to the compressive strength results. The exact opposite behavior (except the mixture cast at 35^{o}C) was observed in the NWA mixtures.

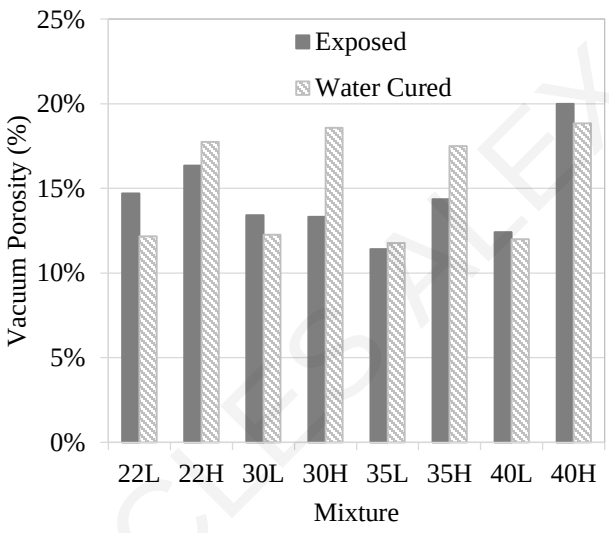

Figure 5-8: Vacuum Porosity (%)

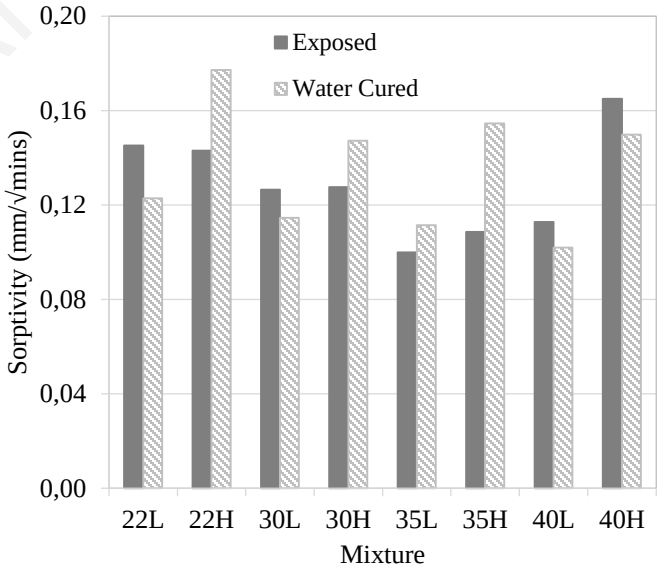

Figure 5-9: Sorptivity (i (mm)/t (√ mins))

Analytically, it was showed that the mixtures cast with HANWA and exposed to the environment, except the mixtures cast at 40^{o}C, observed a significantly lower porosity and sorptivity as opposed to the corresponding mixtures cured in controlled conditions. Comparing the HANWA exposed to the HANWA water cured average values, the mixtures cast at 22°C,

PERICLES ALEXANDROU SAVVA

30°C and 35°C observed a 7.9%, 28.3% and 17.9% lower porosity, and a 19.3%, 13.4% and 29.8% lower sorptivity, respectively. This was considered as a consequence of the enhanced degree of hydration. It is well known, that IC initiates due to the lack of water that causes a suction pressure that results in the IC water withdrawal from the IC medium pores. In this case, the gradient that causes the IC water extraction is the external evaporation, causing a moisture movement that yields in additional hydration. The lower porosity and sorptivity values of the IC exposed mixtures as opposed to the IC water cured mixtures were attributed to the specific pore network sealing. The mixtures cast at 40^{o}C observed a 6.1% and 10.1% higher porosity and sorptivity respectively. On the contrary, the mixtures cast with low absorptive aggregates observed a reverse behavior. Comparing the specific average values, the specimens cast at 22°C, 30°C and 40°C with NWA and exposed to the environment, compared to the water cured, exhibited a 20.8%, 9.4% and 3.5% higher porosity, and a 18.2%, 10.5% and 10.6% higher sorptivity, respectively. The mixtures cast at 35^{o}C observed a 3.0% and 10.3% lower porosity and sorptivity, respectively. The reverse behavior observed in the NWA mixtures is the anticipated behavior of concrete exposed in such environmental conditions and is attributed to the drying, stress cycles, and high restrain. The aforementioned difference between the IC and the NWA mixtures justifies the beneficial effect of IC water and IC medium.

The values presented in Figure 5-10 represent the percentage difference in sorptivity of the HANWA versus the NWA mixtures. The exposed HANWA mixtures, especially in the low cast temperatures (22°C, 30°C and 35°C), observed similar or improved average sorptivity compared to the corresponding NWA mixtures (1.5% lower, 0.8% higher and 8.6% higher). This was attributed to the IC action of the exposed HANWA mixture. The same comparison for the water cured mixtures indicated a 44.2%, 28.5% and a 38.8% lower average sorptivity, for the NWA mixtures cast at 22°C, 30°C and 35°C, respectively. Regarding the mixtures cast at 40°C the sorptivity difference between the HANWA and the NWA mixtures was similar, namely 46.2% for the exposed and 46.8% for the water cured mixtures. The increased cast temperature caused irreversible damage to the material's microstructure.

It was concluded that the IC mechanism was highly efficient in improving the durability properties of the exposed mixtures. Specifically, the results showed that the durability properties of the exposed IC highly-absorptive aggregate mixtures (EH) were considerably improved

PERICLES ALEXANDROUSAVA

compared to the corresponding water cured mixtures (CH). This improvement was not observed in the case of the exposed low-absorptive aggregate mixtures (EL), where no IC was expected.

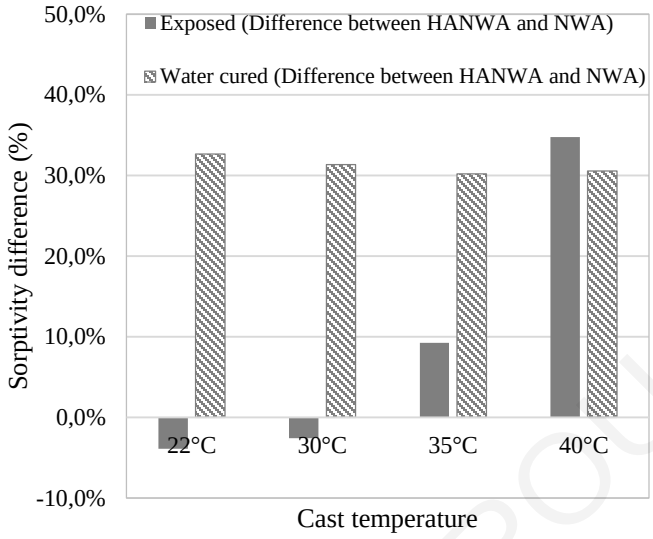

Figure 5-10: Sorptivity average differences

The effect observed in Chapter 4 and explained in Section 4.2.9, for the mixtures sorptivity, is observed in the porosity and sorptivity results of the current chapter as well. It seems that the deteriorating mechanism progresses with time and the damage was extended. As seen in Table 5-6 and, the average values of the open porosity and sorptivity from 90 to 365 days observed a 16.0% and 36.75% increase respectively. The porosity values were plotted against the specimens' density to verify the results. As it is clearly shown in Figure 5-12 and Figure 5-13, the porosity values were in agreement to the density values.

In order to explain the specific degradation, X-ray diffraction, scanning electron microscope and carbonation experiments were conducted. The initial speculation was the formation of ettringite in the region of the ITZ. The results of the specific experiments did not confirm sulfur or ettringite presence. Moreover, carbonation experiments were conducted with the use of 1% of phenolphthalein solution in ethanol. The specific solution is known to change color according to the pH (Figure 5-11). The results showed only minor carbonation for the mixtures exposed to the environment. The carbonation depth was estimated at 1-2 mm. Considering that the specimens were exposed in an industrial area for a time period longer than two years, it was concluded that the specimens had exhibited minor carbonation. The increase was attributed to

PERICLES ALEXANDROU SAVVA

the reaction occurring between the limestone aggregates and the cement paste (Tasong, Lynsdale and Cripps, 1999; Elsharief, Cohen and Olek, 2003; Hussin and Poole, 2011; Kong and Du, 2015). Further research is necessary in order to investigate this topic.

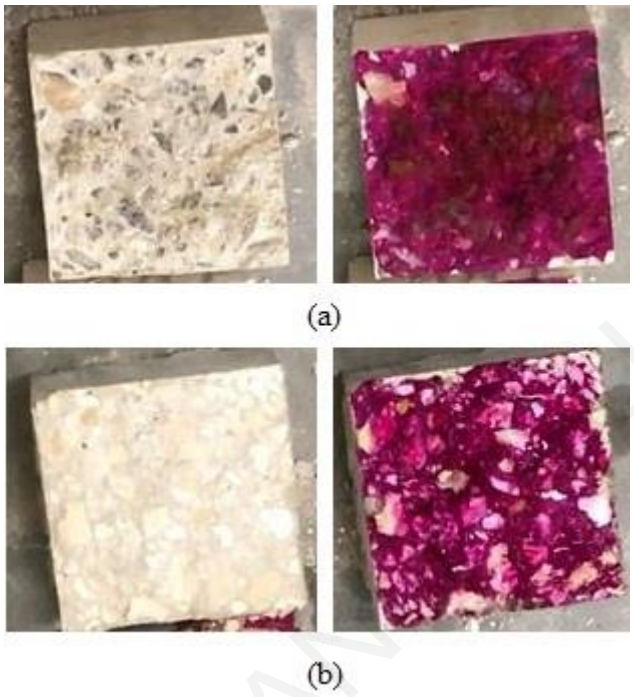

Figure 5-11: Carbonation experiment for NWA (a) and HANWA (b) mixtures

PERICLES ALEXANDROU SAVVA

Table 5-6: Open Porosity (%)

	3 DAYS	7 DAYS	28 DAYS	90 DAYS	365 DAYS
22EL	13.78	14.04	14.71	13.62	17.33
22EH	15.51	14.25	16.25	16.65	19.10
30EL	12.17	11.41	13.69	13.17	16.60
30EH	12.80	11.75	13.73	14.61	13.77
35EL	10.53	10.95	10.54	11.10	13.96
35EH	14.33	14.87	12.82	13.43	16.38
40EL	10.84	12.33	11.94	12.14	14.83
40EH	21.71	18.92	18.73	20.88	19.75
22CL	11.77	11.48	10.62	10.46	16.48
22CH	19.57	15.84	18.43	14.75	20.14
30CL	11.67	11.57	10.46	10.99	16.60
30CH	18.72	17.69	14.98	20.29	21.21
35CL	10.63	10.63	10.54	10.65	16.42
35CH	18.02	14.51	14.27	20.02	20.73
40CL	10.68	10.11	10.00	12.79	16.38
40CH	18.36	18.61	13.98	21.21	22.09

PERICLES ALEXANDROUSAVVA

Table 5-7: Sorptivity (mm/√min)

	3 days	7 days	28 days	90 days	360 days
22EL	1,31E-01	1,30E-01	1,24E-01	1,51E-01	1,90E-01
22EH	1,20E-01	1,05E-01	1,39E-01	1,51E-01	2,00E-01
30EL	1,24E-01	1,23E-01	1,33E-01	8,83E-02	1,65E-01
30EH	9,71E-02	1,06E-01	1,37E-01	1,15E-01	1,82E-01
35EL	8,19E-02	1,06E-01	9,18E-02	9,01E-02	1,31E-01
35EH	9,12E-02	1,06E-01	1,16E-01	8,97E-02	1,40E-01
40EL	8,15E-02	1,06E-01	1,15E-01	9,26E-02	1,27E-01
40EH	1,48E-01	1,06E-01	1,55E-01	1,31E-01	2,36E-01
22CL	1,34E-01	1,24E-01	7,34E-02	1,36E-01	1,47E-01
22CH	2,89E-01	1,16E-01	1,14E-01	1,01E-01	2,66E-01
30CL	1,28E-01	9,13E-02	9,71E-02	8,64E-02	1,70E-01
30CH	1,35E-01	1,30E-01	1,21E-01	1,43E-01	2,07E-01
35CL	1,05E-01	8,67E-02	1,26E-01	9,63E-02	1,43E-01
35CH	1,32E-01	1,34E-01	1,20E-01	1,53E-01	2,34E-01
40CL	1,05E-01	1,05E-01	9,02E-02	8,89E-02	1,21E-01
40CH	1,22E-01	1,46E-01	1,19E-01	1,21E-01	2,41E-01

PERICLES ALEXANDROU SAVVA

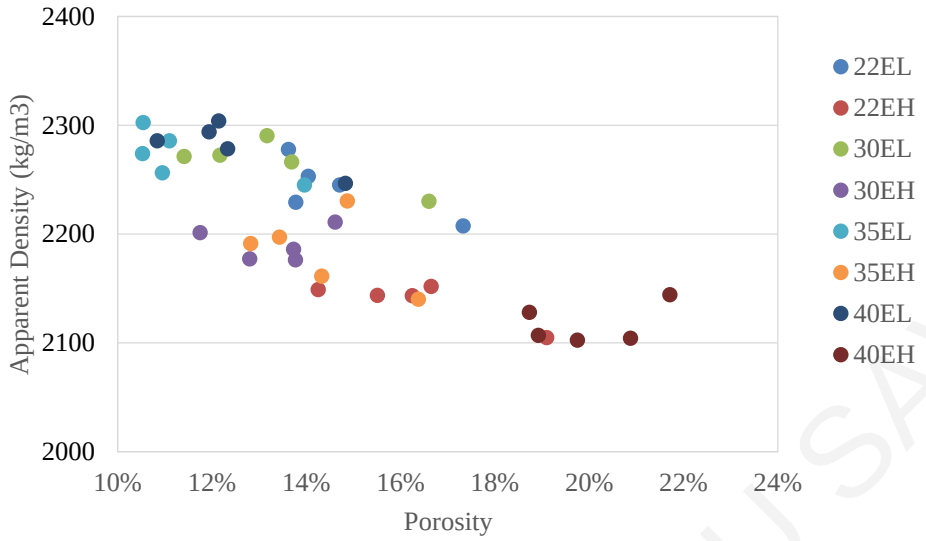

Figure 5-12: Porosity vs Apparent Density for exposed specimens

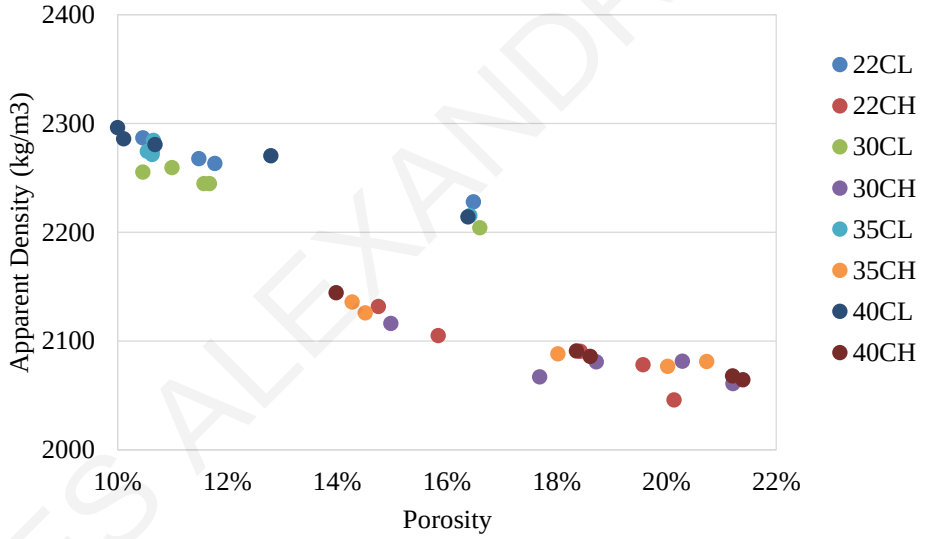

Figure 5-13: Porosity vs Apparent Density for water cured specimens

The rapid chloride permeability experiments were conducted based on ASTM C 1202 2009 tests at the age of 3, 7, 28, 90 and 365 days (Table 5-8). EH mixtures cast at 30°C, 35°C and 40°C observed a moderate permeability up to the age of 28 days, which reduced significantly at the age of 90 and 365 days. Both mixtures cast at 22°C with HANWA observed an increased RCP at the age of 365 days as opposed to the corresponding mixtures cast at higher temperatures. The difference between the aggregates was more intense in the mixtures cast in 22°C. Mixtures

PERICLES ALEXANDROU SAVVA

cast at 22ºC with HANWA observed a 30% higher RCP reduction rate than the corresponding NWA mixtures up to the age of 90 days. Despite the similarities observed up to the age of 90 days, their ultimate performance in RCP was indicative of the HANWA low quality. The significant increase of RCP values observed at 365 days for HANWA mixtures is attributed to a possible malfunction of the RCP test setup. Regarding the mixtures cast at 30ºC and 35ºC, the EH mixtures observed lower RCP than the EL mixtures, which was an indicator of the IC effectiveness. The mixtures cured in controlled conditions and produced with NWA observed lower RCP in all cast temperatures, where the lowest RCP value is exhibited from the mixture cast at 35ºC. The specific finding highlighted the importance of controlling the mixtures curing. Additionally, the exposed mixtures observed a 10% higher average RCP than the controlled cured mixtures. Comparing the RCP based on the curing regime for the NWA mixtures at the age of 365 days, the exposed mixtures observed 30% higher RCP than the controlled cured mixtures. The same comparison for the HANWA mixtures yielded in 3% lower RCP for the exposed mixtures. The specific finding verified the HANWA IC and restrain action and also verifies the damage caused to the NWA exposed mixtures by the high temperature and high temperature fluctuation. Regarding the cast temperature, the average RCP value of the mixtures cast at 22ºC and 40ºC was 5710 coulombs and 5199 Coulombs respectively, whereas the corresponding values for the mixtures cast at 30ºC and 35ºC were 4721 Coulombs and 4582 respectively. Rwo values in Table 5-8, regarding RCP experiments were designated with an asterisk. The specific experiments exceeded the maximum possible value recorded from the RCP configuration which is 10000 Coulombs. Nevertheless, the specific values were included in the analysis because the main objective was to compare the mixtures' behavior and monitor the development of their properties.

PERICLES ALEXANDROUSAKIS

Table 5-8: Rapid chloride permeability (Coulombs)

	3 days	7 days	28 days	90 days	365 days
22EL	8197	6526	5976	4618	2408
22EH	9540	7100	5704	3373	5130
30EL	5858	6242	5784	3711	2510
30EH	6760	5817	5965	5112	2045
35EL	6827	5084	4652	3508	1636
35EH	6324	5044	6252	4445	1493
40EL	10000*	8720	9247	6222	1761
40EH	7051	5840	4681	3979	2187
22CH	8357	6572	4542	2550	4193
22CL	8119	9938	6985	2700	1673
30CL	9969	6286	4179	2060	1264
30CH	7008	6012	2444	2495	2722
35CL	10000*	5733	4052	3400	1140
35CH	8119	5896	3261	2509	2165
40CL	9150	8328	4927	2546	1358
40CH	5581	4893	3244	2201	2171

5.3.1. Statistical analysis

The coefficient of determination was calculated as explained in section 4.4. The specific analysis was conducted for the mixtures' properties up to the age of 90 days (4 points - Table 5-9 and up to the age of 365 days (5 points - Table 5-10). The reason was that the rate of development of several properties was expected to be high in the early-age and decelerate in later-ages. Considering this, the property development versus time was also checked using the coefficient of determination, on a linear and logarithmic scale (Table 5-11 and Table 5-12). Observing

PERICLES ALEXANDROU SAVVA

Table 5-9 and Table 5-10, the first conclusion is the good correlation (R^2 = 0.75) between compressive strength and RCP at the age of 90 days which becomes excellent (R^2 = 0.86) at the age of 365 days. Both properties exhibited an excellent logarithmic correlation with time up to both 90 and 365 days that explains their correlation. More specifically, their compressive strength and the RCP up to the age of 90 days observed an excellent logarithmic behavior (R^2 = 0.79 and 0.96 respectively - Table 5-11) that improved even more at the age of 365 days (R^2 = 0.89 and 0.95 respectively - Table 5-12) as opposed to a good linear correlation. The specific was anticipated, considering that the majority of the cement quantity was hydrated at early ages. However, porosity and sorptivity exhibited significantly better linear than logarithmic rate of development. The two aforementioned properties suffered a great deterioration after the age of 28 days and more clearly from day 90 to day 365. The two specific properties observed similar behavior as shown in Figure 5-8 and Figure 5-9 and indicated from their degree of determination (R^2 = 0.73 at the age of 365 days). The fcm vs RCP correlation for CL mixture was excellent (R^2 = 0.99 at 90 days and R^2 = 0.98 at 365 days). The specific mixture was considered as the reference mixture since it was cured in controlled conditions and manufactured with NWA.

The exposed mixtures' properties observed a poor correlation up to the age of 90 days, which was highly improved at the age of 365 days. The specific observation occurred in every property combination. The water cured specimens observed a poor average correlation. However, several individual properties such as compressive strength versus RCP (R^2 = 0.95) and porosity versus sorptivity (R^2 = 0.90) observed an excellent correlation. The mixtures cast with low absorptive aggregates observed an excellent correlation up to the age of 90 days (R^2 = 0.81) which was good at the age of 365 days (R^2 = 0.61). The specific R^2 reduction was an indicator of the plateau of the properties development that occurred between the age of 90 and 365 days. The specific would be higher if two properties developed in the same rate (linear to linear or logarithmic to logarithmic). This was supported from the average correlation of compressive strength to RCP (R^2 = 0.86) and porosity to sorptivity (R^2 = 0.73) which were properties that developed in the same rate as explained previously and exhibited the best correlation at the age of 365 days.

PERICLES ALEXANDROU SAVVA

Table 5-9: Coefficient of determination (R^2) for each property (90 days)

	RCP	fcm	P	S	Sorptivity	fcm	P	Porosity	fcm
All		0.91	0.03	0.90		0.95	0.01		0.02
E		0.38	0.42	0.03		0.62	0.13		0.08
C		0.98	0.02	0.57		0.68	0.46		0.04
L		0.95	0.81	0.92		0.98	0.56		0.63
H		0.87	0.00	0.49		0.47	0.15		0.14
22ºC		0.70	0.25	0.15		0.59	0.16		0.09
30ºC		0.57	0.14	0.28		0.00	0.23		0.08
35ºC		0.77	0.00	0.44		0.20	0.58		0.05
40ºC		0.82	0.13	0.20		0.00	0.21		0.07
EH		0.26	0.04	0.43		0.88	0.13		0.04
CH		0.93	0.04	0.65		0.77	0.45		0.06
EL		0.56	0.44	0.68		0.10	0.32		0.59
CL		0.99	0.02	0.49		0.56	0.42		0.04
Average		0.75	0.18	0.48		0.52	0.29		0.15

PERICLES ALEXANDROU SAVVA

Table 5-10: Coefficient of determination (R^2) for each property (365 days)

	RCP	fcm	P	S	Sorptivity	fcm	P	Porosity	fcm
All		0.95	0.48	0.33		0.42	0.89		0.48
E		0.76	0.80	0.67		0.82	0.81		0.69
C		0.95	0.22	0.07		0.17	0.90		0.35
L		0.97	0.62	0.23		0.30	0.84		0.69
H		0.91	0.20	0.30		0.42	0.64		0.14
22ºC		0.78	0.15	0.07		0.08	0.71		0.38
30ºC		0.76	0.53	0.34		0.47	0.81		0.36
35ºC		0.88	0.43	0.61		0.56	0.77		0.52
40ºC		0.93	0.56	0.37		0.49	0.37		0.50
EH		0.61	0.47	0.78		0.84	0.38		0.21
CH		0.88	0.03	0.01		0.09	0.76		0.12
EL		0.88	0.83	0.35		0.54	0.68		0.88
CL		0.98	0.39	0.14		0.23	0.89		0.52
Average		0.86	0.44	0.33		0.42	0.73		0.45

PERICLES ALEXANDROU SAVVA

Table 5-11: Coefficient of determination (R^2) for each property plotted versus each time interval (90 days)

	Logarithmic					Linear			
	fcm	P	RCP	S		fcm	P	RCP	S
All	0.90	0.03	0.99	0.87		0.58	0.29	0.85	0.59
E	0.56	0.57	0.91	0.05		0.19	0.75	0.87	0.02
C	0.97	0.00	1.00	0.52		0.74	0.10	0.80	0.18
L	0.96	0.73	0.99	0.96		0.72	0.95	0.89	0.70
H	0.81	0.00	0.99	0.38		0.44	0.19	0.78	0.21
22ºC	0.82	0.21	0.98	0.25		0.45	0.26	0.94	0.03
30ºC	0.52	0.19	0.99	0.27		0.16	0.54	0.81	0.45
35ºC	0.97	0.02	0.90	0.30		0.90	0.24	0.65	0.03
40ºC	0.82	0.08	0.99	0.19		0.63	0.39	0.90	0.38
EH	0.43	0.11	0.91	0.49		0.11	0.38	0.80	0.14
CH	0.92	0.00	0.97	0.53		0.66	0.11	0.72	0.19
EL	0.53	0.71	0.89	0.76		0.28	0.33	0.91	0.89
CL	0.99	0.02	1.00	0.49		0.80	0.06	0.86	0.16
Average	0.79	0.22	0.96	0.43		0.51	0.36	0.83	0.30

PERICLES ALEXANDROUSSAVVA

Table 5-12: Coefficient of determination (R^2) for each property plotted versus each time interval (365 days)

	Logarithmic					Linear			
	fcm	P	RCP	S		fcm	P	RCP	S
All	0.96	0.55	0.99	0.40		0.72	0.93	0.67	0.87
E	0.80	0.72	0.95	0.57		0.72	0.98	0.85	0.86
C	0.98	0.44	0.94	0.23		0.68	0.86	0.51	0.73
L	0.98	0.60	0.99	0.22		0.80	0.97	0.76	0.72
H	0.90	0.36	0.95	0.49		0.62	0.67	0.54	0.92
22ºC	0.92	0.35	0.93	0.16		0.67	0.77	0.52	0.59
30ºC	0.75	0.63	0.99	0.43		0.56	0.95	0.66	0.86
35ºC	0.98	0.52	0.95	0.62		0.71	0.90	0.68	0.94
40ºC	0.92	0.49	1.00	0.32		0.75	0.72	0.78	0.72
EH	0.70	0.51	0.96	0.75		0.56	0.71	0.77	0.86
CH	0.93	0.29	0.82	0.23		0.57	0.63	0.32	0.73
EL	0.78	0.71	0.92	0.17		0.84	0.96	0.90	0.62
CL	1.00	0.52	0.98	0.23		0.74	0.95	0.62	0.73
Average	**0.89**	**0.51**	**0.95**	**0.37**		**0.69**	**0.85**	**0.66**	**0.78**

PERICLES ALEXANDROU SAVVA

5.3.2. Statistical analysis using SPSS

5.3.2.1. Regression analysis

The linear regression analysis for the mixtures up to the age of 28, 90 and 365 days was conducted. Considering compressive strength as the dependent variable and the specimen's age, cast temperature, curing method and aggregates as the independent variables, the results showed that the aggregates source had the largest influence in predicting the compressive strength (ANNEX II - Table 1). In following, the analysis showed that the specimen age and the curing method had similar influence on the compressive strength and the cast temperature showed minor influence.

The significance of all the independent variables was >0.05 except for cast temperature that was 0.875. The meaning of the specific value reflects the degree of confidence that can be given to the outcome values. Therefore, it is implied that the low influence of cast temperature on the compressive strength on the results is more likely an inconclusive value rather than a trend that characterizes the results. Since the results showed high variance for the mixtures cast at 40°C, the specific analysis was repeated without including the specific values. The significance of the cast temperature on the compressive strength was highly improved (0.005) and the influence of the cast temperature on the compressive strength was increased (2.818), as showed in ANNEX II –Table 2. The analysis was also conducted for the compressive strength including the specimens tested at 90 and 365 days. It can be observed in Table 1 to 6 that the influence of the cast temperature on the compressive strength was inconclusive (Low significance) when the mixtures cast at 40°C were included and the level of influence as well as the significance increase when the specific mixtures were excluded. The curing regime exhibited notable influence on the compressive strength at the age of 90 and 365 days (2.128 and 1.103) that increased when the mixtures cast at 40°C were excluded from the calculations (2.715 and 2.377). The significance of the specific values also increased accordingly (0.178 to 0.106 and 0.454 to 0.109). Despite the occasionally good compressive strength exhibited from specimens cast at 40°C, the main conclusion drawn was the high variability of the results.

The analysis was also conducted considering the porosity as dependent variable. The results showed that the only value with significant influence on the results was the aggregates source (Table 7). Repeating the same procedure, as in compressive strength it was showed that the cast

PERICLES ALEXANDROU SAVVA

temperature and curing regime highly improve where the specimen's age shows no significance on the material's porosity (Table 8).

When the regression analysis was conducted for the RCP and sorptivity results, the influence and the significance of the cast temperature on the results was highly improved when the mixture cast at 40°C was excluded. The specific was observed at 28, 90 and 365 days.

5.3.2.2. General remarks

Based on the regression analysis and according to the equations predicting the future behavior of the tested properties (Table 1 up to Table 24), the following conclusions were drawn. The conclusions presented below are written in an ascending order beginning with the most influential.

5.3.2.2.1. 28 days

Compressive strength

- Decreased when aggregates absorption increased
- Increased with age
- Increased when exposed
- Increased with cast temperature

Porosity

- Increased when aggregates absorption increased
- Decreased with age
- Decreased when exposed
- Cast temperature had no influence

Rapid chloride permeability

- Decreased with age
- Decreased when aggregates absorption increased
- Increased when exposed
- Decreased with cast temperature increased

Sorptivity

- Increased when aggregates absorption increased
- Decreased with age
- Decreased with cast temperature increased
- Decreased when exposed

PERICLES ALEXANDROU SAVVA

5.3.2.2.2. 90 days

Compressive strength

- Decreased when aggregates absorption increased
- Increased with age
- Increased when exposed
- Increased with cast temperature increased

Porosity

- Increased when aggregates absorption increased
- Decreased when exposed
- Increased with cast temperature increased
- Increased with age

Rapid chloride permeability

- Decreased with age
- Decreased when aggregates absorption increased
- Increased when exposed
- Decreased when cast temperature increased

Sorptivity

- Increased when aggregates absorption increased
- Increased with cast temperature increased
- Increased with age
- Increased when exposed

PERICLES ALEXANDROU SAVVA

5.3.2.3. Descriptive analysis

Due to large volume of data, a descriptive analysis was conducted using the specific statistical software, in order to extract general trends of the material properties (ANNEX II – Figure 1 to Figure 16). In addition, since the current chapter focuses on the IC, the NWA were excluded in order to extract possible trends of the IC mixtures (ANNEX II –Figure 17 to Figure 28). It has to be clarified that the line bars in Figure 1 up to Figure 28 in ANNEX II , represent the minimum and the maximum value of each tested parameter where the solid bars represent the lower and the upper bound of the 95% confidence interval for mean.

The specific analysis showed an increasing trend (versus age) of the mixtures' compressive strength in the case where both NWA and HANWA were included (Figure 1) and in the case where only HANWA were tested (Figure 17). Decreasing trend was observed in the RCP results in both cases up to the age of 365 days (Figure 3 and Figure 19). The porosity results in both case of the analysis showed a continuous decrease up to the age of 28 days that reversed at the age of 90 and 365 days (Figure 2 and Figure 18). The average increase observed in the porosity values from day 28 to day 365 was 29.7% for all the mixtures and 24.0% for the HANWA mixtures. The specific increase was 29.9% and 43.8% respectively, when the mixtures cast at 40°C were excluded from the analysis. The reason was the high porosity values and high variability exhibited from the specific mixtures from early ages. The sorptivity values in both cases (Figure 4 and Figure 20) a stable behaviour from day 3 up to day 90, but were highly increased at the age of 365 days (581.1% for all the mixtures and 69.8% for the HANWA mixtures)

The mixtures cast at 40°C showed the higher variability, with compressive strength and porosity values varying from 30.2 MPa to 89.2 MPa and 10.0% to 22.1% respectively (Figure 6, Figure 22, Figure 5 and Figure 21). The mixtures cast at 35°C observed the higher average compressive strength and the lowest spread. The porosity of the specific mixtures for both cases (NWA + HANWA and HANWA) was the lowest average porosity among the series (Figure 6 and Figure 22). The same conclusions stood for the RCP and sorptivity when all the mixtures were tested (Figure 7 and Figure 8) which was changed when only HANWA mixtures were tested (Figure 23 and Figure 24). According to Figure 9 and Figure 25 the compressive strength of the mixtures cured in controlled environment was higher than the mixtures exposed to the environment,

PERICLES ALEXANDROU SAWA

which however was reversed when the NWA were excluded from the calculations. Figure 10 and Figure 26 showed that the porosity values were similar when the two curing regimes were compared and reduced slightly for the exposed mixtures when the NWA were excluded from the calculations. The RCP results were similar according to Figure 11 for both methods of curing where the exposed mixtures exhibited lower RCP values when the NWA were excluded from the calculations (Figure 27). Similar trend was observed in the sorptivity values (Figure 28). However the exposed mixtures observed higher values when both types of aggregate specimens were included (Figure 12).

5.4. Conclusions

It was showed that the exposure of concrete in severe environmental conditions increased the negative impact on the material's performance. Based on the current chapter, the following conclusions were drawn:

- The compressive strength of the IC mixtures exposed to the environment performed significantly better (11.5%), considering the curing conditions, than the corresponding mixtures cured in controlled conditions. The specific characteristic was attributed to the IC which replenished the water in the material's porosity and enhanced the degree of hydration. The IC enhanced also the bond between the aggregates and cement paste (mortar), due to higher absorptivity and increased of degree of hydration near the aggregates surface. On average, the IC mixtures exposed to the environment, exhibited a similar (7.8% difference) compressive strength, with the corresponding NWA mixtures.
- Regarding the porosity and sorptivity, the mixtures cast with HANWA and exposed to the environment (EH) showed an improved performance as opposed to the corresponding water cured mixtures. However, the specific mixtures exhibited a poorer performance compared to the corresponding NWA mixtures (EL). The improved porosity of the EH mixtures was attributed to the action of IC, which however, due to the poor IC agents' dispersion was not that effective to overcome the NWA mixtures. The exact opposite behavior was observed in the NWA mixtures. The specific behavior was anticipated since the exposed mixtures undergone intense stress cycles from their early-age.

PERICLES ALEXANDROU SAWA

- The HANWA RCP values of both the exposed and water cured specimens performed better than the corresponding NWA mixtures. This was attributed to the IC and the low aggregates modulus of elasticity. RCP is an indicator of the material's pore network instead of the voids total fraction (porosity). It has to be mentioned that the effectiveness of IC is expected to be more pronounced at a small distance from the IC source. Therefore, the pore network sealing is more likely than the total porosity reduction.
- The correlation of the material properties indicated a good correlation between compressive strength and porosity, when the results were averaged and plotted in terms of the cast temperature. The compressive strength also exhibited an excellent correlation with the RCP when the specific analysis was conducted using the time interval based values. Compressive strength and RCP exhibited an excellent correlation when their independent plot was conducted versus time on a logarithmic scale.
- The mixtures cast at 40^{o}C showed a poor and unpredictable behavior. The major issue rising from the specific mixtures is the uncertainty regarding their property evolution.
- It is presumed that the exposure of concrete mixtures cast with NWA caused significant damage to the materials' microstructure. The utilization of aggregates with low modulus of elasticity such as HANWA offered a lower degree of restrain, which allowed greater deformations of the cement paste. The employment of IC compensated for the lack of water and contributed to an enhanced microstructure, which was reflected on the results.

The main conclusions drawn from the current research highlight the importance of maintaining the cast temperature at low levels and the importance of providing proper curing to concrete mixtures. In addition, the conversion of a low quality material (HANWA) into a useful IC agent was achieved. It was proven that an IC mixture including HANWA, performed very well, converting an otherwise "waste" material into a high performance IC agent. However, a degradation mechanism was observed, that occurred at later ages. The specific mechanism appeared in both HANWA and NWA mixtures.

It was expected that the exposure of concrete to an environment where high temperatures and temperature fluctuations occur would eventually damage the material's mechanical and durability performance. It was shown that the curing conditions had a great impact on the materials' final performance. The reference mixtures performed better than the IC mixtures due

PERICLES ALEXANDROU SAWA

to the better quality of aggregates. However, the hot temperatures had a severe impact on the reference mixtures. On the contrary, the exposed IC mixtures exhibited improved behavior in terms of mechanical and durability properties than the corresponding water cured. HANWA IC is a cost-effective method to improve the behavior of concrete.

PERICLES ALEXANDROU SAVVA

6. Internal curing theoretical verification

6.1. Water binding in cementitious system

6.1.1. Brunauer, Emmett and Teller (B.E.T.) theory

B.E.T. theory explains the physical adsorption of gas molecules on solid surfaces in order to measure the specific surface area of various materials (Nina and Andrew, 1987). In a cementitious system, various forces are responsible for binding water molecules. The water is classified according to the forces and the mechanism binding its molecules. Feldman and Sereda stated that water included in pores greater than 50 Angstroms is classified as capillary water in two subcategories (Feldman and Sereda, 1970): The water in pores greater than 50 nm is considered as free water whose evaporation will not affect the system, whereas the amount of water in pores 5-50 nm is still free to evaporate; however, its egress will cause shrinkage. Capillary water is considered as free water and therefore it does not participate in the process of hydration. It was mentioned previously, that one gram of cement requires 0.42 gram of water to become fully hydrated (Powers and Brownyard, 1947). The capillary water is not included in the specific calculation. Powers mentioned that 0.23 g of water is chemically bounded (not presented in Figure 6-1) and 0.19 g of water is physically adsorbed (Adsorbed water and Interlayer water - Figure 6-1).

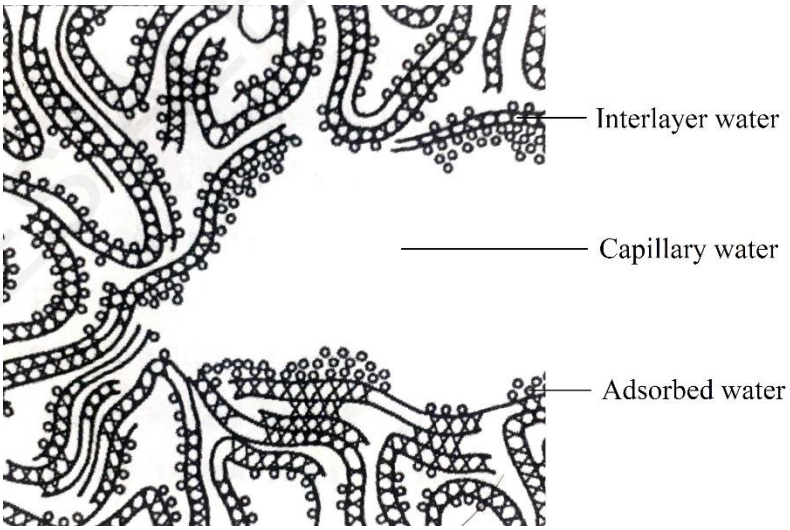

Figure 6-1: Water in C-S-H structure (Feldman and Sereda, 1970)

Several useful conclusions can be drawn from B.E.T. theory regarding the binding mechanism between a solid surface and a gas or a vapor. The B.E.T. theory explains that the mechanism of

physical adsorption is the result of attractive van der Waal's forces acting between solid and gas molecules. The specific forces are of lower intensity than the forces involved in chemical reactions. When water vapor is in motion above a solid surface, the molecules attracted on the surface are in condensed phase and may be considered as a different phase. The net result of the specific process is a continuous molecule interaction between the solid surface and the vapor phase, where the solid surface concentration remains higher than the vapor concentration, due to the surface attraction. In addition, the water molecules may be adsorbed directly on the surface or on a previously adsorbed molecule. The main difference between the energy binding the two molecules is that the energy required for the first layer adsorbed to evaporate has to be the sum of its heat of vaporization and the energy of the attractive forces (Powers and Brownyard, 1947). The theory states that the amount of the adsorbed molecules is directly proportional to the surface area of the solid.

6.1.2. Capillary condensation

Powers and Brownyard elaborated B.E.T. theory and provided its application on water vapor moving above a water surface (Powers and Brownyard, 1947). At first, it was provided that the surface of attraction is the water or pore fluid surface itself and that a convex surface (meniscus) leads to an increased surface area. On the other hand, the surface tension strives to reduce the meniscus curvature, the water in the cylinder is continuously under tension, reducing the vapor pressure for a given temperature. Therefore, it is concluded that the greater the curvature, the greater the surface tension and the lower the vapor pressure. The specific relationship between the vapor pressure and the pores curvature leads to the Kelvin equation.

6.2. Kelvin's Law

The equation that connects the surface tension of a liquid with its vapor pressure was established in 1871 by Sir William Thomson also known as Lord Kelvin (Sir William Thomson, 1871). The specific theorem states that the pressure of a vapor above a liquid surface varies in height according to the hydrostatic law. Therefore, a saturated vapor above a concave surface has less pressure than a saturated vapor above a convex surface. It continues saying that vapor from different vessels all enclosed in a single vessel will evaporate from the higher surfaces and condense on the lower surfaces until hydrostatic equilibrium is reached.

PERICLES ALEXANDROU SAVVA

6.3. Kelvin theorem and mercury intrusion porosimeter – Application on HANWA

The capillary pressure needed to drain a pore is controlled by its minimum radius where the capillary pressure needed to fill a pore is controlled by its maximum radius (Charbeneau, 2002). Henkensiefken (Henkensiefken, Bentz, *et al.*, 2009) stated that the larger pores are the first to empty in a capillary system. This was also supported by Castro et al. (Castro, Bentz and Weiss, 2011) who supported that in higher RH values the larger pores are the first that exhaust their water (Figure 6-2). Bentz et al. specified that during desorption, a pore is getting empty only when its size equals or exceeds the Kelvin/ Young Laplace equation (6-3) radius and when the surrounding wall is not depercolated (Bentz, Garboczi and Quenard, 1998). It was mentioned above that the compression forces that develop on the pores surrounding wall counteract the tension forces and disjoining pressure reduction, are responsible for the material's contraction. The first mechanism is reflected in Young-Laplace equation (6-1) in terms of surface tension increase and in Kelvin equation (6-2) in terms of RH decrease. Additionally, knowing the RH, the capillary pressure can be extracted using Kelvin equation (6-2) or the meniscus radius using Kelvin/ Young Laplace equation (6-3), where molar volume in pore solution (V_m) is ~ 18 x 10^{-6} m^3/mol (Radlinska *et al.*, 2008; Henkensiefken, Bentz, *et al.*, 2009). The combination of Young-Laplace equation (6-1) and Kelvin equation (6-2) can be useful in order to evaluate the relation between the equilibrated RH and the radius of the smallest empty pore (Kelvin/ Young Laplace equation (6-3)).

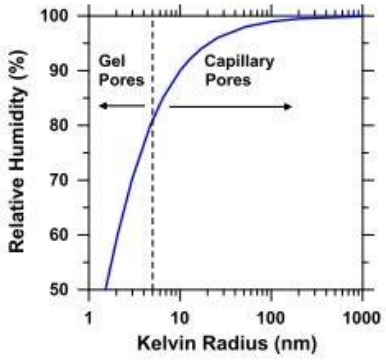

Figure 6-2: Relation between RH and partially empty pores in cement paste (Castro, Bentz and Weiss, 2011)

PERICLES ALEXANDROU SAWA

$$\sigma_{cap} = -\frac{2\gamma\cos(\theta)}{r} \quad \text{Young-Laplace equation} \quad (6\text{-}1)$$

$$\sigma_{cap} = \frac{RTln(RH)}{V_m} \quad \text{Kelvin equation} \quad (6\text{-}2)$$

$$r = -\left(\frac{2\gamma\cos(\theta)}{ln(RH)}\right)\left(\frac{V_m}{RT}\right) \quad \text{Kelvin/ Young Laplace equation} \quad (6\text{-}3)$$

where σ_{cap} is the capillary pressure, γ is the surface tension, $\cos(\theta)$ is the contact angle and r is the radius of curvature, R is the Universal gas constant, T is the absolute temperature, RH is the relative humidity and V_m is the molecular mass.

Henkensiefken illustrated the concept of IC, where the large pores are expected to be emptied first (Henkensiefken, Bentz, *et al.*, 2009) - Figure 6-3. HANWA and cement paste (7 days) were tested in MIP (Figure 6-4). Considering Figure 6-3 and Figure 6-4, it was clearly observed that the HANWA would provide their moisture in the cement paste, since the aggregates pores were larger than the cement paste pores (Figure 6-3). Both aggregates (HANWA and NWA) were tested in MIP in order to demonstrate their difference in porosity and pore distribution. Their cumulative and incremental pore distribution are showed in Figure 6-5 and Figure 6-6 respectively whereas their basic pore network properties are provided in Table 6-1. It has to be mentioned that the IC mechanism has the ability to self-enhance its action, because the IC water withdrawal force is the pores underpressure, which increases as the pore size decreases. Considering the action of IC water is to enhance the degree of hydration, thus reducing pore size, the mechanism is expected to function up to the HANWA pores fully IC water utilization. Therefore, the key factor of IC in the case of HANWA is the initiation. The results provided verify that HANWA had such a pore size distribution that allowed the cement paste to withdraw water from its pores, namely to initiate IC. The specific was also verified in Figure 6-7 where the cement paste showed a continuously lower size of empty pores as compared to HANWA, which reflects the continuous action of IC. The specific is analyzed in greater detail in section 6.5.

PERICLES ALEXANDROU SAVVA

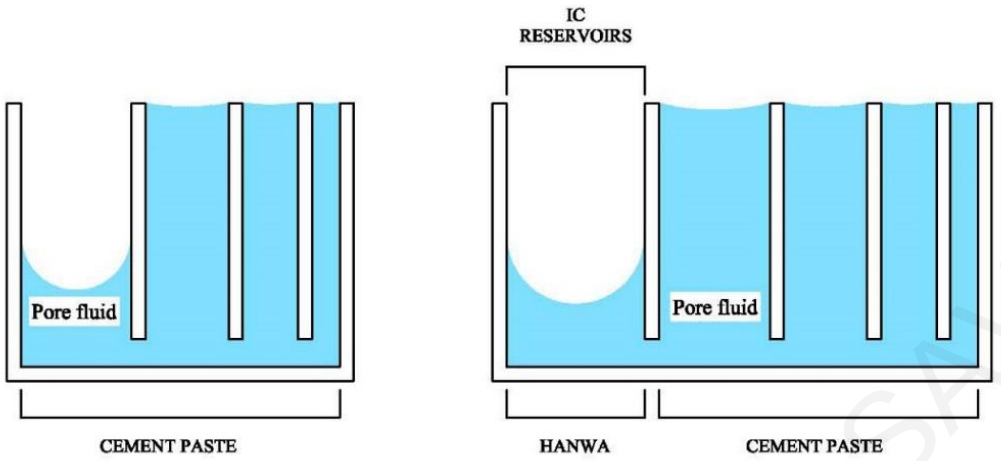

Figure 6-3: Illustration of menisci formation in sealed specimens (Concept based on Henkensiefken, Bentz, et al. 2009)

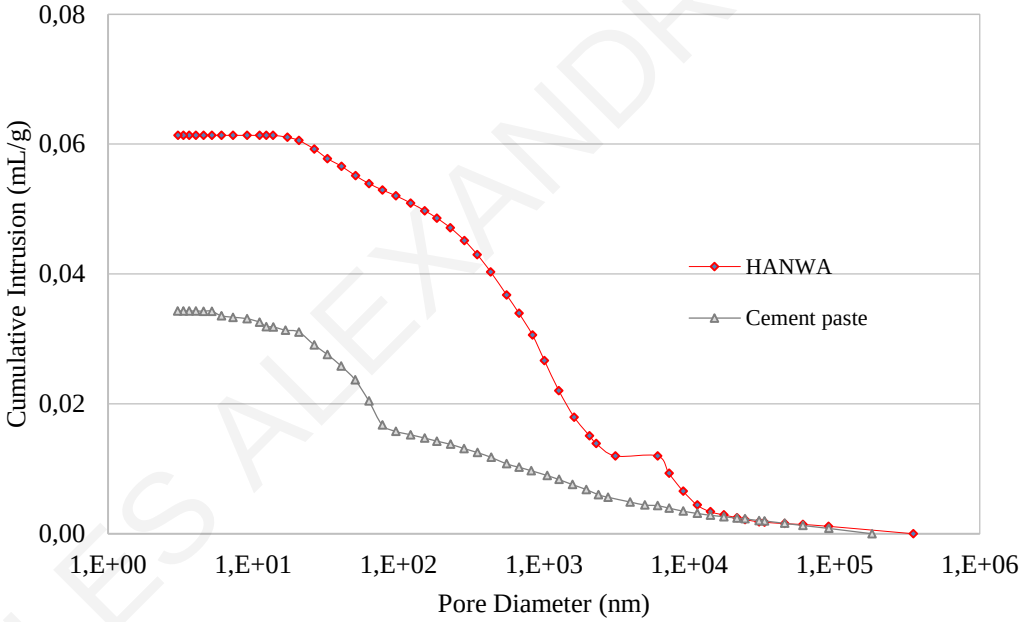

Figure 6-4: HANWA and cement paste cumulative intrusion in MIP

PERICLES ALEXANDROU SAWA

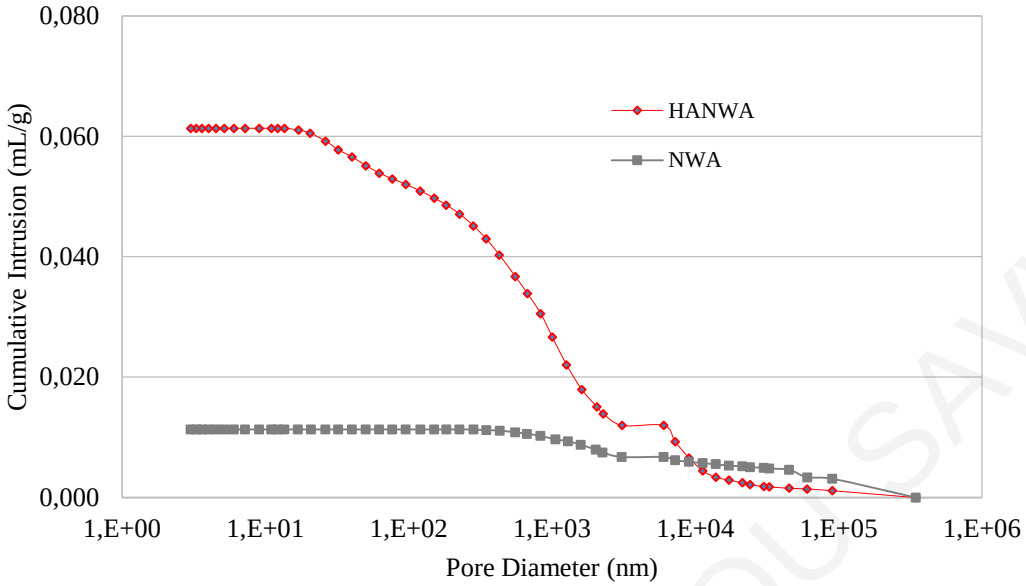

Figure 6-5: Aggregates cumulative intrusion (mL/g)

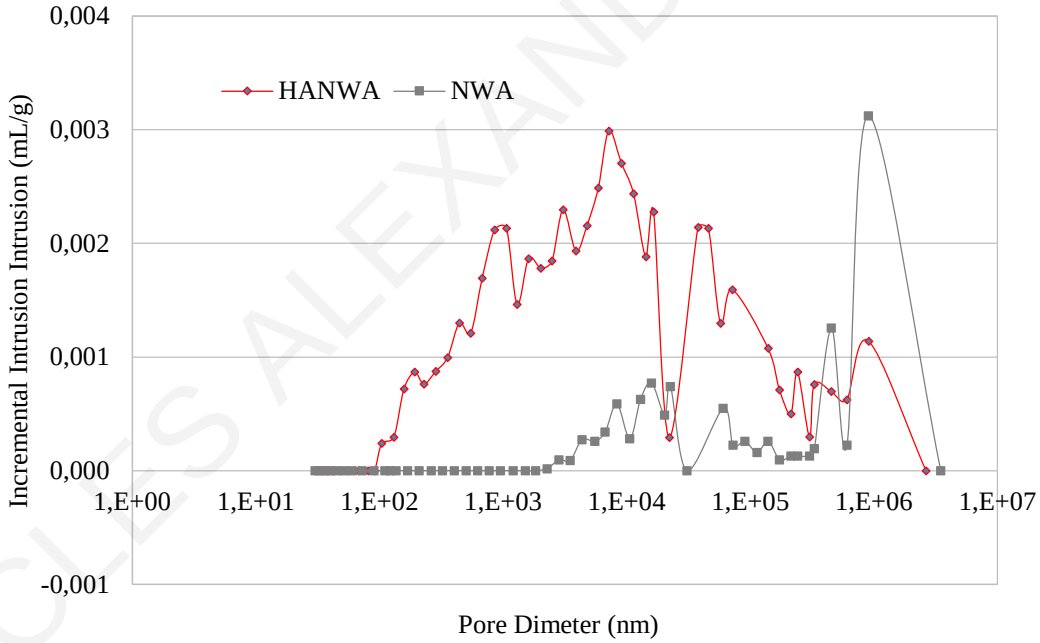

Figure 6-6: Aggregates incremental intrusion (mL/g)

PERICLES ALEXANDROUSAVVA

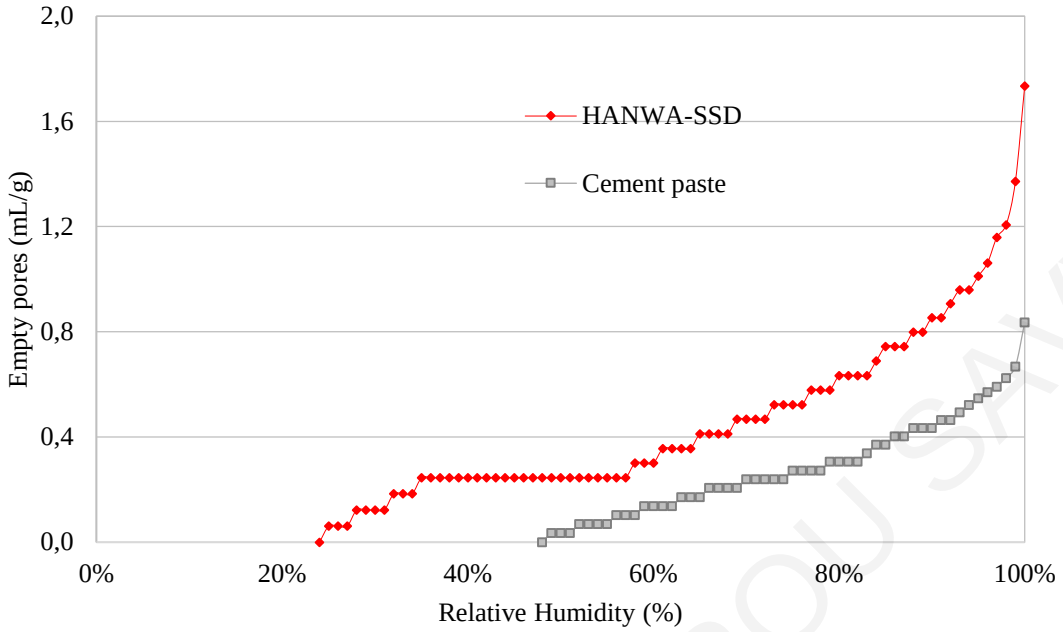

Figure 6-7: Theoretical empty pores (mL/g) of HANWA-SSD and cement paste according to Kelvin equation

Table 6-1: Mercury porosimeter results for both types of aggregates

		HANWA	NWA
Total Intrusion Volume	mL/g	0.055	0.0113
Total Pore Area	m^2/g	1.622	0.018
Apparent (skeletal) Density	g/mL	2.61	2.88
Porosity	%	12.64	3.15
Tortuosity		16.87	6.49

The evaluation of the HANWA and cement pore distribution verified the ability of HANWA to be utilized as IC agents. In order to develop a desorption isotherm curve, the Kelvin/ Young Laplace equation (6-3) equation was used. The theoretical desorption curve (Figure 6-8) was plotted against the experimental desorption curve provided in Section 4.2.2 (Figure 4-4). The most important conclusion is that the theoretical desorption curve is in accordance to the experimental desorption curve, especially at high RH values. It has to be mentioned that the

PERICLES ALEXANDROU SAVVA

MIP experiment is conducted on a single grain where the experimental desorption isotherm experiment is conducted on a sample of 100 g aggregates, which is more representative.

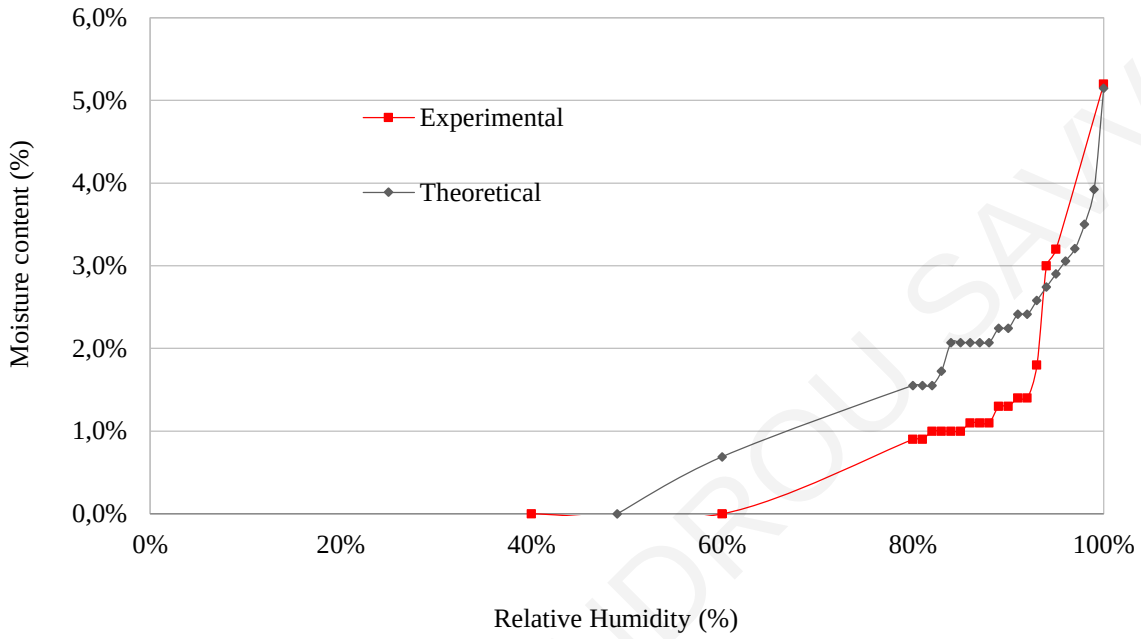

Figure 6-8: HANWA theoretical and experimental desorption

6.4. Mercury Intrusion Porosimeter on mixtures

The two basic mixtures presented in Chapter 4 (Control and HANWA-SSD) were examined in MIP, at three different ages, in order to evaluate the progress of their pore distribution as well as their porosity (Figure 6-9 and Figure 6-10). At the age of 3 days, a high percentage (67%) of the pores of the control mixture was concentrated in the range of 10-100 nm, which according to Snoeck, Velasco, et al. 2015, falls in the lower limit of the capillary porosity. At the age of 7 days, a small percentage (1.7%) shifted to the range of 600-1500 nm where the percentage concentrated at the range of 10-100 nm reduced to 59%. Correspondingly, at the age of 28 days a higher percentage (18%) was concentrated at the range of 25-45 μm where the percentage concentrated at the range of 10-100 nm was reduced to 51%. The specific was a result of the chemical shrinkage pores nucleation, which increased with respect to time. In the case of HANWA-SSD mixture, the pore formation exhibited a different behavior. The majority of the pores (77%) was concentrated in the range of 10-100 nm at the age of 3 days. At the age of 7 days the specific percentage was reduced to 64% and a slight increase of the porosity (2%) at

PERICLES ALEXANDROU SALVA

the range of 20-30μm. It is important to note that the HANWA-SSD mixture did not exhibit the porosity increase attributed to the chemical shrinkage pores, as opposed to the control mixture. At the age of 28 days, the HANWA mixture observed an additional reduction (58%) of the porosity in the range of 10-100nm. The reduction of the porosity concentrated in the range of 10-100nm – which was the range with the highest porosity – was 11.9% for the control mixture (from 67% to 59%) and 24.9% for the HANWA-SSD mixture (from 77% to 54%). The specific, in addition to the continuous reduction of the pore diameter, indicated the effect of IC in the HANWA-SSD mixture.

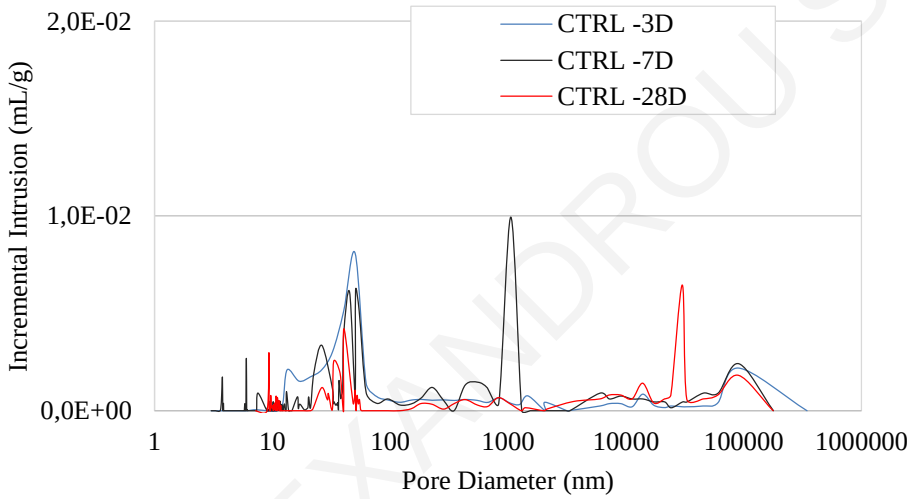

Figure 6-9: Mercury incremental intrusion for control mixture (mL/g)

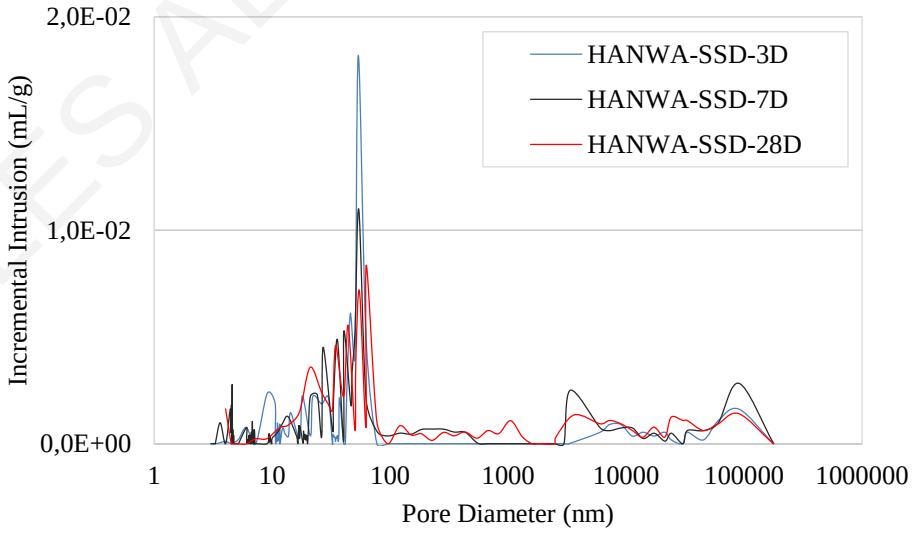

Figure 6-10: HANWA-SSD mixture mercury incremental intrusion (mL/g)

PERICLES ALEXANDROU SAVVA

6.5. Evaluation of HANWA-SSD efficiency using the results of mercury intrusion porosimeter

In order to verify the IC action of mixtures including HANWA, the principle illustrated by Henkensiefken (Figure 6-3) was examined using mercury intrusion porosimeter. In Figure 6-12, the pore distribution of HANWA and HANWA mixture at different ages was presented. It is observed in Figure 6-12 that the majority of the pores in the case of HANWA was concentrated in pores with a diameter higher than 100 nm (80%). The cement paste from HANWA mixtures observed only 10.7% pores with diameter higher than 100 nm, at the age of 3 days. One would expect that the corresponding porosity would decrease with respect to time. However, the pore size increased from day 3 to day 7 (18.1%) and day 28 (23.5%) was attributed to the chemical shrinkage pore nucleation that was expected to occur at later ages (Figure 6-11). The IC initiation due to higher pore diameter in the aggregates than the cement paste was confirmed. However, the IC action was not quantified, because of an opposite action yielding from the chemical shrinkage. In order to assess the effect of IC during the mixtures aging, the same calculations were conducted on the control mixture, where no IC was employed. The corresponding percentage of NWA mixture was significantly higher than the HANWA-SSD mixture. More specifically, the percentage of pores with diameter higher than 100 nm was 33.1%, 32.3% and 42.6% at the age of 3, 7 and 28 days respectively. This highlighted the effect of IC on the cement paste that reduces the pore diameter due to extended hydration.

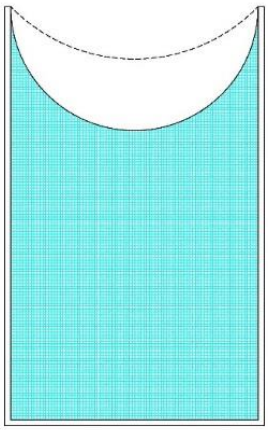

Figure 6-11: Liquid meniscus in a cylindrical pore (Powers and Brownyard, 1947)

PERICLES ALEXANDROU SAWA

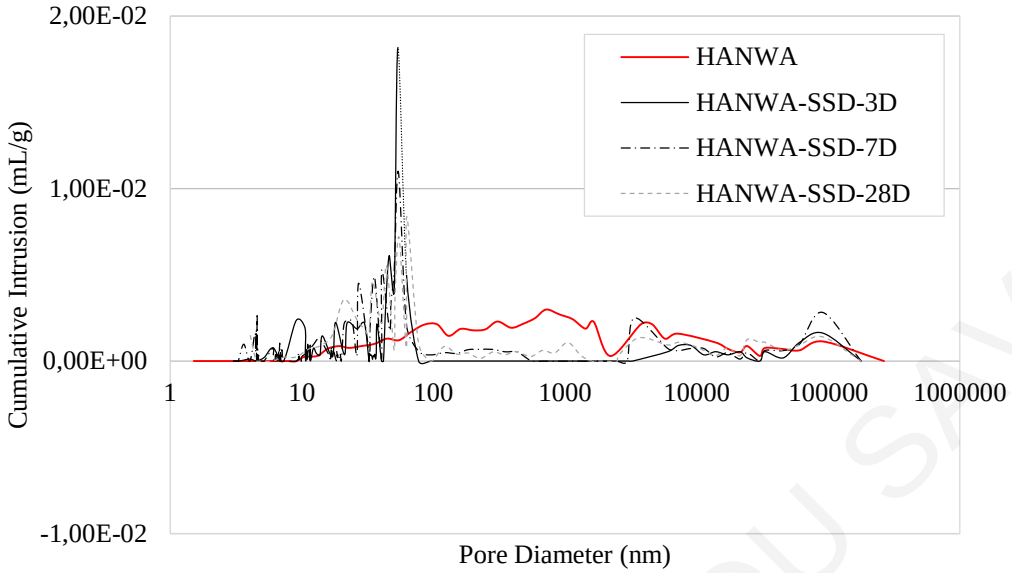

Figure 6-12: Incremental intrusion of HANWA compared to HANWA mixtures (mL/g)

Table 6-2: Aggregates (HANWA and NWA) and mixtures pore size distribution

	HANWA	HANWA-SSD-3D	HANWA-SSD-7D	HANWA-SSD-28D
Total Intrusion (mL/g)	5.55E-02	7.27E-02	8.75E-02	8.21E-02
Intrusion in pores > 100nm	4.44E-02	7.75E-03	1.58E-02	1.93E-02
Percentage	80.0%	10.7%	18.1%	23.5%

	NWA	Control -3D	Control -7D	Control -28D
Total Intrusion (mL/g)	1.13E-02	4.01E-02	8.35E-02	4.80E-02
Intrusion in pores > 100nm	1.13E-02	1.33E-02	2.69E-02	2.04E-02
Percentage	100.0%	33.1%	32.3%	42.6%

PERICLES ALEXANDROU SAWA

Table 6-3: Mixtures pores classification

	Control			HANWA-SSD		
	3 days	7 days	28 days	3 days	7 days	28 days
Gel pores <10nm	0.13%	9.20%	11.24%	4.81%	17.92%	18.63%
Capillary pores 10nm-10μm	87.43%	81.96%	59.35%	87.76%	73.93%	71.05%
Voids<10μm	12.44%	8.84%	29.41%	7.43%	8.15%	10.32%
	Normalized according to mixture porosity					
Gel pores <10nm	0.01%	1.53%	1.18%	0.72%	3.32%	3.25%
Capillary pores 10nm-10μm	8.12%	13.61%	6.21%	13.23%	13.68%	12.38%
Voids<10μm	1.16%	1.47%	3.08%	1.12%	1.51%	1.80%
Total Porosity %	9.29%	16.60%	10.46%	15.08%	18.50%	17.43%

Snoeck et al. categorized the pores as gel pores (<10nm), capillary pores (10nm-10μm) and voids (>10μm) (Snoeck *et al.*, 2015). The specific was conducted as shown Table 6-3 in order to get a better understanding of the mixtures' microstructure. The MIP experiments revealed a higher porosity for the HANWA-SSD mixture (17.43%) as opposed to the control mixture, at the age of 28days. However, as indicated in Table 6-3, only 10.32% of the HANWA-SSD pores is higher than 10 μm compared to a 29.41% of the control mixture. Snoeck et al. mentioned that mixtures with the same w/c ratio should have the same capillary porosity (Snoeck *et al.*, 2015). The 28-day porosity of HANWA-DRY mixture was almost identical with HANWA-SSD.

6.6. Volumetric phase distribution

Based on the approach derived by Jensen and Hansen (Jensen and Hansen, 2000) we extracted from Powers' model (Powers and Brownyard, 1947) the phase distribution of the cement paste of the two mix designs presented in Chapter 4, Section 4.2.1 (Table 4-4) and Chapter 5, Section 5.2.1 (Table 5-3) was calculated using the equations of Initial porosity (6-4), Chemical shrinkage (6-5), Capillary water (6-6), Gel water (6-7), Gel solid (6-8) and Unhydrated cement (6-9) The phase distribution was calculated without the effect of IC for the w/c 0.25 (Figure 6-13) and the 0.40 (Figure 6-15) mixtures. Additionally, the maximum expected degree of

PERICLES ALEXANDROUSAKIS

hydration was derived from the specific calculations based on Powers' model which suggests that for w/c ratio < 0.42, a_{max} = 1 is not possible. Jensen mentioned that only free water or capillary water is unimpededly available for hydration (Jensen and Hansen, 2000).

$$p = (w/c)/(w/c + \rho_w/\rho_c)$$ Initial porosity (6-4)

$$V_{cs} = \rho_c 6.410^{-5} (1-p)\, a = 0.20\,(1-p)\, a$$ Chemical shrinkage (6-5)

$$V_{cw} = p - (\rho_c/\rho_w)\,(0.19 + 0.23)\,(1-p)\, a = p - 1.32\,(1-p)\, a$$ Capillary water (6-6)

$$V_{gw} = (\rho_c/\rho_w)\, 0.19\,(1-p)\, a = 0.60\,(1-p)\, a$$ Gel water (6-7)

$$V_{gs} = (1 - \rho_c 6.410^{-5} + (\rho_c/\rho_w)0.23)\,(1-p)\, a = 1.52\,(1-p)\, a$$ Gel solid (6-8)

$$V_{uc} = (1-p)\,(1-a)$$ Unhydrated cement (6-9)

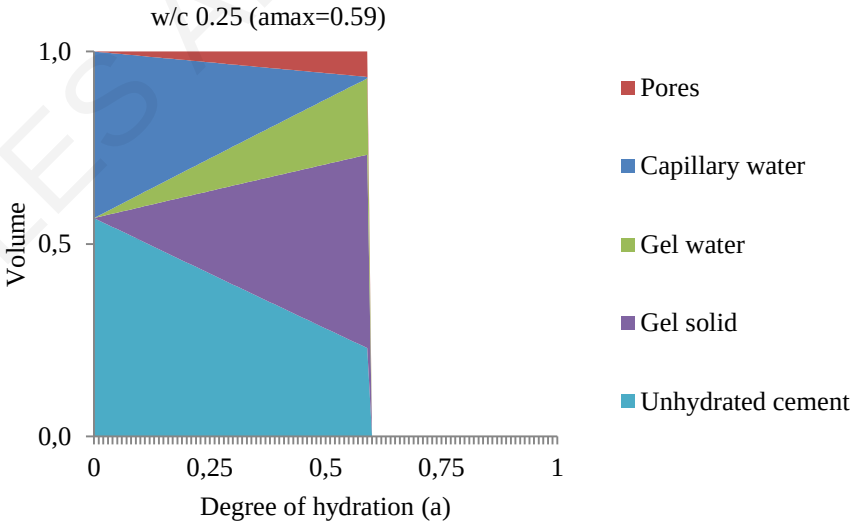

Figure 6-13: Phase distribution of HANWA w/c 0.25 mixture

PERICLES ALEXANDROU SAWA

According to Figure 6-13, the maximum degree of hydration of the mixtures cast with w/c ratio 0.25 is 0.59. Including the IC water (Figure 6-14), according to the volumetric phase distribution, the maximum degree of hydration may reach 0.71. In addition, since the specific volume distribution represents only the cement phase, it is not expected to increase the capillary porosity due to water consumption. Therefore, porosity remains constant and the effect of additional water is reflected on the gel water, gel solid and unhydrated cement phase. This is a simplified approach and its scope is to represent the effect of IC on the degree of hydration without producing additional porosity. It has to be mentioned that the addition of SAP in concrete produces extra porosity, since the water in SAP is considered as bulk water and its consumption will result in additional porosity (Jensen and Hansen, 2000). On the other hand, the action of LWA in concrete is identical to the action of HANWA, since the specific is not part of the cement system.

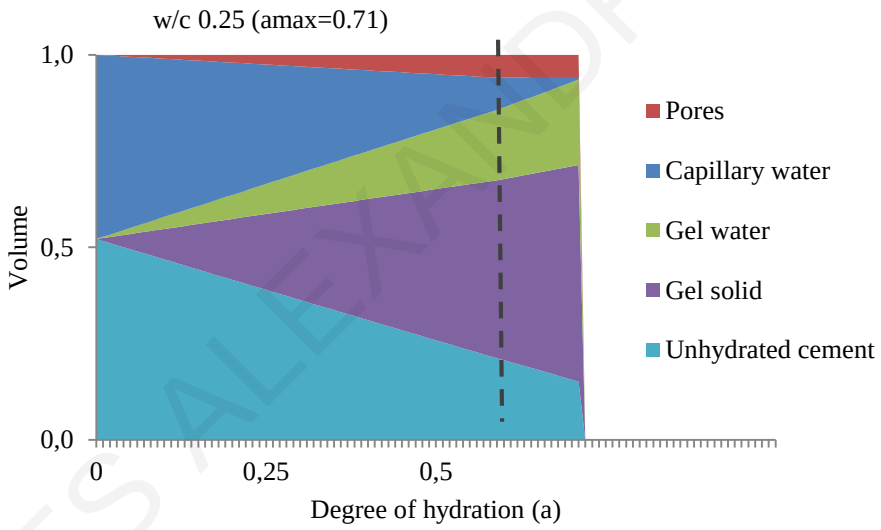

Figure 6-14: Phase distribution of HANWA w/c 0.25 mixture including 0.05 IC water

The IC water in mixtures cast with 0.40 w/c ratio was not expected to contribute in the degree of hydration extension, since the maximum expected degree of hydration according to the volumetric phase distribution was 0.95. However, the value that yielded from the specific calculations suggested that when the a_{max} was reached, 0.95 in this case, 0 grams of cement would remain unhydrated (Figure 6-15).

PERICLES ALEXANDROU SAVVA

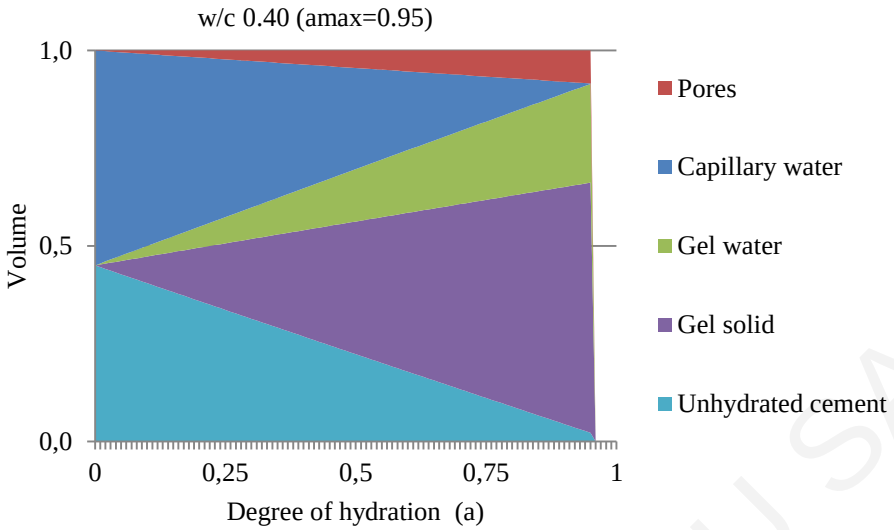

Figure 6-15: Phase distribution of HANWA 0.40 mix design

6.7. Conclusions

The current chapter presents the evaluation of HANWA (aggregates and mixtures), using equations from the literature and advanced testing techniques such as mercury intrusion porosimeter. The results showed that the HANWA aggregates pores have an average pore size larger than the cement paste, which implies that the water evaporation will begin from the aggregates before initiating from the cement paste. The evaporation form the HANWA mixtures cement paste will initiate after the aggregates water exhaustion, since the pore fluid replenishment form the aggregates will continuously increase the capillary pressure. Based on Powers and Brownyard, 1947, it was showed that a low w/c ratio mixture will exhibit, among others, lack of adequate water for hydration. Using internal curing, it was demonstrated that water can be provided from the inside of the structure, enhancing significantly the cement hydration.

PERICLES ALEXANDROU SAVVA

7. Innovative techniques for measuring relative humidity in concrete

7.1. Introduction

The most prominent effect of internal curing in concrete is the maintenance of the RH values at high levels, in order to minimize self-desiccation. The development of RH sensors was decided since the commercial RH sensors are expensive and thus not appropriate for concrete applications. For comparison reasons, commercial moisture sensors were initially utilized. The configuration utilized for the specific experiment was ML3 thetaprobe connected on a general-purpose data logger, with two analogue, two resistances, one event, one counter and one alarm channel. The data logger was connected to a personal computer and the data were recorded using a specialized software. The mixtures tested in the specific experiment were the control and the HANWA-SSD described in Chapter 4. The mixtures were cast in plastic molds and cured in an environmental chamber at constant RH and temperature for the whole duration. The mixtures' RH was recorded for a time-period of 15 days and the results demonstrated that the HANWA-SSD mixture exhibited higher RH than the control mixture. The control mixture observed a steep drop in RH from day three up to day five. The specific drop is expected in mixtures with low w/c ratio. The drop in HANWA-SSD RH was smoother than in the control. The reason was the IC water carried in the aggregates pore network. It was explained previously that the specific amount of water will be utilized to the mixture through the mechanism of diffusion, when the capillary pressure drops.

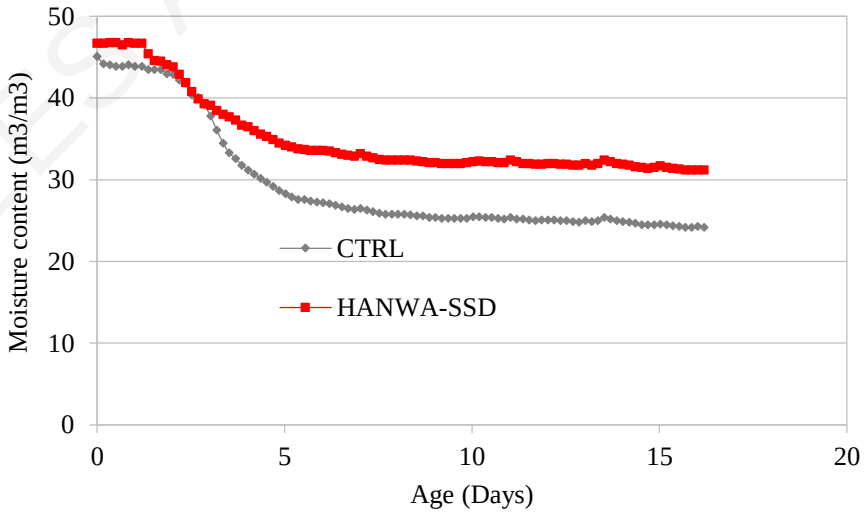

Figure 7-1: Moisture measurement of HANWA-SSD and control mixtures

PERICLES ALEXANDROU SAVVA

It was decided that an innovative configuration was going to be investigated because the high accuracy commercial sensors are very expensive and cannot be used to measure RH inside the concrete structures. The cost-effectiveness along with the high accuracy and repeatability were the major objectives of the sensor development. Therefore, the development of two alternative methods (electrical sensors and fibre optic sensors) was investigated.

7.2. Electrical sensors embedment for the measurement of RH

7.2.1. Introduction

In recent years, there was an escalating trend for developing new technology suitable for smart cities and smart buildings. The concept of implementing the Internet of Things (IoT) with smart cities and buildings created a need for real-time sensors to monitor the condition of important structures such as bridges and skyscrapers (Norris, Saafi and Romine, 2008; Alam *et al.*, 2010). Real-time condition monitoring of concrete is under extensive investigation during the last decade (Ong *et al.*, 2008).

The main objective of this research was to develop an electrical sensor able to measure concrete moisture in real-time. Although several moisture content sensors were reported, their manufacturing and instrumentation costs are rather high, which does not allow their implementation in everyday structures (Chiarello and Zinno, 2005; Han, Yu and Kwon, 2009). In this section, a low-cost, screen-printed sensor is described that is cheap enough to allow its implementation even in residential buildings with the ability to be implanted in concrete during construction and provide real-time readings for an extended period.

7.2.2. Sensor Fabrication

The sensor's operating principle was based on the four electrodes method of conductivity measurement. In these experiments an alternating square wave current source was used as the excitation signal. The conventional four electrodes theoretical method is simple and well known and more details can be found elsewhere (Nabighian, 2006). The sensor was fabricated using Thick-Film Technology and the electrode layers were printed onto two 50 mm × 25 mm, 0.625 mm thick, 96% alumina substrates (Coorstech). The inks were printed using stainless steel screens with a mesh count of 250 lines per inch, 15 μm emulsion thickness and a 45^{o} mesh. The

PERICLES ALEXANDROU SAVVA

screen designs for each layer were created on AUTOCAD and were manufactured by MCI Cambridge for the Aurel C880 Printer.

The first layer printed on the alumina substrate was the gold conductor with three rectangular screen mesh openings and dimensions of 4.5 mm × 45 mm. A waterproofing layer was printed on top of the gold electrodes, with a rectangular shape of 6.5 mm × 14 mm to leave an exposed electrode area of 26 mm × 4.5 mm. The distance between the electrodes of the same substrate was approximately 5 mm. Wires were soldered on one end of the gold electrodes being approximately 5 mm × 4.5 mm in size. The gold electrodes were printed using ESL 8844 ink (Electro Science) and the glass dielectric insulator was printed using ESL 4905-C (Electro Science) to expose a precise surface area of the electrodes. The individual sensor layers were printed and cured sequentially with the specific printing and curing procedure and temperatures as described previously (Atkinson and Sophocleous, 2014).

The sensor was constructed by placing two identical substrates, with three electrodes each, facing each other with a spacing distance between opposite electrodes of 10 mm. The sensor was designed such that the drive current is applied across the two outer sets of electrodes, while the resulting potential across the cell is measured by the inner electrode on each substrate (Sophocleous and Atkinson, 2015). The final construction of the sensor is shown in Figure 7-2.

Figure 7-2: Construction of the screen-printed resistivity sensor (left), Concrete cube in an extruded polystyrene box (right)

This geometry was specifically used to minimise any fringing effects and to remove the susceptibility of the sensor to rotational movements of each individual substrate. The resistivity

of the material between the two substrates will be proportional to the voltage measured across the inner voltage electrode pair.

7.2.3. Experimental Setup

Two concrete mixtures (control and HANWA-SSD – Chapter 4) with low w/c ratio (0.25) were designed. The mixtures' constituents are shown in Table 4-4. The aggregates utilized in both types of concrete were limestone from local quarries. The specific mixtures were utilized to evaluate the sensor performance, since it was expected that the HANWA-SSD mixture would maintain a high RH value at the same instant with the control mixture. The concrete was cast in a plastic non-absorptive mold of dimensions 100 x 100 x 100 mm. The specimen was insulated with a plastic membrane to prevent moisture loss and an extruded polystyrene (XPS) box with a lambda value in the range 0.029 to 0.039 ($Wm^{-1}K^{-1}$) to ensure adiabatic conditions (Figure 7-2). The sensor employed an alternating square wave current source of 1 mA at a frequency of 1 kHz, which is low enough to measure resistivity independently of any electrode capacitance but high enough to prevent any polarisation effects on the electrodes. The voltage was logged using a commercial data logger (Campbell Scientific CR1000).

7.2.4. Results & Discussion

The data logger recorded voltage with respect to time, for a given drive current (A) hence the measured resistance R (ohms) was obtained by applying Ohm's Law. Hence, the resistivity, ρ (ohm m) of the sample was calculated as:

$$\rho = R(A/L) \qquad \text{Resistivity equation} \qquad (7\text{-}1)$$

where A/L is the cell constant of the sensor, with A being the cross-sectional area of the cell (m^2) and L the distance between opposite facing electrodes (m). The measured voltages were translated to resistivity values based on the assumption that the cell constant of the sensor does not change within the measured resistivity range. Based on the sensor's performance in previous experiments (Sophocleous and Atkinson, 2015), the cell constant can safely be assumed to be equal to the calculated geometrical value of 0.0611 metres within the range of resistivity values obtained here. Figure 7-3 shows the resulting resistivity data obtained from the sensor for both concrete types during a 9-day period.

PERICLES ALEXANDROU SAVVA

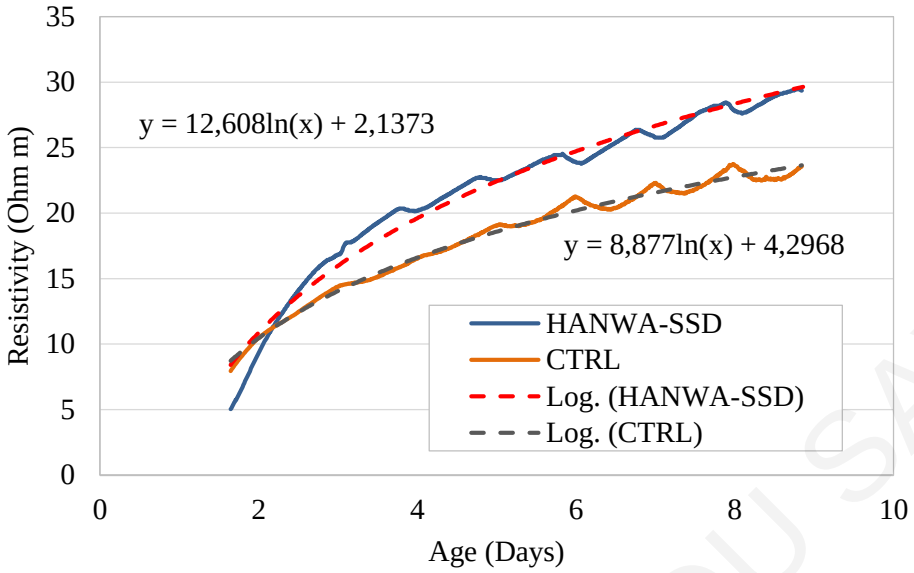

Figure 7-3: Sensor output for the two concrete types

The shape of the graph was anticipated since the resistivity of concrete is highly depended on its moisture content. As hydration progresses the resistivity of the mixture increases. Moisture content reaches an equilibrium point that depends on the relative humidity of the environment. This resistivity change profile of concrete was consistent with the trend identified in the literature (Bjegović *et al.*, 2016), which was obtained by taking resistivity measurements with commercial sensors and very similar methods. The initial and final absolute resistivity values of the two concrete types were different and also their drying rates were different; this was confirmed by the different equation coefficients suggesting that each concrete type would have its own unique curve equation. The rate and the extent of hydration, were expected to be different due to IC, which was expected to extent the hydration and provide water from the inner structure.

The resistivity fluctuations observed during the period of 24 hours, were in accordance with predictions, since the resistivity of concrete is highly dependent on temperature, even if the water content is the same. Thus, existing commercially available resistivity probes incorporate temperature compensation algorithms. Due to high chemical activity during the first hours, it was anticipated that high temperature fluctuations would occur during the specific time interval, despite the external thermal insulation.

PERICLES ALEXANDROU SAVVA

From Figure 7-3, one would expect that the water content of HANWA-SSD mixture would be higher than that of control mixture. Due to IC, it was expected that HANWA-SSD mixture would retain a much higher water content. The measured resistivity was normalised based on the initial minimum value of each concrete type. Initial resistivity readings of both types are not showed in Figure 7-4 since no big changes were observed but they were taken into account for the normalisation process. The normalisation was conducted as follows:

$$n\rho = \rho/\min(\rho) \qquad \text{Normalized Resistivity} \qquad (7\text{-}2)$$

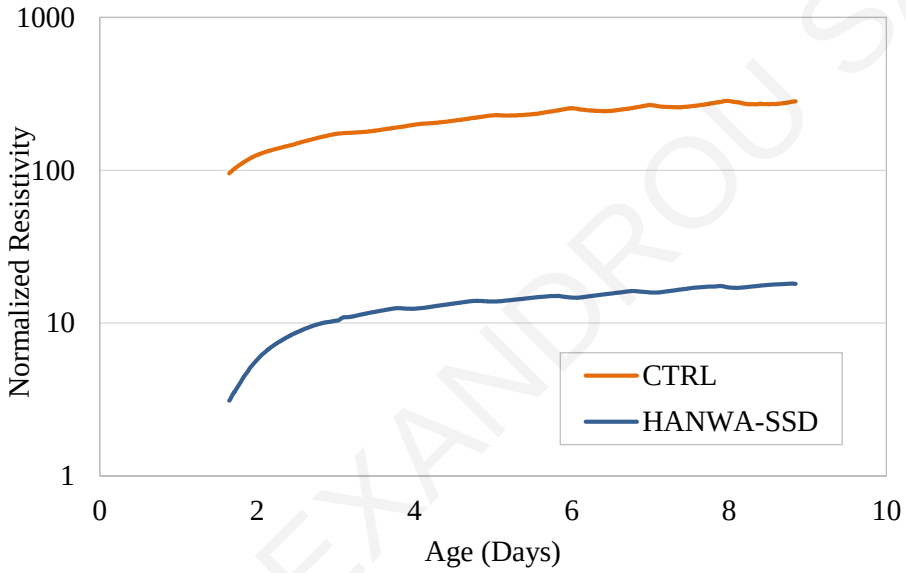

Figure 7-4: Normalised resistivity values of the two concrete types

Figure 7-4 shows that control changes its resistivity value by almost 300 times while HANWA-SSD changes its resistivity value by almost 20 times in the same time period suggesting that although the absolute resistivity values of the two concrete types are similar, there is a major difference of the resistivity changes during the tested period.

7.2.5. Conclusions

This section demonstrated a low-cost, screen printed resistivity sensor capable of monitoring the moisture content of concrete in real-time. The sensor is suitable for application to smart structures and can be integrated in the IoT. Results agree with predicted sensor behaviour and they further suggest that monitoring the resistivity of the concrete in its initial stages, can

PERICLES ALEXANDROU SAVVA

distinguish between different concrete types. Further research is necessary to calibrate the sensor in order to measure the actual RH inside concrete structures.

7.3. Fibre optics for measuring relative humidity

The science of fibre optic sensors relies on the scientific advancements made from 1960 and on, including the laser and the modern low-loss optical fibre (Grattan and Sun, 2000; Fidanboylu and Efendioglu, 2009). Nowadays fibre optic sensors are low-cost, compact, immune to electromagnetic interference, lightweight and highly accurate (Grattan and Sun, 2000). The utilization of fibre optics for the monitoring of relative humidity was developed at the early 2000's (Limberger, Giaccari and Kronenberg, 2001; Kronenberg *et al.*, 2002), whereas multiple concrete applications were developed since. Fibre optics are being used increasingly in applications other than telecommunications, due to the various advantages that they offer.

7.3.1. Polymer optical fibres

The use of fibre Bragg gratings (FBGs) as sensing elements for measuring different mechanical and physical parameters such as temperature, strain, and pressure is not new, since from 1978 when Hill et al. (Hill *et al.*, 1978 & Kawasaki *et al.*, 1978) inscribed the first FBG in glass fibre a significant number of publications were reported (Lau *et al.*, 2001; Ferraro and De Natale, 2002; Zhao, Liao and Lai, 2002; Leng and Asundi, 2003; Staszewski, 2003; Liang *et al.*, 2005; Lima *et al.*, 2008; Theodosiou, Lacraz, *et al.*, 2016). Their immunity to the electromagnetic interference, the light design and small size are the main advantages compared to the conventional electronic sensors. In the last two decades, the scientific community showed high interest for the polymer optical fibres (POFs) due to their unique characteristics for sensing applications. The POFs are well-known for their lower Young's modulus compared to the glass fibres, about ~23 times less, which allows better strain and pressure responses, higher wavelength shift and also due to their elasticity they are fundamentally safer for in-vivo measurements (Xiong *et al.*, 1999; Liu, Peng and Chu, 2001; Johnson *et al.*, 2010; Peters, 2011; Yuan, Stefani, *et al.*, 2011; Theodosiou, Polis, *et al.*, 2016). Till now, the main drawback of the POFs was the massive transmission losses at the near-infrared band which sometimes is more than 100 dB/m and as a result, the operating length of the POF sensors for satisfactory measuring signal is limited to few centimeters especially for Poly(methyl methacrylate) fibres (H., A.K.Y. and L.R., 2002; Yeniay *et al.*, 2004). Ma et al. (H., A.K.Y. and L.R., 2002) and Yeniay et al.

PERICLES ALEXANDROU SAVVA

(Yeniay *et al.*, 2004) had studied the transmission losses in polymers and reported that the increased losses on this particular wavelength range is associated with the molecules having high spring constants and/or small masses, and this occurs when one of the atoms is hydrogen. However, when fluorine replaces hydrogen, the absorption losses at the particular wavelength range decreased significantly. Hence, perfluorinated polymer fibres made of the cyclized transparent optical polymer (CYTOP) having much higher transparency and much lower losses, less than 60 dB/km at 1300 nm were employed (Lacraz, Theodosiou and Kalli, 2016). However, the only commercially available form of CYTOP fibre is gradient index multimode fibre. The particular fibre was design for short distance communication networks up to 100 m, and the large core diameters reduced the costs of the maintenance and handling since the high numerical aperture (NA) made the coupling from and to the fibre much easier. From the sensing point of view, the multimode fibres and not preferred for sensing applications because of a large number of supported modes (Liu *et al.*, 2005; Schmid and Müller, 2015). Traditional inscription methods such as the phase mask method are creating interference phase pattern that covers most of the core's diameter. The size of the pattern is not able to be controlled, and as a result, a significant number of modes are excited and detected in the spectrum as multiple peaks for the reflection or multiple deeps in the transmission spectrum (Statkiewicz-Barabach *et al.*, 2013). This fact made the interrogation process complicated since the different transmission modes are behaving differently and observed as mode overlapping in the spectrum.

Giaccari et al. examined the influence of humidity and temperature on a polymer coated in-fibre Bragg grating (Limberger, Giaccari and Kronenberg, 2001). Kronenberg et al. presented the concept of relative humidity sensor using polyimide-recoated fibre Bragg gratings (Kronenberg *et al.*, 2002). Ghandehari and Vimer replaced the cladding of silica fibre with polymethyl methacrylate doped with pH sensitive chromoionophores to monitor the pH level using the evanescent field spectroscopy (Ghandehari and Vimer, 2004). Yeo et al. examined the characteristics of a polymer-coated fibre Bragg grating sensor for relative humidity (Yeo *et al.*, 2005). Viviani et al. used fibre optic sensors to decouple the effect of thermal and autogenous deformation of concrete (Viviani, Glisic and Smith, 2007). Huang et al. utilized thermoplastic polyimide-coated fibre Bragg grating to measure relative humidity (Huang *et al.*, 2007). Wong et al. employed a photonic crystal fibre optic coated with polyvinyl alcohol to measure relative humidity, forming a Michelson interferometer with cladding mode excitation at both ends of the

PERICLES ALEXANDROU SAVVA

fibre (Wong *et al.*, 2012). André et al. used plastic optical fibres to monitor the curing of concrete, based on the scattering of the propagated optical signal in grooves imposed on to the fibre (André *et al.*, 2012). Ghandehari et al. used molecular vibration spectroscopy to evaluate the capillary absorption and evaporation of cementitious materials using near-infrared electromagnetic energy (Ghandehari *et al.*, 2012). Zou et al. used Fabry-Pérot fibre optic temperature sensors to describe concrete hydration (Zou *et al.*, 2012). An et al. used a single mode – multimode – single mode fibre with polyvinyl alcohol coated on the multimode structure to measure relative humidity (An *et al.*, 2013). Yehia et al. utilized a Fabry-Pérot fibre optic sensor to investigate the hydration of concrete (Yehia *et al.*, 2014). Wei et al. developed a fibre optic chloride chemical sensor based on long period gratings inscribed in a photonic crystal fibre for steel corrosion monitoring (Wei, Tao and Krishnaswamy, 2016). Butler et al. used distributed and discrete fibre optic sensors to evaluate the early-age behavior of prestressed concrete beams (Butler *et al.*, 2016). Yazdizadeh et al. used fibre Bragg grating sensors to monitor the dynamic response of a bridge alongside to the creep and shrinkage of the bridge's piers (Yazdizadeh, Marzouk and Hadianfard, 2017).

7.3.2. Concrete relative humidity

The reasons why RH is a key indicator in IC applications were analysed previously. Beside those, RH in concrete is a determining factor for various other deteriorating mechanisms. Many problems could be prevented and mitigated if the RH value of the inner matrix of concrete could be monitored in real time. Concrete carries compressive stresses where reinforcement is embedded to carry tensile stresses. Both materials are sensitive to specific environments. The embedded steel in concrete forms a protective layer after cement hydration that consists of maghemite, which is an iron oxide (γ-Fe_2-O_3). As long as the specific oxide is tightly adhered to the steel, the latest is protected against oxidization. A key prerequisite for the maintenance of the specific layer is the alkaline environment (pH >12.5). High alkalinity of concrete is provided from the dissolution of calcium oxides in water. The depassivation threshold pH value of the specific layer is approximately 9.5. In the presence of chloride ions, the iron oxide is perforated, providing access to oxygen and water. Chloride ions penetrate the passivate layer and form an anode region as follows: $Fe^2 + 2Cl^- \rightarrow FeCl_2$, $FeCl_2 + 2H_2O \rightarrow Fe(OH)_2 + 2HCl$. The oxidization process proceeds as follows. The difference in the electrical potential across a steel bar forms an electrochemical cell where anion and cation occur connected from porous solution, which is

PERICLES ALEXANDROU SAVVA

an electrolyte. The positively charged ferrous ions Fe^{2+} from the anode pass into the solution where the negatively charged free electrons e^- pass through the steel into the cathode. The constituent of the electrolyte absorbs the free electrons and their combination with water and oxygen forms hydroxyls OH^-. The hydroxyls travel through the electrolyte and combined with Fe^{2+} produce ferric hydroxide or rust. The chemical reactions are as follows. Anodic reaction: $Fe \rightarrow Fe^2 + 2e^-$, $Fe^2 + 2OH^- \rightarrow Fe(OH)_2$ (ferrous hydroxide), $4Fe(OH)_2 + 2H_2O + O_2 \rightarrow 4Fe(OH)_3$ (ferric hydroxide), Cathodic reaction: $4e^- + O_2 + 2H_2O \rightarrow 4OH^-$. It is therefore understandable that no corrosion would exist if oxygen, water or chloride ions existed (Neville, 2002). Neville stated that corrosion may not exist in RH values lower than 60%, or in an immersed element (Neville, 1995). It was specifically stated that the most optimum RH values for corrosion were 70-80%. The oxidization products occupy several times more volume than the initial products. This leads in microcracks and consequently in an increase in transport properties. Moreover, corrosion results in a reduction of the reinforcement cross-sectional area and a consequent decreased load carrying capacity (Verma, Bhadauria and Akhtar, 2013). Concrete exposed in areas with high concentrations in carbon dioxide such as industrial areas is prone to carbonation. Carbonation is the process where carbon dioxide ingress the material's structure and reacts with hydrates. The pore solution acts as the transport medium that diffuses carbonic acid (gaseous CO_2 is not reactive) throughout the material's structure (Neville, 2002). The chemical reactions are as follows: $Ca(OH)_2 + CO_2 \rightarrow CaCO_3 + H_2O$. Calcium hydroxide reacts more readily among all hydrates with carbonic acid to form mainly calcium carbonate ($CaCO_3$) (Šavija and Luković, 2016). $CaCO_3$ creates stress on the material's structure during its crystallization that may result in fracture. Local fragmentations increase the material's transport properties and allow increased amounts of deleterious substances to ingress, leading to a vicious cycle, which will reduce the material's life cycle. Moreover, carbonation of concrete results in the reduction of the pH value causing the dissolution of the iron oxide layer exposing the reinforcement's surface to deleterious substances. The progression of corrosion may lead in concrete spalling that will completely expose the reinforcement to the environment. A key parameter that affects the carbonation efficiency is the inner RH value of concrete. Moreover, the reduction of RH in concrete causes shrinkage to the material due to a physical mechanism known as self-desiccation. Self-desiccation is mainly governed by two physical mechanisms. The reduction of disjoining pressure and the meniscus formation. The disjoining pressure occurs

PERICLES ALEXANDROU SAWA

when the attractive forces between the calcium silicate hydrate (C-S-H) gels are counteracted from the multi-layer water molecules adsorbed on their surface (Taylor, 1990). It is developed as a result of adequate amount of water. A drop in RH - which is known to occur earlier in low w/b ratio mixtures - causes the reduction of disjoining pressure, resulting in additional shrinkage (Lura, Jensen and Van Breugel, 2003). Moreover, the second physical mechanism that describes self-desiccation is the water-air meniscus which appears in unsaturated pores due to pressure decrease (Kelvin's Law) (Lura, Jensen and Van Breugel, 2003). It results in tensile stress development within the pore fluid and subsequent compressive stress development from the surrounding material that causes further contraction (Lura, Jensen and Van Breugel, 2003; Barcelo, Moranville and Clavaud, 2005; Schröfl, Mechtcherine and Gorges, 2012).

The most common methods for measuring the internal RH in concrete mixtures are conventional humidity sensors (D.A. Lange and R. Rodden, no date; Bentz, Geiker and Jensen, 2002; Jensen and Hansen, 2002). However, electronic sensors exhibit specific drawbacks such as cost, electromagnetic interference and a relative "bulky" design, few millimeters, often influencing the design of the structure.

In order to measure RH in concrete, several requirements need to be considered. Concrete is characterized by high alkalinity (pH=~13), various chemical reactions and shrinkage that takes place during its maturing period. Other deteriorating chemical reactions such as carbonation may also occur at later ages. The immunity of the sensor to these parameters need to be considered in order to measure RH in concrete using an embedded sensor. Indeed, optical fibres exhibit immunity to electromagnetic interference, durability, chemical resistance and consistency (Alwis, Sun and Grattan, 2013) as opposed to other electric/electronic sensors. In addition, the glass or polymer fibre is a cost-effective material which can be embedded in concrete at several locations as opposed to other sensors. Finally, optical fibres provide the ability to measure RH at micro and macro level at any time without losing their reference value.

7.3.2.1. Principles of Fibre Bragg Gratings in Polymer Optical Fibres (FBG-POF)

The FBGs consist of periodic modulated refractive index zones in the center of the core which reflects the resonance wavelength that satisfies the equation of the Bragg condition shown below (Bragg condition (7-3)).

PERICLES ALEXANDROU SAVVA

$$\lambda_{Bragg} = 2n_{eff}\Lambda \qquad \text{Bragg condition} \qquad (7\text{-}3)$$

where n_{eff} is the effective refractive index of the fibre and Λ is the period of the modulation. The resonance wavelength depends on the effective refractive index of the core and the periodicity of the grating.

Temperature, strain, and pressure are the main external parameters that can influence the resonance wavelength of the FBGs inscribed in common glass fibres. These factors cause permanent modulation either on refractive index and/or on the period of the modulation and this result in permanent shift of the resonance Bragg wavelength, that is described by the equation bellow.

$$\Delta\lambda_B = 2\left[\Lambda\frac{\partial n_{eff}}{\partial l} + n_{eff}\frac{\partial\Lambda}{\partial l}\right]\Delta l + 2\left[\Lambda\frac{\partial n_{eff}}{\partial T} + n_{eff}\frac{\partial\Lambda}{\partial T}\right]\Delta T \qquad (7\text{-}4)$$

Shift of the resonance Bragg wavelength

where the first part of the Shift of the resonance Bragg wavelength (7-4) refers to the strain effect on an optical fibre and the second part to the temperature effect (Othonos *et al.*, 2006).

However, FBGs in specialty fibres such as the polymer optical fibres are sensitive to other environmental parameters such as the relative humidity (RH) due to their hydrophilic aptitude. The RH changes are detected by the POF-FBGs by two mechanisms. The first mechanism has to do with increased water content absorbed by the polymer, which results in a change in the refractive index of the polymer. The other mechanism is related to the increase of the volume of the polymer due to swelling by water absorption and as a result, to the change in the period of the index modulation.

The POF-FBGs are offering higher strain and pressure sensitivity due to the lower Young's modulus, higher temperature response but much lower temperature threshold because of the lower melting point. The corresponding reported POF-FBG sensitivities were up to 1.5 pm/με for strain compared to 1.1 pm/ με for common glass fibres (Johnson et al., 2010; Peters, 2011; Yuan, Stefani, et al., 2011) and up to 73 nm wavelength shift (Xiong et al., 1999; Liu, Peng and Chu, 2001), -55 pm/oC for temperature compared to 14 pm/oC for common glass fibres (Liu, Peng and Chu, 2002; Prabhugoud and Peters, 2004; Webb et al., 2008; Alwis, Sun and Grattan,

PERICLES ALEXANDROU SAVVA

2013) and 35.2pm/%RH for humidity (Yuan, Khan, et al., 2011; Alwis, Sun and Grattan, 2013; Zhang and Webb, 2014; Woyessa et al., 2017).

7.3.3. Experimental Program

Measurement of RH changes using embedded uniform fibre Bragg gratings (FBGs) inscribed in multimode gradient-index polymer fibres in a concrete mixture was conducted. The constituent materials of the concrete mixture can be found in section 4.2.1. The optical fibre was embedded in the mixtures where RH variation was known, in order to establish and optimize the methodology.

7.3.3.1. Fibre Bragg inscription

The inscription of Bragg grating on polymer fibre showed a very high strain response and a high wavelength tuning range, due to their lower Young's modulus, as compared to silica fibres (Theodosiou, Polis, *et al.*, 2016). In addition, the majority of commercially available polymer fibres are multimode, namely, the inscription occurs on more than one fibres, and therefore, the interrogation of the fibre Bragg grating spectrum is uncertain because of the multi-peak response spectrum. The polymer fibre also exhibits high water absorption and optical losses that limit their applicability to short distances. The requirements of a fibre-optic application applicable in measuring RH are water absorption, low optical losses in order to fulfil the accuracy requirements and single-peak response spectrum in order to enhance the interrogation accuracy.

The use a low-loss perfluorinated graded index multimode CYTOP fibre with core diameter 62.5 μm, a 20 μm cladding layer diameter and an additional polyester and polycarbonate outer over-cladding of 490 μm was decided. The fibre sample was mounted on a microscope glass slide and using two supported fibres it was immersed in a refractive index oil matching and wascovered using thin glass coverslips to overcome any curvature effects due to the shape of the fibre during the inscription. Subsequently, the glass sample was mounted on a nanometer-accuracy air bearing stage for two-dimension controlled motion. The FBGs were inscribed by guiding the laser pulse of a femtosecond laser system (femtoRegen HighQ) operating at 517 nm with 220-fs (Figure 7-5) pulse duration through the mirror above of the sample and using a second vertical translation stage, and a microscope lens x50 (Mitutoyo) was focused inside to the core of the fibre (Figure 7-6). The pulse energies at the exit of the laser were set at ~70 nJ/pulse and using a mechanical pulse speaker we set the repetition rate at 2 kHz. We performed

PERICLES ALEXANDROU SAVVA

transversal motion across the core of the fibre creating three-dimension planes that were fully controlled by depth, width, and duty cycle. The gratings inscribed for this work were 4th order gratings inscribed using the Plane-by-Plane femtosecond laser inscription method with a period of ~2.2 μm (Figure 7-7), to minimize the index overlapping between the grating planes and with a 15 μm plane width in the center of the core, to minimize the coupling between the grating and high order modes supported by the fibre. Using the Plane-by-Plane femtosecond laser inscription method we managed to control the physical dimensions of the grating structure inscribed in a multimode CYTOP polymer fibre to overcome the multiple peak issues (Lacraz *et al.*, 2015; Theodosiou, Lacraz, *et al.*, 2016; Fokine *et al.*, 2017; Theodosiou *et al.*, 2017). The gratings were connected with single mode glass pigtails to be compatible with the interrogation devices and calibrated under strain, temperature and humidity. After that, the sensors were embedded into two concrete mixtures. The reflection spectrum of the gratings monitored for six days, and the internal RH change was noted for a sampling rate 2 hour.

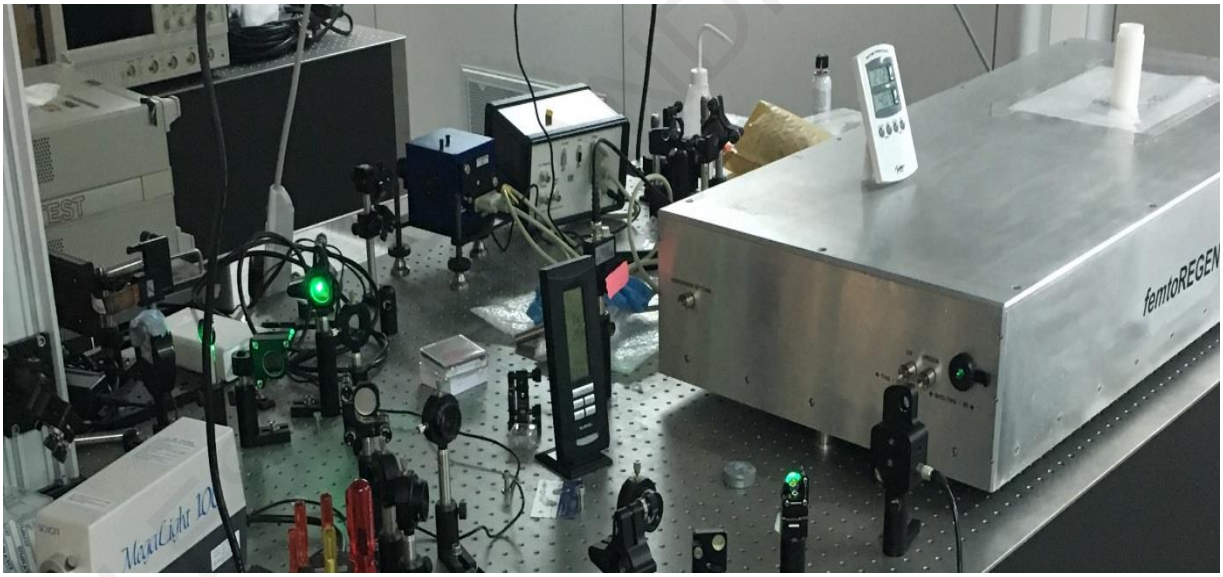

Figure 7-5: femtosecond laser (HighQ – femtoRegen)

PERICLES PAPADOPOULOS SAVVA

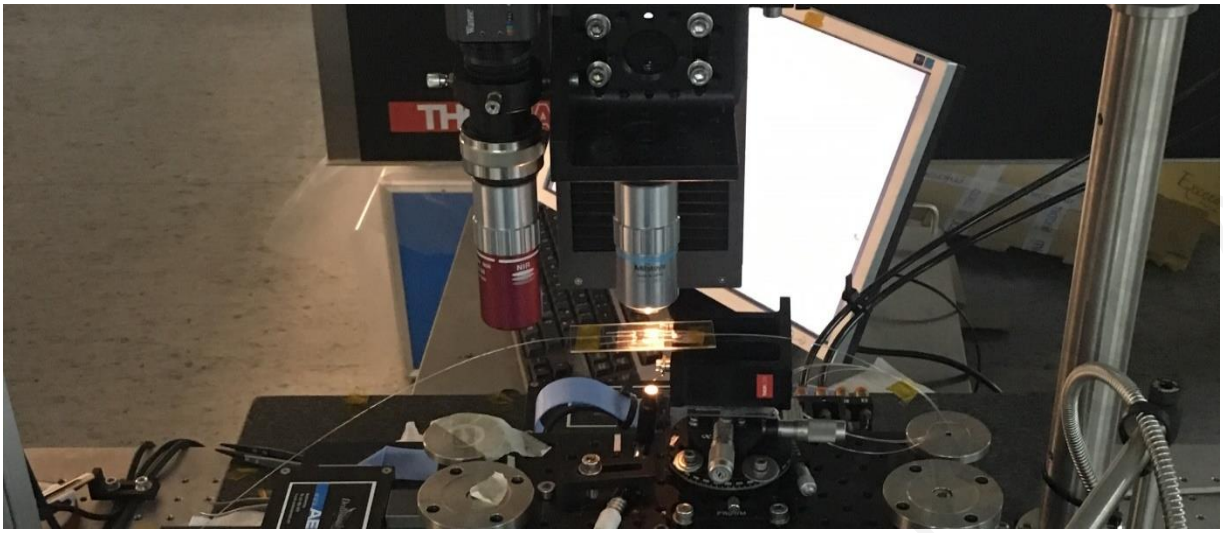

Figure 7-6: Fibre on translation stage for FBG inscription

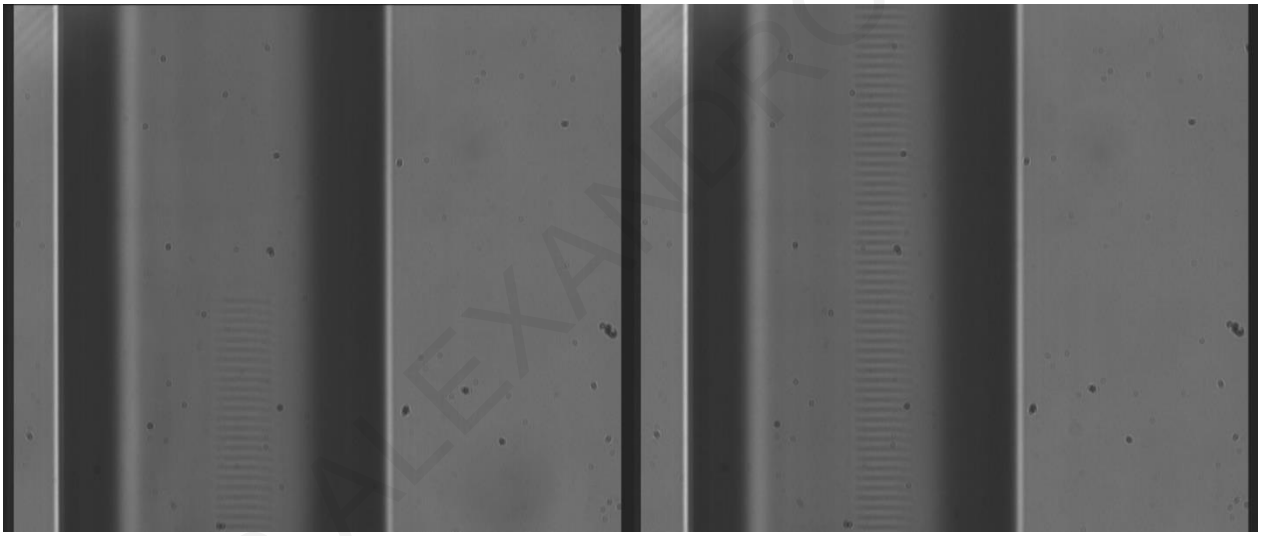

Figure 7-7: Optical microscope image of the femtosecond-laser inscribing FBG in multimode CYTOP fibre using the *Pl-by-Pl* (*Pl*~2-μm apart and 30-μm width) – Left in progress, right completed

The fibre sample was illuminated using a broadband light source (Thorlabs-ASE730) through a circulator and the reflection spectrum was measured using a commercial spectrometer (Ibsen IMON). The fibre sample was then UV-glued to the one end of a multimode gradient index glass fibre with 62.5 μm core diameter that was spliced from the other end with an SMF28 pigtail. The multimode glass fibre was selected for easier coupling and more stable joint. The reflection amplitude spectrum is shown in Figure 7-8. The tuning of the optical fibre is shown in Figure 7-9. The UV-glued polymer sample was embedded in the concrete mixture. The RH drop in concrete was not expected to begin before its third day of life.

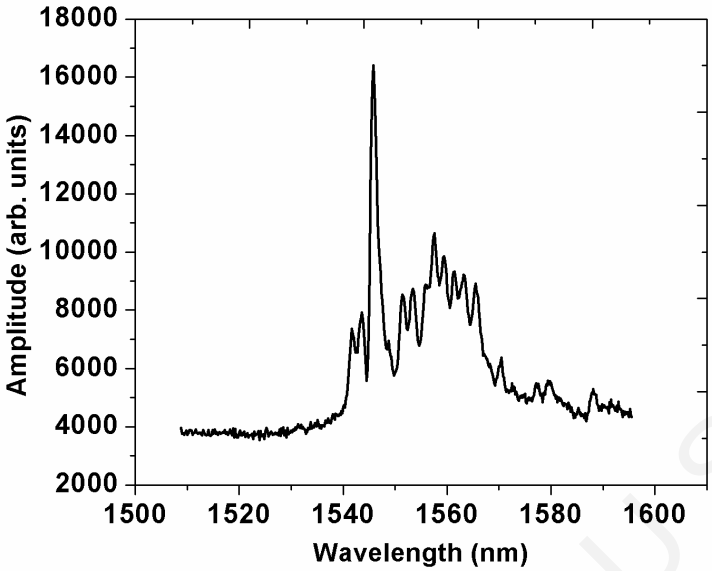

Figure 7-8: Reflection spectrum of FBG inscribed in CYTOP polymer fibre

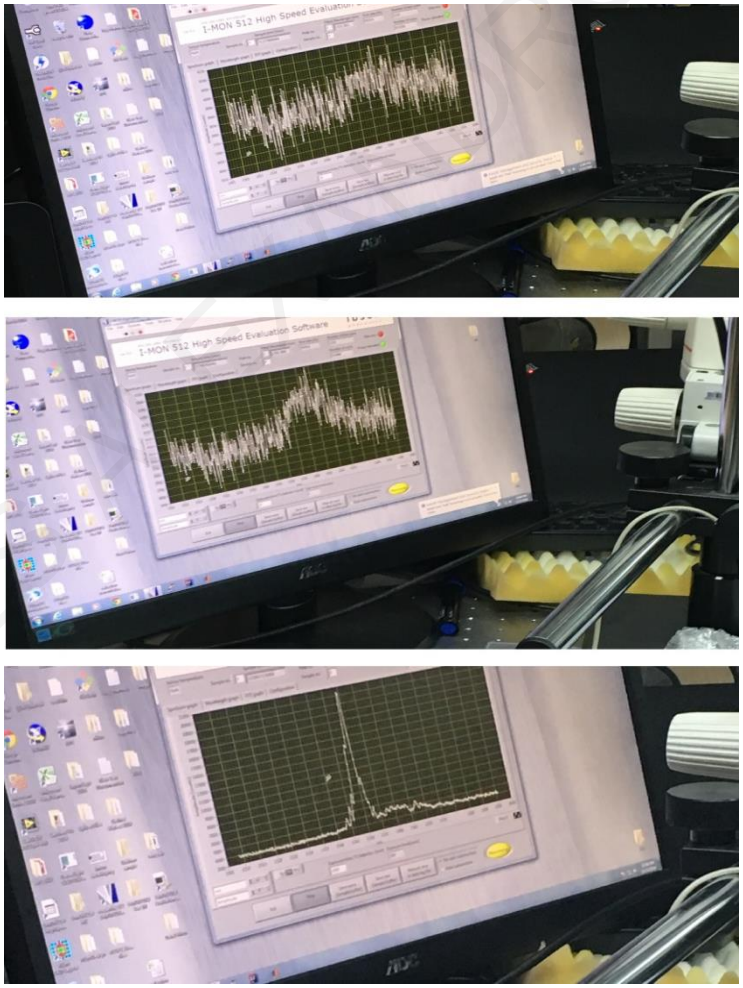

Figure 7-9: Fibre optic tuning

PERICLES SAVVIDOU SAVVA

7.3.3.2. Experimental investigation I

7.3.3.2.1. Methodology

The current work includes the innovative technique of inscribing Bragg grating on a cyclic transparent optical polymer (CYTOP) perfluorinated polymer optical fibres (POFs) (Lacraz *et al.*, 2015). The specific methodology employs a direct write method with a femtosecond laser operating in the visible spectrum. CYTOP offers specific advantages as opposed to polymethyl methacrylate optical fibres, namely, lower optical loss in the near-infrared optical communications window, lower affinity for water absorption and a refractive index similar to the aqueous refractive index.

7.3.3.2.2. Results

The reflection spectrum of the FBG was captured once a day during the first two days. Figure 7-10 shows the wavelength shift variation of the FBG sensor. During the first two days, a wavelength shift of ~2.7 nm was observed. This was attributed to the cross sensitivity between the strain occurring due to the swelling and shrinkage of the mixture. After day 3 to day 7, the grating went a continuous wavelength blueshift (peak descending). Considering that the specimen was kept at a controlled room temperature during the experiment, and the intrinsic temperature variations of the material (due to chemical activity) were greatly reduced after the 30th hour of casting the only variable parameter was the humidity of the mixture. However, small strain fluctuations always introduced cross sensitivity errors in the results.

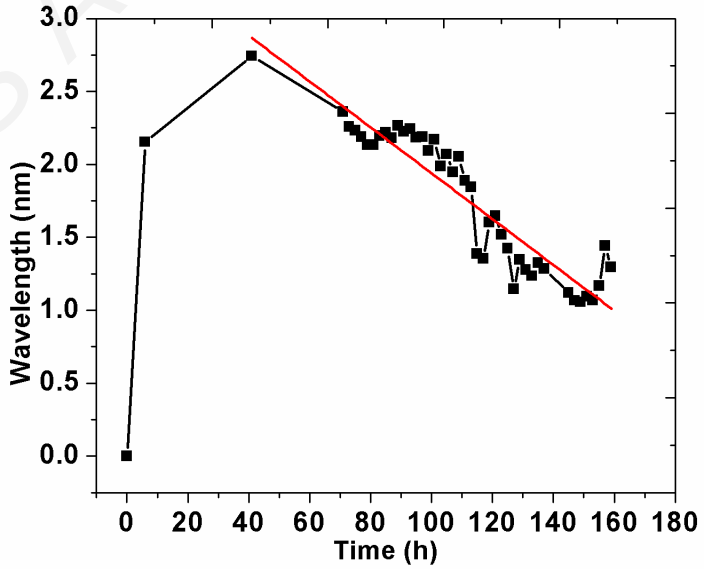

Figure 7-10: Humidity measurements

PERICLES ALEXANDROU SAVVA

7.3.3.2.3. Conclusions

The specific section reports on measuring relative humidity changes using embedded uniform fibre Bragg gratings (FBGs) inscribed in multimode gradient-index CYTOP polymer fibres in concrete. From day 3 to day 7, the FBG was undergoing a continuous wavelength blueshift that was interpreted as an RH drop. However, the results were interfering with strain causing a cross-sensitivity especially the first two days.

7.3.3.3. Experimental Investigation II

7.3.3.3.1. Sensing calibration

After the inscription, the gratings were mounted on a manual stage and using a single mode standard glass SMF-28 fibre a stable joint between them using the UV-glue method was established. This was an important fact to ensure stable connection and coupling between the fibres, no mode interchange and compatibility with the peripheral devices such as spectrometers and light sources. A proper UV joint between the two fibres is shown in Figure 7-11.

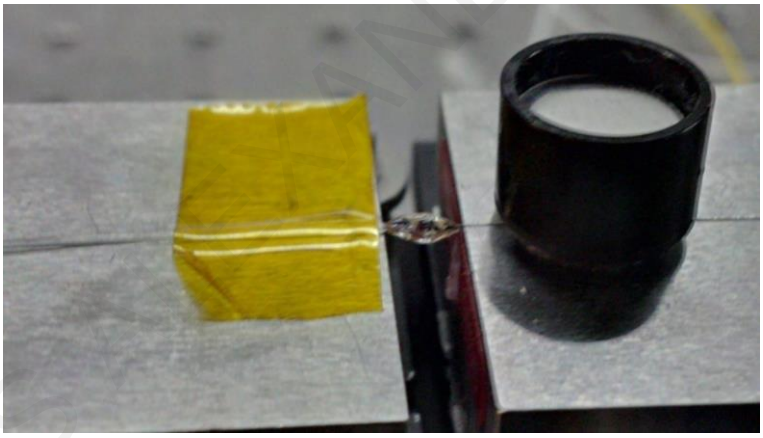

Figure 7-11: Connection between a multimode gradient index CYTOP polymer fibre and a standard glass fibre SMF-28 using the UV-glue method.

The POF-FBG was illuminated using a broadband light source (Thorlabs ASE730) through a circulator, and the reflection spectrum of the grating was captured using an FBG commercial demodulator (IBSEN IMON 512 high speed). To calibrate and characterize the strain of the sensor the fibre sample was fixed using an epoxy glue between a manual translation stage and a stable surface and axial strain was applied on the ends of fibre sample. The reflection spectrum of the grating was measured using the commercial demodulator having optical resolution ~169

PERICLES PAPANDROU SAVVA

pm for each step and then was post-processed using a specialized custom made algorithm (ZCA) to improve the resolution and the accuracy of the POF-FBG wavelength shift. The strain sensitivity was found to be 1.44 pm/με while a maximum wavelength~18 nm at ~1.3% strain as shown in Figure 7-12 was achieved.

The POF-FBG was placed in a climate chamber to measure the response of the grating to the temperature and relative humidity changes. Firstly, the climate chamber was set to a constant humidity, 23%, and the temperature was increased from 35^0C to 60^0C for 80 minutes while the reflection spectrum of the grating was captured every 1 minute. From the reflection spectra and suing the ZCA algorithm the response of the POF-FBG to temperature was found to be 17.62 pm/^{0}C as shown in Figure 7-13.

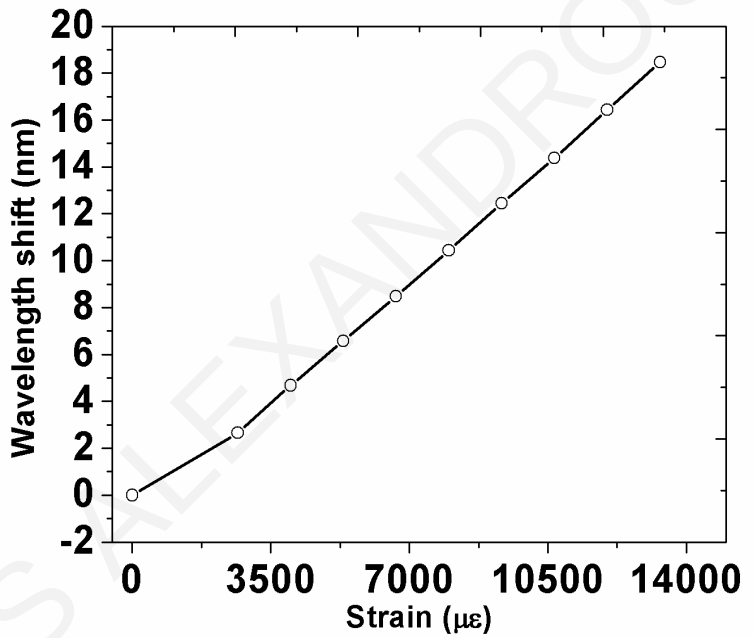

Figure 7-12: Strain response of a POF-FBG inscribed in multimode gradient index CYTOP polymer fibre using the Pl-by-Pl femtosecond laser inscription method. The grating achieved maximum wavelength shift ~18nm.

PERICLES ALEXANDROU SAVVA

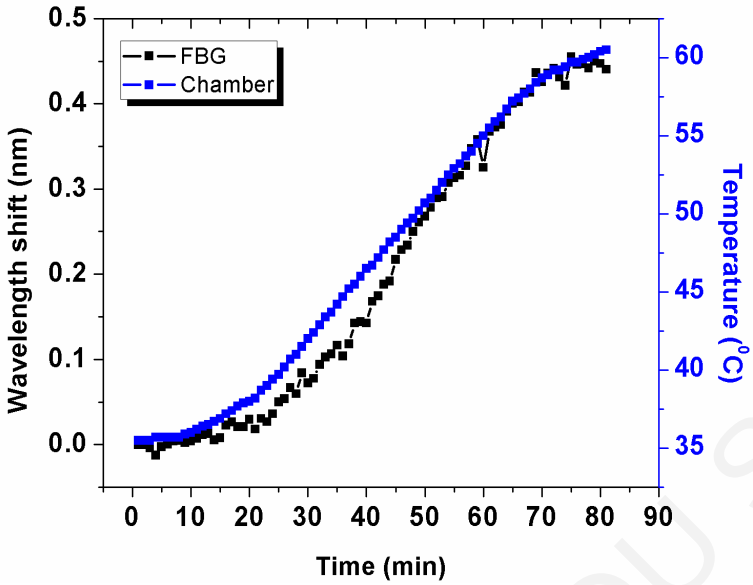

Figure 7-13: Temperature response of POF-FBG inscribed in multimode gradient index CYTOP fibre for 35 to 60^{0}C according to the climate chamber temperature sensor.

Finally, the behavior of the grating under relative humidity changes was calibrated. A similar methodology with the temperature calibration was followed. The temperature was kept constant at 30^{o}C and the response of the grating spectrum from 50% to 90% RH with interval steps of 10% after a stabilization period of 90 minutes for each step was conducted. The corresponding humidity sensitivity was approximately 37.6 pm/%RH as shown in Figure 7-14. The response of POF-FBGs due to the water absorption was based on two primary mechanisms: either due to the change of the refractive index or by the modification of the gratings period. The refractive index changes due to the increased water content absorbed by the polymer. The grating period changes by the swelling of the polymer. In our case, the RH sensitivity of the CYTOP POF-FBG occurred due to the second mechanism since previous studies showed perfluorinated polymers having a similar response to humidity as glass fibres. Thus, the swelling of the polycarbonate-based outer jacket of the fibre influences the period of POF-FBG and as a result the resonance wavelength of the grating it took 5 hours to diffuse water and absorption.

PERICLES ALEXANDROU SAVVA

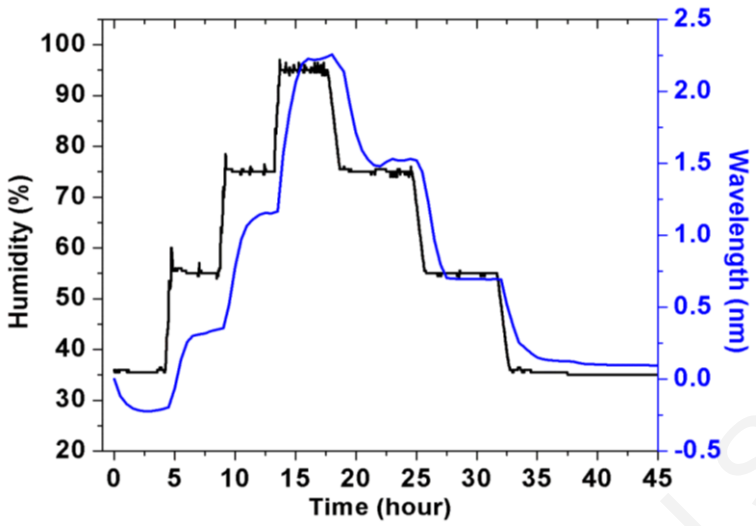

Figure 7-14: The RH response of a CYTOP POF-FBG when using a climate chamber

7.3.3.3.2. Concrete mixtures

The mixtures were manufactured in controlled conditions, cast in plastic non-absorbent cubic molds and sealed to prevent moisture loss. Two mixtures with low w/c ratio were intensively designed to increase autogenous shrinkage according to the mixtures designed in Chapter 4 (Table 4-4) (Control and HANWA-SSD). In order to maintain RH levels high and reduce or diminish autogenous shrinkage, the first mixture was manufactured using HANWA in a saturated-surface dry condition. The reference mixture was manufactured using NWA. The HANWA and NWA properties are presented in Table 4-2.

7.3.3.3.3. Results and Discussion

Two pigtailed POF-FBGs were embedded separately into the two concrete mixtures (Control and HANWA-SSD). A broadband light source (Thorlabs ASE730) operating from 1520 nm to 1600 nm illuminating the two POF-FBGs through an optical circulator that was connected to a 100 m spool of SMF28 fibre cable. The other side of the spool was connected to an optical coupler that was attached to the pigtailed POF-FBGs as shown in Figure 7-15. The reflection spectrum of the FBGs was monitored using a commercial demodulator from IBSEN Photonics (IMON 512 High speed) with optical resolution ~169 pm for six days with an interval sampling period of 1 hour. Since the temperature changes influence the wavelength shift of the gratings, the material temperature was continuously monitored using type J thermocouples with an identical junction length. It is important to note that the both concrete samples were covered

PERICLES ALEXANDROU SAVVA

with a 4 mm thin rectangular glass to prevent moisture exchange with the environment as shown in Figure 7-15 and Figure 7-16.

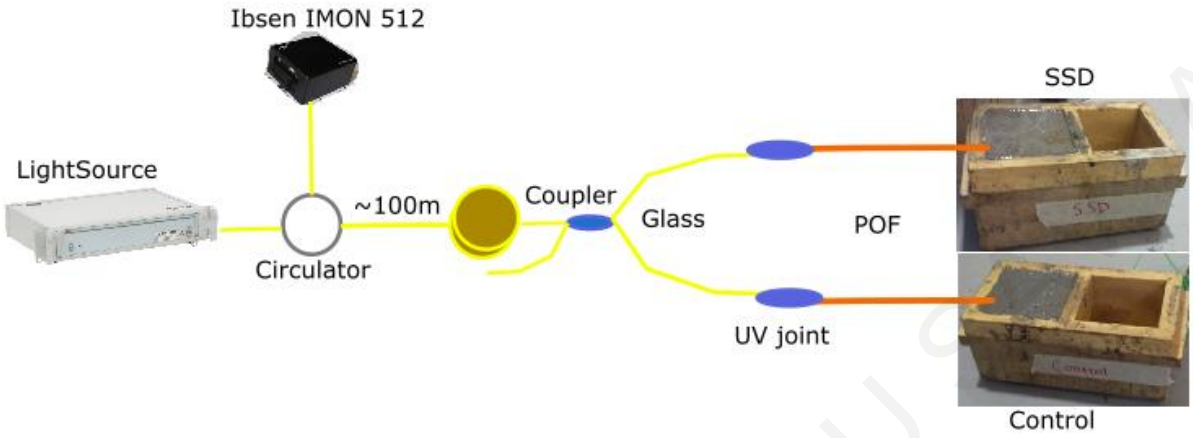

Figure 7-15: Experimental setup for the RH monitoring of the two concrete mixtures using polymer optical fibre Bragg grating sensors

After six days of monitoring the reflection spectra of the two FBGs were imported in Matlab and were post-processed using the ZCA demodulation algorithm for higher optical resolution (< 1pm) and accuracy (Theodosiou, Komodromos and Kalli, 2017). The raw results taken on the sixth day are shown in Figure 7-17. The specific graphs include the contribution of the temperature, strain and RH. At this moment it was unable to recover the strain induced on the POF-FBG sensors due to shrinkage. However, the temperature fluctuation on the concrete samples was monitored using the thermocouples and based on the temperature calibration of the gratings the thermal effect was disregarded. The temperature of concrete samples as recovered with the thermocouples for six days is shown in Figure 7-18, and the response of the gratings after removing the contribution of temperature is shown in Figure 7-19. The results in Figure 7-19 represent the wavelength shift of the POF-FBG 10 minutes after embedded in the concrete samples. The gratings were expected to show an initial increase in wavelength due to concrete swelling followed by a continuous decrease because of the RH drop in the concrete sample that yielded in vapor desorption from the polymer. According to Figure 7-19, it is clear that the two samples behaved differently. The slope of the two curves showed that the SSD sample maintained a higher RH value compared to the control mixture. This was attributed to the IC mechanism.

PERICLES ALEXANDROU

Figure 7-16: The two concrete samples (control and SSD) were covered using a rectangular glass cover and a J-type thermocouple monitoring their temperature while optical fibre sensors were recovering the RH change.

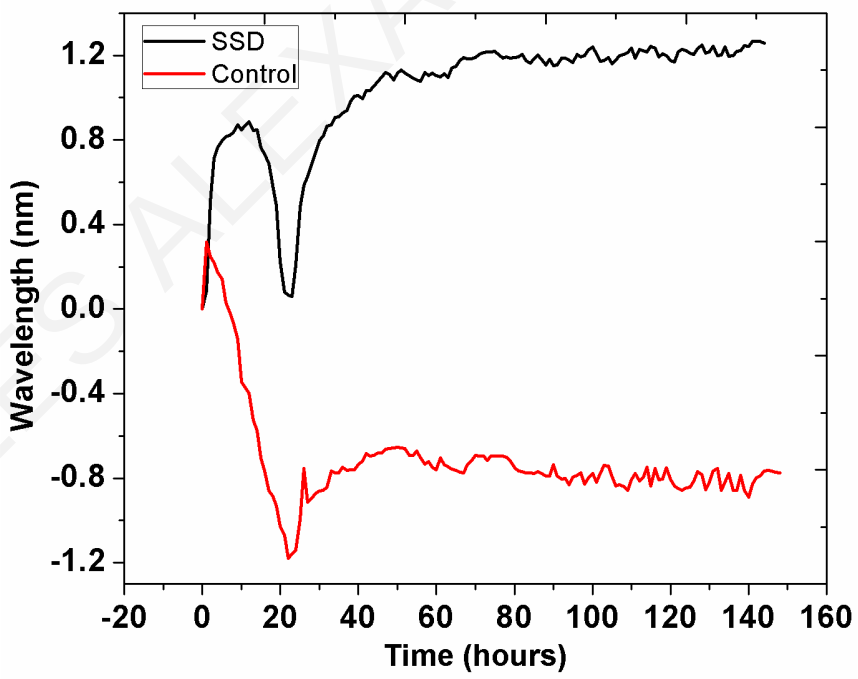

Figure 7-17: The response of the POF-FBGs with the temperature contribution

PERICLES ALEXANDROS SAVVA

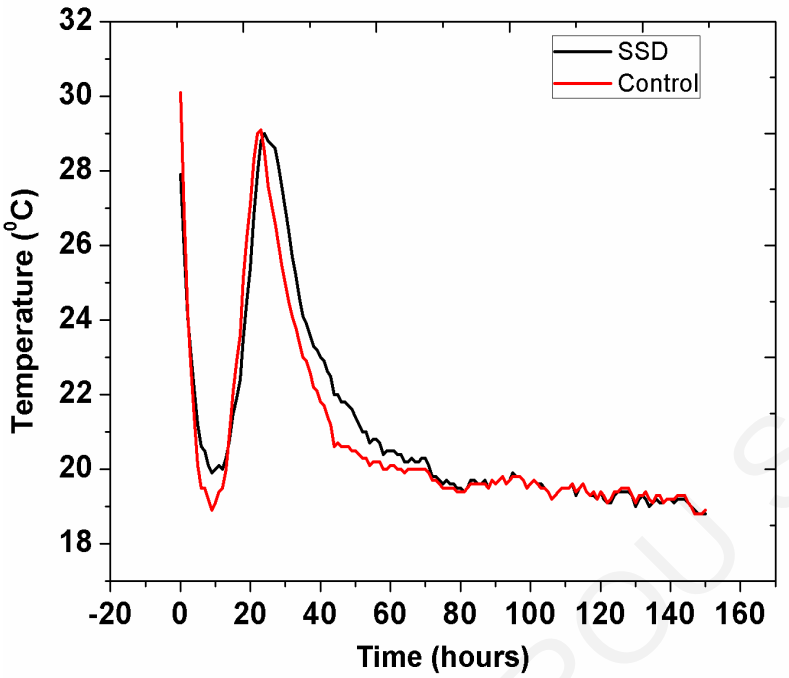

Figure 7-18: Response of the thermocouples during the six day period

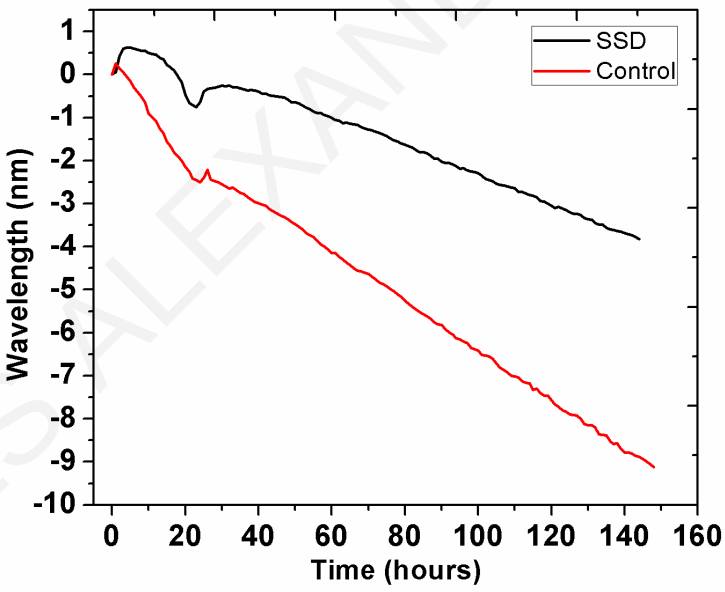

Figure 7-19: Response of the POF-FBGs after the temperature contribution according to the thermocouples was removed

7.3.3.3.4. Conclusions

Two polymer fibre Bragg gratings sensors, inscribed in a CYTOP multimode fibre were embedded in two similar concrete samples that differ only on the type of aggregate. The polymer

PERICLES ALEXANDROU SAVVA

sensors were initially characterized and calibrated under temperature, strain, and relative humidity. After embedding in the concrete samples the reflection spectrum of both sensors was captured for six days with sampling rate one per hour while the temperature of the samples was monitored using thermocouples. Since FBG sensors are sensitive to temperature fluctuations, the two concrete samples were kept at a constant room temperature 20°C ± 2°C while the temperature contribution due to the chemical reactions into the samples were monitored and excluded from the results. The results showed different drying rate between the two samples, as expected. The HANWA-SSD sample showed three times lower drying rate compared to the control sample. However, the exact internal RH state of the samples was not possible to be measured at this stage since the induced strain was also included in our measurements. The measurement approach can be improved by using another FBG sensor inscribed in glass fibre that is not sensitive to RH to remove the strain contribution or by using more advanced fibre sensors such as fibre Fabry-Perrot cavities (Theodosiou *et al.*, 2018).

PERICLES ALEXANDROU SAWA

8. Conclusions and future research

The current thesis evaluated the possibility of employing highly absorptive normal weight aggregates for internal curing, in high and normal strength concrete mixtures. This was tested in various curing and environmental conditions. The methodology was tested using simple and advanced techniques. The most prominent conclusions and the most promising outcomes for further investigation are summarized below.

The objective of this research was to develop an IC method, aiming to reduce early-age shrinkage and maintain the materials' properties intact. The specific objective was fulfilled considering that the IC mixtures including HANWA-SSD exhibited similar mechanical and durability properties with the control mixture. HANWA-SSD performed very well in reducing autogenous shrinkage and improving mechanical properties and durability. The ring test showed that the HANWA-SSD mixture cracked 6 days after both control and SAP mixtures and exhibited 87.5% and 86.5% lower crack width than the control and the SAP mixture. The performance of concrete including RCA can be improved using the method of IC. The mixture design has to be conducted based on the cement requirements, in order to compensate self-desiccation. It was shown that the RCA mixtures exhibited identical or even better properties with the conventional concrete mixture (i.e. control) in both compressive strength and RCP experiments. The specific results constitute the extension of the current research and prepare the field for an extended research regarding IC on waste materials such as recycled aggregates, regardless of their poor properties. It also supports the argument of extending the principles of IC on materials other than LWAs and HANWAs, succeeding in yielding low quality materials into high performance materials with a wide range of applications. The successful implementation of IC in RCA concrete mixtures will contribute to a better utilization of waste materials, ensuring environmental sustainability.

The compressive strength of the IC mixtures exposed to the environment performed significantly better (11.5%), considering the curing conditions, than the corresponding mixtures cured in controlled conditions. The specific characteristic was attributed to the IC which replenished the water in the material's porosity and enhanced the degree of hydration. The IC enhanced also the bond between the aggregates and cement paste (mortar), due to higher absorptivity and increased degree of hydration near the aggregates surface. On average, the IC

PERICLES ALEXANDROU SAVVA

mixtures exposed to the environment, exhibited a similar (7.8% difference) compressive strength, with the corresponding NWA mixtures. Regarding the porosity and sorptivity, the mixtures cast with HANWA and exposed to the environment (EH) shown an improved performance as opposed to the corresponding water cured mixtures. However, the specific mixtures exhibited a poorer performance compared to the corresponding NWA mixtures (EL). The improved porosity of the EH mixtures was attributed to the action of IC, which however, due to poor IC agents' dispersion was not that effective to overcome the NWA mixtures. The exact opposite behavior was observed in the NWA mixtures. The specific behavior was anticipated since the exposed mixtures undergone intense stress cycles from their early-age. The HANWA RCP values of both exposed and water cured specimens were lower than the corresponding NWA mixtures. The specific was attributed to the IC and the low aggregates modulus of elasticity. The HANWA mixtures overcame the NWA mixtures in the specific tests. RCP is an indicator of the materials pore network instead of the voids total fraction (porosity). It has to be mentioned that the effectiveness of IC is expected to be more pronounced at a small distance from the IC source. Therefore, the pore network sealing is more likely than the total porosity reduction. The mixtures cast at 40^{o}C showed a poor and unpredictable behavior. The major issue rising from the specific mixtures is the uncertainty regarding their properties evolution. The exposure of concrete mixtures cast with NWA to the environment caused significant damage to the materials' microstructure. The utilization of aggregates with low modulus of elasticity such as HANWA offered a lower degree of restraint, which allowed greater deformations of the cement paste. The employment of IC compensated the lack of water and contributed to an enhanced microstructure, which was reflected on the results. The main conclusions drawn from the specific section highlight the importance of maintaining the cast temperature at low levels and the importance of providing proper curing to concrete mixtures. In addition, the conversion of a low quality material (HANWA) into a useful IC agent was achieved. It was proven that an IC mixture including HANWA, performed very well, converting an otherwise "waste" material into a high performance IC agent. However, a degradation mechanism was observed, that occurred at later ages. The specific mechanism appeared in both HANWA and NWA mixtures and was attributed to a possible interaction between the limestone aggregates and cement paste. HANWA IC is a cost-effective method to improve the behavior of concrete.

PERICLES ALEXANDROUSAVA

The current manuscript presents the evaluation of HANWA aggregates and mixtures, using equations from the literature and advanced testing techniques such as mercury intrusion porosimeter. The results showed that the HANWA aggregates pores have an average pore size larger than the cement paste, which implies that the water evaporation will begin from the aggregates before initiating from the cement paste. The evaporation form the HANWA mixtures cement paste will initiate after the aggregates water exhaustion, since the pore fluid replenishment form the aggregates will continuously increase the capillary pressure. Based on Powers and Brownyard, 1947, it was showed that a low w/c ratio mixture will exhibit, among others, lack of adequate water for hydration. Using internal curing, it was demonstrated that water can be provided from the inside of the structure, enhancing significantly the cement hydration.

Finally, two innovative methodologies were developed in order to measure RH in concrete. The first development was a low-cost, screen printed resistivity sensor capable of monitoring the moisture content of concrete in real-time. The sensor is suitable for application to smart structures and can be integrated in the IoT. Experimental results agree with predicted sensor behaviour and they further suggest that monitoring the resistivity of the concrete in its initial stages, can distinguish between different concrete types. Further research is necessary to calibrate the sensor in order to measure the actual RH inside concrete structures. In the second methodology, two polymer fibre Bragg gratings sensors were inscribed in a CYTOP multimode fibre embedded in two similar concrete samples that differed only on the type of aggregate. The polymer sensors' temperature sensitivity was investigated. After embedded into the concrete samples, the reflection spectrum of both sensors was captured for six days with sampling rate one per hour while the temperature of the samples was monitored using thermocouples. Since FBG sensors are sensitive to temperature fluctuations, the two concrete samples were kept at a constant room temperature 20°C ± 2°C while the temperature contribution due to the chemical reactions into the samples were monitored and excluded from the results. The results showed different drying rate between the two samples, as expected. The HANWA-SSD sample showed three times lower drying rate compared to the control sample. However, the exact internal RH state of the samples was not possible to measure at this stage since the induced strain was also included in our measurements. The measurement approach can be improved by using another FBG sensor inscribed in glass fibre that is not sensitive to RH to remove the strain contribution

PERICLES ALEXANDROUSAKIS

or by using more advanced fibre sensors such as fibre Fabry-Perrot cavities (Theodosiou *et al.*, 2018).

8.1. Summary of Conclusions

- HANWA can be effectively used for internal curing in order to replenish the consumed water and reduce autogenous shrinkage in low w/c ratio mixtures.
- Despite their low mechanical properties (compressive strength and elastic modulus), HANWA helped the concrete mixtures to perform better than the control mixtures in occasions were concrete mixtures were exposed in adverse environmental conditions.
- HANWA were employed and tested in restrained shrinkage and exhibited great effectiveness in reducing the material's cracking due to water evaporation, compared to control mixtures and SAP mixtures.
- Various theoretical models from the literature were used to evaluate the mercury intrusion porosimeter results. The specific calculations verified the effectiveness of HANWA – IC in low w/c ratio mixtures.
- Innovative electrical and optical fiber sensors were developed in order to measure concrete RH. The results of the developed sensors were very promising whereas the internally cured mixtures showed a humidity retainment within the matrix, which is a direct proof of internal curing action.
- The method of IC was successfully utilized in concrete mixtures with recycled aggregates.

The methodologies described in this thesis were tested, experimentally and theoretically, under various conditions. Cyprus construction industry has to deal with two main issues, aggregates high absorptivity and high temperatures. It was showed that simple techniques and a specialized design can be utilized to reduce the variability in mechanical properties and durability of concrete and improve its quality. A first measure has to be the obligatory presoaking of the aggregates, in order to partially offset the negative effects of aggregates' high water absorption.

8.2. Recommendations for future research

From the specific dissertation, the possibilities for extending the work of internal curing are listed below:

PERICLES ALEXANDROU SAWA

- Evaluation of the internal curing products using advanced methods, such as scanning electron microscope and x-ray diffraction. Investigate the ITZ for both NWA and HANWA materials.
- Evaluation of the mechanism that deteriorated limestone aggregate mixtures in later ages. Speculations include the calcium leaching, a slow reaction of cement paste and aggregates in the interfacial transition zone and less likely the formation of ettringite in the specific region.
- Restrained shrinkage specific testing (on a couple of mixtures) accompanied with finite elements modelling.
- Evaluation of the degree of hydration using isothermal calorimetry.
- Extend the development of electrical sensors to measure RH.
- Extend the development of optical fiber sensors to measure RH, strain and pH. The ultimate goal should be low cost health monitoring devices that can be used for conventional concrete structures. The major advantage of these sensors is that they do not lose their reference point and therefore, continuous monitoring is not necessary.
- Extended research for internal curing using recycled aggregates. The specific is much more challenging since the aggregate (fraction and source) combinations are infinite and also fine recycled aggregates are mostly disregarded nowadays.

PERICLES ALEXANDROU SAVVA

Publications

International Journal Publications

PhD Related Journal Publications

1. **Savva, A.P**., Nicolaides, G.D. and Petrou, F.M., 2016. High Absorptive Normal Weight Aggregates Used as Internal Curing Agents to Reduce Hot Weather Concreting and Curing Detrimental Effects. *Key Engineering Materials*, 711, pp.420–427.
2. G. Dimitriou, **P. Savva** and M.F. Petrou, Enhancing mechanical and durability properties of recycled aggregate concrete, *Construction and Building Materials*. 158 (2018), pp.228-235.
3. **Savva, A.P**., Nicolaides, G.D. and Petrou, F.M. 2018, Internal curing for mitigating high temperature concreting effects (In press, *Construction and Building Materials* - Elsevier)
4. **Savva, A.P**., Petrou, F.M., 2018. Internal curing using high absorptive normal weight aggregates (Accepted, *Construction and Building Materials* - Elsevier)
5. Theodosiou, A., **Savva, A.P**, Petrou, M.F. and Kalli, K. An Innovative Fibre Optic methodology for measuring Relative Humidity in Concrete – (Under Preparation)
6. Sophokleous, M., **Savva, A.P**, Petrou, M.F., Atkinson J.K. and Georgiou, J., Screen-printed resistivity sensor for in-situ and real-time monitoring of concrete moisture content suitable for smart buildings/cities and IoT (Under Preparation)

Other Journal Publications

7. Nicolaides, D., Kanellopoulos, A., Petrou, M., **Savva, P.** and Mina, A., 2015. Development of a new Ultra High Performance Fibre Reinforced Cementitious Composite (UHPFRCC) for impact and blast protection of structures. *Construction and Building Materials*, 95, pp.667–674.
8. Nicolaides, D., Kanellopoulos, A., **Savva, P**. and Petrou, M., 2015. Experimental field investigation of impact and blast load resistance of Ultra High Performance Fibre Reinforced Cementitious Composites (UHPFRCCs). *Construction and Building Materials*, 95, pp.566–574.

PERICLES ALEXANDROU SAVVA

9. Kanellopoulos, A., **Savva, P**., Petrou, M. F, Ioannou, I., Pantazopoulou, S., Image analysis methodology for the qualitative characterisation of the interface between concrete and steel reinforcement in self-compacting and normal vibrated concretes (Under preparation).

PERICLES ALEXANDROU SAVVA

Conference Proceedings

PhD Related Conference Proceedings

1. **Savva, P.A.** and Petrou, M.F., 2015. A new approach for internal curing of high performance concrete to reduce early-age volume variations. In *Concrete Repair, Rehabilitation and Retrofitting IV, Leipzig, Germany*. pp. 435–441.

2. **Savva, P.A.** and Petrou, M.F., 2015. High-Absorptive Normal-Weight Aggregates used as Internal Curing Agent. In *27th Biennial National Conference of the Concrete Institute of Australia in conjuction with the 69th RILEM week*. pp. 1305–1313.

3. **Savva, P.,** Theodosiou, A., Petrou F.M. and Kalli, K., 2017. Concrete RH monitoring using embedded FBG sensors inscribed in multimode CYTOP fibre. (Submitted in *the 5th on Specialty Optical Fibres and Their Applications* - WSOF 2107)

4. **Σάββα, Π.** Αϊβαλιώτης, Κ., Νικολαΐδης, Δ. και Πέτρου, Μ.Φ., 2018. Χρήση μηχανισμού αυτοσυντήρησης με σκοπό το μετριασμό δυσμενών επιπτώσεων σκυροδέτησης και συντήρησης σε υψηλές θερμοκρασίες. *18ο Συνέδριο Σκυροδέματος* – Αθήνα, Ελλάδα

Other Conference Proceedings

5. Nicolaides, D., Kanellopoulos, A., **Savva, P.** and Mina, A., Petrou, M., 2013. Mix Design and Mechanical Properties of Ultra High Performance Fibre Reinforced Cementitious Composites (UHPFRCC). In Paper presented at the *7th International RILEM Symposium on SCC*. p. (electronic copy).

6. Nicolaides, D., Lampropoulos, A., Kanellopoulos, A., **Savva, P.** and Mina, A., Petrou, M., 2013. Static Response and Modelling of Impact Resistance of UHPFRCC Slab Specimens. In A. V. Dancygier, ed. Proceedings of the *fib Symposium, Engineering a Concrete Future: Technology, Modeling & Construction*. Tel-Aviv, Israel, pp. 605–608.

7. Nicolaides, D., Kanellopoulos, A., **Savva, P.** and Petrou, M., 2012. Static response of UHPFRCC slab specimens. In D. H. Bager & J. Silfwerbrand, eds. Proceedings of the *fib Symposium, Concrete Structures for Sustainable Community*. pp. 597–600.

PERICLES ALEXANDROU SAVVA

Bibliography

(APHA) Association American Public Health (2005) *Standard methods for the examination of water and wastewater*. 21st edn.

ACI Committee 308 and 213 (2013) 'Report on Internally Cured Concrete Using Prewetted Absorptive Lightweight Aggregate'.

Akcay, B. and Tasdemir, M. A. (2009) 'Optimisation of using lightweight aggregates in mitigating autogenous deformation of concrete', *Construction and Building Materials*. Elsevier Ltd, 23(1), pp. 353–363. doi: 10.1016/j.conbuildmat.2007.11.015.

Akcay, B. and Tasdemir, M. A. (2010) 'Effects of distribution of lightweight aggregates on internal curing of concrete', *Cement and Concrete Composites*. Elsevier Ltd, 32(8), pp. 611–616. doi: 10.1016/j.cemconcomp.2010.07.003.

Alam, M. N. *et al.* (2010) 'Concrete moisture content measurement using interdigitated near-field sensors', *IEEE Sensors Journal*, 10(7), pp. 1243–1248. doi: 10.1109/JSEN.2010.2040175.

Alwis, L., Sun, T. and Grattan, K. T. V (2013) 'Optical fibre-based sensor technology for humidity and moisture measurement: Review of recent progress', *Measurement: Journal of the International Measurement Confederation*. Elsevier Ltd, 46(10), pp. 4052–4074. doi: 10.1016/j.measurement.2013.07.030.

America Concrete Institute (2002) 'Standard Practice for Selecting Proportions for Normal Heavyweight, and Mass Concrete, ACI 211.1-91', *Manual of Concrete Practice*, (Reapproved), pp. 1–38.

An, J. *et al.* (2013) 'Relative humidity sensor based on SMS fiber structure with polyvinyl alcohol coating', *Optik - International Journal for Light and Electron Optics*. Elsevier GmbH., 124(23), pp. 6178–6181. doi: 10.1016/j.ijleo.2013.04.095.

André, P. S. *et al.* (2012) 'Monitoring of the concrete curing process using plastic optical fibers', *Measurement*, 45(3), pp. 556–560.

Assmann, A. and Reinhardt, H. W. (2014) 'Tensile creep and shrinkage of SAP modified concrete', *Cement and Concrete Research*, 58, pp. 179–185. doi: 10.1016/j.cemconres.2014.01.014.

PERICLES ALEXANDROU SAVVA

ASTM (2015) ‘Standard Practice for Preparing Precision and Bias Statements for Test Methods for Construction Materials’, *American Society for Testing and Materials*, pp. 1–9. doi: 10.1520/C0670-10.2.

ASTM C1608 (2008) *Standard Test Method for Chemical Shrinkage of Hydraulic Cement Paste*.

ASTM C 1202 *et al.* (2008) ‘Standard Test Method for Electrical Indication of Concrete ’ s Ability to Resist Chloride’, *Annual Book of ASTM Standards*, (95 mm), pp. 1–6. doi: 10.1520/C1202-10.2.

ASTM C 1202 (2009) ‘Standard Test Method for Electrical Indication of Concrete ’ s Ability to Resist Chloride’, pp. 1–6.

ASTM C 1581 (2009) ‘Standard Test Method for Determining Age at Cracking and Induced Tensile Stress Characteristics of Mortar and Concrete under Restrained Shrinkage’, pp. 1–8.

Atkinson, J. K. and Sophocleous, M. (2014) ‘A novel thick-film screen printed electrical conductivity sensor for measurement of liquid and soil conductivity’, *IEEE SENSORS 2014 Proceedings*, pp. 86–89. doi: 10.1109/ICSENS.2014.6984939.

Azarijafari, H. *et al.* (2016) ‘Effects of pre-soaked super absorbent polymers on fresh and hardened properties of self-consolidating lightweight concrete’, *Construction and Building Materials*. Elsevier Ltd, 113, pp. 215–220. doi: 10.1016/j.conbuildmat.2016.03.010.

Barcelo, L., Moranville, M. and Clavaud, B. (2005) ‘Autogenous shrinkage of concrete: A balance between autogenous swelling and self-desiccation’, *Cement and Concrete Research*, 35, pp. 177–183.

Bentur, A., Igarashi, S. I. and Kovler, K. (2001) ‘Prevention of autogenous shrinkage in high-strength concrete by internal curing using wet lightweight aggregates’, *Cement and Concrete Research*, 31, pp. 1587–1591. doi: 10.1016/S0008-8846(01)00608-1.

Bentz, D. P. *et al.* (1997) ‘Microstructural modelling of self-desiccation during hydration’, pp. 132–140. Available at: http://fire.nist.gov/concpubs/conc98/PDF/c98003.pdf.

Bentz, D. P. (2007) ‘A virtual rapid chloride permeability test’, *Cement and Concrete Composites*, 29, pp. 723–731. doi: 10.1016/j.cemconcomp.2007.06.006.

PERICLES ALEXANDROU SAWA

Bentz, D. P. (2009) ‘Influence of internal curing using lightweight aggregates on interfacial transition zone percolation and chloride ingress in mortars’, *Cement and Concrete Composites*. Elsevier Ltd, 31(5), pp. 285–289. doi: 10.1016/j.cemconcomp.2009.03.001.

Bentz, D. P., Garboczi, E. J. and Quenard, D. A. (1998) ‘Modelling drying shrinkage in reconstructed porous materials: application to porous Vycor glass’, *Modelling and Simulation in Materilas Science and Engineering*, 6, pp. 211–236.

Bentz, D. P., Geiker, M. and Jensen, O. M. (2002) ‘ON THE MITIGATION OF EARLY AGE CRACKING’, in *The Third International Research Seminar in Lund,*.

Bentz, D. P., Lura, P. and Roberts, J. W. (2005) ‘Mixture proportioning for internal curing’, *Concrete International*, 27(2), pp. 35–40. Available at: http://concrete.nist.gov/~bentz/Mixpropfin/CI2702Bentz.pdf.

Bentz, D. P. and Snyder, K. A. (1999) ‘Protected paste volume in concrete’, *Cement and Concrete Research*, pp. 1863–1867.

Bentz, P. D. and Snyder, K. A. (1999) ‘Protected paste volume in concrete Extension to internal curing using saturated lightweight fine aggregates’, *Cement and Concrete Research*, 29, pp. 1863–1867.

Bjegović, D. *et al.* (2016) ‘Test Methods for Concrete Durability Indicators’, in *Performance-Based Specifications and Control of Concrete Durability*, pp. 51–105.

Briffaut, M. *et al.* (2011) ‘A thermal active restrained shrinkage ring test to study the early age concrete behaviour of massive structures’, *Cement and Concrete Research*. Elsevier Ltd, 41(1), pp. 56–63. doi: 10.1016/j.cemconres.2010.09.006.

Browning, J. A. *et al.* (2011) ‘Lightweight aggregate as internal curing agent to limit concrete shrinkage’, *ACI Materials Journal*, 108(6), pp. 638–644.

Butler, L. J. *et al.* (2016) ‘Evaluating the early-age behaviour of full-scale prestressed concrete beams using distributed and discrete fibre optic sensors’, *Construction and Building Materials*. The Authors, 126, pp. 894–912. doi: 10.1016/j.conbuildmat.2016.09.086.

Byard, B. E., Schindler, A. K. and Barnes, R. W. (2012) ‘Early-Age Cracking Tendency and Ultimate Degree of Hydration of Internally Cured Concrete’, *Journal of Materials in Civil*

PERICLES ALEXANDROU SAVVA

Engineering, 24(August), pp. 1025–1033.

Castro, J. *et al.* (2011) 'Absorption and desorption properties of fine lightweight aggregate for application to internally cured concrete mixtures', *Cement and Concrete Composites*. Elsevier Ltd, 33(10), pp. 1001–1008. doi: 10.1016/j.cemconcomp.2011.07.006.

Castro, J., Bentz, D. and Weiss, J. (2011) 'Effect of sample conditioning on the water absorption of concrete', *Cement and Concrete Composites*. Elsevier Ltd, 33(8), pp. 805–813. doi: 10.1016/j.cemconcomp.2011.05.007.

Cervera, M. *et al.* (2002) 'Numerical modelling of concrete curing, regarding hydration and temperature phenomena', *Computers & Structures*, 80(18–19), pp. 1511–1521.

Charbeneau, R. (2002) *Groundwater Hydraulics and Pollutant Transport*, *Applied Mechanics Reviews*. Waveland Press, Inc. doi: 10.1115/1.1451232.

Chiarello, M. and Zinno, R. (2005) 'Electrical conductivity of self-monitoring CFRC', *Cement and Concrete Composites*, 27(4), pp. 463–469. doi: 10.1016/j.cemconcomp.2004.09.001.

Choi, H. *et al.* (2015) 'Restrained shrinkage behavior of expansive mortar at early ages', *Construction and Building Materials*. Elsevier Ltd, 84, pp. 468–476. doi: 10.1016/j.conbuildmat.2015.03.075.

Chu, I. *et al.* (2012) 'Estimation of temperature effects on autogenous shrinkage of concrete by a new prediction model', *Construction and Building Materials*. Elsevier Ltd, 35, pp. 171–182. doi: 10.1016/j.conbuildmat.2012.03.005.

Collins, F. and Sanjayan, J. G. (1999) 'Strength and shrinkage properties of alkali-activated slag concrete placed into a large column', *Cement and Concrete Research*, 29(5), pp. 659–666. doi: 10.1016/S0008-8846(99)00011-3.

Craeye, B., Geirnaert, M. and Schutter, G. D. (2011) 'Super absorbing polymers as an internal curing agent for mitigation of early-age cracking of high-performance concrete bridge decks', *Construction and Building Materials*. Elsevier Ltd, 25(1), pp. 1–13. doi: 10.1016/j.conbuildmat.2010.06.063.

Craeye, B. and Schutter, G. (2006) 'Experimental evaluation of mitigation of autogenous shrinkage by means of a vertical dilatometer for concrete', *International RILEM Conference on*

PERICLES ALEXANDROUSAWA

Volume Changes of Hardening Concrete: Testing and Mitigation, C(August), pp. 21–30. doi: 10.1617/2351580052.003.

Cusson, D., Lounis, Z. and Daigle, L. (2010) 'Benefits of internal curing on service life and life-cycle cost of high-performance concrete bridge decks - A case study', *Cement and Concrete Composites*. Elsevier Ltd, 32(5), pp. 339–350. doi: 10.1016/j.cemconcomp.2010.02.007.

Cyprus Geological Survey Department (2016) *Cyprus Geological Survey Department*. Available at: http://www.moa.gov.cy/moa/gsd/gsd.nsf/dmlPentadaktylos_en/dmlPentadaktylos_en?OpenDocument (Accessed: 3 November 2016).

D.A. Lange and R. Rodden, Z. C. G. (no date) 'Embedded Sensors for Measuring Environmental Parameters in Concrete', *Special Publication*, 252. doi: 10.14359/20156.

Demetriou, G. (2014) *Enhancing Mechanical and Durability Properties of Recycled Aggregate Concrete*.

Deo, S. V and Pofale, A. D. (2015) 'Parametric Study for Replacement of Sand by Fly Ash for Better Packing and Internal Curing', (March), pp. 118–130. doi: 10.4236/ojce.2015.51012.

Ding, H., Zhang, L. and Zhang, P. (2017) 'Factors Influencing Strength of Super Absorbent Polymer (SAP) Concrete', *Transactions of Tianjin University*. Tianjin University, 23(3), pp. 245–257. doi: 10.1007/s12209-017-0049-y.

Dong, W. *et al.* (2016) 'Effects of specimen size on assessment of shrinkage cracking of concrete via elliptical rings: Thin vs. thick', *Computers & Structures*. Elsevier Ltd. doi: 10.1016/j.compstruc.2015.12.005.

Double, D. D. and Hellawell, A. (1977) 'The Solidification of Cement', *Scientific American*, pp. 82–90.

Dudziak, L. and Mechtcherine, V. (2010) 'Deliberations on Kinetics of Internal Curing Water Migration and Consumption Based on Experimental Studies on Sap-Enriched Uhpc', (August).

Elsharief, A., Cohen, M. D. and Olek, J. (2003) 'Influence of aggregate size, water cement ratio and age on the microstructure of the interfacial transition zone', *Cement and Concrete Research*, 33(11), pp. 1837–1849. doi: 10.1016/S0008-8846(03)00205-9.

PERICLES ALEXANDROU SAVVA

EN 1097 (2013) ‘Tests for mechanical and physical properties of aggregates Part 6: Determination of particle density and water absorption’. BSI Standards Publication.

EN 12390 - 3 (2002) ‘Testing hardened concrete - Part 3: Compressive strength of test specimens’.

EN 14580 (2005) *Natural stone test methods. Determination of static elastic modulus*.

EN 1926 (2006) ‘Natural stone test methods - Determination of uniaxial compressive strength’.

Eppers, S. (2010) *Assessing the autogenous shrinkage cracking propensity of concrete by means of the restrained ring test*. University of Dresden.

Espinoza-Hijazin, G. and Lopez, M. (2011) ‘Extending internal curing to concrete mixtures with W/C higher than 0.42’, *Construction and Building Materials*. Elsevier Ltd, 25(3), pp. 1236–1242. doi: 10.1016/j.conbuildmat.2010.09.031.

Esteves, L. P. (2011) ‘Superabsorbent polymers: On their interaction with water and pore fluid’, *Cement and Concrete Composites*, 33(7), pp. 717–724. doi: 10.1016/j.cemconcomp.2011.04.006.

Esteves, P. (2010) ‘On the absorption kinetics of superabsorbent polymers’, *International RILEM Conference on Use of Superabsorbent Polymers and Other New Additives in Concrete 15-18 August*, (August), pp. 77–84.

Feldman, R. F. and Sereda, P. J. (1970) ‘A new model for hydrated cement and its practical implications’, *Engineering Journal*, 53(8/9), pp. 53–59.

Ferraro, P. and De Natale, G. (2002) ‘On the possible use of optical fiber Bragg gratings as strain sensors for geodynamical monitoring’, *Optics and Lasers in Engineering*, 37(2), pp. 115–130. doi: https://doi.org/10.1016/S0143-8166(01)00141-5.

Ferreira, T. and Rasband, W. (2012) *ImageJ User Guide*, *IJ 1.46r*. Available at: http://rsbweb.nih.gov/ij/docs/guide/146-30.html (Accessed: 10 February 2015).

Fidanboylu, K. and Efendioglu, H. (2009) ‘Fiber optic sensors and their applications’, *Proceedings of 5th …*, pp. 199–201.

Fokine, M. *et al.* (2017) ‘Laser structuring, stress modification and Bragg grating inscription in silicon-core glass fibers’, *Optical Materials Express*. OSA, 7(5), pp. 1589–1597. doi:

PERICLES ALEXANDROU SAVVA

10.1364/OME.7.001589.

Gao, Y., Zhang, J. and Han, P. (2013) 'Determination of stress relaxation parameters of concrete in tension at early-age by ring test', *Construction and Building Materials*, 41, pp. 152–164. doi: 10.1016/j.conbuildmat.2012.12.004.

Ghandehari, M. *et al.* (2012) 'In-situ measurement of liquid phase moisture in cement mortar', *NDT & E International*, 45(1), pp. 162–168.

Ghandehari, M. and Vimer, C. S. (2004) 'In situ monitoring of pH level with fiber optic evanescent field spectroscopy', *NDT and E International*, 37, pp. 611–616. doi: 10.1016/j.ndteint.2004.03.007.

Giannaros, P., Kanellopoulos, A. and Al-Tabbaa, A. (2016) 'Sealing of cracks in cement using microencapsulated sodium silicate'.

Gjorv, M.-H. Z. and O. E. (1991) 'Characteristics of Lightweight Aggregates for High-Strength Concrete', *Materials Journal*, 88(2). doi: 10.14359/1924.

Golias, M., Castro, J. and Weiss, J. (2012) 'The influence of the initial moisture content of lightweight aggregate on internal curing', *Construction and Building Materials*. Elsevier Ltd, 35, pp. 52–62. doi: 10.1016/j.conbuildmat.2012.02.074.

Grattan, K. T. V. and Sun, T. (2000) 'Fiber optic sensor technology: an overview', *Sensors and Actuators A: Physical*, 82, pp. 40–61. doi: 10.1016/S0924-4247(99)00368-4.

H., M., A.K.Y., J. and L.R., D. (2002) 'Polymer-Based Optical Waveguides: Materials, Processing, and Devices', *Advanced Materials*. Wiley-Blackwell, 14(19), pp. 1339–1365. doi: 10.1002/1521-4095(20021002)14:19<1339::AID-ADMA1339>3.0.CO;2-O.

Han, B., Yu, X. and Kwon, E. (2009) 'A self-sensing carbon nanotube/cement composite for traffic monitoring', *Nanotechnology*, 20(44), p. 445501. doi: 10.1088/0957-4484/20/44/445501.

Han, Y. *et al.* (2014) 'Effect of internal curing on internal relative humidity and shrinkage of high strength concrete slabs', *Construction and Building Materials*. Elsevier Ltd, 61, pp. 41–49. doi: 10.1016/j.conbuildmat.2014.02.060.

Hasholt, M. T. and Jensen, O. M. (2015) 'Chloride migration in concrete with superabsorbent polymers', *Cement and Concrete Composites*. Elsevier Ltd, 55, pp. 290–297. doi:

PERICLES ALEXANDROU SAVVA

10.1016/j.cemconcomp.2014.09.023.

Hasholt, M. T., Jespersen, M. H. S. and Jensen, O. M. (2010a) 'Mechanical properties of Concrete with SAP Part I: Development of compressive strength', (August).

Hasholt, M. T., Jespersen, M. H. S. and Jensen, O. M. (2010b) 'Mechanical properties of Concrete with SAP Part II: Modulus of Elasticity', (August).

Henkensiefken, R. *et al.* (2008) 'Comments on the Shrinkage of Paste in Mortar', *Concrete*, (May), pp. 707–714.

Henkensiefken, R., Bentz, D., *et al.* (2009) 'Volume change and cracking in internally cured mixtures made with saturated lightweight aggregate under sealed and unsealed conditions', *Cement and Concrete Composites*. Elsevier Ltd, 31(7), pp. 427–437.

Henkensiefken, R., Castro, J., *et al.* (2009) 'Water absorption in internally cured mortar made with water-filled lightweight aggregate', *Cement and Concrete Research*. Elsevier Ltd, 39(10), pp. 883–892. doi: 10.1016/j.cemconres.2009.06.009.

Hill, K. O. *et al.* (1978) 'Photosensitivity in optical fiber waveguides: Application to reflection filter fabrication', *Applied Physics Letters*. American Institute of Physics, 32(10), pp. 647–649. doi: 10.1063/1.89881.

Holm, T. A. (1980) 'Performance of Structural Lightweight Concrete in Marine Environment', in *Performance of Concrete in Marine Environments*.

Hossain, A. B. and Weiss, J. (2004) 'Assessing residual stress development and stress relaxation in restrained concrete ring specimens', *Cement and Concrete Composites*, 26(5), pp. 531–540. doi: 10.1016/S0958-9465(03)00069-6.

Huang, H., Ye, G. and Breugel, K. Van (2010) 'Numerical Simulation on Moisture Transport From Super Absorbent Polymers To Concrete', (October), pp. 185–194.

Huang, X. F. *et al.* (2007) 'Low-cost relative humidity sensor based on thermoplastic polyimide-coated fiber Bragg grating', *Sensors and Actuators B: Chemical*, 127(2), pp. 518–524. doi: 10.1016/j.snb.2007.05.007.

Husem, M. (2003) 'The effects of bond strengths between lightweight and ordinary aggregate-mortar, aggregate-cement paste on the mechanical properties of concrete', *Materials Science*

PERICLES ALEXANDROUSAWA

and Engineering A, 363, pp. 152–158. doi: 10.1016/S0921-5093(03)00595-1.

Hussin, A. and Poole, C. (2011) 'Petrography evidence of the interfacial transition zone (ITZ) in the normal strength concrete containing granitic and limestone aggregates', *Construction and Building Materials*. Elsevier Ltd, 25(5), pp. 2298–2303. doi: 10.1016/j.conbuildmat.2010.11.023.

Iffat, S., Manzur, T. and Noor, M. A. (2016) 'Durability performance of internally cured concrete using locally available low cost LWA', *KSCE Journal of Civil Engineering*, 21(4), pp. 1256–1263. doi: 10.1007/s12205-016-0793-x.

Igarashi, S. and Watanabe, A. (2006) 'Experimental study on prevention of autogenous deformation by internal curing using super-absorbent polymer particles', *International RILEM Conference on Volume Changes of Hardening Concrete: Testing and Mitigation*, C(August), pp. 77–86. doi: 10.1617/2351580052.009.

Ioannou, I. *et al.* (2010) 'Crushed limestone as an aggregate in concrete production: the Cyprus case', *Geological Society, London, Special Publications*, 331(1), pp. 127–135.

Jensen, O. M. and Hansen, P. F. (2000) 'Water-entrained cement-based materials I . Principle and theoretical background', *Cement and Concrete Research*, 31, pp. 1–13.

Jensen, O. M. and Hansen, P. F. (2001) 'Autogenous deformation and RH-change in perspective', *Cement and Concrete Research*, 31(March), pp. 1859–1865.

Jensen, O. M. and Hansen, P. F. (2002) 'Water-entrained cement-based materials II. Experimental observations', 32, pp. 973–978.

Jensen, O. M. and Lura, P. (2006) 'Techniques and materials for internal water curing of concrete', *Materials and Structures*, 39, pp. 817–825. doi: 10.1617/s11527-006-9136-6.

Jin, F., Gu, K. and Al-Tabbaa, A. (2014) 'Strength and drying shrinkage of reactive MgO modified alkali-activated slag paste', *Construction and Building Materials*. Elsevier Ltd, 51, pp. 395–404. doi: 10.1016/j.conbuildmat.2013.10.081.

Johnson, I. P. *et al.* (2010) 'Multiplexed FBG sensor recorded in multimode microstructured polymer optical fibre', in, p. 77140D–7714–10. Available at: https://doi.org/10.1117/12.854410.

PERICLES ALEXANDROU SAVVA

Justs, J. *et al.* (2015) 'Internal curing by superabsorbent polymers in ultra-high performance concrete', *Cement and Concrete Research*. Elsevier Ltd, 76, pp. 82–90.

Kanellopoulos, A., Petrou, M. F. and Ioannou, I. (2012) 'Durability performance of self-compacting concrete', *Construction and Building Materials*. Elsevier Ltd, 37, pp. 320–325. doi: 10.1016/j.conbuildmat.2012.07.049.

Kanellopoulos, A., Qureshi, T. and Al-Tabbaa, A. (2015) 'Glass encapsulated minerals for self-healing in cement based composites', *Construction and Building Materials*, pp. 780–791.

Kang, S. H., Hong, S. G. and Moon, J. (2017) 'Absorption kinetics of superabsorbent polymers (SAP) in various cement-based solutions', *Cement and Concrete Research*. Elsevier Ltd, 97, pp. 73–83. doi: 10.1016/j.cemconres.2017.03.009.

Kawasaki, B. S. *et al.* (1978) 'Narrow-band Bragg reflectors in optical fibers', *Optics Letters*. OSA, 3(2), pp. 66–68. doi: 10.1364/OL.3.000066.

Kim, H. K. *et al.* (2014) 'Improved chloride resistance of high-strength concrete amended with coal bottom ash for internal curing', *Computers and Chemical Engineering*. Elsevier Ltd, 71, pp. 334–343. doi: 10.1016/j.conbuildmat.2014.08.069.

Kjellsen, O. K. and Detwiller, J. . (1992) 'Reaction kinetics of portland cement mortars hydrated at different temperatures', *Cement and Concrete Research*, 22, pp. 112–120.

Kohno, K. *et al.* (1999) 'Effects of artificial lightweight aggregate on autogenous shrinkage of concrete', *Cement and Concrete Research*, 29, pp. 611–614. doi: 10.1016/S0008-8846(98)00202-6.

Kong, L. and Du, Y. (2015) 'Interfacial interaction of aggregate-cement paste in concrete', *Journal of Wuhan University of Technology-Mater. Sci. Ed.*, 30(1), pp. 117–121. doi: 10.1007/s11595-015-1111-z.

Kronenberg, P. *et al.* (2002) 'Relative humidity sensor with optical fiber Bragg gratings.', *Optics letters*, 27(16), pp. 1385–1387. doi: 10.1364/OL.27.001385.

De La Varga, I. *et al.* (2012) 'Application of internal curing for mixtures containing high volumes of fly ash', *Cement and Concrete Composites*. Elsevier Ltd, 34(9), pp. 1001–1008. doi: 10.1016/j.cemconcomp.2012.06.008.

PERICLES ALEXANDROUSAVVA

De La Varga, I. *et al.* (2014) 'Fluid transport in high volume fly ash mixtures with and without internal curing', *Cement and Concrete Composites*. Elsevier Ltd, 45, pp. 102–110. doi: 10.1016/j.cemconcomp.2013.09.017.

Lacraz, A. *et al.* (2015) 'Femtosecond Laser Inscribed Bragg Gratings in Low Loss CYTOP Polymer Optical Fiber', *IEEE Photonics Technology Letters*, 27(7), pp. 693–696. doi: 10.1109/LPT.2014.2386692.

Lacraz, A., Theodosiou, A. and Kalli, K. (2016) 'Femtosecond laser inscribed Bragg grating arrays in long lengths of polymer optical fibres; a route to practical sensing with POF', *Electronics Letters*, 52(19), pp. 1626–1627. doi: 10.1049/el.2016.2238.

Lau, K. T. *et al.* (2001) 'Strain monitoring in FRP laminates and concrete beams using FBG sensors', *Composite Structures*, 51(1), pp. 9–20. doi: 10.1016/S0263-8223(00)00094-5.

Leemann, A., Nygaard, P. and Lura, P. (2014) 'Impact of admixtures on the plastic shrinkage cracking of self-compacting concrete', *Cement and Concrete Composites*. Elsevier Ltd, 46, pp. 1–7. doi: 10.1016/j.cemconcomp.2013.11.002.

Leng, J. and Asundi, A. (2003) 'Structural health monitoring of smart composite materials by using EFPI and FBG sensors', *Sensors and Actuators A: Physical*, 103(3), pp. 330–340. doi: https://doi.org/10.1016/S0924-4247(02)00429-6.

Li, M. *et al.* (2017) 'Efficacy of internal curing combined with expansive agent in mitigating shrinkage deformation of concrete under variable temperature condition', *Construction and Building Materials*. Elsevier Ltd, 145, pp. 354–360. doi: 10.1016/j.conbuildmat.2017.04.021.

Liang, W. *et al.* (2005) 'Highly sensitive fiber Bragg grating refractive index sensors', *Applied Physics Letters*. American Institute of Physics, 86(15), p. 151122. doi: 10.1063/1.1904716.

Lima, H. F. *et al.* (2008) 'Structural Health Monitoring of the Church of Santa Casa da MisericÓrdia of Aveiro Using FBG Sensors', *IEEE Sensors Journal*, 8(7), pp. 1236–1242. doi: 10.1109/JSEN.2008.926177.

Limberger, H., Giaccari, P. and Kronenberg, P. (2001) 'Influence of humidity and temperature on polyimide-coated fiber Bragg gratings', *Bragg Gratings, Photosensitivity, and Poling in Glass Waveguides*, (I). doi: 10.1364/BGPP.2001.BFB2.

PERICLES ALEXANDROU SAVVA

Litina, C., Kanellopoulos, A. and Al-Tabbaa, A. (2014) 'Alternative repair system for concrete using microencapsulated healing agents', *Concrete solutions*, p. 97.

Liu, F. *et al.* (2017) 'Internal curing of high performance concrete using cenospheres', *Cement and Concrete Research*. Elsevier Ltd, 95, pp. 39–46. doi: 10.1016/j.cemconres.2017.02.023.

Liu, H. Y., Peng, G. D. and Chu, P. L. (2001) 'Thermal tuning of polymer optical fiber Bragg gratings', *IEEE Photonics Technology Letters*, 13(8), pp. 824–826. doi: 10.1109/68.935816.

Liu, H. Y., Peng, G. D. and Chu, P. L. (2002) 'Thermal stability of gratings in PMMA and CYTOP polymer fibers', *Optics Communications*, 204(1), pp. 151–156. doi: https://doi.org/10.1016/S0030-4018(02)01216-6.

Liu, J. *et al.* (2017) 'An overview on the effect of internal curing on shrinkage of high performance cement-based materials', *Construction and Building Materials*. Elsevier Ltd, 146, pp. 702–712. doi: 10.1016/j.conbuildmat.2017.04.154.

Liu, Y. *et al.* (2005) 'Fiber comb filters based on UV-writing Bragg gratings in graded-index multimode fibers', *Optics Express*. OSA, 13(21), pp. 8508–8513. doi: 10.1364/OPEX.13.008508.

Lo, Y., Gao, X. F. and Jeary, A. P. (1999) 'Microstructure of pre-wetted aggregate on lightweight concrete', *Building and Environment*, 36(6), pp. 759–764.

Lopes, A. N. M. *et al.* (2013) 'Shrinkage-Reducing Admixture: Effects on Durability of High-Strength Concrete', *ACI Materials Journal*, 110(4), pp. 365–374.

Lura, P. (2003) *Autogenous Deformation and Internal Curing of Concrete*. Technische Universiteit Delft.

Lura, P. *et al.* (2006) 'Compressive strength of cement pastes and mortars with superabsorbent polymers', in *RILEM conference on Volume Changes of Hardening Concrete: Testing and Mitigation*. Lyngby, pp. 117–126.

Lura, P. and Bisschop, J. (2004) 'On the origin of eigenstresses in lightweight aggregate concrete', *Cement and Concrete Composites*, 26(5), pp. 445–452. doi: 10.1016/S0958-9465(03)00072-6.

Lura, P., Jensen, O. M. and Van Breugel, K. (2003) 'Autogenous shrinkage in high-performance

PERICLES ALEXANDROU SAVVA

cement paste: An evaluation of basic mechanisms', *Cement and Concrete Research*, 33, pp. 223–232.

Lura, P., Jensen, O. M. and Igarashi, S.-I. (2007) 'Experimental observation of internal water curing of concrete', *Materials and Structures*, 40, pp. 211–220. doi: 10.1617/s11527-006-9132-x.

Lura, P. and Terrasi, G. Pietro (2014) 'Reduction of fire spalling in high-performance concrete by means of superabsorbent polymers and polypropylene fibers: Small scale fire tests of carbon fiber reinforced plastic-prestressed self-compacting concrete', *Cement and Concrete Composites*. Elsevier Ltd, 49, pp. 36–42. doi: 10.1016/j.cemconcomp.2014.02.001.

Lynam, C. G. (1934) *Growth and Movement in Portland Cement Concrete*, *Oxford University Press*. London: Oxford University Press.

Ma, X. *et al.* (2017) 'Effects of SAP on the properties and pore structure of high performance cement-based materials', *Construction and Building Materials*. Elsevier Ltd, 131, pp. 476–484. doi: 10.1016/j.conbuildmat.2016.11.090.

Maekawa, K., Chaube, R. and Kishi, T. (1999) *Modelling of concrete Perfomance*. E&FN Spon.

Maruyama, I. *et al.* (2009) 'Evaluation of water transfer from saturated lightweight aggregate to cement paste matrix by neutron radiography', *Nuclear Instruments and Methods in Physics Research, Section A: Accelerators, Spectrometers, Detectors and Associated Equipment*, 605, pp. 159–162. doi: 10.1016/j.nima.2009.01.138.

Matschei, T., Lothenbach, B. and Glasser, F. P. (2007) 'The role of calcium carbonate in cement hydration', *Cement and Concrete Research*, 37(4), pp. 551–558. doi: 10.1016/j.cemconres.2006.10.013.

Mechtcherine, V. *et al.* (2006) 'Internal curing by Superabsorbent Polymers (SAP) – Effects on material properties of self-compacting fibre-reinforced high performance concrete', *International RILEM Conference on Volume Changes of Hardening Concrete: Testing and Mitigation, 20-23 August*, C(August), pp. 87–96.

Mechtcherine, V. *et al.* (2013) 'Effect of internal curing by using superabsorbent polymers (SAP) on autogenous shrinkage and other properties of a high-performance fine-grained concrete: results of a RILEM round-robin test', *Materials and Structures*, 47, pp. 541–562.

PERICLES ALEXANDROU SAWA

Mechtcherine, V., Secrieru, E. and Schröfl, C. (2015) ‘Effect of superabsorbent polymers (SAPs) on rheological properties of fresh cement-based mortars - Development of yield stress and plastic viscosity over time’, *Cement and Concrete Research*, 67, pp. 52–65. doi: 10.1016/j.cemconres.2014.07.003.

Mejlhede Jensen, O. and Freiesleben Hansen, P. (1995) ‘A dilatometer for measuring autogenous deformation in hardening portland cement paste’, *Materials and Structures*, 28, pp. 406–409. doi: 10.1007/BF02473076.

Milestone, N. B. and Gorce, J. P. (2012) ‘Determining how water is held in composite cement binders’, *Journal of the Australian Ceramic Society*, 48, pp. 244–248.

Mönnig, S. and Reinhardt, H.-W. (2006) ‘Results of a comparative study of the shrinkage behaviour of concrete and mortar mixtures with different internal water sources’, *International RILEM Conference on Volume Changes of Hardening Concrete: Testing and Mitigation*, C(August), pp. 67–75. doi: 10.1617/2351580052.008.

Mousa, M. I. *et al.* (2014a) ‘Mechanical properties of self-curing concrete (SCUC)’, *HOUSING AND BUILDING NATIONAL RESEARCH CENTER*. Housing and Building National Research Center. doi: 10.1016/j.hbrcj.2014.06.004.

Mousa, M. I. *et al.* (2014b) ‘Physical properties of self-curing concrete (SCUC)’, *HOUSING AND BUILDING NATIONAL RESEARCH CENTER*. Housing and Building National Research Center, pp. 1–9. doi: 10.1016/j.hbrcj.2014.05.001.

Mousa, M. I. *et al.* (2015) ‘Self-curing concrete types; Water retention and durability’, *Alexandria Engineering Journal*. Faculty of Engineering, Alexandria University, 54(3), pp. 565–575.

Nabighian, M. N. (2006) *Electromagnetic Methods in Applied Geophysics, Theory, vol.1*.

Neville, A. (1995) ‘Chloride Attack of Reinforcement Conccrete an Overview.Pdf’, *Materials and Structures*, pp. 63–70. doi: 10.14359/10569.

Neville, A. M. (2002) *Properties of Concrete*. Pearson Education Limited.

Nina, H. and Andrew, R. B. (1987) ‘BET Surface Area Analysis of Nanoparticles’, 2(Figure 1), pp. 1–11.

PERICLES ALEXANDROU SAVVA

Norris, A., Saafi, M. and Romine, P. (2008) 'Temperature and moisture monitoring in concrete structures using embedded nanotechnology/microelectromechanical systems (MEMS) sensors', *Construction and Building Materials*, 22(2), pp. 111–120. doi: 10.1016/j.conbuildmat.2006.05.047.

Olawuyi, B. J. and Boshoff, W. P. (2017) 'Influence of SAP content and curing age on air void distribution of high performance concrete using 3D volume analysis', *Construction and Building Materials*. Elsevier Ltd, 135, pp. 580–589. doi: 10.1016/j.conbuildmat.2016.12.128.

Ong, J. B. *et al.* (2008) 'A Wireless, Passive Embedded Sensor for Real-Time Monitoring of Water Content in Civil Engineering Materials', *IEEE Sensors Journal*, 8(12), pp. 2053–2058. doi: 10.1109/JSEN.2008.2007681.

Othonos, A. *et al.* (2006) *Fiber Bragg Gratings : Fundamentals and Applications in Telecommunications and Sensing*. Springer Series in Optical Sciences.

Page, C. L. and Vennesland (1983) 'Pore solution composition and chloride binding capacity of silica-fume cement pastes', *Mat??riaux et Constructions*, 16, pp. 19–25. doi: 10.1007/BF02474863.

Peters, K. (2011) 'Polymer optical fiber sensors—a review', *Smart Materials and Structures*, 20(1), p. 13002. Available at: http://stacks.iop.org/0964-1726/20/i=1/a=013002.

Piérard, J., Pollet, V. and Cauberg, N. (2006) 'Mitigating autogenous shrinkage in HPC by internal curing using superabsorbent polymers', *International RILEM Conference on Volume Changes of Hardening Concrete: Testing and Mitigation, 20-23 August*, C(August), pp. 97–106.

Poon, C. S. *et al.* (2004) 'Influence of moisture states of natural and recycled aggregates on the slump and compressive strength of concrete', *Cement and Concrete Research*, 34(1), pp. 31–36. doi: 10.1016/S0008-8846(03)00186-8.

Poon, C. S., Shui, Z. H. and Lam, L. (2004) 'Effect of microstructure of ITZ on compressive strength of concrete prepared with recycled aggregates', *Construction and Building Materials*, 18(6), pp. 461–468. doi: 10.1016/j.conbuildmat.2004.03.005.

Powers, T. C. and Brownyard, T. L. (1947) 'Studies of the physical properties of hardened Portland cement paste', *Journal ACI*, 18.

PERICLES ALEXANDROU SAWA

Prabhugoud, M. and Peters, K. (2004) 'Modified transfer matrix formulation for bragg grating strain sensors', *Journal of Lightwave Technology*, 22(10), pp. 2302–2309. doi: 10.1109/JLT.2004.833281.

Radlinska, A. *et al.* (2008) 'Shrinkage Mitigation Strategies in Cementitious Systems: A Closer Look at Differences in Sealed and Unsealed Behavior', *Transportation Research Record: Journal of the Transportation Research Board*, 2070(1), pp. 59–67. doi: 10.3141/2070-08.

Reinhardt, H. W., Assmann, a and Mönnig, S. (2008) 'Superabsorbent polymers (SAP) - An admixture to increase the durability of concrete', *1st International Conference on Microstructure Related Durability of Cementitious Composites 13-15 October*, (October), pp. 313–322.

Reinhardt, H. W. and Mönnig, S. (2006) 'Basic Concepts for a Model of Different Internal Water Sources', in *ConcreteLife'06 - International RILEM-JCI Seminar on Concrete Durability and Service Life*, pp. 235–244.

Riding, K. a. *et al.* (2008) 'Simplified concrete resistivity and rapid chloride permeability test method', *ACI Materials Journal*, 105(105), pp. 390–394.

RILEM TC 196-ICC Rep 41-4 (2007) *State of the Art Report of RILEM technical committee Internal curing of concrete*. Edited by K. Kovler and O. M. Jensen. Bagneux, France: RILEM Publications S.A.R.L.

RILEM TC 196-ICC Rep 41-5 (2007) *State of the Art Report of RILEM technical committee Internal curing of concrete*. Edited by K. Kovler and O. M. Jensen. Bagneux, France: RILEM Publications S.A.R.L.

RILEM TC 196-ICC Rep 41-6 (2007) *State of the Art Report of RILEM technical committee Internal curing of concrete*. Edited by K. Kovler and O. M. Jensen. Bagneux, France: RILEM Publications S.A.R.L.

RILEM TC 225-SAP (2012) *State of the Art Report of RILEM tecnical committee Application of Superabsorbent Polymers (SAP) in Concrete Construction*. Edited by V. Mechtcherine and H.-W. Reinhardt. Springer Dordrecht Heidelberg London New York.

Le Roy, R., Parant, E. and Boulay, C. (2005) 'Taking into account the inclusions' size in lightweight concrete compressive strength prediction', *Cement and Concrete Research*, 35(4),

PERICLES ALEXANDROU SAVVA

pp. 770–775. doi: 10.1016/j.cemconres.2004.06.002.

Sant, G., Bentz, D. and Weiss, J. (2011) ‘Capillary porosity depercolation in cement-based materials: Measurement techniques and factors which influence their interpretation’, *Cement and Concrete Research*. Elsevier Ltd., 41(8), pp. 854–864.

Sant, G., Lura, P. and Weiss, J. (2006) ‘Measurement of Volume Change in Cementitious Materials at Early Ages: Review of Testing Protocols and Interpretation of Results’, *Transportation Research Record*, 1979, pp. 21–29. doi: 10.3141/1979-05.

Šavija, B. and Luković, M. (2016) ‘Carbonation of cement paste: Understanding, challenges, and opportunities’, *Construction and Building Materials*, 117, pp. 285–301. doi: 10.1016/j.conbuildmat.2016.04.138.

Schmid, M. J. and Müller, M. S. (2015) ‘Measuring Bragg gratings in multimode optical fibers’, *Optics Express*, 23(6), p. 8087. doi: 10.1364/OE.23.008087.

Schroefl, C. *et al.* (2015) ‘Sorption kinetics of superabsorbent polymers (SAPs) in fresh Portland cement-based pastes visualized and quantified by neutron radiography and correlated to the progress of cement hydration’, *Cement and Concrete Research*, 75, pp. 1–13. doi: 10.1016/j.cemconres.2015.05.001.

Schröfl, C., Mechtcherine, V. and Gorges, M. (2012) ‘Relation between the molecular structure and the efficiency of superabsorbent polymers (SAP) as concrete admixture to mitigate autogenous shrinkage’, *Cement and Concrete Research*, 42, pp. 865–873.

Shen, D. *et al.* (2015a) ‘Effect of internal curing with super absorbent polymers on autogenous shrinkage of concrete at early age’, *Construction and Building Materials*. Elsevier Ltd, 99(1), pp. 246–253. doi: 10.1016/j.conbuildmat.2015.08.042.

Shen, D. *et al.* (2015b) ‘Effect of internal curing with super absorbent polymers on the relative humidity of early-age concrete’, *Construction and Building Materials*. Elsevier Ltd, 99, pp. 246–253. doi: 10.1016/j.conbuildmat.2015.08.042.

Shen, D. *et al.* (2017) ‘Prediction of internal relative humidity in concrete modified with super absorbent polymers at early age’, *Construction and Building Materials*. Elsevier Ltd, 149, pp. 543–552. doi: https://doi.org/10.1016/j.conbuildmat.2017.05.121.

PERICLES ALEXANDROU SAVVA

Siramanont, J., Vichit-Vadakan, W. and Siriwatwechakul, W. (2010) 'The impact of SAP structure on the effectiveness of internal curing', *International RILEM Conference on Use of Superabsorbent Polymers and Other New Additives in Concrete*, (August), pp. 243–252.

Sir William Thomson (1871) *The London, Edinburgh and Dublin Philosophical Magazine and Journal of Science - Google Books*. Available at: https://books.google.com.cy/books?id=ZeYXAAAAYAAJ&pg=PA448&redir_esc=y#v=onepage&q&f=false (Accessed: 29 May 2017).

Skourides, I. (2015) *Παραγωγική διαδικασία στη τσιμεντοποιία βασιλικού*.

Snoeck, D. *et al.* (2015) 'The effects of superabsorbent polymers on the microstructure of cementitious materials studied by means of sorption experiments', *Cement and Concrete Research*. Elsevier Ltd, 77(November), pp. 26–35. doi: 10.1016/j.cemconres.2015.06.013.

Snoeck, D., Jensen, O. M. and De Belie, N. (2015) 'The influence of superabsorbent polymers on the autogenous shrinkage properties of cement pastes with supplementary cementitious materials', *Cement and Concrete Research*. Elsevier Ltd, 74, pp. 59–67. doi: 10.1016/j.cemconres.2015.03.020.

Sophocleous, M. and Atkinson, J. K. (2015) 'A novel thick-film electrical conductivity sensor suitable for liquid and soil conductivity measurements', *Sensors and Actuators, B: Chemical*. Elsevier B.V., 213, pp. 417–422. doi: 10.1016/j.snb.2015.02.110.

Staszewski, D. C. B. and G. T. and B. C. and W. J. (2003) 'Acousto-ultrasonic sensing using fiber Bragg gratings', *Smart Materials and Structures*, 12(1), p. 122. Available at: http://stacks.iop.org/0964-1726/12/i=1/a=314.

Statkiewicz-Barabach, G. *et al.* (2013) 'Fabrication of multiple Bragg gratings in microstructured polymer fibers using a phase mask with several diffraction orders', *Optics Express*. OSA, 21(7), pp. 8521–8534. doi: 10.1364/OE.21.008521.

Sumanasooriya, M. S. and Neithalath, N. (2009) 'Stereology and morphology based pore structure descriptors of Enhanced Porosity (Pervious) Conretes', *ACI Materials Journal*, 106(5), pp. 429–438.

Sun, X. *et al.* (2015) 'Investigation of internal curing effects on microstructure and permeability of interface transition zones in cement mortar with SEM imaging, transport simulation and

PERICLES ALEXANDROU SAVVA

hydration modeling techniques', *Construction and Building Materials*. Elsevier Ltd, 76, pp. 366–379. doi: 10.1016/j.conbuildmat.2014.12.014.

Tasong, W. A., Lynsdale, C. J. and Cripps, J. C. (1999) 'Aggregate-cement paste interface: Part I. Influence of aggregate geochemistry', *Cement and Concrete Research*, 29(7), pp. 1019–1025. doi: 10.1016/S0008-8846(99)00086-1.

Taylor, H. F. W. (1990) 'Cement chemistry', *Library*.

Theodosiou, A., Polis, M., *et al.* (2016) 'Comparative study of multimode CYTOP graded index and single- mode silica fibre Bragg grating array for the mode shape capturing of a free-free metal beam', in *Micro-Structured and Specialty Optical Fibres IV*. Brussels.

Theodosiou, A., Lacraz, A., *et al.* (2016) 'Modified fs-Laser Inscribed FBG Array for Rapid Mode Shape Capture of Free-Free Vibrating Beams', *IEEE Photonics Technology Letters*, 28(14), pp. 1509–1512. doi: 10.1109/LPT.2016.2555852.

Theodosiou, A. *et al.* (2017) 'Plane-by-Plane Femtosecond Laser Inscription Method for Single-Peak Bragg Gratings in Multimode CYTOP Polymer Optical Fiber', *Journal of Lightwave Technology*. OSA, 35(24), pp. 5404–5410. Available at: http://jlt.osa.org/abstract.cfm?URI=jlt-35-24-5404.

Theodosiou, A. *et al.* (2018) 'Bragg gratings and Fabry-Perot cavities in low-loss multimode CYTOP polymer fibre', *IEEE Photonics Technology Letters*, p. 1. doi: 10.1109/LPT.2018.2820381.

Theodosiou, A., Komodromos, M. and Kalli, K. (2017) 'Accurate and Fast Demodulation Algorithm for Multipeak FBG Reflection Spectra Using a Combination of Cross Correlation and Hilbert Transformation', *Journal of Lightwave Technology*, 35(18), pp. 3956–3962. doi: 10.1109/JLT.2017.2723945.

Torikai, Y., Sato, S. and Ohashi, H. (1996) 'Thermodynamic Properties of Water in Compacted Sodium Montmorillonite', *Nuclear Technology*. Taylor & Francis, 115(1), pp. 73–80. doi: 10.13182/NT96-A35276.

Tritsch, N., Darwin, D. and Browning, J. (2005) 'Evaluating Shrinkage and Cracking Behavior of Concrete Using Restrained Ring and Free Shrinkage Tests', *THE TRANSPORTATION POOLED FUND PROGRAM Project No. TPF-5(051)*, SM Report(Report), p. 178.

PERICLES ALEXANDROUSAVVA

Twelvetress, W. N. (1905) *Concrete and Reinforced Concrete*. London: Sir Isaac Pitman & Sons Ltd.

Van, V.-T.-A. *et al.* (2014) 'Rice husk ash as both pozzolanic admixture and internal curing agent in ultra-high performance concrete', *Cement and Concrete Composites*. Elsevier Ltd, 53, pp. 270–278. doi: 10.1016/j.cemconcomp.2014.07.015.

Vaysburd, A. M. (1996) 'Durability of lighweight concrete bridges in severe environments', *American Concrete Institute*, 18(7), pp. 33–38.

Verma, S. K., Bhadauria, S. S. and Akhtar, S. (2013) 'Evaluating effect of chloride attack and concrete cover on the probability of corrosion', *Frontiers of Structural and Civil Engineering*, 7(4), pp. 379–390. doi: 10.1007/s11709-013-0223-9.

Viviani, M., Glisic, B. and Smith, I. F. C. (2007) 'Separation of thermal and autogenous deformation at varying temperatures using optical fiber sensors', *Cement and Concrete Composites*, 29(6), pp. 435–447.

Wang, F. *et al.* (2016) 'Influence of superabsorbent polymers on the surrounding cement paste', *Cement and Concrete Research*. Elsevier Ltd, 81, pp. 112–121. doi: 10.1016/j.cemconres.2015.12.004.

Wasserman, R. and Bentur, A. (1996) 'Interfacial interactions in lightweight aggregate concretes and their influence on the concrete strength', *Cement and Concrete Composites*, 18(1), pp. 67–76.

Webb, D. J. *et al.* (2008) 'Temperature sensitivity of Bragg gratings in PMMA and TOPAS microstructured polymer optical fibres', in, p. 69900L–6990–10. Available at: https://doi.org/10.1117/12.781019.

Weber, S. and Reinhardt, H. W. (1997) 'A new generation of high performance concrete: concrete with autogenous curing', *Advanced cement based materials*, 6(97), pp. 59–68.

Wehbe, Y. and Ghahremaninezhad, A. (2017) 'Combined effect of shrinkage reducing admixtures (SRA) and superabsorbent polymers (SAP) on the autogenous shrinkage, hydration and properties of cementitious materials', *Construction and Building Materials*. Elsevier Ltd, 138, pp. 151–162. doi: 10.1016/j.conbuildmat.2016.12.206.

PERICLES ALEXANDROU SAVVA

Wei, H., Tao, C. and Krishnaswamy, S. (2016) 'Photonic crystal fiber based chloride chemical sensors for corrosion monitoring', (April), p. 98052A. doi: 10.1117/12.2217700.

Weiss, J., Yang, W. and Shah, S. (2000) 'Influence of Specimen Size/Geometry on Shrinkage Cracking of Rings', *Journal of Engineering Mechanics*, 126(3), pp. 233–242. doi: 10.1061/(ASCE)0733-9399(2000)126.

Wong, W. C. *et al.* (2012) 'Polyvinyl alcohol coated photonic crystal optical fiber sensor for humidity measurement', *Sensors and Actuators, B: Chemical*. Elsevier B.V., 174, pp. 563–569. doi: 10.1016/j.snb.2012.07.032.

Woyessa, G. *et al.* (2017) 'Low Loss Polycarbonate Polymer Optical Fiber for High Temperature FBG Humidity Sensing', *IEEE Photonics Technology Letters*, 29(7), pp. 575–578. doi: 10.1109/LPT.2017.2668524.

Wyrzykowski, M. and Lura, P. (2013) 'Controlling the coefficient of thermal expansion of cementitious materials - A new application for superabsorbent polymers', *Cement and Concrete Composites*. Elsevier Ltd, 35(1), pp. 49–58. doi: 10.1016/j.cemconcomp.2012.08.010.

Xiang, H. *et al.* (2010) 'Self-Sealing Cement-Based Materials Using Superabsorbent Polymers', (August).

Xiong, Z. *et al.* (1999) 'Highly tunable Bragg gratings in single-mode polymer optical fibers', *IEEE Photonics Technology Letters*, 11(3), pp. 352–354. doi: 10.1109/68.748232.

Yazdizadeh, Z., Marzouk, H. and Hadianfard, M. A. (2017) 'Monitoring of concrete shrinkage and creep using Fiber Bragg Grating sensors', *Construction and Building Materials*. Elsevier Ltd, 137, pp. 505–512. doi: 10.1016/j.conbuildmat.2017.01.084.

Yehia, S. *et al.* (2014) 'Monitoring of strain induced by heat of hydration, cyclic and dynamic loads in concrete structures using fiber-optics sensors', *Measurement: Journal of the International Measurement Confederation*, 52(1), pp. 33–46. doi: 10.1016/j.measurement.2014.02.030.

Yeniay, A. *et al.* (2004) 'Ultra-low-loss polymer waveguides', *Journal of Lightwave Technology*, 22(1), pp. 154–158. doi: 10.1109/JLT.2003.822206.

Yeo, T. L. *et al.* (2005) 'Characterisation of a polymer-coated fibre Bragg grating sensor for

PERICLES ALEXANDROU SAVVA

relative humidity sensing', *Sensors and Actuators, B: Chemical*, 110(1), pp. 148–156. doi: 10.1016/j.snb.2005.01.033.

Yuan, W., Khan, L., *et al.* (2011) 'Humidity insensitive TOPAS polymer fiber Bragg grating sensor', *Optics Express*. OSA, 19(20), pp. 19731–19739. doi: 10.1364/OE.19.019731.

Yuan, W., Stefani, A., *et al.* (2011) 'Improved thermal and strain performance of annealed polymer optical fiber Bragg gratings', *Optics Communications*, 284(1), pp. 176–182. doi: https://doi.org/10.1016/j.optcom.2010.08.069.

Zhang, T. *et al.* (2013) 'Measurement of chemical shrinkage of cement paste: Comparison study of ASTM C 1608 and an improved method', *Construction and Building Materials*. Elsevier Ltd, 48, pp. 662–669. doi: 10.1016/j.conbuildmat.2013.07.086.

Zhang, W. and Webb, D. J. (2014) 'Humidity responsivity of poly(methyl methacrylate)-based optical fiber Bragg grating sensors', *Optics Letters*. OSA, 39(10), pp. 3026–3029. doi: 10.1364/OL.39.003026.

Zhao, Y., Liao, Y. and Lai, S. (2002) 'Simultaneous measurement of down-hole high pressure and temperature with a bulk-modulus and FBG sensor', *IEEE Photonics Technology Letters*, 14(11), pp. 1584–1586. doi: 10.1109/LPT.2002.803914.

Zhutovsky, S. and Kovler, K. (2010) 'Durability Aspects of Internally Cured High Performance Concrete', in *International RILEM Conference on Use of Superabsorbent Polymers and Other New Additives in Concrete*, pp. 305–314.

Zhutovsky, S. and Kovler, K. (2012) 'Effect of internal curing on durability-related properties of high performance concrete', *Cement and Concrete Research*. Elsevier Ltd, 42(1), pp. 20–26. doi: 10.1016/j.cemconres.2011.07.012.

Zhutovsky, S. and Kovler, K. (2017) 'Influence of water to cement ratio on the efficiency of internal curing of high-performance concrete', *Construction and Building Materials*. Elsevier Ltd, 144, pp. 311–316. doi: 10.1016/j.conbuildmat.2017.03.203.

Zhutovsky, S., Kovler, K. and Bentur, A. (2002) 'Autogenous Curing of High-Strength Concrete Using Pre-Soaked Pumice and Perlite Sand', *The Third International Research Seminar in Lund*, (JANUARY 2002), pp. 161–173.

PERICLES ALEXANDROU SAVVA

Zhutovsky, S., Kovler, K. and Bentur, A. (2004) ‘Influence of cement paste matrix properties on the autogenous curing of high-performance concrete’, *Cement and Concrete Composites*, 26, pp. 499–507. doi: 10.1016/S0958-9465(03)00082-9.

Zhutovsky, S., Kovler, K. and Bentur, A. (2011) ‘Revisiting the protected paste volume concept for internal curing of high-strength concretes’, *Cement and Concrete Research*. Elsevier Ltd, 41(9), pp. 981–986. doi: 10.1016/j.cemconres.2011.05.007.

Zou, X. *et al.* (2012) ‘An experimental study on the concrete hydration process using Fabry-Perot fiber optic temperature sensors’, *Measurement: Journal of the International Measurement Confederation*. Elsevier Ltd, 45(5), pp. 1077–1082. doi: 10.1016/j.measurement.2012.01.034.

PERICLES ALEXANDROU SAVVA

ANNEX I: Cement clinker concentration analysis (XRD)

CEM I 52.5N

Run	SiKa1,2	AlKa1,2	TiKa1,2	FeKa1,2	CaKa1,2	MgKa1,2	Ska1,2	PKa1,2	NaKa1,2
Avg	17.842	3.822	0.206	3.057	63.197	1.579	5.570	0.194	0.417
Sd	0.016	0.001	0.001	0.006	0.011	0.003	0.007	0.003	0.003
Sd%	0.089	0.022	0.607	0.195	0.017	0.213	0.129	1.573	0.824
	KKa1,2	CrKa1,2	MnKa1,2	SrKa1,2	ZnKa1,2	FKa1,2	ClKa1,2	Alkalies	Sum
Avg	0.626	0.014	0.249	0.174	0.010	0.045	0.031	0.828	97.0.34
Sd	0.001	0.000	0.002	0.000	0.000	0.006	0.000	0.003	0.019
Sd%	0.219	1.379	0.606	0.042	1.495	12.517	0.645	0.306	0.020
	LSF	SM	AM						
Avg	111.940	2.594	1.250						
Sd	0.063	0.004	0.003						
Sd%	0.057	0.164	0.217						

PERICLES ALEXANDROU SAVVA

CEM II 42.5R

Run	SiKa1,2	AlKa1,2	TiKa1,2	FeKa1,2	CaKa1,2	MgKa1,2	Ska1,2	PKa1,2	NaKa1,2
Avg	16.902	3.621	0.207	2.974	63.337	1.502	5.472	0.158	0.441
Sd	0.012	0.007	0.002	0.002	0.024	0.002	0.004	0.002	0.002
Sd%	0.073	0.196	0.776	0.071	0.038	0.101	0.064	1.193	0.399
	KKa1,2	CrKa1,2	MnKa1,2	SrKa1,2	ZnKa1,2	FKa1,2	ClKa1,2	Alkalies	Sum
Avg	0.619	0.014	0.220	0.169	0.021	0.033	0.036	0.849	95.727
Sd	0.000	0.000	0.000	0.000	0.000	0.008	0.001	0.002	0.053
Sd%	0.028	0.434	0.103	0.168	0.118	23.156	2.063	0.194	0.056
	LSF	SM	AM						
Avg	118.320	2.563	1.218						
Sd	0.052	0.002	0.002						
Sd%	0.044	0.067	0.125						

PERICLES ALEXANDROU SAVVA

ANNEX II: Statistical analysis with SPSS

Regression analysis tables

Table 1 – ANNEX II: Linear regression analysis up to the age of 28 days for compressive strength

Coefficients[a]

Model		Unstandardized Coefficients		Standardized Coefficients	t	Sig.
		B	Std. Error	Beta		
1	(Constant)	52,754	4,507		11,704	,000
	Specimens Age	4,892	1,008	,471	4,854	,000
	Cast temperature	,117	,736	,015	,159	,875
	Curing Regime	4,369	1,646	,258	2,655	,011
	Aggregates	-9,372	1,646	-,553	-5,695	,000

a. Dependent Variable: Compressive strength

Table 2 – ANNEX II: Linear regression analysis up to the age of 28 days for compressive strength (excluding mixtures cast at 40°C)

Coefficients[a]

Model		Unstandardized Coefficients		Standardized Coefficients	t	Sig.
		B	Std. Error	Beta		
1	(Constant)	42,618	4,255		10,017	,000
	Specimens Age	5,195	,936	,545	5,551	,000
	Cast temperature	2,818	,936	,296	3,011	,005
	Curing Regime	5,316	1,528	,341	3,478	,002
	Aggregates	-6,968	1,528	-,448	-4,560	,000

a. Dependent Variable: Compressive strength

PERICLES ALEXANDROUSAVVA

Table 3 – ANNEX II: Linear regression analysis up to the age of 90 days for compressive strength

Coefficients[a]

Model		Unstandardized Coefficients		Standardized Coefficients	t	Sig.
		B	Std. Error	Beta		
1	(Constant)	58,193	4,199		13,857	,000
	Specimens Age	3,645	,697	,461	5,225	,000
	Cast temperature	,399	,697	,050	,572	,570
	Curing Regime	2,128	1,560	,120	1,364	,178
	Aggregates	-9,841	1,560	-,557	-6,310	,000

a. Dependent Variable: Compressive strength

Table 4 – ANNEX II: Linear regression analysis up to the age of 90 days for compressive strength (excluding mixtures cast at 40°C)

Coefficients[a]

Model		Unstandardized Coefficients		Standardized Coefficients	t	Sig.
		B	Std. Error	Beta		
1	(Constant)	49,306	4,498		10,963	,000
	Specimens Age	3,617	,734	,491	4,925	,000
	Cast temperature	3,152	1,006	,312	3,134	,003
	Curing Regime	2,715	1,642	,165	1,653	,106
	Aggregates	-7,516	1,642	-,456	-4,577	,000

a. Dependent Variable: Compressive strength

PERICLES ALEXANDROU SAVVA

Table 5 – ANNEX II: Linear regression analysis up to the age of 365 days for compressive strength

Coefficients[a]

Model		Unstandardized Coefficients		Standardized Coefficients	t	Sig.
		B	Std. Error	Beta		
1	(Constant)	59,752	3,916		15,260	,000
	Specimens Age	4,009	,519	,569	7,729	,000
	Cast temperature	,365	,656	,041	,557	,579
	Curing Regime	1,103	1,467	,055	,752	,454
	Aggregates	-10,285	1,467	-,516	-7,012	,000

a. Dependent Variable: Compressive strength

Table 6 – ANNEX II: Linear regression analysis up to the age of 365 days for compressive strength (excluding mixtures cast at 40°C)

Coefficients[a]

Model		Unstandardized Coefficients		Standardized Coefficients	t	Sig.
		B	Std. Error	Beta		
1	(Constant)	51,067	3,967		12,874	,000
	Specimens Age	3,924	,516	,604	7,599	,000
	Cast temperature	2,855	,894	,254	3,192	,002
	Curing Regime	2,377	1,461	,129	1,627	,109
	Aggregates	-8,366	1,461	-,455	-5,728	,000

a. Dependent Variable: Compressive strength

PERICLES ALEXANDROU SAVVA

Table 7 – ANNEX II: Linear regression analysis up to the age of 28 days for porosity

Coefficients[a]

Model		Unstandardized Coefficients		Standardized Coefficients	t	Sig.
		B	Std. Error	Beta		
1	(Constant)	,081	,016		4,896	,000
	Specimens Age	-,005	,004	-,128	-1,307	,198
	Cast temperature	-,001	,003	-,025	-,252	,803
	Curing Regime	,000	,006	-,004	-,037	,970
	Aggregates	,046	,006	,756	7,730	,000

a. Dependent Variable: Porosity

Table 8 – ANNEX II: Linear regression analysis up to the age of 28 days for porosity (excluding mixtures cast at 40°C)

Coefficients[a]

Model		Unstandardized Coefficients		Standardized Coefficients	t	Sig.
		B	Std. Error	Beta		
1	(Constant)	,118	,016		7,588	,000
	Specimens Age	-,004	,003	-,111	-1,032	,310
	Cast temperature	-,010	,003	-,309	-2,881	,007
	Curing Regime	-,007	,006	-,142	-1,322	,196
	Aggregates	,037	,006	,718	6,689	,000

a. Dependent Variable: Porosity

PERICLES ALEXANDROU SAVVA

Table 9 – ANNEX II: Linear regression analysis up to the age of 90 days for porosity

Coefficients[a]

Model		Unstandardized Coefficients		Standardized Coefficients	t	Sig.
		B	Std. Error	Beta		
1	(Constant)	,064	,015		4,370	,000
	Specimens Age	,001	,002	,020	,238	,812
	Cast temperature	,002	,002	,052	,618	,539
	Curing Regime	-,001	,005	-,022	-,265	,792
	Aggregates	,049	,005	,759	9,002	,000

a. Dependent Variable: Porosity

Table 10 – ANNEX II: Linear regression analysis up to the age of 90 days for porosity (excluding mixtures cast at 40°C)

Coefficients[a]

Model		Unstandardized Coefficients		Standardized Coefficients	t	Sig.
		B	Std. Error	Beta		
1	(Constant)	,103	,014		7,181	,000
	Specimens Age	,000	,002	-,006	-,059	,953
	Cast temperature	-,007	,003	-,224	-2,330	,025
	Curing Regime	-,007	,005	-,126	-1,303	,199
	Aggregates	,040	,005	,732	7,599	,000

a. Dependent Variable: Porosity

PERICLES ALEXANDROU SAVVA

Table 11 – ANNEX II: Linear regression analysis up to the age of 365 days for porosity

Coefficients[a]

Model		Unstandardized Coefficients		Standardized Coefficients	t	Sig.
		B	Std. Error	Beta		
1	(Constant)	,063	,014		4,483	,000
	Specimens Age	,007	,002	,306	3,928	,000
	Cast temperature	,001	,002	,038	,495	,622
	Curing Regime	-,006	,005	-,084	-1,083	,282
	Aggregates	,045	,005	,667	8,572	,000

a. Dependent Variable: Porosity

Table 12 – ANNEX II: Linear regression analysis up to the age of 28 days for porosity (excluding mixtures cast at 40°C)

Coefficients[a]

Model		Unstandardized Coefficients		Standardized Coefficients	t	Sig.
		B	Std. Error	Beta		
1	(Constant)	,098	,015		6,560	,000
	Specimens Age	,007	,002	,341	3,761	,000
	Cast temperature	-,007	,003	-,199	-2,187	,033
	Curing Regime	-,010	,005	-,170	-1,868	,067
	Aggregates	,036	,005	,602	6,632	,000

a. Dependent Variable: Porosity

PERICLES ALEXANDROU SAVVA

Table 13 – ANNEX II: Linear regression analysis up to the age of 28 days for RCP

Coefficients[a]

Model		Unstandardized Coefficients		Standardized Coefficients	t	Sig.
		B	Std. Error	Beta		
1	(Constant)	11189,604	1112,587		10,057	,000
	Specimens Age	-1412,219	248,782	-,615	-5,677	,000
	Cast temperature	-162,000	181,685	-,097	-,892	,378
	Curing Regime	242,583	406,259	,065	,597	,554
	Aggregates	-1208,250	406,259	-,322	-2,974	,005

a. Dependent Variable: Rapid chloride permeability

Table 14 – ANNEX II: Linear regression analysis up to the age of 28 days for RCP (excluding mixtures cast at 40°C)

Coefficients[a]

Model		Unstandardized Coefficients		Standardized Coefficients	t	Sig.
		B	Std. Error	Beta		
1	(Constant)	11845,444	1123,361		10,545	,000
	Specimens Age	-1470,083	247,106	-,682	-5,949	,000
	Cast temperature	-679,667	247,106	-,315	-2,751	,010
	Curing Regime	-212,222	403,523	-,060	-,526	,603
	Aggregates	-538,333	403,523	-,153	-1,334	,192

a. Dependent Variable: Rapid chloride permeability

PERICLES ALEXANDROU SAVVA

Table 15 – ANNEX II: Linear regression analysis up to the age of 90 days for RCP

Coefficients[a]

Model		Unstandardized Coefficients		Standardized Coefficients	t	Sig.
		B	Std. Error	Beta		
1	(Constant)	10171,000	891,856		11,404	,000
	Specimens Age	-1478,513	148,129	-,763	-9,981	,000
	Cast temperature	-86,663	148,129	-,045	-,585	,561
	Curing Regime	634,313	331,227	,146	1,915	,060
	Aggregates	-972,813	331,227	-,224	-2,937	,005

a. Dependent Variable: Rapid chloride permeability

Table 16 – ANNEX II: Linear regression analysis up to the age of 90 days for RCP (excluding mixtures cast at 40°C)

Coefficients[a]

Model		Unstandardized Coefficients		Standardized Coefficients	t	Sig.
		B	Std. Error	Beta		
1	(Constant)	10644,938	931,385		11,429	,000
	Specimens Age	-1501,267	152,094	-,812	-9,871	,000
	Cast temperature	-490,344	208,264	-,194	-2,354	,023
	Curing Regime	216,750	340,094	,052	,637	,527
	Aggregates	-384,750	340,094	-,093	-1,131	,264

a. Dependent Variable: Rapid chloride permeability

PERICLES ALEXANDROU SAWA

Table 17 – ANNEX II: Linear regression analysis up to the age of 365 days for RCP

Coefficients[a]

Model		Unstandardized Coefficients		Standardized Coefficients	t	Sig.
		B	Std. Error	Beta		
1	(Constant)	9786,556	778,438		12,572	,000
	Specimens Age	-1438,969	103,107	-,836	-13,956	,000
	Cast temperature	-170,470	130,421	-,078	-1,307	,195
	Curing Regime	561,600	291,629	,115	1,926	,058
	Aggregates	-556,850	291,629	-,114	-1,909	,060

a. Dependent Variable: Rapid chloride permeability

Table 18 – ANNEX II: Linear regression analysis up to the age of 365 days for RCP (excluding mixtures cast at 40°C)

Coefficients[a]

Model		Unstandardized Coefficients		Standardized Coefficients	t	Sig.
		B	Std. Error	Beta		
1	(Constant)	10088,600	805,663		12,522	,000
	Specimens Age	-1404,967	104,888	-,856	-13,395	,000
	Cast temperature	-563,725	181,672	-,198	-3,103	,003
	Curing Regime	239,700	296,669	,052	,808	,423
	Aggregates	-67,367	296,669	-,015	-,227	,821

a. Dependent Variable: Rapid chloride permeability

PERICLES ALEXANDROU SAWA

Table 19 – ANNEX II: Linear regression analysis up to the age of 28 days for RCP

Coefficients[a]

Model		Unstandardized Coefficients		Standardized Coefficients	t	Sig.
		B	Std. Error	Beta		
1	(Constant)	,000	,000		4,890	,000
	Specimens Age	-4,788E-6	,000	-,124	-,857	,396
	Cast temperature	-3,800E-6	,000	-,135	-,931	,357
	Curing Regime	-3,342E-6	,000	-,053	-,366	,716
	Aggregates	1,527E-5	,000	,243	1,673	,102

a. Dependent Variable: Sorptivity

Table 20 – ANNEX II: Linear regression analysis up to the age of 28 days for RCP (excluding mixtures cast at 40°C)

Coefficients[a]

Model		Unstandardized Coefficients		Standardized Coefficients	t	Sig.
		B	Std. Error	Beta		
1	(Constant)	,000	,000		5,130	,000
	Specimens Age	-7,329E-6	,000	-,180	-1,130	,267
	Cast temperature	-1,266E-5	,000	-,310	-1,952	,060
	Curing Regime	-1,086E-5	,000	-,163	-1,025	,313
	Aggregates	1,662E-5	,000	,249	1,569	,127

a. Dependent Variable: Sorptivity

PERICLES ALEXANDROU SAVVA

Table 21 – ANNEX II: Linear regression analysis up to the age of 90 days for RCP

Coefficients[a]

Model		Unstandardized Coefficients		Standardized Coefficients	t	Sig.
		B	Std. Error	Beta		
1	(Constant)	,000	,000		6,120	,000
	Specimens Age	-3,817E-6	,000	-,142	-1,170	,247
	Cast temperature	-4,851E-6	,000	-,180	-1,486	,142
	Curing Regime	-3,034E-6	,000	-,050	-,416	,679
	Aggregates	1,692E-5	,000	,281	2,319	,024

a. Dependent Variable: Sorptivity

Table 22 – ANNEX II: Linear regression analysis up to the age of 90 days for RCP (excluding mixtures cast at 40°C)

Coefficients[a]

Model		Unstandardized Coefficients		Standardized Coefficients	t	Sig.
		B	Std. Error	Beta		
1	(Constant)	,000	,000		6,117	,000
	Specimens Age	-3,891E-6	,000	-,137	-1,015	,316
	Cast temperature	-1,293E-5	,000	-,332	-2,463	,018
	Curing Regime	-9,421E-6	,000	-,148	-1,099	,278
	Aggregates	1,682E-5	,000	,264	1,962	,056

a. Dependent Variable: Sorptivity

PERICLES ALEXANDROU SAVVA

Table 23 – ANNEX II: Linear regression analysis up to the age of 365 days for RCP

Coefficients[a]

Model		Unstandardized Coefficients		Standardized Coefficients	t	Sig.
		B	Std. Error	Beta		
1	(Constant)	8,402E-5	,000		3,793	,000
	Specimens Age	1,046E-5	,000	,356	3,566	,001
	Cast temperature	-5,430E-6	,000	-,146	-1,463	,148
	Curing Regime	-6,377E-6	,000	-,077	-,768	,445
	Aggregates	2,634E-5	,000	,317	3,174	,002

a. Dependent Variable: Sorptivity

Table 24 – ANNEX II: Linear regression analysis up to the age of 28 days for RCP (including mixtures cast at 40°C)

Coefficients[a]

Model		Unstandardized Coefficients		Standardized Coefficients	t	Sig.
		B	Std. Error	Beta		
1	(Constant)	,000	,000		4,460	,000
	Specimens Age	1,048E-5	,000	,356	3,164	,003
	Cast temperature	-1,422E-5	,000	-,279	-2,478	,016
	Curing Regime	-1,284E-5	,000	-,154	-1,370	,176
	Aggregates	2,289E-5	,000	,275	2,443	,018

a. Dependent Variable: Sorptivity

PERICLES ALEXANDROU SAVVA

Descriptive analysis

Descriptive analysis using all the results included in Chapter 6

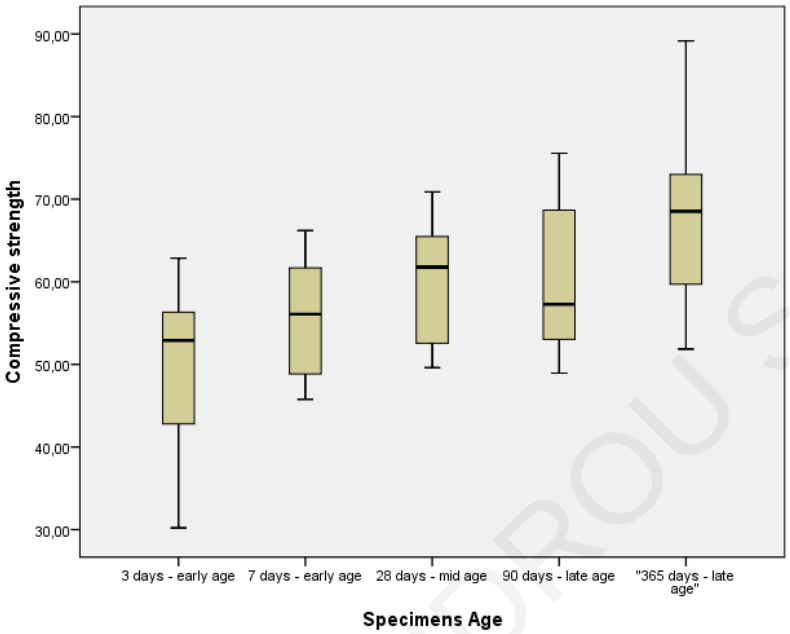

Figure 1 – ANNEX II: Compressive strength vs Specimens age for all mixtures (including NWA and HANWA)

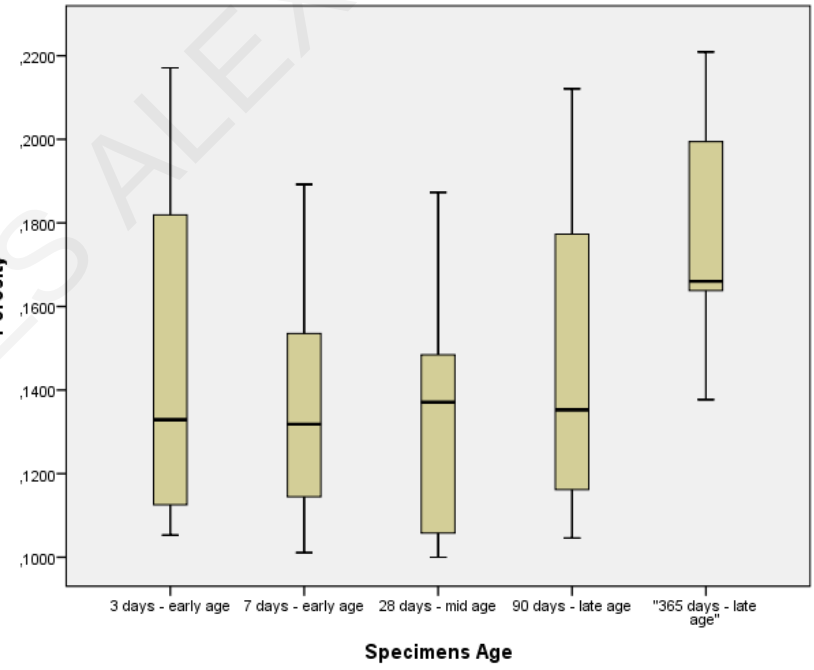

Figure 2 – ANNEX II: Porosity vs Specimens age for all mixtures (including NWA and HANWA)

PERICLES ALEXANDROU SAVVA

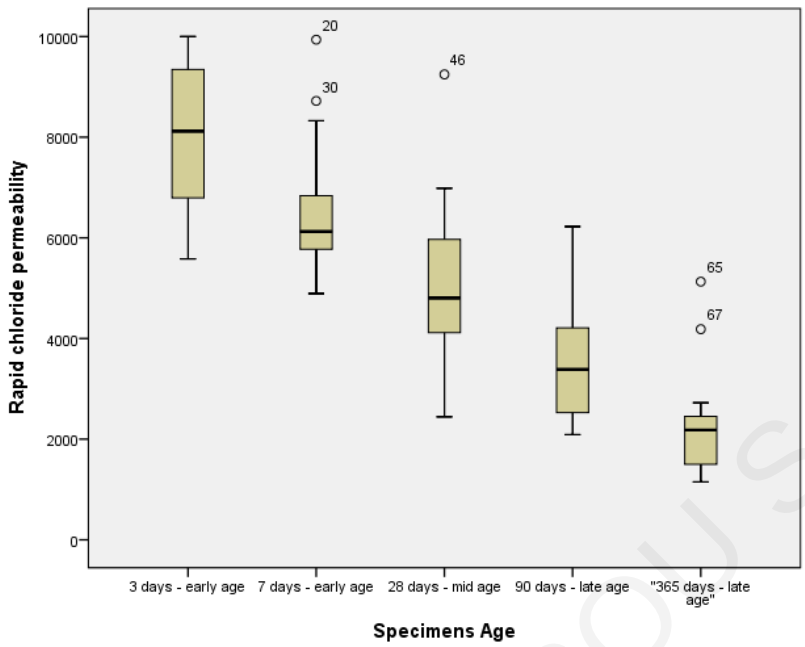

Figure 3 – ANNEX II: RCP vs Specimens age for all mixtures (including NWA and HANWA)

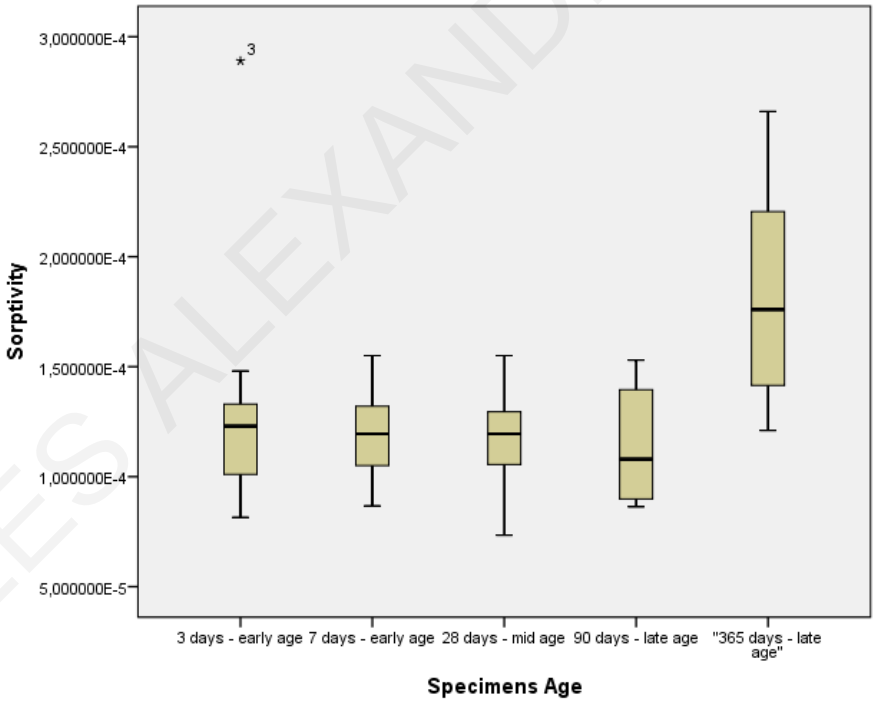

Figure 4 – ANNEX II: Sorptivity vs Specimens age for all mixtures (including NWA and HANWA)

PERICLES ALEXANDROU SAVVA

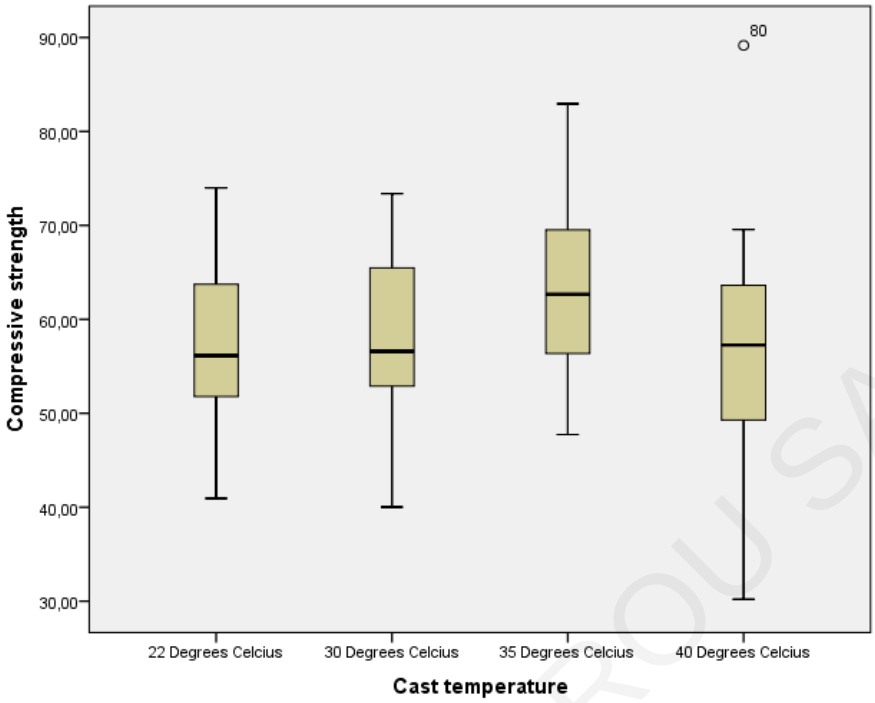

Figure 5 – ANNEX II: Compressive strength vs Cast temperature for all mixtures (including NWA and HANWA)

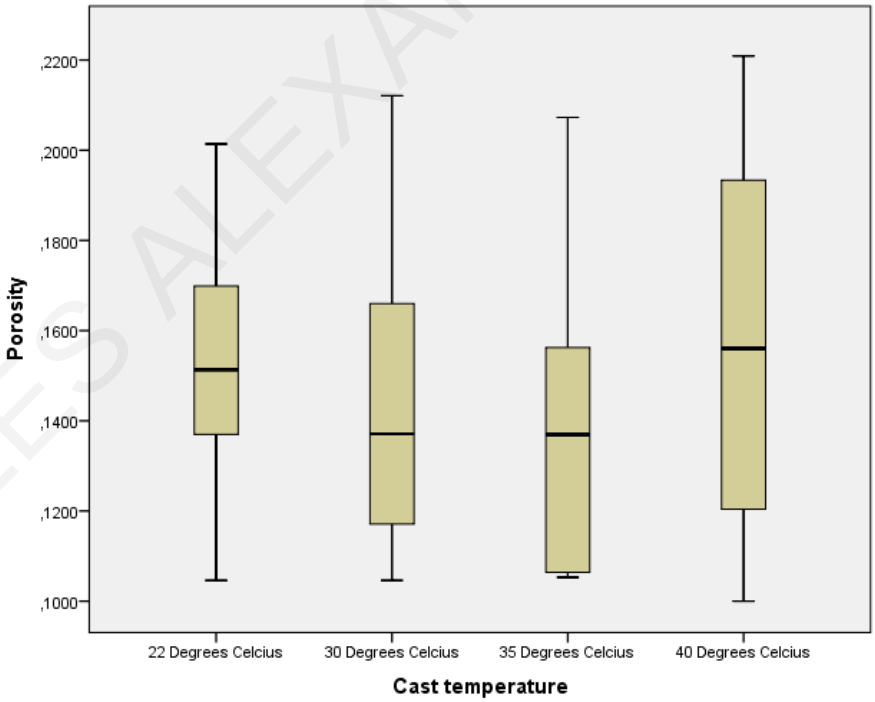

Figure 6 – ANNEX II: Porosity vs Cast temperature for all mixtures (including NWA and HANWA)

PERICLES ALEXANDROU SAVVA

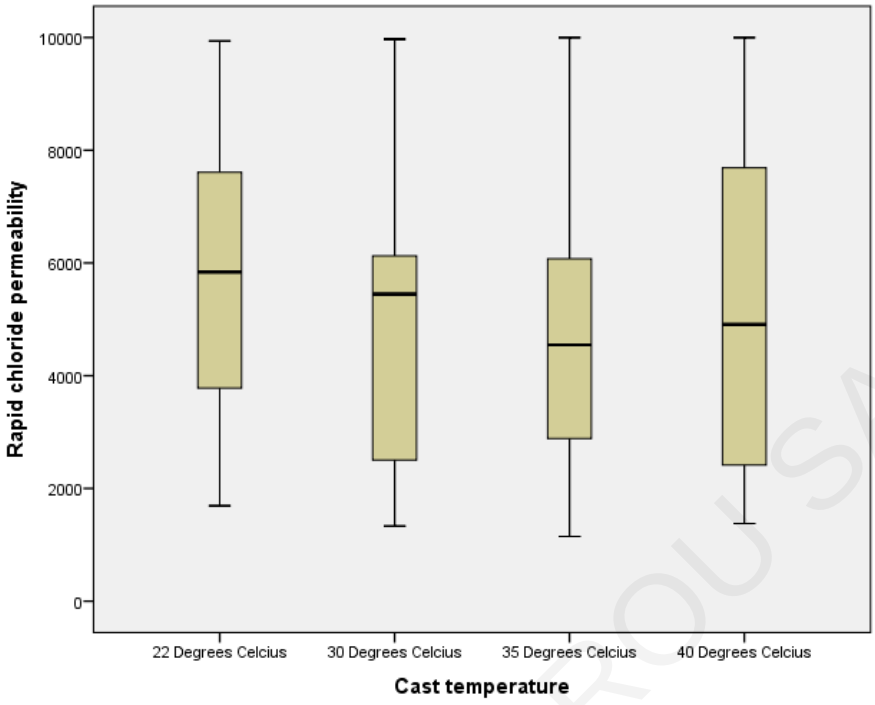

Figure 7 – ANNEX II: RCP vs Cast temperature for all mixtures (including NWA and HANWA)

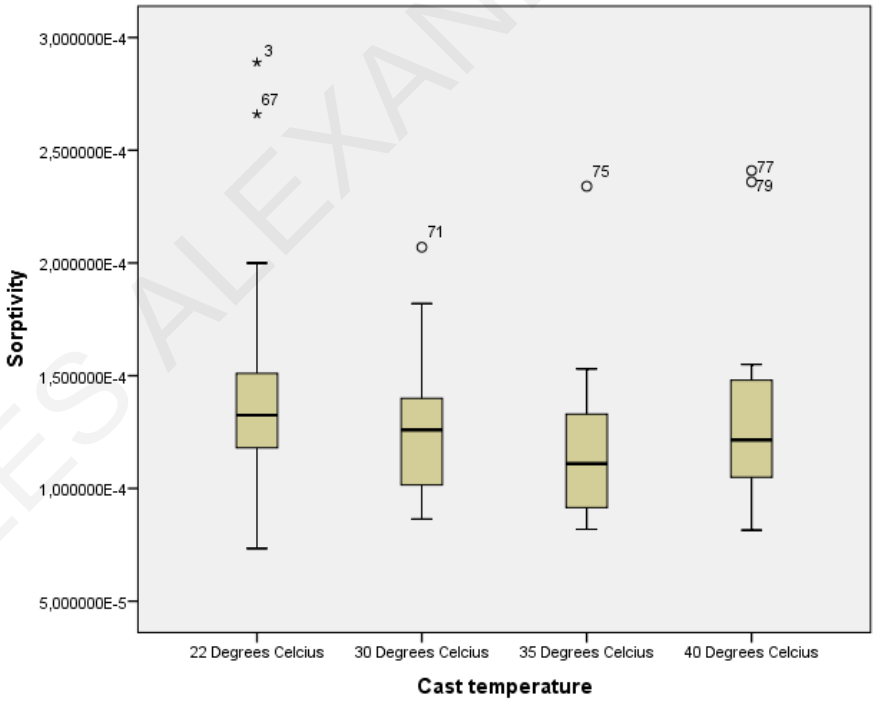

Figure 8 – ANNEX II: Sorptivity vs Cast temperature for all mixtures (including NWA and HANWA)

PERICLES ALEXANDROU SAVVA

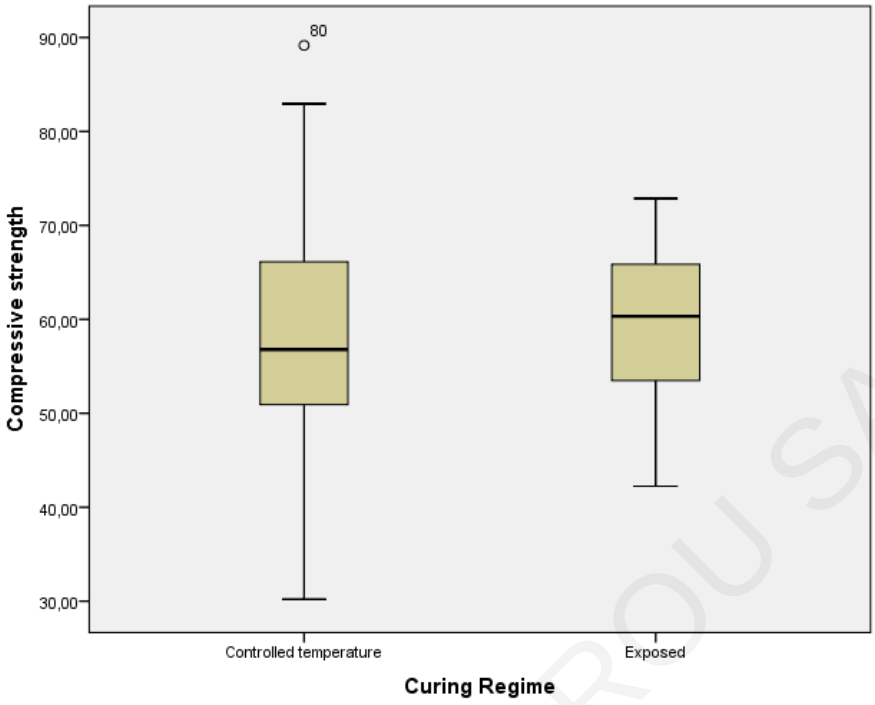

Figure 9 – ANNEX II: Compressive strength vs Curing regime (including NWA and HANWA)

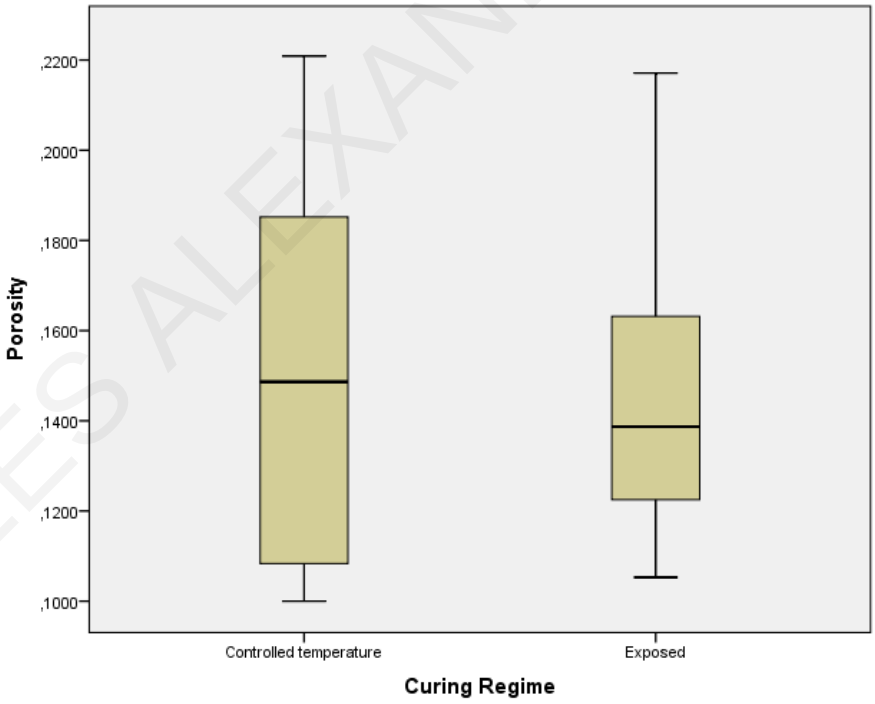

Figure 10 – ANNEX II: Porosity vs Curing regime (including NWA and HANWA)

PERICLES ALEXANDROU SAVVA

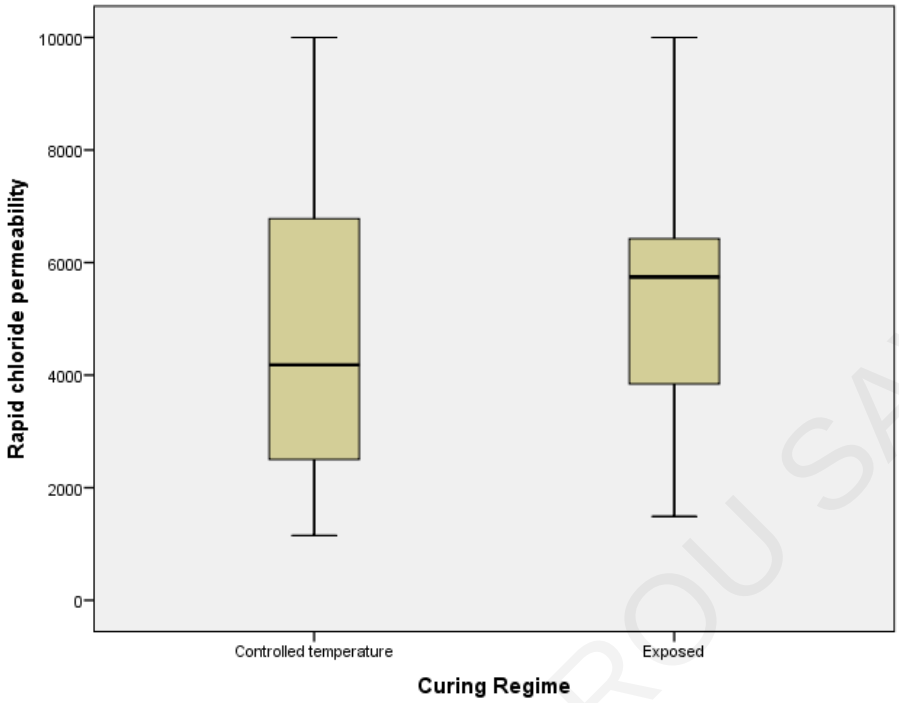

Figure 11 – ANNEX II: RCP vs Curing regime (including NWA and HANWA)

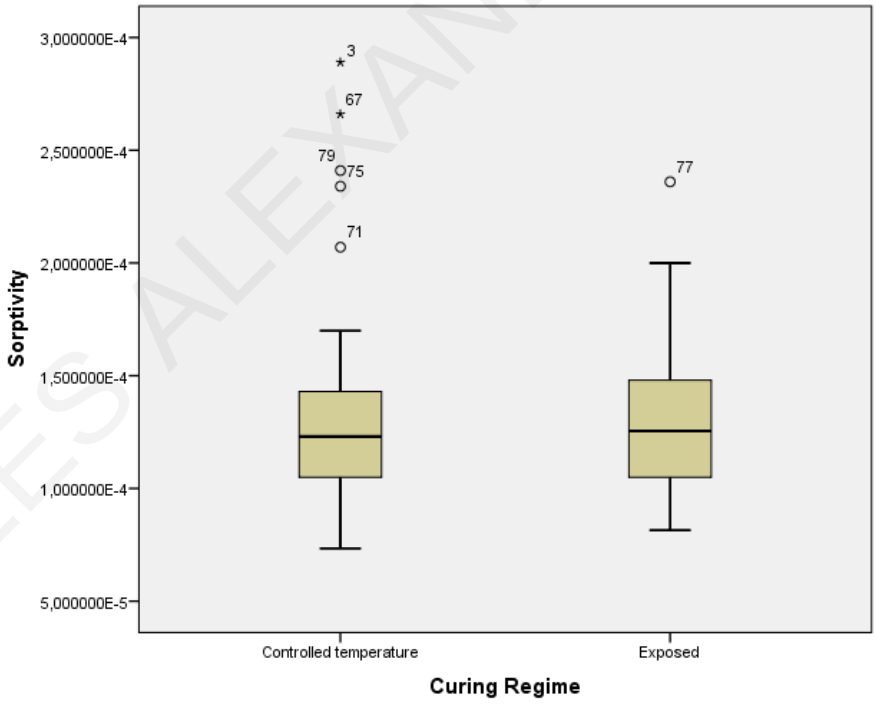

Figure 12 – ANNEX II: Sorptivity vs Curing regime (including NWA and HANWA)

PERICLES ALEXANDROU SAVVA

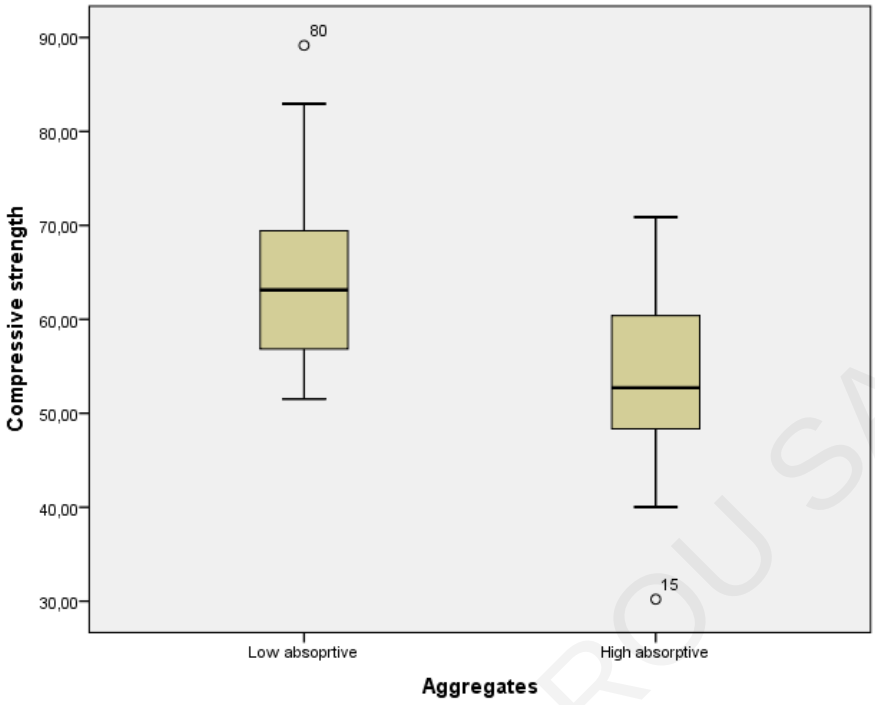

Figure 13 – ANNEX II: Compressive strength vs Aggregates type

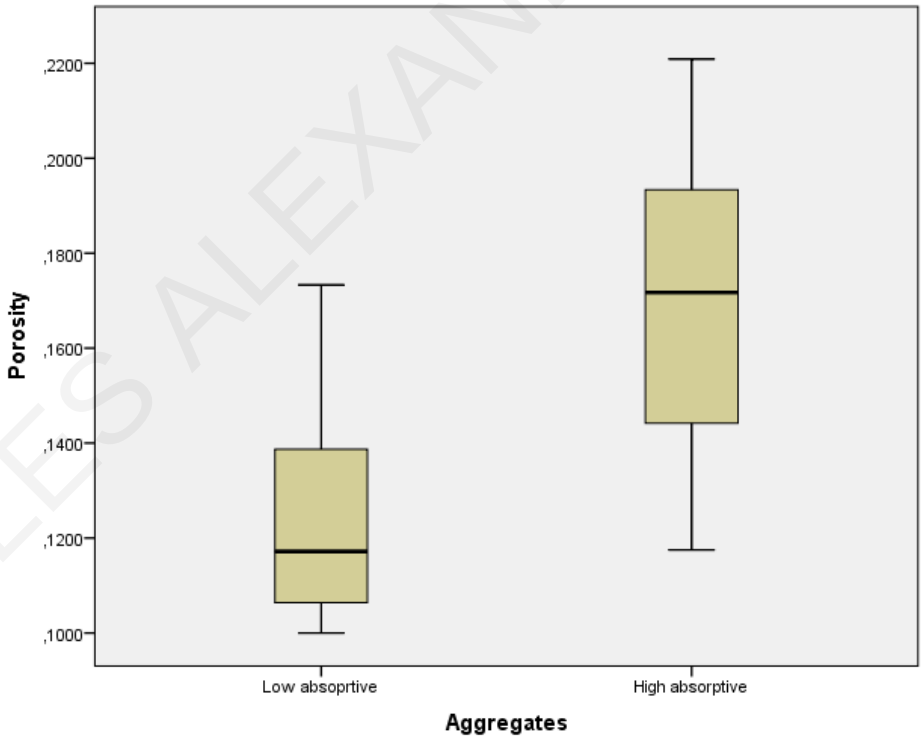

Figure 14 – ANNEX II: Porosity vs Aggregates type

PERICLES ALEXANDROU SAVVA

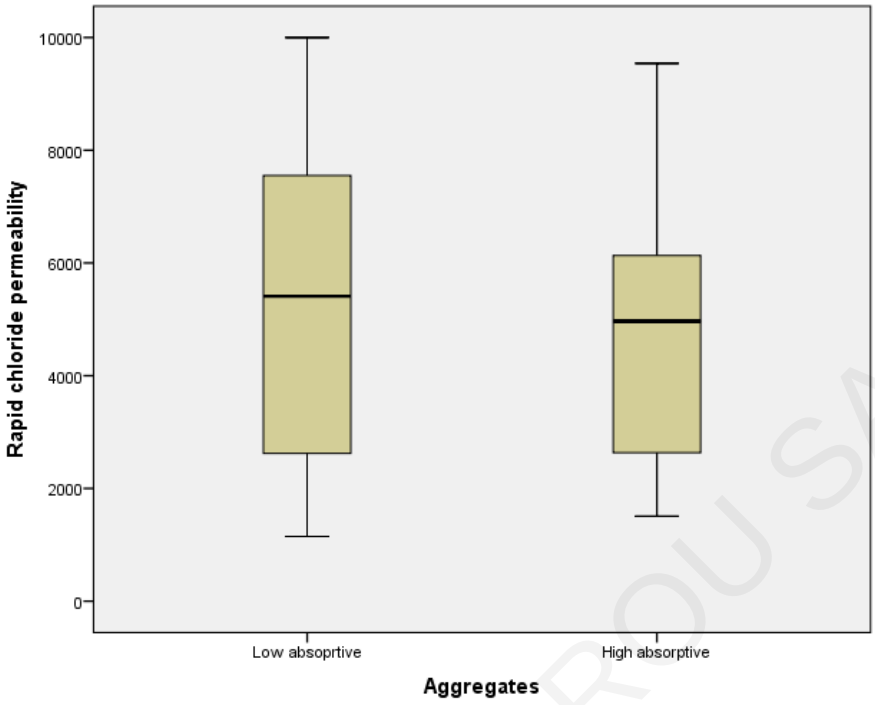

Figure 15 – ANNEX II: RCP vs Aggregates type

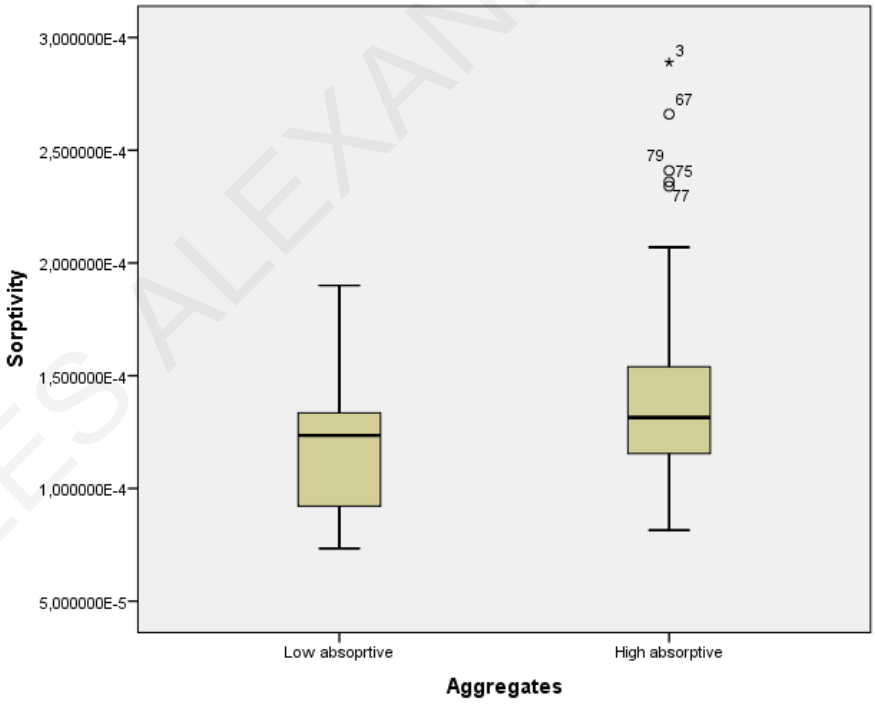

Figure 16 – ANNEX II: Sorptivity vs Aggregates type

PERICLES ALEXANDROU SAVVA

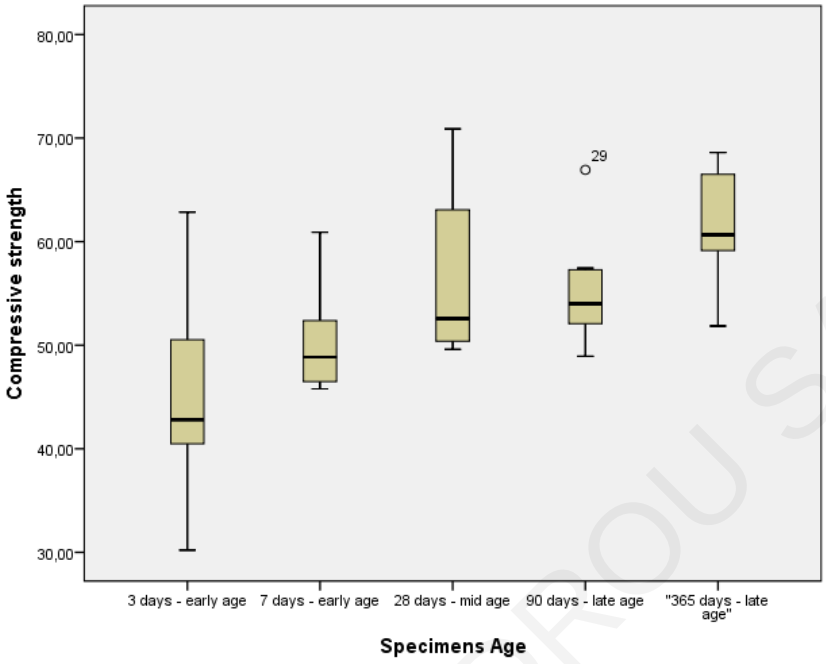

Figure 17 – ANNEX II: Compressive strength vs Specimens age for HANWA mixtures

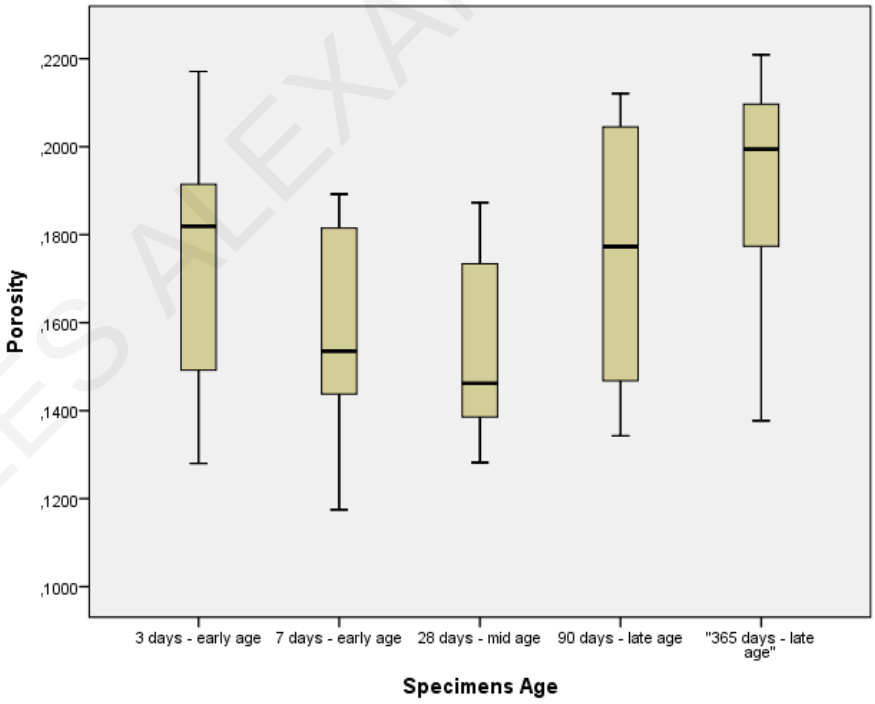

Figure 18 – ANNEX II: Porosity vs Specimens age for HANWA mixtures

PERICLES ALEXANDROU SAVVA

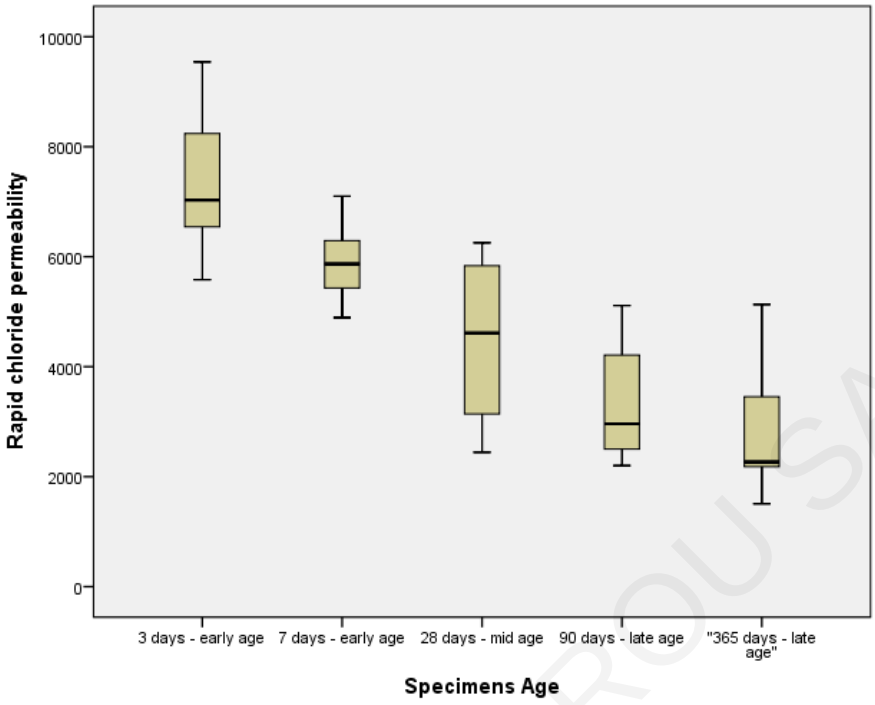

Figure 19 – ANNEX II: RCP vs Specimens age for HANWA mixtures

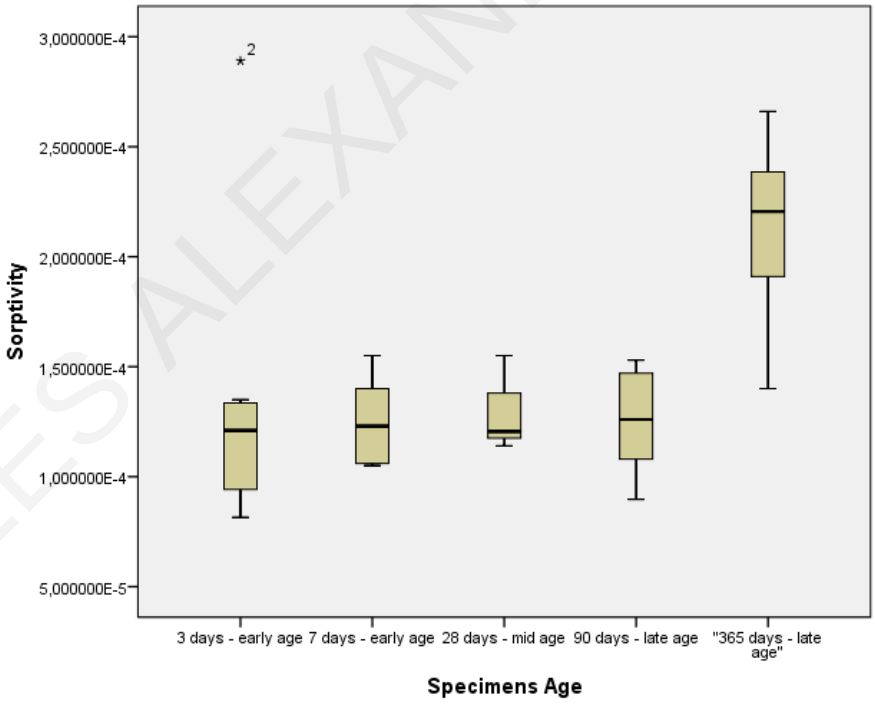

Figure 20 – ANNEX II: Sorptivity vs Specimens age for HANWA mixtures

PERICLES ALEXANDROU SAVVA

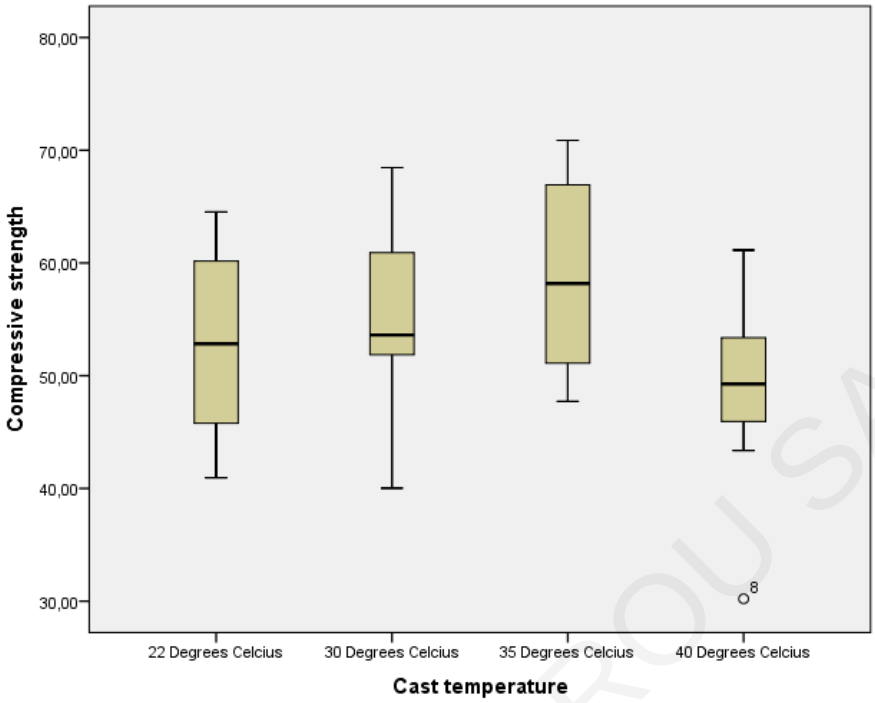

Figure 21 – ANNEX II: Compressive strength vs Cast temperature for HANWA mixtures

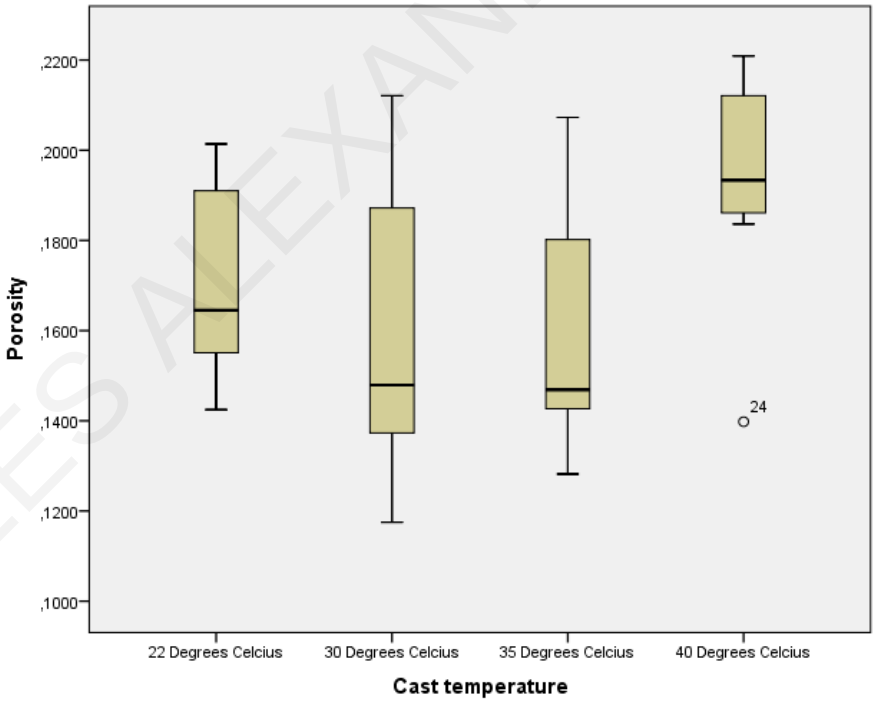

Figure 22 – ANNEX II: Porosity vs Cast temperature for HANWA mixtures

PERICLES ALEXANDROU SAVVA

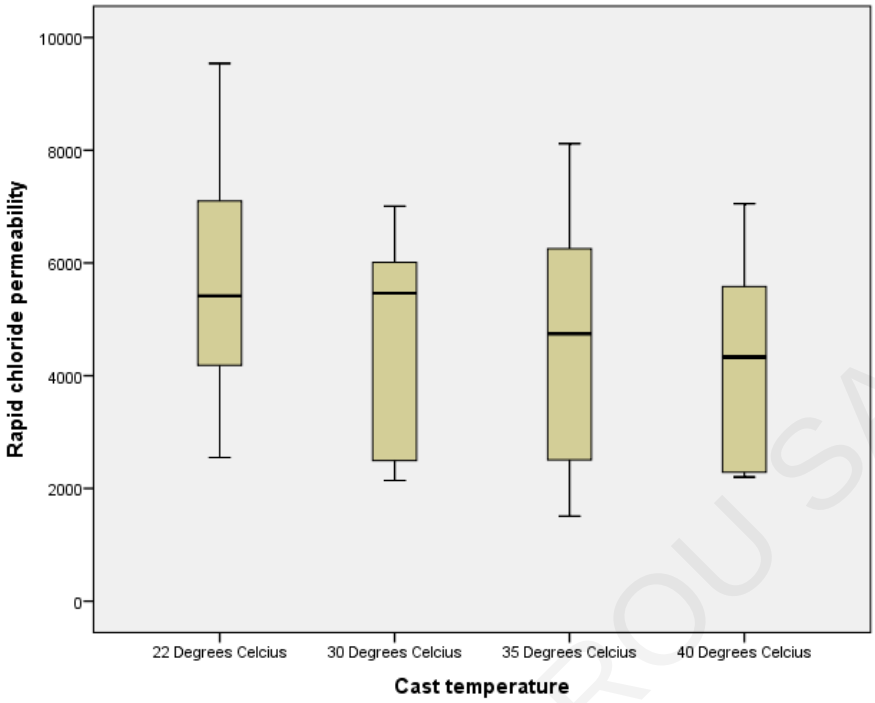

Figure 23 – ANNEX II: RCP vs Cast temperature for HANWA mixtures

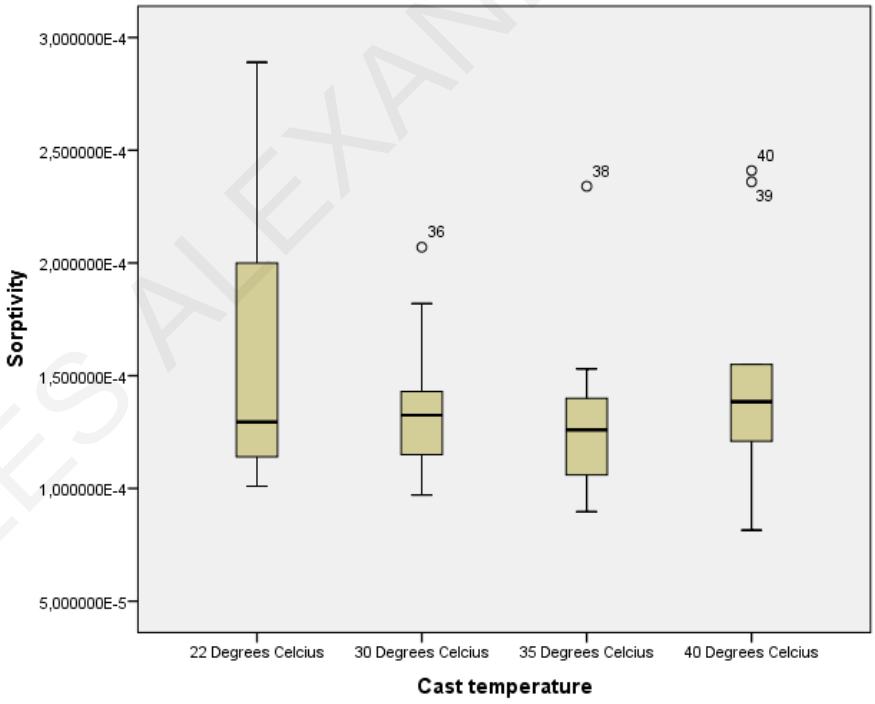

Figure 24 – ANNEX II: Sorptivity vs Cast temperature for HANWA mixtures

PERICLES ALEXANDROU SAVVA

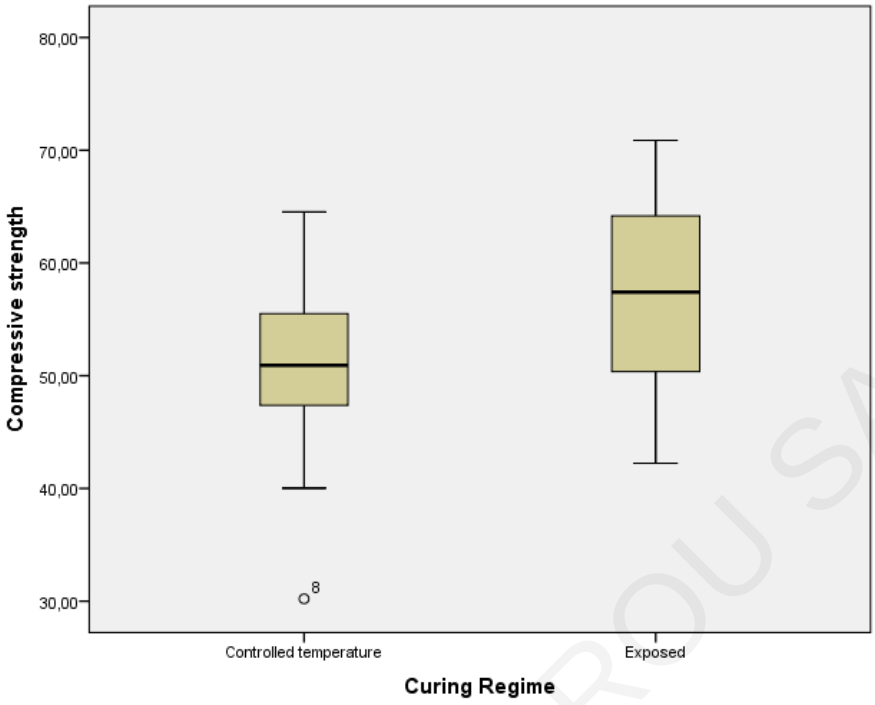

Figure 25 – ANNEX II: Compressive strength vs Curing regime for HANWA mixtures

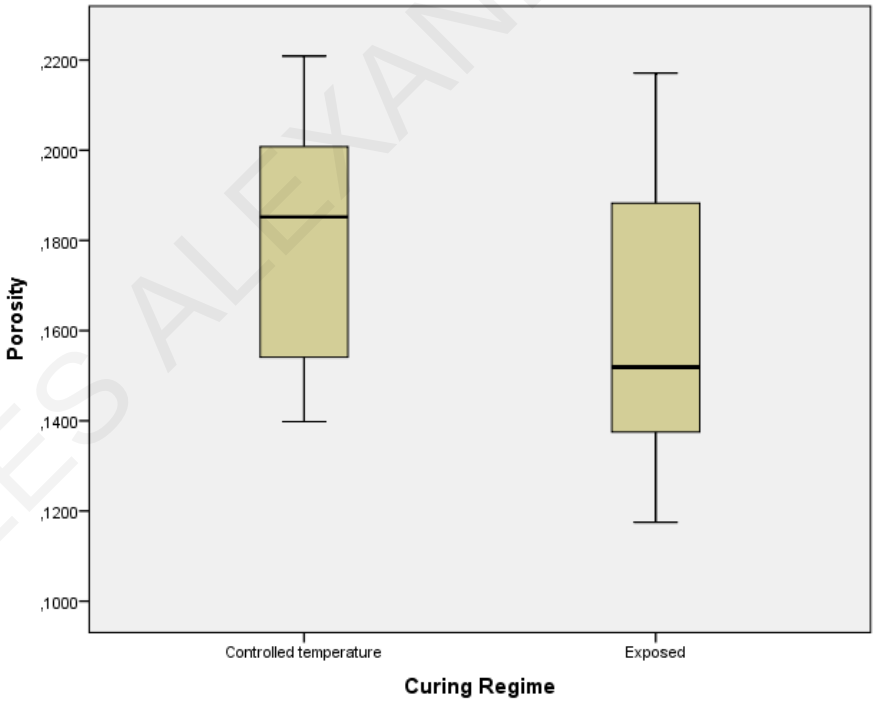

Figure 26 – ANNEX II: Porosity vs Curing regime for HANWA mixtures

PERICLES ALEXANDROU SAVVA

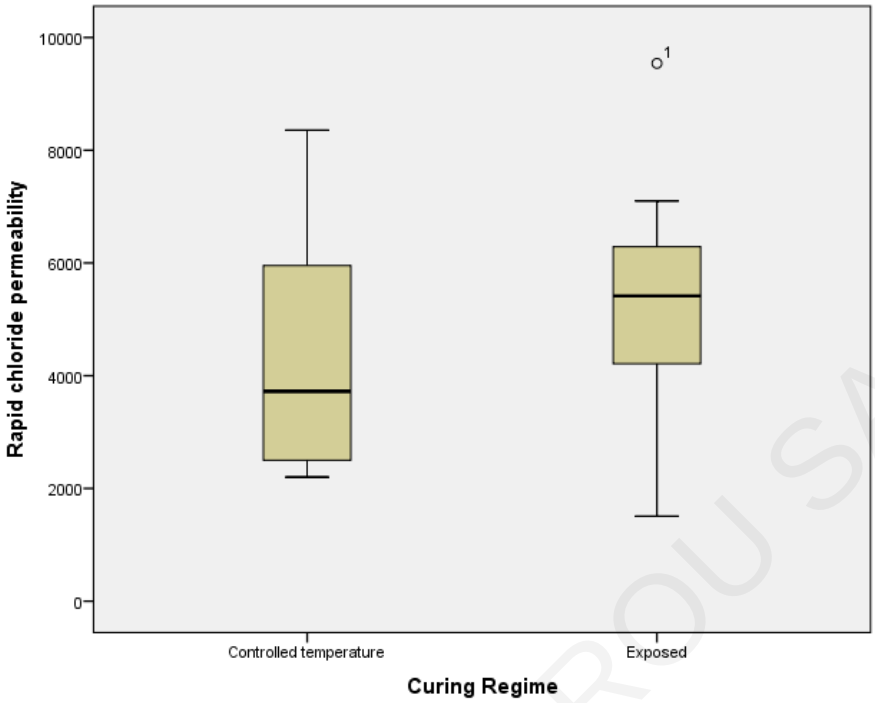

Figure 27 – ANNEX II: RCP vs Curing regime for HANWA mixtures

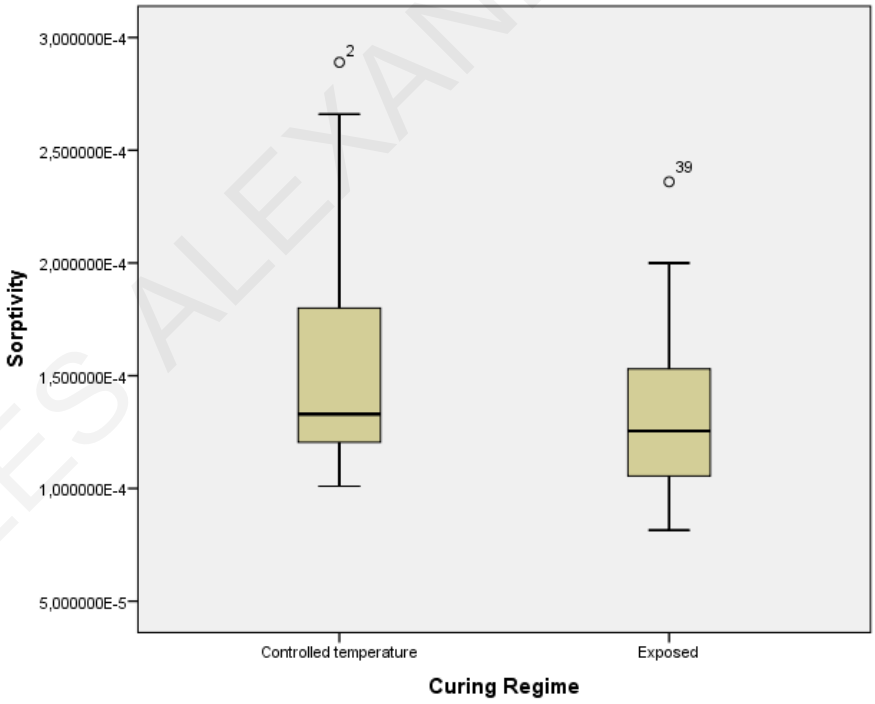

Figure 28 – ANNEX II: Sorptivity vs Curing regime for HANWA mixtures

PERICLES ALEXANDROU SAVVA